

**IMPAIRED REGULATION OF HEPATIC GLUCOSE DISPOSITION BY HIGH
DIETARY FAT AND FRUCTOSE**

By

Kathryn Eileen Colbert Coate

Dissertation

Submitted to the Faculty of the
Graduate School of Vanderbilt University
in partial fulfillment of the requirements for

the degree of

DOCTOR OF PHILOSOPHY

in

Molecular Physiology and Biophysics

December, 2011

Nashville, Tennessee

Approved:

Professor Richard M. O'Brien

Professor Owen P. McGuinness

Professor Larry L. Swift

Associate Professor Alyssa H. Hasty

Assistant Professor Masakazu Shiota

To my family, Dad, Mom, Robin, Holly, Lee Ann, Angela,

Anna Caitlin, Graham, Stephen, Braden,

And my wonderful husband, Matt

For your love, support, encouragement, and ceaseless prayers throughout this journey.

ACKNOWLEDGEMENTS

First, I would like to thank my mentor, Dr. Alan D. Cherrington, for believing in me and providing me with the opportunity to train under him over the last 4 years. It has been such a fulfilling and enriching experience for me, and I am so blessed to have had the opportunity to work one-on-one with such a brilliant scientist. He has played an integral role in molding me into the scientist that I am today, and has undoubtedly equipped me with the skills necessary to become a successful academic scientist in the near future. I will be indebted to Dr. Cherrington for the remainder of my career for the opportunities that he has provided for me. For his generosity, loyalty, dedication, patience, encouragement, positive attitude, sense of humor, words of wisdom, and guidance, I thank him.

I would also like to thank my dissertation committee, Dr. Richard O'Brien, Dr. Owen McGuinness, Dr. Masakazu Shiota, Dr. Alyssa Hasty, and Dr. Larry Swift. They have provided me with invaluable feedback and suggestions over the last three years, and I am truly grateful for their time, generosity, and scientific contributions to this body of work.

It goes without saying that my success as a graduate student was made possible in part by the incredibly talented staff of technicians that work in our laboratory. Without the help of Marta Smith, Maggie Lautz, Ben Farmer, Doss Neal, Erik Nass, Josh Roop, Melanie Scott, and Jon Hastings, I would not have completed all of this work in 4 years time. I owe each of them a great deal of gratitude for their time, hard work, dependability, technical proficiency, and patience. They embody the characteristics of what it means to be a team and to work together towards a common goal, and for that I am truly grateful.

In addition, I would like to thank Dr. Dale Edgerton and Dr. Genie Moore for being wonderful colleagues, mentors, and friends. Genie taught me how to perform a pancreatic clamp study from start to finish, and has spent countless hours proofreading my manuscripts and looking over my talks. I am sincerely grateful for her generosity, time, and willingness to help in every circumstance. I would also like to thank several of my friends from the lab (past and present), including Guillaume Kraft, Zhibo An, Noelia Rivera, Tiffany Farmer, Marta Smith, Melanie Scott, Josh Roop, and Jon Hastings. Each of you has made the lab a pleasant and enjoyable place to come to every day, and I cherish the moments that we have spent together over the last 4 years. Thank you for your encouragement and help along the way.

Finally, God has blessed me with an amazing family and husband who have enabled me to persevere through the good times and bad. They have been my support system and source of strength throughout this entire process, and I am truly a testament to the power of prayer. I am also so fortunate to have a husband that supports me, loves me, encourages me, listens to my frustrations, and shares in my joys. He has made numerous sacrifices for me to pursue the career of my dreams, and I am sincerely grateful for his support and love. I am confident that God has amazing experiences and opportunities in store for us both, and my desire is that we continue to obey Him and to use the talents and abilities that He has blessed us with to the best of our abilities.

Financial support for this work was provided by the Vanderbilt University Molecular Endocrinology Training Program, a National Institute of Diabetes and Digestive Kidney Diseases (NIDDK) Grant, NIH RO1-DK18243, and a National Institute of Health Diabetes Research and Training Center Grant, DK-020593.

TABLE OF CONTENTS

	Page
DEDICATION.....	ii
ACKNOWLEDGEMENTS.....	iii
LIST OF TABLES.....	ix
LIST OF FIGURES.....	xi
Chapter	
I. INTRODUCTION.....	1
Dietary Fat.....	4
Dietary Fat and Obesity in Humans.....	4
Dietary Fat, Insulin Resistance, and Type 2 Diabetes in Humans...8	8
Dietary Fat Quality and Insulin Sensitivity in Humans.....	12
Dietary Fat, Adiposity, and Insulin Action in Experimental Animals Models.....	14
Dietary Fructose.....	19
Dietary Fructose Consumption in the U.S.....	19
Metabolism of Dietary Fructose.....	20
Dietary Fructose and Obesity in Humans.....	22
Dietary Fructose, Insulin Resistance, and Type 2 Diabetes in Humans.....	23
Dietary Fructose, Insulin Action, and Dyslipidemia in Experimental Animal Models.....	27
Catalytic Quantities of Fructose and Hepatic Glucose Metabolism.....	30
Cellular Mechanisms of Diet-Induced Hepatic Insulin Resistance.....	32
Molecular Changes Associated with High-Fat or High-Fructose Feeding.....	32
Regulation of Hepatic Glucose Uptake.....	35
Regulation of Net Hepatic Glucose Uptake by Hyperglycemia.....	37
Regulation of Net Hepatic Glucose Uptake by Hyperinsulinemia.....	39
Regulation of Net Hepatic Glucose Uptake by Hyperinsulinemia and Hyperglycemia.....	41
Regulation of Net Hepatic Glucose Uptake by Portal Glucose Delivery.....	43
Interaction Between the Portal Glucose Signal, Insulin, and the Hepatic Glucose Load.....	46

	Mechanism of Portal Signaling.....	48
	Mechanism of Action of the Portal Glucose Signal.....	50
	Impaired Regulation of Splanchnic Glucose Uptake with Diabetes.....	52
	Specific Aims.....	54
II.	MATERIALS AND METHODS.....	58
	Animal Care and Surgical Procedures.....	58
	Animal Care.....	58
	Surgical Procedures.....	58
	Hepatic Catheterization.....	58
	Partial Pancreatectomy.....	61
	Experimental Diets.....	63
	Collection and Processing of Samples.....	64
	Blood Samples.....	64
	Tissue Samples.....	66
	Sample Analysis.....	67
	Whole Blood Metabolites.....	67
	Alanine.....	68
	Glycerol.....	68
	Lactate.....	69
	Plasma Metabolites.....	69
	Glucose.....	69
	3-[³ H]-Glucose.....	70
	Non-esterified Fatty Acids.....	71
	Triglycerides.....	72
	Hormones.....	72
	Insulin.....	73
	Glucagon.....	74
	C-peptide.....	75
	Glucagon-like Peptide-1.....	76
	Acetaminophen.....	76
	Hepatic Blood Flow.....	78
	Liver Tissue Analysis.....	79
	Glycogen Content.....	79
	Total Triglyceride Content.....	80
	RNA Extraction, cDNA Synthesis, and Real-Time PCR.....	81
	Western Blotting.....	82
	Glucokinase Activity.....	84
	Glycogen Synthase and Phosphorylase Activity.....	84
	Calculations.....	85
	Net Hepatic Substrate Balance.....	85
	Net Gut Substrate Balance.....	85
	Net Hepatic Substrate Fractional Extraction.....	86
	Hepatic Sinusoidal Substrate Concentration.....	86

	Glucose Mixing in the Portal Vein.....	86
	Unidirectional Hepatic Glucose Uptake.....	88
	Hepatic Glucose Production.....	90
	Glucose Turnover.....	90
	Net Hepatic Carbon Retention (Net Glycogen Synthesis).....	92
	Nonhepatic Glucose Uptake.....	92
	Statistical Analysis.....	93
III.	SPECIFIC AIM I: CHRONIC CONSUMPTION OF A HIGH-FAT, HIGH-FRUCTOSE DIET RENDERS THE LIVER INCAPABLE OF NET HEPATIC GLUCOSE UPTAKE.....	94
	Aim.....	94
	Experimental Timeline.....	95
	Experimental Design.....	95
	Results.....	97
	Discussion.....	102
	Figures.....	111
	Tables.....	118
IV.	SPECIFIC AIM II: A HIGH-FAT, HIGH-FRUCTOSE DIET ACCELERATES NUTRIENT ABSORPTION AND IMPAIRS NET HEPATIC GLUCOSE UPTAKE IN RESPONSE TO A MIXED MEAL IN PARTIALLY PANCREATCTOMIZED DOGS.....	123
	Aim.....	123
	Experimental Design.....	124
	Results.....	125
	Discussion.....	128
	Figures.....	134
	Tables.....	138
V.	SPECIFIC AIM III: PORTAL VEIN GLUCOSE ENTRY TRIGGERS A COORDINATED MOLECULAR RESPONES THAT ACTIVATES HEPATIC GLUCOSE UPTAKE AND GLYCOGEN SYNTHESIS IN NORMAL, BUT NOT HIGH-FAT, HIGH-FRUCTOSE-FED DOGS.....	142
	Aim.....	142
	Experimental Design.....	144
	Results.....	145
	Discussion.....	152
	Figures.....	166
	Tables.....	172

VI.	SPECIFIC AIM IV: THE EFFECT OF SHORT-TERM HIGH-FAT VS. HIGH-FRUCTOSE FEEDING ON HEPATIC GLUCOSE UPTAKE AND DISPOSITION.....	175
	Aim.....	175
	Experimental Design.....	175
	Results.....	177
	Discussion.....	181
	Figures.....	191
	Tables.....	197
VII.	SUMMARY AND CONCLUSIONS.....	199
	REFERENCES.....	212

LIST OF TABLES

Table		Page
2.1	Macronutrient compositions of experimental diets utilized in Specific Aims I-IV.....	63
2.2	Experimental diet assignment, feeding duration (weeks), and sample size (<i>n</i>) for Specific Aims I-IV.....	64
3.1	Venous plasma glucagon concentrations during OGTTs.....	118
3.2	Venous plasma glucose, insulin, glucagon, free fatty acid, and triglyceride concentrations during hyperinsulinemic euglycemic clamps.....	119
3.3	Body weight, fasting plasma glucose, and insulin.....	120
3.4	Tracer-determined rate of endogenous glucose appearance (Endo R_a), net hepatic glucose balance (NHGB), estimated hepatic glucose uptake (Est HGU = Endo R_a -NHGB), and rate of glucose disappearance (Glucose R_d) during hyperinsulinemic hyperglycemic clamps in a subset of dogs	121
3.5	Total hepatic blood flow, total glucose infusion rate, arterial blood lactate and glycerol concentrations, arterial plasma NEFA concentration, net hepatic lactate, glycerol and NEFA balance, and net hepatic carbon retention during hyperinsulinemic hyperglycemic clamps.....	122
4.1	Composition of the experimental diets.....	138
4.2	Portal vein plasma glucagon like peptide-1 (GLP-1), arterial plasma glucagon, and hepatic sinusoidal plasma glucagon concentrations during the basal (60 to 120 min) and experimental (120 to 390 min) periods following oral administration of a liquid mixed meal to 24-h-fasted dogs that had been fed a control diet (CTR) or a high-fat, high-fructose diet (HFFD) for 8 weeks.....	139
4.3	Arterial blood glycerol, net hepatic glycerol uptake, and arterial plasma FFA and TG concentrations during the basal (60 to 120 min) and experimental (120 to 390 min) periods following oral administration of a liquid mixed meal to 24-h-fasted dogs that had been fed a control diet (CTR) or a high-fat, high-fructose diet (HFFD) for 8 weeks.....	140
4.4	Arterial blood alanine, gut production of alanine, net hepatic alanine uptake, fractional extraction of alanine during the basal (60 to 120 min) and experimental (120 to 390 min) periods following oral administration of a	

	liquid mixed meal in 24-h-fasted dogs that had been fed a control diet (CTR) or a high-fat, high-fructose diet (HFF) for 8 weeks.....	141
5.1	Mean values for total hepatic blood flow and glucose infusion rate during the basal (-20 to 0 min) and experimental periods (P1, 60 to 90 min; P2, 150-180 min) of a hyperinsulinemic hyperglycemic clamp.....	172
5.2	Mean values for unidirectional hepatic glucose uptake, hepatic glucose production, and net hepatic glucose balance during the basal (-20 to 0 min) and experimental (P1, 30 to 90 min; P2, 120-180 min) periods of a hyperinsulinemic hyperglycemic clamp in the CTR-PoG, HFFD-PoG, CTR+PoG, and HFFD+PoG groups.....	173
5.3	Mean values for lactate, glycerol, and NEFA concentrations, and their net hepatic balance during the (-20 to 0 min) and experimental (P1, 30 to 90 min; P2, 120-180 min) periods of a hyperinsulinemic hyperglycemic clamp in the CTR-PoG, HFFD-PoG, CTR+PoG, and HFFD+PoG groups.....	174
6.1	Mean values for hepatic arterial and portal venous blood flow, as well as total glucose infusion rate during the basal (-20 to 0 min) and experimental periods (P1, 60 to 90 min; P2, 150 to 180 min) of a hyperinsulinemic hyperglycemic clamp.....	197
6.2	Mean values for lactate, glycerol, and NEFA concentrations, and their net hepatic balance during the (-20 to 0 min) and experimental (P1, 30 to 90 min; P2, 120-180 min) periods of a hyperinsulinemic hyperglycemic clamp in CTR, HFA, and HFR groups.....	198

LIST OF FIGURES

Figure		Page
3.1	Experimental timeline. Numbers below the horizontal line indicate the week in which an experiment or surgery was conducted relative to initiation of the experimental diets (CTR or HFFD). CTR, standard meat and laboratory chow diet; HFFD, high-fat, high-fructose diet; VU, Vanderbilt University; OGTT, oral glucose tolerance test; HIEG, hyperinsulinemic-euglycemic clamp; Px, partial pancreatectomy; HIHG, hyperinsulinemic-hyperglycemic clamp.....	111
3.2	OGTTs in CTR group. OGTTs were conducted in 24-h-fasted dogs at baseline (BL; circles), and after 4 (squares) and 8 (triangles) weeks of feeding a CTR diet ($n = 4$). Polycose was administered orally (0.9 g/kg), and plasma glucose (A), c-peptide (B), and insulin (C) concentrations were measured over 180 min. <i>Insets:</i> Delta AUCs over 180 min for glucose (A), c-peptide (B), and insulin (C). Data are means \pm SE.....	112
3.3	OGTTs in HFFD-Sh group. OGTTs were conducted in 24-h-fasted dogs at baseline (BL; circles), and after 4 (squares) and 8 (triangles) weeks of feeding a HFFD to sham-operated dogs (HFFD-Sh; $n = 4$). Polycose was administered orally (0.9 g/kg), and plasma glucose (A), c-peptide (B), and insulin (C) concentrations were measured over 180 min. <i>Insets:</i> Delta AUCs over 180 min for glucose (A), c-peptide (B), and insulin (C). Data are means \pm SE. * $P < 0.05$ vs. baseline Δ AUC.....	113
3.4	OGTTs in HFFD-Px group. OGTTs were conducted in 24-h-fasted dogs at baseline (BL; circles), and after 4 (squares) and 8 (triangles) weeks of feeding a HFFD to partially pancreatectomized dogs (HFFD-Px; $n = 6$). Polycose was administered orally (0.9 g/kg), and plasma glucose (A), c-peptide (B), and insulin (C) concentrations were measured over 180 min. <i>Insets:</i> Delta AUCs over 180 min for glucose (A), c-peptide (B), and insulin (C). Data are means \pm SE. * $P < 0.05$ vs. baseline Δ AUC.....	114
3.5	Hyperinsulinemic euglycemic clamps in CTR and HFFD groups. Mean glucose infusion rates (GIR; A and B) during HIEG clamps conducted in 18-h-fasted dogs at baseline (BL; circles) and after 10 weeks (squares) of feeding a CTR ($n = 4$; A) or a HFFD to Sh or Px ($n = 10$; B) dogs. Average GIR (C) and GIR-to-insulin ratios (D) during 90-120 min of HIEGs conducted at BL (filled bars) and after 10 weeks (patterned bars) of feeding. Data from the HFFD-Sh and HFFD-Px groups were combined in B-D because the reduction in GIR (mg/kg/min) after 10 weeks of HFFD feeding was similar between groups (HFFD-Sh, BL: 18.5 ± 1.7 , 10wk: 13.9 ± 0.7 ; HFFD-Px, BL: 19.2 ± 1.3 , 10wk: 14.1 ± 1.1). Data are means \pm SE. * $P < 0.05$ vs. baseline; NS, not significant....	115

- 3.6 **Plasma hormone concentrations during hyperinsulinemic hyperglycemic clamps in CTR and HFFD groups.** Arterial plasma insulin (A) and glucagon (C), and hepatic sinusoidal insulin (B) and glucagon (D) during the basal (-20 to 0 min) and experimental periods (0 to 180 min) of HIHG clamps conducted in 18-h-fasted dogs after 13 weeks of feeding a CTR diet ($n = 4$; □) or a HFFD ($n = 8$; ●). Data from the HFFD-Sh and HFFD-Px groups were combined in this figure because there were no differences between groups for these clamped parameters. Two dogs in the HFFD-Px group had to be dropped from the cohort, one because of catheter failure and one because of an infusion error. Data are means \pm SE. † $P < 0.05$ vs. basal period (HFFD and CTR groups).....116
- 3.7 **Hyperinsulinemic hyperglycemic clamps in CTR and HFFD groups.** Arterial blood glucose (A), nonhepatic glucose uptake (B), hepatic glucose load (C) and net hepatic glucose balance (NHGB; D) during the basal (-20 to 0 min) and experimental periods (0 to 180 min) of HIHG clamps conducted in 18-h-fasted dogs after 13 weeks of feeding a CTR diet ($n = 4$; □) or a HFFD ($n = 8$; ●). Negative values for NHGB indicate net hepatic uptake; positive values indicate net hepatic production. Data from the HFFD-Sh and HFFD-Px groups were combined for HIHG analyses because there was no difference in NHGB (mg/kg/min) between the two groups (average during last 30 min of the 2 subperiods; HFFD-Sh: -0.1 ± 0.5 ; HFFD-Px: 0.3 ± 0.8). Data are means \pm SE. † $P < 0.05$ vs. basal period (HFFD and CTR groups); * $P < 0.05$ vs. CTR group.....117
- 4.1 Arterial plasma glucose (A), net gut glucose balance (B), and arterial plasma acetaminophen (C) concentrations during the basal (60 to 120 min) and experimental (120 to 390 min) periods following oral administration of a liquid mixed meal to 24-h-fasted dogs that had been fed a CTR ($n = 5$; ●) or HFFD ($n = 5$; ○) for 8 weeks. Data are means \pm SE. † $P < 0.05$ vs. basal period; * $P < 0.05$ vs. CTR group.....134
- 4.2 Arterial plasma insulin (A), c-peptide (B), and glucagon like peptide-1 (GLP-1, active) (C) concentrations during the basal (60 to 120 min) and experimental (120 to 390 min) periods following oral administration of a liquid mixed meal to 24-h-fasted dogs that had been fed a CTR ($n = 5$; ●) or HFFD ($n = 5$; ○) for 8 weeks. Data are means \pm SE. † $P < 0.05$ vs. basal period; * $P < 0.05$ vs. CTR group...135
- 4.3 Net hepatic glucose balance (NHGB) (A), net hepatic carbon retention (NHCR; mg of glucose equivalents) (B), and nonhepatic glucose uptake (C) during the basal (60 to 120 min) and experimental (120 to 390 min) periods following oral administration of a liquid mixed meal to 24-h-fasted dogs that had been fed a CTR ($n = 5$; ●) or HFFD ($n = 5$; ○) for 8 weeks. Negative values for NHGB or NHCR indicate net hepatic glucose uptake or glycogen synthesis, respectively; positive values indicate net hepatic glucose output or glycogen breakdown, respectively. Data are means \pm SE. † $P < 0.05$ vs. basal period; * $P < 0.05$ vs. CTR group.....136

- 4.4 Arterial blood lactate (A) and net hepatic lactate balance (B) during the basal (60 to 120 min) and experimental (120 to 390 min) periods following oral administration of a liquid mixed meal to 24-h-fasted dogs that had been fed a CTR ($n = 5$; ●) or HFFD ($n = 5$; ○) for 8 weeks. Negative values for net hepatic lactate balance indicate net hepatic lactate uptake; positive values indicate net hepatic lactate output. Data are means \pm SE. † $P < 0.05$ vs. basal period; * $P < 0.05$ vs. CTR group.....137
- 5.1 **Schematic representation of the hyperinsulinemic hyperglycemic clamp protocol.** The protocol consisted of basal (-20 to 0 min) and experimental periods (1: 0-90 min; 2: 90-180 min). Somatostatin and 3-[³H] glucose were infused peripherally, insulin (3-fold basal) and glucagon (basal) were infused intraportally, and glucose was infused peripherally at a variable rate to increase the hepatic glucose load 2-fold basal during periods 1 and 2. During period 2, glucose was also infused intraportally to activate the portal glucose signal.....166
- 5.2 **Plasma hormone concentrations during hyperinsulinemic hyperglycemic clamps in CTR and HFFD groups.** Arterial plasma insulin (A) and glucagon (C), and hepatic sinusoidal insulin (B) and glucagon (D) during basal (-20 to 0 min) and experimental periods (0 to 180 min) of HIHG clamps conducted in 18-h-fasted dogs after 4 weeks of feeding a CTR (HIHG-PoG CTR, $n = 5$; HIHG+PoG CTR, $n = 5$; □) or HFFD (HIHG-PoG HFFD, $n = 5$; HIHG+PoG HFFD, $n = 6$; ●). Data are means \pm SE. † $P < 0.05$ vs. basal period.....167
- 5.3 **Arterial blood glucose, hepatic glucose load, and hepatic glucose uptake during hyperinsulinemic hyperglycemic clamps in CTR and HFFD groups.** Arterial blood glucose (A), hepatic glucose load (B), and hepatic glucose uptake in the portal saline (C) and portal glucose (D) groups during the basal (-20 to 0 min) and experimental periods (0 to 180 min) of HIHG clamps conducted in 18-h-fasted dogs after 4 weeks of feeding a CTR (HIHG-PoG CTR, $n = 5$; HIHG+PoG CTR, $n = 5$; □) or HFFD (HIHG-PoG HFFD, $n = 5$; HIHG+PoG HFFD, $n = 6$; ●). Data are means \pm SE. † $P < 0.05$ vs. basal period; * $P < 0.05$ vs. corresponding CTR group; § $P < 0.05$, HIHG - PoG HFFD vs. CTR; # $P < 0.05$, HIHG+PoG HFFD vs. CTR.....168
- 5.4 **Hepatic glucokinase (GK) and glucokinase regulatory protein (GKRP) in CTR and HFFD groups.** Levels of GK mRNA (A) and protein (B), GK activity (C), and levels of GKRP protein (D). A, B, and D are expressed relative to levels observed in basal CTR animals. Data are means \pm SE; $n = 5-6$ per group. ‡ $P < 0.05$, basal HFFD vs. CTR; † $P < 0.05$ vs. basal CTR; * $P < 0.05$ vs. corresponding CTR group; § $P < 0.05$, HIHG - PoG HFFD vs. CTR; # $P < 0.05$, HIHG + PoG HFFD vs. CTR.....169
- 5.5 **Markers of hepatic insulin signaling in CTR and HFFD groups.** Phosphorylation of Akt on Ser473 (A) and GSK3 β on Ser9 (B) relative to levels observed in basal CTR animals. Data are means \pm SE; $n = 5-6$ per group. † $P <$

	0.05 vs. basal CTR; § <i>P</i> < 0.05, HIHG - PoG HFFD vs. CTR; # <i>P</i> < 0.05, HIHG + PoG HFFD vs. CTR.....	170
5.6	Markers of hepatic glycogen metabolism in CTR and HFFD groups. Phosphorylation of glycogen synthase (GS) on Ser641 (A) relative to levels observed in basal CTR animals. Activity ratios of GS (B), glycogen phosphorylase (GP) (C), and GS/GP (D). Calculated increment in liver glycogen from basal (E). Glycogen synthesized through the direct pathway (F). Data are means ± SE; <i>n</i> = 5-6 per group. † <i>P</i> < 0.05 vs. basal CTR; * <i>P</i> < 0.05 vs. corresponding CTR group; § <i>P</i> < 0.05, HIHG - PoG HFFD vs. CTR; # <i>P</i> < 0.05, HIHG + PoG HFFD vs. CTR.....	171
6.1	Mean daily energy intake. Mean daily energy intake was recorded in dogs fed control diet (CTR, <i>n</i> = 5), a high-fat diet (HFA, <i>n</i> = 5), or a high-fructose diet (HFR, <i>n</i> = 5) for 4 weeks. Dogs fed the HFA or HFR diet were provided isoenergetic quantities of their respective diets over the course of 4 weeks, but both were hypercalorically-fed relative to CTR dogs.....	191
6.2	Plasma hormone concentrations during hyperinsulinemic hyperglycemic clamps in CTR, HFA, and HFR groups. Arterial plasma insulin (A) and glucagon (C), and hepatic sinusoidal insulin (B) and glucagon (D) during basal (-20 to 0 min) and experimental periods (0 to 180 min) of HIHG clamps conducted in 18-h-fasted dogs after 4 weeks of feeding a CTR (HIHG+PoG, <i>n</i> = 5; □), HFA (HIHG+PoG, <i>n</i> = 5; ▲), or HFR (HIHG+PoG HFR, <i>n</i> = 5; ●) diet. Data are means ± SE. † <i>P</i> < 0.05 vs. basal period.....	192
6.3	Arterial blood glucose, hepatic glucose load, and hepatic glucose uptake during hyperinsulinemic hyperglycemic clamps in CTR, HFA, and HFR groups. Arterial blood glucose (A), hepatic glucose load (B), and hepatic glucose uptake in the portal saline (C) and portal glucose (D) groups during the basal (-20 to 0 min) and experimental periods (0 to 180 min) of HIHG clamps conducted in 18-h-fasted dogs after 4 weeks of feeding a CTR (HIHG+PoG, <i>n</i> = 5; □), HFA (HIHG+PoG, <i>n</i> = 5; ▲), or HFR (HIHG+PoG HFR, <i>n</i> = 5; ●) diet. Data are means ± SE. † <i>P</i> < 0.05 vs. basal period; * <i>P</i> < 0.05 vs. CTR; # <i>P</i> < 0.05, HFR vs. HFA.....	193
6.4	Hepatic glucokinase (GK) and glucokinase regulatory protein (GKRP) in CTR, HFA, and HFR groups. Levels of GK mRNA (A) and protein (B), GK activity (C), and levels of GKRP protein (D). A, B, and D are expressed relative to levels observed in CTR animals. Data are means ± SE; <i>n</i> = 5 per group. * <i>P</i> < 0.05 vs. CTR; # <i>P</i> < 0.05, HFR vs. HFA.....	194
6.5	Markers of hepatic insulin signaling in CTR, HFA, and HFR groups. Phosphorylation of Akt on Ser473 (A) and GSK3β on Ser9 (B) relative to levels observed in CTR animals. Data are means ± SE; <i>n</i> = 5 per group. * <i>P</i> < 0.05 vs. CTR.....	195

6.6	Markers of hepatic glycogen metabolism in CTR, HFA, and HFR groups. Activity ratios of glycogen synthase (GS) (A), glycogen phosphorylase (GP) (B), GS/GP (C), and total GS activity (D). Terminal liver glycogen levels (E), and glycogen synthesized through the direct pathway (F). Data are means \pm SE; $n = 5$ per group. * $P < 0.05$ vs. CTR; # $P < 0.05$, HFR vs. HFA.....	196
7.1	Schematic of altered hepatic glucose flux by high-fat, high-fructose diet feeding in the presence of hyperglycemia and hyperinsulinemia.....	210
7.2	Summary schematic of the metabolic staging of type 2 diabetes in the context of western diet-induced insulin resistance.....	211

CHAPTER I

INTRODUCTION

In 2008, the World Health Organization (WHO) estimated that 1.5 billion adults over the age of 20 were overweight (body mass index [BMI] of 25.0 - 29.9 kg/m²), and over 500 million men and women were obese (BMI \geq 30.0 kg/m²). In the U.S. alone, the prevalence of obesity exceeds 30% in men and women across most age groups [1]. Strikingly, nearly 43 million children under the age of five were classified as overweight, as defined by a BMI greater than or equal to the 85th percentile but less than the 95th percentile (for children of the same age and sex) [2, 3]. Collectively, overweight and obesity are the most prevalent nutritionally-linked problems in the developed world [4]. Furthermore, type 2 diabetes is one of the most common health consequences associated with overweight and obesity, and is the seventh leading cause of death within the U.S. [5]. Current estimates from the Centers for Disease Control and Prevention indicate that 8.3% of the U.S. population, or 25.8 million individuals, have diabetes [5]; of the diagnosed cases, 90% to 95% are type 2 diabetes. In 2010, there were 1.9 million newly diagnosed cases of diabetes within the U.S., indicating that the incidence of the disease is continuing to rise concomitant with the increasing prevalence of obesity [5].

Although interaction among environmental exposures and genetic susceptibility ultimately determines the phenotypic characteristics of an individual, population gene pools shift very slowly over time and thus, are not likely to explain the rapid growth rates in obesity and diabetes in recent decades. In contrast, changes in lifestyle characterized

by excess energy consumption and decreased energy expenditure (physical activity) might be causally linked to the increased prevalence of obesity and type 2 diabetes [4]. Thus, scientists have directed substantial effort towards understanding the influence of environmental factors, such as the type of diet that one consumes, on the obesity and diabetes epidemic. Given that high-fat and high-sugar-containing, energy dense and nutrient deficient foods have become increasingly available and preferentially consumed in Westernized cultures [6-12], considerable emphasis has been placed on their respective contributions to the development of obesity, insulin resistance, and type 2 diabetes. Indeed, excessive consumption of dietary fat and fructose has been associated with adipose tissue accrual, ectopic lipid deposition, whole-body insulin resistance, and perturbations in the regulation of glucose metabolism in laboratory animals and in humans. Thus, studies aimed at investigating the link(s) between diet and metabolic diseases are warranted.

Previous studies have indicated that the liver is particularly vulnerable to nutritional insults induced by consumption of a high-fat or high-fructose diet [13-23]. In fact, several have suggested that hepatic insulin resistance, manifested as a diminished ability of insulin to suppress hepatic glucose production (HGP), is the first metabolic consequence to emerge upon initiation of high-fat or high-fructose feeding in laboratory animals [16-18, 23]. This is problematic because the liver serves as one of the principal regulators of whole-body glucose homeostasis, given its dynamic ability to switch from glucose production to glucose consumption during a fasting to fed transition. Thus, inappropriate suppression of HGP, or inadequate activation of hepatic glucose uptake (HGU) in response to a meal may contribute to the development of postprandial

hyperglycemia, and increase the load of glucose that must be disposed of by peripheral tissues. Specifically, individuals with diabetes display a marked impairment not only in the ability of hyperinsulinemia and hyperglycemia to suppress HGP, but also in the ability of those postprandial stimuli to activate splanchnic (liver and gut tissues) glucose uptake and glycogen synthesis. As a result, diabetic individuals experience frequent bouts of postprandial hyperglycemia, one of the sequelae of the disease that contributes to the elevation of their hemoglobin A1c and many of the complications associated with diabetes [24, 25].

While the effects of high dietary fat and fructose on HGP have been extensively studied, their chronic effects on HGU are poorly understood. This is due to both the complexity of its regulatory signals, and because it cannot be measured directly in humans or small animals [26]. On the other hand, HGU can be measured directly in the dog, given the accessibility of both the hepatic and portal veins. This allows for repeated direct measurements of HGU in the course of experimental perturbations. In addition, the response to glucose ingestion is very similar in dogs and humans [27]. Thus, the dog model is uniquely suited for the investigation of the adverse effects of high dietary fat and fructose consumption on HGU and glycogen synthesis *in vivo*.

The goal of this dissertation was to elucidate the metabolic and hepatocellular consequences associated with chronic consumption of a high-fat and/or high-fructose diet, focusing on perturbations in the regulation of HGU and disposition by hyperglycemia, hyperinsulinemia, and portal vein glucose delivery – the three primary determinants of hepatic glucose uptake *in vivo* [26]. My hope is that the studies described herein expose in part, the metabolic and molecular underpinnings of impaired hepatic

glucose flux associated with diet-induced obesity and insulin resistance, thereby shedding light on the pathogenesis of type 2 diabetes.

Dietary Fat

Dietary Fat and Obesity in Humans

As alluded to earlier, many have attributed the global surge in obesity and diabetes to a change in dietary consumption patterns favoring energy dense foods that are high in fat and sugar. These types of foods have been categorized as typical constituents of a Western diet. Thus, a Western dietary pattern is characterized by excess consumption of processed and red meat, high-fat dairy products, refined grains, french fries, and high-sugar and fructose-containing desserts and sweets [28, 29]. Several mechanisms have been proposed to explain the link between high dietary fat consumption and adiposity accretion. For example, dietary fat imparts flavor and palatability to foods, which might lead to a preferential increase in the consumption of high-fat foods by virtue of their hedonic effects [30, 31]. In addition, the thermic effect of fat, or the increment in energy expended as heat after a meal, is lower than that of carbohydrate and protein, enabling more efficient metabolism and storage of fat calories [31, 32]. Another potential mechanism that has received considerable attention is the fact that fat is the most energy dense of all macronutrients, providing 9 kcal/g (as opposed to 4 kcal/g for protein and carbohydrate). Based on the First Law of Thermodynamics and the principles governing energy balance, an increase in dietary fat intake in the absence of an offsetting increase in energy expenditure should promote body weight gain and an increase in adiposity over

time. As such, dietary fat might play an exaggerated role in contributing to the chronic positive energy balance required to produce obesity simply because of its caloric density [33]. Indeed, an increase in the food energy supply was reported by Swinburn and colleagues [34] to be more than sufficient to account for weight gain in the U.S. from 1971 – 2002. Likewise, energy density was found to be an independent predictor of augmented fasting insulin concentrations, obesity, and the metabolic syndrome among U.S. adults, suggesting that excess dietary fat consumption might contribute to the development of these metabolic abnormalities [35]. There also appears to be something unique about the consumption of high-fat and/or high-sugar-containing foods that perturbs the normal regulation of energy intake. For example, Bray and colleagues [36] analyzed food records from free-living adults over two, 7-day periods and found that the number of calories consumed per day was significantly and positively correlated with dietary fat consumption. Further clinical evidence supporting the notion that energy dense foods promote excess energy intake was provided by the studies of Blundell et al. [37] and Green et al. [38] in which subjects were given lunches differing in energy, sucrose, and fat content, but only those consuming lunches containing the high-fat, high-sucrose and/or energy dense combinations were likely to overeat at their next meal [37, 38]. These data are in agreement with other human studies which demonstrated an impaired ability to reduce energy intake at subsequent meals to compensate for food eaten earlier when the preceding food choices were high in fat or high in fat and sugar [38-42]. Altogether, these data suggest that one of the means through which a high-fat diet may promote the development of obesity is by perturbing the normal homeostatic mechanisms that govern energy intake. In such a case, decreasing one's consumption of foods that

drive energy overconsumption might be an effective approach in preventing or reversing obesity.

Nevertheless, the role of high dietary fat in contributing to the worldwide obesity epidemic is a controversial topic [10, 30]. One reason for this is because a reduction in the percentage of energy consumed from fat occurred during the 1990s despite explosive growth in the incidence of obesity [43-46]. However, it was estimated that the decrease in energy consumption from fat was only 3-5%, which would not necessarily be expected to result in a coordinate decline in body weight [10, 11]. In addition, it was postulated that the absolute amount of dietary fat remained elevated during this time period, whereas the percentage of energy intake from fat decreased as a result of an increase in energy intake from dietary carbohydrates [47, 48]. Despite the controversy, several epidemiological studies have supported the assertion that a positive relationship exists between total dietary fat intake and obesity prevalence. One of the most cited epidemiologic reports was provided by Bray and Popkin [10, 49], in which they performed a least-squares regression analysis to assess the relationship between an increase in the proportion of dietary energy intake from fat and the prevalence of overweight among adult participants from twenty different countries. A large significant positive association was found between the percentage of energy from dietary fat intake and the proportion of individuals in the population who were overweight [10, 49]. In addition, by use of time-trend analysis to examine obese individuals and their preceding diet history, Sonne-Holm and Sorensen [50] demonstrated a significant positive association between dietary fat consumption and subsequent development of obesity among nearly 400,000 Danish military recruits. Furthermore, data acquired from research on the Western-diet

influenced nutrition transition in countries such as China, South Africa, and Brazil have also demonstrated a positive relationship between increases in dietary fat intake and increases in the incidence of obesity [10, 51, 52]. To ascertain whether an increase in energy intake from fat as opposed to other non-fat sources (e.g. protein and carbohydrate) had an independent effect on adiposity in the China Health and Nutrition Survey [53], Popkin and colleagues [54] examined the effect of fat per se after controlling for the effects of total energy intake, and changes in energy intake from non-fat sources (e.g. protein and carbohydrate). The modified regression analysis displayed an independent effect of dietary fat intake on body weight [10, 49, 54]. Collectively, these studies are in agreement with the concept that dietary fat per se might play a role in the obesity epidemic worldwide.

Although useful for generating hypotheses, epidemiologic studies are often prone to confounding factors and are not indicative of a causal relationship. Thus, many randomized controlled dietary trials have been conducted to circumvent some of the weaknesses inherent in non-experimental studies, and to clarify the role of total dietary fat in obesity. Bray and Popkin [10] conducted a meta-analysis of 28 short-term, controlled clinical trials that studied the effects of reductions in dietary fat on weight loss. When fitted into a regression model, with the main explanatory variable as the change in percentage of energy from fat, their analysis concluded that a 10% reduction in the percentage of energy from fat would result in a marginally significant decline in body weight of 16 g/d; however, a large degree of heterogeneity existed among the studies [10, 49].

One of the criticisms of short-term dietary trials is that they are not thought to be predictive of long-term weight control, given that the weight loss experienced during the first 6 to 12 months of intervention is usually regained. Indeed, based on the analysis of Bray and Popkin [10], one would expect a body weight reduction of 6 kg over one year if a 10% reduction in the percentage of energy from fat was sustained, but that did not occur in studies that have lasted for one year or greater [31, 55-60]. In fact, the long-term randomized trials of fat reduction showed little if any impact of total dietary fat on body weight, given that fat consumption within the range of 18% to 40% of energy had no significant effect on body fatness [30, 31]. Thus, considerable controversy continues to exist regarding the role of total dietary fat per se in the obesity epidemic.

Dietary Fat, Insulin Resistance, and Type 2 Diabetes in Humans

In addition to being a major predictor for the progression to type 2 diabetes [61], insulin resistance is a common pathogenic link underlying many of the metabolic abnormalities clustered under the term, “metabolic syndrome” [62, 63]. Thus, several studies have been conducted to investigate the complex relationship between overnutrition/obesity and insulin resistance/diabetes. The Insulin Resistance and Atherosclerosis Study (IRAS) found a significant inverse association between the percentage of energy from total fat and the degree of whole-body insulin sensitivity, as measured by the frequently sampled intravenous glucose tolerance test (FSIGTT); however, this relationship was partly attributable to the effect of dietary fat on obesity [64]. Likewise, Van Dam and colleagues [29] assessed the impact of dietary fat and processed meat, typical constituents of a Western diet, on risk of type 2 diabetes in a

large prospective, 12-year follow-up of U.S. men in the Health Professionals Follow-up Study. Their results indicated that total dietary fat, saturated fat, and frequent consumption of processed meats were associated with an increased risk of type 2 diabetes, albeit not independent of BMI [29].

On the other hand, several studies have reported a direct relationship between total fat intake and risk of type 2 diabetes that is independent of obesity and/or BMI. For example, in a large prospective study of U.S. men [28], their habitual dietary consumption patterns were divided into two groups: a prudent pattern, characterized by increased intakes of fruits, vegetables, fish, poultry, and whole grains, and a Western pattern, characterized by processed foods rich in total fat, saturated fat, and sugar, as outlined previously under *Dietary Fat and Obesity in Humans*. Their analysis demonstrated a slight reduction in the risk for type 2 diabetes in men that consumed the prudent diet, whereas men that consumed the Western pattern diet displayed a substantially higher risk for type 2 diabetes [28]. This risk was magnified when the Western pattern diet was coupled with low physical activity and/or obesity [28]. Furthermore, the association between Western diet consumption and type 2 diabetes risk was independent of BMI [28], suggesting that foods consumed as part of a Western diet may directly promote the development of insulin resistance and type 2 diabetes, regardless of overweight or obesity. This finding is at odds with the author's previous study [29], in which the association between total dietary fat intake and type 2 diabetes was not independent of BMI. The disparity in their findings suggests that components of a Western diet other than dietary fat may be independently associated with the development of type 2 diabetes, such as refined grains and/or high-sugar and fructose-

containing desserts and sweets. In addition, these data indicate that the association between a Western pattern diet and type 2 diabetes is stronger than the association between any one dietary factor and type 2 diabetes.

Data suggestive of a link between high-fat foods and glucose abnormalities was provided by Gulliford and colleagues [65], in which they found that use of solid fat for cooking, consumption of whole milk, or use of butter and/or margarine spreads was associated with higher hemoglobin A1c in healthy adults, even after adjustment for BMI, age, waist-hip ratio, and activity. Further epidemiologic evidence supporting the relationship between high dietary fat and type 2 diabetes risk independent of obesity was provided by the San Luis Valley Diabetes Study [66], in which consumption of a very high-fat, low-carbohydrate diet, as assessed by 24-hour diet recalls, was associated with a 3.4-fold increase in the risk of type 2 diabetes after adjustment for obesity. In addition, the percentage of energy consumed from fat was a significant predictor of conversion from impaired glucose tolerance to type 2 diabetes, even after adjusting for energy intake, obesity, and markers of glucose metabolism [67]. Collectively, these studies and others demonstrate that an association exists between total dietary fat intake and risk of type 2 diabetes, although that relationship is sometimes dependent upon the effects dietary changes have on BMI or obesity.

Several controlled clinical trials have been conducted to assess the impact of dietary fat on insulin sensitivity and glucose metabolism. Contrary to the equivocal findings regarding low-fat diets and weight loss, data from studies addressing the ability of a reduction in dietary fat to modulate insulin sensitivity independent of obesity are more conclusive. For example, in studies of healthy individuals, short-term consumption

of a low-fat diet, in which 14% to 25% of the energy was derived from fat, resulted in significant improvements in insulin sensitivity as measured by the FSIVGTT or hyperinsulinemic euglycemic clamp [68-73]. Moreover, the improvements in insulin sensitivity were independent of changes in body weight [68-73]. Conversely, short-term consumption of a high-fat diet elicits adverse metabolic consequences. In young healthy men, 5 days of hypercaloric (50% extra kcal/d) high-fat feeding (60% of kcal from fat) resulted in an increase in fasting plasma glucose levels secondary to an elevation in hepatic glucose production [74], whereas 11 days of high-fat feeding (83% of kcal from fat) attenuated the suppressive action of insulin on endogenous glucose production and diminished its stimulatory effects on glucose oxidation [75].

Swinburn and colleagues assessed the long-term effects of a reduced-fat ad-libitum diet in glucose intolerant individuals [76]. After five years, participants who were compliant with low-fat dietary recommendations maintained a significant reduction in fasting and 2-hour plasma glucose concentrations despite having the same body weight as they had five years prior [76]. Plasma triglyceride concentrations in the low-fat diet group were not reported. In support of the effectiveness of dietary interventions in disease prevention, data from the multicenter clinical research study entitled, "Diabetes Prevention Program (DPP)," demonstrated a 58% reduction in the development of type 2 diabetes over a 3-year period in overweight individuals with impaired glucose tolerance that were assigned to an intensive lifestyle intervention group, which lost a modest amount of weight through dietary changes (specifically, a 6% decrease in the percentage of energy from fat coupled with a reduction in total energy intake) and increased physical activity (150 min of exercise per week) [77]. After an average 10 year follow-up period,

study participants that had been enrolled in the intensive lifestyle modification program maintained an average 34% reduction in the rate of type 2 diabetes development compared to the placebo group, as reported in the Diabetes Prevention Program Outcomes Study [78]. The Finnish Diabetes Prevention Study also reported a significant reduction in the development of type 2 diabetes in participants that had reduced their total dietary fat intake and increased their physical activity levels [79]. However, neither study was designed to delineate between the relative contributions of changes in diet, exercise, and weight loss to diabetes risk reduction. In addition, neither study classified the quality of the carbohydrate consumed by the participants. Altogether, these data suggest that changes in the constituents of the diet that one consumes, particularly with regard to dietary fat, can have a remarkable impact on glucose metabolism and risk of diabetes.

Dietary Fat Quality and Insulin Sensitivity in Humans

Some of the discordance in the findings regarding the role of total dietary fat in obesity, or the direct effects of dietary fat in the risk for type 2 diabetes might be explained by the fact that all dietary fats are not created equal. Thus, assessing the impact of total dietary fat in the absence of consideration of the quality (whether saturated, monounsaturated, or polyunsaturated) of dietary fat consumed might be misleading. In general, most epidemiologic studies have found a positive association between saturated fat intake and hyperinsulinemia, glucose intolerance, and type 2 diabetes that is independent of body fat [80-85]. In addition, Stein and et al. [86] and Dobbins et al. [87] demonstrated that saturated fatty acids have a greater insulinotropic potency than unsaturated fatty acids, suggesting that chronic consumption of Western diet rich with

saturated fat might contribute to hyperinsulinemia, which in and of itself can impair whole-body insulin action and glucose uptake, as demonstrated previously in dogs [88, 89]. Conversely, diets rich in monounsaturated and polyunsaturated fatty acids have generally been shown to exert beneficial effects on insulin sensitivity [80, 90-92]. Vessby and colleagues [93] best exemplified this in the KANWU (Kuopio, Aarhus, Naples, Wollongong, and Uppsala) study, a large multicenter, controlled intervention trial. Healthy participants were randomly assigned to consume isocaloric quantities of either a saturated fat diet (17% of energy) or a monounsaturated fat diet (23% of energy), while the total amount of fat (37% of energy) and other dietary constituents remained constant. After 3 months, subjects that consumed the saturated fat diet displayed a significant reduction (10%) in insulin sensitivity as assessed by the FSIVGTT, whereas subjects that consumed the monounsaturated diet displayed no change in insulin sensitivity despite consuming the same percentage of total energy from fat. The difference between groups was most striking in subjects that consumed less than 37% of energy from fat, whereas the improvement in insulin sensitivity brought about by the substitution of saturated fat with monounsaturated fat was abolished at dietary fat intakes greater than 37% of total energy [80, 93]. Collectively, these data provide strong evidence that both fat quality and quantity play a role in modulating insulin sensitivity in humans and thus, might be causally linked to the diabetes epidemic in association with consumption of a Western diet.

Dietary Fat, Adiposity, and Insulin Action in Experimental Animal Models

Given that high-fat-fed laboratory animals are useful models for investigating the putative effects of a Western diet in humans, numerous studies have been conducted in the rodent and dog in attempts to elucidate the metabolic pathogenesis of obesity and insulin resistance induced by a nutritional insult in the form of high dietary fat. It is evident from most studies that high-fat feeding impairs insulin action in experimental animal models; however, the duration of high-fat feeding required to elicit insulin resistance, and the temporal manifestation of insulin resistance in the liver, skeletal muscle, brain, and/or adipose tissue are issues that remain incompletely understood. Some studies have suggested that the initial defect in insulin action in response to a high-fat diet occurs in the liver in a relatively short period of time. For example, Kraegen et al. [17] performed hyperinsulinemic euglycemic clamp experiments in male Wistar rats that were fed isocaloric high-fat (59% of energy from fat) or high-starch (10% of energy from fat) diets for three days or three weeks, in order to assess the progressive changes in insulin sensitivity following a nutritional challenge. Three days of high-fat feeding was sufficient to induce whole-body insulin resistance, as evidenced by a significant decrease (46%) in the glucose infusion rate required to maintain euglycemia during the clamp; however, this was attributable to a significant decline in the ability of insulin to suppress hepatic glucose production, with no difference between groups in insulin-stimulated whole-body glucose uptake (R_d). These data were confirmed by additional studies in which [^3H]-2-deoxyglucose was administered during the clamp, and tissue-specific glucose metabolic index (R_g) was measured. Indeed, there was no difference between groups in R_g in any of the hindlimb muscles tested after only three days of high-fat

feeding. On the other hand, three weeks of high-fat feeding resulted in a further decline in hepatic insulin sensitivity and a significant decrease (35%) in insulin-stimulated whole-body glucose disposal (R_d), indicative of the emergence of impaired insulin-mediated muscle glucose uptake. Similar studies conducted by the same group of investigators demonstrated that the suppressive effects of a high-fat diet on insulin-mediated peripheral glucose uptake after three weeks of feeding occurred predominantly in oxidative skeletal muscles [94, 95]. Taken together, these data suggest that hepatic insulin resistance develops prior to skeletal muscle insulin resistance in the context of high-fat feeding [17, 94, 95].

Although marked impairments in whole-body insulin sensitivity and glucose metabolism induced by short-term (three days or three weeks) high-fat feeding occurred in the absence of an increase in body weight or energy consumption relative to chow-fed control animals, high-fat-fed rats accumulated more white adipose tissue in association with a significant reduction in energy expenditure and brown adipose tissue [94, 95]. Other studies have also demonstrated that pair feeding of high-fat and low-fat diets to rats results in greater adipose tissue accretion in high-fat-fed animals despite similar body weights and energy consumption between groups [96, 97]. Thus, as growing rodents are fed a high-fat diet, the excess energy is preferentially deposited as fat, whereas feeding of a standard rodent chow supports the growth of the rodent by means of increasing lean body mass. Thus, the proportion of dietary fat consumed can affect fat deposition, insulin action, and whole-body glucose metabolism independent of total energy intake or changes in body weight.

Samuel et al. [23] also demonstrated liver-specific effects of short-term high-fat feeding in male Sprague-Dawley rats, which were fed either a high-fat diet (59% of energy from fat) or regular rodent chow (10% of energy from fat) for three days. In agreement with the findings of Kraegen and colleagues [17], insulin suppression of endogenous glucose production during a hyperinsulinemic-euglycemic clamp was significantly reduced in high-fat fed rats compared to chow-fed controls (74% vs. 8% suppression, respectively), whereas insulin-stimulated whole-body glucose utilization was similar between groups [23]. In addition, three days of high-fat feeding was associated with a significant reduction in hepatic glycogen synthase activity and in the percentage of glycogen synthesized through the direct pathway [23]. These data are indicative of a selective impairment in insulin regulation of hepatic glucose production and storage after only three days of high-fat feeding in rodents, and support the concept that hepatic insulin resistance precedes skeletal muscle insulin resistance.

The temporal development of hepatic insulin resistance in relation to the pathogenesis of diet-induced obesity and whole-body insulin resistance was investigated in a canine model over a 12 week feeding period, in which the animal's normal daily diet was supplemented with 2g/kg of cooked bacon grease [16]. This constituted a total increase in dietary fat energy of approximately 8% (from 36% to 44% of total energy from fat), and was termed a "moderate-fat diet" [16]. The authors reported that this moderate increase in dietary fat did not result in a significant change in total daily energy intake [16]. After twelve weeks of moderate-fat feeding, there was a two-fold increase in total trunk fat and fasting hyperinsulinemia, despite little change in total body weight. Furthermore, moderate-fat feeding was associated with a progressive decline in hepatic

insulin sensitivity, as indicated by a deterioration in the ability of insulin to suppress hepatic glucose production during a hyperinsulinemic euglycemic clamp after 6 and 12 weeks of fat feeding [16]. Despite clear evidence of hepatic insulin resistance at week 12, rates of insulin-stimulated whole-body glucose uptake were not significantly reduced after 6 or 12 weeks of a moderate-fat diet, even after adjustment for elevations in the steady-state plasma insulin levels over time [16]. Altogether, these data support the notion that hepatic insulin resistance precedes muscle insulin resistance in the context of high-fat diet-induced increases in adiposity [16].

In contrast, other studies have suggested that peripheral insulin resistance precedes hepatic insulin resistance with high-fat diet-induced obesity. For example, Rocchini et al [98] observed a significant reduction in insulin-mediated whole body glucose uptake at 1 week in dogs placed on a high-fat diet (regular diet supplemented with 0.9 kg of cooked beef fat), whereas the ability of insulin to suppress hepatic glucose production was retained for the duration of the study (6 weeks). Similarly, Kim et al [99] reported a significant decrease in insulin-stimulated whole body glucose uptake, with only a tendency towards reduced suppression of hepatic glucose production by insulin in dogs fed a hypercaloric, high-fat diet (standard diet supplemented with 6 g/kg of cooked bacon grease, corresponding to 54% of total energy from fat) for 6 weeks. The impairment in insulin-mediated peripheral glucose uptake was attributed to nocturnal elevations in free fatty acid levels in dogs maintained on the high-fat diet [100]. Ironically, that study was conducted by the same laboratory which previously reported no change in insulin-stimulated peripheral glucose uptake after 6 weeks of moderate-fat feeding, whereas the ability of insulin to suppress endogenous glucose production was

markedly impaired by this time [16]. The reason for the disparities in their findings is not clear. Nevertheless, the literature describing the metabolic consequences of high-fat feeding in laboratory animals provides evidence that high dietary fat is associated with insulin resistance and aberrant glucose metabolism, depending on the amount and duration of high-fat feeding.

One potential reason for the heterogeneity in the metabolic responses to high-fat feeding in animal models is that the composition of dietary fat differs among studies. For example, in the studies by Samuel et al. [23], Storlein et al. [94], and Kraegen et al. [17, 95], the lipid component of the high-fat diet was safflower oil, which consists predominantly (over 80%) of polyunsaturated omega-6 fatty acid species in the form of linoleic acid. On the other hand, bacon grease was utilized in the studies of Rocchini et al. [98] and Kim et al. [16, 100], which consists predominantly of saturated and monounsaturated fatty acid species. Indeed, Storlein and colleagues [101] demonstrated that the fatty acid composition and the lipid environment in which they are presented in high-fat diets is a determinant of insulin sensitivity in rats. However, as demonstrated in the KANWU study [93], it is possible that a threshold of total dietary fat consumption exists above which differences in the quality of dietary fat might have little impact on the metabolic phenotype. Thus, the debate continues regarding the temporal manifestation of hepatic vs. peripheral insulin resistance in the pathogenesis of diet-induced obesity and whole-body insulin resistance. Part of the goal of Specific Aim I is to shed light on the temporal manifestation of glucose intolerance and whole-body insulin resistance in response to excess consumption of a diet high in fat and fructose.

Dietary Fructose

Dietary Fructose Consumption in the U.S.

Changes in food technology over the last several decades resulted in a shift in the sweetener composition of the food supply from predominantly cane sugar in the form of sucrose, to predominantly corn sugar in the form of high-fructose corn syrup [102]. Initially, dietary fructose was investigated as a beneficial sweetener for individuals with type 2 diabetes given its low glycemic index, a way of classifying carbohydrate-containing foods based on the incremental area under the curve (AUC) for the glucose response they elicit; however, it became evident that chronic consumption of a high-fructose diet leads to the development of many of the features of the metabolic syndrome [12].

Between 1978 and 2004, there was a 61% increase in the per capita availability of high-fructose corn syrup [103]. This was associated with a 32% increase in average individual intakes of dietary fructose concomitant with a 41% increase in carbohydrate intake and an 18% increase in total energy intake, according to Nationwide Food Consumption Survey (1977-1978) and NHANES (1999-2004) data [103]. Much of the increase in sugar and carbohydrate intake within this time frame was attributed to a marked elevation in the consumption of high-fructose corn syrup-sweetened beverages [9, 104-106]. When expressed in a different way, the per capita consumption of high-fructose corn syrup increased from approximately 0.3 kg/person/year in 1970 to 33 kg/person/year in 2000 [9, 107]. Given that sucrose (50% glucose/50% fructose) and high-fructose corn syrup (either 42% fructose/58% glucose or 55% fructose/45%

glucose) have very similar compositions in terms of their molar ratios of glucose and fructose, the positive associations between high-fructose corn syrup consumption, obesity, and risk of type 2 diabetes is most likely due to the steady overconsumption of total sugar, of which fructose is the major contributor. Indeed, consumption of sugar-sweetened beverages has been associated with the development of insulin resistance [108], type 2 diabetes [109, 110], fatty liver [111, 112], and cardiovascular disease [46, 113], underscoring the clinical significance of a potential link between dietary sugar consumption and metabolic disease.

Metabolism of Dietary Fructose

Fructose is a monosaccharide with a chemical formula identical to that of glucose ($C_6H_{12}O_6$); however, the presence of a keto group on the second carbon of fructose makes it distinct from glucose, which contains an aldehyde group at carbon number one. The liver is largely responsible for the metabolism of dietary fructose given that the enzymes essential for its catabolism (fructokinase, aldolase B, and triokinase) are highly expressed in the liver, and that first pass hepatic extraction of fructose is greater than 50% [114]. Loss of fructose into the urine of individuals with an inherited deficiency of fructokinase (hereditary fructosuria) lends support to the fact that fructose is poorly metabolized in extrahepatic tissues [12]. Shiota et al. [115, 116] demonstrated that net hepatic fructose uptake (first pass and recirculated) accounted for ~80% of the fructose delivered into the portal vein.

The hepatic metabolism of fructose is distinct from that of glucose at several steps. Although both glucose and fructose enter the hepatocyte through the bidirectional

glucose transporter, GLUT2 [117, 118], fructose is rapidly phosphorylated by fructokinase, which has a low K_m for fructose [119, 120] and a high V_{max} [119, 121]. Glucose, on the other hand, is phosphorylated by glucokinase, which has a high K_m for glucose [122]. The product of the fructokinase reaction, fructose-1-phosphate, is a potent stimulator of hepatic glucokinase translocation from the nucleus to the cytosol [123], thereby facilitating the uptake and storage of glucose by the liver in an acute setting. The six-carbon fructose-1-phosphate metabolite is further catabolized into triose phosphates through the enzymatic action of aldolase B and triokinase [124], thereby bypassing one of the main rate-determining enzymes of glycolysis, phosphofructokinase-1 (PFK-1) [13]. Fructose is also unique in that its metabolism is not regulated by insulin or negative feedback (e.g. ATP or citrate), whereas the rate-limiting enzymes involved in the catabolism of glucose through the glycolytic pathway (glucokinase, PFK-1, and pyruvate kinase) are regulated by the energy status of the cell and by insulin [12].

Fructose ultimately has several fates within the liver, including oxidation to CO_2 , or conversion into glucose, glycogen, lactate, or lipid, but their relative contributions to fructose disposal differ [124]. For example, gluconeogenically-derived glucose and glycogen are the predominant fates of triose phosphates produced from the hepatic metabolism of fructose [125, 126]. In addition, catheterization studies performed in humans have consistently demonstrated that administration of ^{13}C -labeled fructose results in approximately 50% of the fructose load recirculating as ^{13}C -labeled glucose, suggesting that glucose synthesis is quantitatively the largest pathway of hepatic fructose disposal [127-130]. On the other hand, in vitro studies have suggested that the predominant fate of lactate produced by the catabolism of fructose is lipid via de novo

lipogenesis [131-133]. Inhibition of pyruvate dehydrogenase kinase and subsequent activation of pyruvate dehydrogenase is thought to facilitate de novo lipogenesis in response to high-fructose feeding [131-133], resulting in an unregulated supply of carbon (via acetyl-CoA and glycerol-3-phosphate) for the synthesis of fatty acids through de novo lipogenesis [12, 124]; however, the precise mechanism through which fructose decreases PDK activity is not clear. Furthermore, this pathway constitutes only a minor portion of fructose disposal [134-136].

Dietary Fructose and Obesity in Humans

In 2004, Bray and colleagues [9] used age-standardized, nationally representative measures of obesity from 1960 to 1999, and data on the availability of high-fructose corn syrup collected annually over the same time period, to demonstrate that the rising prevalence of obesity was temporally associated with an increase in the consumption of high-fructose corn syrup, predominantly in the form of calorically sweetened beverages. In support of this hypothesis, Ludwig and colleagues [137] conducted a longitudinal (19 months) study in adolescents in which they found that each additional serving of sugar-sweetened beverage consumption was associated with an increase in BMI and in the frequency of obesity after adjustment for anthropometric, demographic, dietary, and lifestyle variables. Furthermore, baseline consumption of sugar-sweetened drinks was independently associated with change in BMI [137], suggesting that high-fructose corn syrup might contribute to obesity in adolescents as well. In another study, consumption of high-fructose corn syrup-sweetened soda for 3 weeks resulted in significant increases in total energy intake and body weight in male and female participants when compared to

consumption of an equivalent quantity of artificially-sweetened (aspartame) diet soda [138]. Likewise, middle-aged men with type 1 or type 2 diabetes reported an increase in body weight upon the addition of 50-60 g fructose/day into their diets for 24 weeks [139]. Taken together, these studies raise the possibility that a link exists between high dietary fructose consumption and increased body weight.

On the other hand, a meta-analysis of intervention studies investigating the effects of fructose intake (less than 100 g fructose/day) on body weight found no significant relationship between the dose of fructose ingested and body weight [140]. In addition, the hypothesis proposed by Bray and colleagues [9] has been disputed by others given that a rise in other macronutrient intakes also occurred during the same time frame, which might have been linked to the increased prevalence of overweight and obesity [141]. Furthermore, there has been little evidence from studies conducted in humans demonstrating that high-fructose corn syrup acts in an exclusive manner to promote obesity [141]. Thus, much like the proposed association between total dietary fat and obesity, considerable controversy exists regarding the purported causal relationship between dietary fructose and obesity prevalence within the U.S.

Dietary Fructose, Insulin Resistance, and Type 2 Diabetes in Humans

In contrast to the tenuous link between increased consumption of dietary fructose and the obesity epidemic, numerous studies have provided clear evidence that excess consumption of dietary fructose is associated with the development of insulin resistance and an increased risk for type 2 diabetes. With regard to epidemiologic evidence, Gross et al. [105] compared the per capita nutrient consumption in the U.S. between 1909 and

1997 with data from the Centers for Disease Control and Prevention regarding the prevalence of type 2 diabetes. Their findings indicated that corn syrup (which largely consists of fructose) was positively associated with the prevalence of type 2 diabetes, even after adjustment for total energy intake in a multivariate nutrient-density model [105]. Conversely, fiber intake was negatively associated with the prevalence of type 2 diabetes, suggesting that changes in the quality and composition of carbohydrate consumed during the 20th century paralleled the upward trend in the prevalence of type 2 diabetes [105]. In addition, analysis of nearly 3000 cases over 20 years of data collection from the Health Professionals Follow-Up Study indicated that consumption of sugar-sweetened beverages was associated with a significant elevation in risk of type 2 diabetes, whereas a 17% reduction in risk was achieved by replacement of one serving of sugar-sweetened beverage with 1 cup of coffee [142]. In a separate study, combined intakes of fructose and glucose were associated with a significant increase in risk of type 2 diabetes during a 12 year follow-up of over 4000 middle-aged men and women that were free of diabetes at baseline [109]. Lastly, Malik and colleagues [143] conducted a meta-analysis to ascertain whether consumption of sugar-sweetened beverages was associated with risk of type 2 diabetes and the metabolic syndrome. Their analysis provided abundant evidence to support the contention that the caloric and fructose content of sugar-sweetened beverages are associated with obesity and risk of type 2 diabetes, gout, and heart disease [143].

With regard to experimental studies, Hallfrisch et al. [144] demonstrated that consumption of a diet containing 15% of energy from fructose for 5 weeks resulted in augmented fasting plasma glucose concentrations and exaggerated glycemic and

insulinemic responses to a sucrose load in healthy men, suggesting that a moderate increase in dietary fructose impairs glucose tolerance and insulin sensitivity. In addition, six days of eating a high-fructose diet, in which 25% of total energy was derived from fructose, resulted in an increase in fasting plasma glucose and triglyceride levels, and a significant impairment in the ability of insulin to suppress adipose tissue lipolysis and hepatic glucose production during a hyperinsulinemic euglycemic clamp in normal men [145]. Interestingly, supplementation of the high-fructose diet with fish oil normalized the perturbations in lipid metabolism, but not insulin sensitivity [145]. These data imply that high dietary fructose elicits dyslipidemia and insulin resistance through separate mechanisms, and that the deterioration of insulin sensitivity induced by high-fructose feeding might not be associated with hypertriglyceridemia or augmented lipolysis in normal men.

Recently, Stanhope and colleagues [146] conducted a well-controlled intervention study in older, overweight or obese subjects in which they compared the effects of consuming fructose-sweetened versus glucose-sweetened beverages, providing 25% of their energy requirements, for ten weeks. Participants were instructed to ingest the sugar-sweetened beverages as three servings a day with meals, while continuing to consume their usual diet *ad libitum*. At the end of the ten week study, both groups had gained comparable amounts of body weight (~ 1.4 kg) and body fat (~ 0.8 kg); however, participants consuming the fructose-sweetened beverages deposited a significantly greater proportion of their fat in visceral adipose tissue depots, whereas subjects consuming glucose-sweetened beverages preferentially accrued fat in subcutaneous adipose tissue depots [146]. Differential effects in glucose metabolism and insulin

sensitivity were also evident following consumption of glucose-sweetened versus fructose-sweetened beverages, in which the latter was associated with increased fasting glucose and insulin concentrations, impaired glucose tolerance, and decreased whole-body glucose disposal and insulin sensitivity [146]. Furthermore, consumption of fructose-sweetened beverages promoted dyslipidemia in that twenty-four-hour postprandial plasma triglyceride levels were significantly increased in association with decreased lipoprotein lipase activity and an elevated rate of hepatic de novo lipogenesis [146]. Likewise, fasting plasma concentrations of low-density lipoprotein (LDL) cholesterol, apolipoprotein B, oxidized LDL, and small-dense LDL, and postprandial levels of remnant-like particle-triglyceride and -cholesterol were all significantly augmented after ten weeks of increased fructose consumption [146]. Despite similar body weight gain, these other changes did not occur in subjects consuming the glucose-sweetened beverages for ten weeks, demonstrating that the adverse effects of excess dietary fructose were not solely attributable to weight gain [146, 147]. In fact, postprandial triglyceride concentrations were increased within twenty-four hours after consumption of fructose-sweetened versus glucose-sweetened beverages (providing 30% of total kcal) in short-term studies in younger adults [148], suggesting that postprandial hypertriglyceridemia, perhaps mediated by an increase in hepatic de novo lipogenesis, is one of the earliest metabolic perturbations associated with excess fructose intake [149]. Taken together, these data provided experimental evidence to suggest that relatively short-term consumption of high dietary fructose elicits adverse metabolic and cardiovascular effects by promoting visceral adipose tissue accretion, aberrant lipid

metabolism, and decreased insulin sensitivity, thereby increasing the risk for type 2 diabetes and cardiovascular disease [146, 147].

Dietary Fructose, Insulin Action, and Dyslipidemia in Experimental Animal Models

Numerous studies have also demonstrated the capacity of dietary fructose (either free fructose or complexed with glucose as sucrose) to induce insulin resistance, hepatic lipid accumulation, and hypertriglyceridemia in experimental animal models. For example, Storlein and colleagues [150] compared the effects of feeding isocaloric quantities of a high-starch diet or high-sucrose (50% glucose, 50% fructose) diet (69% of total kcal as sucrose or cornstarch) on whole-body insulin action in adult male Wistar rats. After four weeks of feeding, the glucose infusion rate required to maintain euglycemia during a hyperinsulinemic euglycemic clamp was significantly lower in high-sucrose fed rats, indicative whole-body insulin resistance. The decrease in the clamp glucose infusion rate was the result of a significant impairment in the ability of insulin to suppress endogenous glucose production, whereas insulin-mediated whole-body glucose uptake was only slightly reduced, corresponding to a 10% reduction in tissue-specific glucose metabolic index (R_g) in skeletal muscle [150]. The perturbations in glucose metabolism in high-sucrose-fed rats occurred in the absence of an increase in body fat. These data suggest that four weeks of high-sucrose feeding produced a major impairment in insulin action at the liver that was independent of changes in body weight or adiposity [150]. In a follow-up study [151], the same group of investigators assessed the contribution of the fructose moiety of sucrose versus that of glucose in the development of insulin resistance after 4 weeks of feeding a high-fructose or high-glucose diet (35% of

total kcal as fructose or glucose combined with another 35% of kcal as cornstarch) to adult male Wistar rats. Four weeks of high-fructose versus high-glucose feeding was associated with a significant decrease in the ability of insulin to suppress hepatic glucose production coupled with an equivalent decline in insulin-mediated peripheral glucose disposal during a hyperinsulinemic-euglycemic clamp [151]. The authors concluded that fructose, not glucose, was the deleterious factor associated with impaired insulin action after high-sucrose feeding [151].

Pagliassotti and colleagues [19] also demonstrated that 8 weeks of high-sucrose feeding (68% of kcal from sucrose) in rats was sufficient to induce whole-body insulin resistance, as indicated by a significant reduction in the glucose infusion rate required to maintain euglycemia with increasing insulin concentrations, and impaired suppression of hepatic glucose production by hyperinsulinemia. These changes were associated with an increase in hepatic PEPCK activity [18, 152], increased G6Pase expression and activity [14, 153, 154], and lower GK activity [14]. Next, Pagliassotti et al [18] investigated whether the amount of sucrose consumed and the duration of dietary sucrose exposure influenced the temporal development of insulin resistance in a tissue-specific manner. Three groups of male Wistar rats were fed a low-sucrose diet (18% of total energy from sucrose), a high-sucrose diet, or a high-starch diet (68% of total kcal from sucrose or cornstarch, respectively) for 8, 16, or 30 weeks [18]. Sucrose-fed rats were pair-fed to their respective starch control rats. Despite no difference among diet groups in body weight gain or percentage of body fat, both the low-sucrose and high-sucrose diets induced whole-body insulin resistance; however, the time course of induction and tissue distribution of insulin resistance was influenced by the quantity of dietary sucrose

consumed [18]. For example, consumption of the high-sucrose diet resulted in hepatic and peripheral insulin resistance within 8 weeks, as demonstrated by a decline in the ability of insulin to suppress endogenous glucose production concomitant with decreased insulin-mediated whole-body glucose disposal [18]. On the other hand, consumption of the low-sucrose diet required at least 16 weeks to elicit hepatic insulin resistance, whereas there was no significant decline in insulin-mediated peripheral glucose disposal after 30 weeks of feeding [18]. In agreement with the findings of Thorburn and colleagues [151], Thresher et al. [155] also demonstrated that dietary fructose was the primary mediator of sucrose-induced impairments in insulin action and glucose intolerance *in vivo*.

A more detailed analysis of the temporal development of insulin resistance in the liver versus muscle after 1, 2, 5, or 8 weeks of high-sucrose versus high-starch (68% of total kcal as sucrose or cornstarch, respectively) feeding demonstrated that hepatic insulin resistance precedes muscle insulin resistance as determined by sequential hyperinsulinemic euglycemic testing [156]. In addition, the reduction in hepatic insulin sensitivity was accompanied by increases in liver triglyceride levels in sucrose-fed animals, but the rate of hepatic triglyceride accumulation was dependent upon the quantity of dietary sucrose consumed [18]. Furthermore, rats fed a high-sucrose diet developed fasting hypertriglyceridemia and hyperinsulinemia, whereas those fed a low-sucrose diet did not [18]. Nevertheless, a decrease in hepatic insulin sensitivity was evident in both high- and low-sucrose-fed groups, suggesting that hyperinsulinemia and hypertriglyceridemia per se are not causally linked to hepatic insulin resistance induced by an increase in dietary sucrose consumption. On the other hand, the time course of the

changes in fasting plasma insulin and triglyceride levels in high-sucrose-fed rats was consistent with the time course of the development of peripheral insulin resistance in those animals, suggesting that perhaps hyperinsulinemia and/or hypertriglyceridemia are linked to impaired insulin action in skeletal muscle following consumption of high dietary sucrose, and by extension [151, 155], fructose. In support of this hypothesis, there was a significant inverse association between fasting plasma triglyceride concentrations and clamp rates of whole-body glucose disposal and insulin-stimulated muscle glycogen synthesis [156] in high-sucrose-fed rats. All together, the aforementioned studies provide evidence to suggest that the liver is particularly susceptible to the adverse effects of dietary fructose, whether consumed in moderate or high quantities, whereas peripheral tissues (primarily skeletal muscle) appear to be vulnerable to the adverse effects of dietary fructose only when consumed in high quantities.

Catalytic Quantities of Fructose and Hepatic Glucose Metabolism

In contrast to the studies which have defined the metabolic consequences of chronic high dietary fructose consumption, other studies have demonstrated that the acute administration of small quantities of fructose actually improves postprandial glycemic and insulinemic responses. For example, inclusion of 7.5 g of fructose with a standard 75 g oral glucose load substantially reduced the glycemic response during an oral glucose tolerance test in both normal and type 2 diabetic individuals [157, 158]. In addition, infusion of catalytic quantities of fructose with an intraportal or intraduodenal glucose load markedly enhanced net hepatic glucose uptake (NHGU) and hepatic glycogen synthesis (GSYN) in conscious dogs [115, 116, 159]. Augmented NHGU was attributed

to the ability of fructose-1-phosphate (the product of fructokinase) to stimulate the translocation of hepatic glucokinase from the nucleus to the cytosol, thereby facilitating NHGU [116, 160-162]. Indeed, low-dose fructose infusion partially restored hepatic glucose effectiveness in individuals with type 2 diabetes, as evidenced by a 44% decline in endogenous glucose production during hyperglycemia and euinsulinemia, whereas no further improvement in glucose effectiveness was evident in non-diabetic subjects in response to fructose infusion [163]. Furthermore, Petersen et al. [164] demonstrated that low-dose fructose infusion increased carbon flux through glycogen synthase and stimulated hepatic glycogen synthesis [164]. Altogether, the beneficial effects of catalytic quantities of fructose on hepatic glucose flux appear to be mediated by the activation of hepatic glucokinase and glycogen synthase [165].

Wei and colleagues [154] proposed that the differential effects of low-dose fructose versus chronic high-dose fructose exposure might be mediated by its effects on glucose-6-phosphatase expression. For example, the gene expression of the catalytic subunit of glucose-6-phosphatase was reduced during a hyperinsulinemic hyperglycemic clamp combined with low-dose fructose infusion into the portal venous circulation, but significantly augmented in the presence of a high-dose fructose infusion [154]. Although the acute regulation of hepatic glucose uptake by low-dose intraportal fructose infusion cannot be explained by a decrease in glucose-6-phosphatase gene expression, it is possible that chronic consumption of high dietary fructose might lead to persistent elevations in glucose-6-phosphatase mRNA and protein, thereby antagonizing the balance between hepatic glucose output via glucose-6-phosphatase, and hepatic glucose uptake via glucokinase.

Cellular Mechanisms of Diet-Induced Hepatic Insulin Resistance

Molecular Changes Associated with High-Fat or High-Fructose Feeding

The cellular mechanisms by which high dietary fat or high dietary fructose confer metabolic abnormalities are overlapping in some respects, and distinct in others. One similarity amongst fat and fructose is that both nutrients in excessive amounts have profound effects on the liver, particularly in the early stages of feeding. In rodent models, high-fat and high-fructose feeding has been associated with hepatic lipid deposition, impaired regulation of glucokinase and glucose-6-phosphatase, decreased activation of insulin signaling intermediates, impaired regulation of glycogen synthase, and activation of stress signaling pathways. For example, the accumulation of triacylglycerol and diacylglycerol (DAG) in the livers of rats after three days of high-fat feeding was associated with a decrease in insulin-stimulated tyrosine phosphorylation of the insulin receptor and IRS 1/2, a reduction in the association of IRS proteins with PI-3K, a decrease in Akt and glycogen synthase activity, and an increase in GSK3 β and JNK activity [23]. Impaired insulin signaling was associated with activation of PKC ϵ secondary to liver lipid accumulation, whereas impaired activation of liver glycogen synthase was associated with a significant decrease in the incorporation of glucose into glycogen through the direct pathway, although the percentage of glycogen synthesized through the indirect pathway was slightly increased [23]. Furthermore, Oakes and colleagues [22] reported that three weeks of high-fat feeding in rats resulted in a significant impairment in the ability of insulin to suppress hepatic glucose production in association with impaired suppression of glucose-6-phosphatase activity, and

significantly reduced glucokinase activity during a hyperinsulinemic-euglycemic clamp. Altogether, these data indicate that high-dietary fat exerts adverse effects on the regulation of hepatic glucose metabolism in part by promoting liver lipid accumulation, by impairing the balance between glucose-6-phosphatase and glucokinase activity, and by attenuating the activation of insulin signaling intermediates, which translates into impaired activation of liver glycogen synthase.

Consumption of a high-fructose (or sucrose) diet has also been associated with a decrease in insulin-stimulated tyrosine phosphorylation of the IR, a reduction in insulin stimulated tyrosine phosphorylation of IRS 1/2, a reduction in the association of IRS proteins with PI-3K, a reduction in Akt and glucokinase activity, and an increase in G6Pase mRNA and activity [13, 14, 18, 19, 152, 154, 155, 166-170]. These changes were associated with an increase in JNK1 activity, an increase in protein tyrosine phosphatase 1b (PTP1b) and inducible nitric oxide synthase (iNOS) protein levels, an increase in hepatic lipid peroxidation, an increase in liver lipid and DAG concentrations, and activation of PKC ϵ [168-173]. The transcriptional changes that frequently accompany high-fructose feeding include hepatic induction of the lipogenic transcription factors SREBP-1c and ChREBP [126, 174, 175]. In fact, Koo and colleagues demonstrated an induction of ChREBP and fructose metabolic enzymes (fructokinase and aldolase B), along with pyruvate kinase, fatty acid synthase, and glycerol-3-phosphate acyltransferase in the livers of high-fructose fed rats, suggesting that ChREBP is a mediator of the lipogenic effects of fructose along with SREBP1c [126]. Furthermore, high fructose diet-induced hyperlipidemia and insulin resistance was ameliorated when the expression of hepatic ChREBP was knocked down *in vivo* [176]. On the other hand, knockdown of

ChREBP in high-fat-fed rodents had no beneficial metabolic effects [174]. Collectively, these data indicate that high-dietary fructose also exerts adverse effects on the regulation of hepatic glucose metabolism by promoting liver lipid accumulation, by impairing insulin signal transduction to Akt, and by increasing the ratio of glucose-6-phosphatase to glucokinase activity.

One of the common links underlying the adverse metabolic effects of excess dietary fat or fructose consumption in rodents is hepatic lipid accumulation. High-fat diets are thought to promote hepatic lipid deposition through increased delivery of dietary fat to the liver that exceeds its ability to oxidize the fatty acids or export them in VLDL particles [177], whereas high-fructose diets are thought to promote hepatic lipid deposition by stimulating *de novo* lipogenesis [146, 149, 171]. Recently, Ren and colleagues [178] investigated the role of endoplasmic reticulum (ER) stress and inflammation in hepatic steatosis and insulin resistance during high-fat feeding (lipid oversupply) versus high-fructose feeding (excess *de novo* lipogenesis). After only three days of feeding, both diets resulted in an increase in hepatic triglyceride levels and in SREBP1c mRNA expression; however, only the high-fructose diet increased hepatic *de novo* lipogenesis and the expression of ChREBP, acetyl-CoA carboxylase, fatty acid synthase, and stearoyl-CoA desaturase [178]. Furthermore, high-fructose feeding was associated with activation of ER stress signaling pathways (PERK/eIF α and IRE/XBP-1) but not JNK, whereas high-fat feeding was associated with activation of JNK but not ER stress [178]. These data suggest that different mechanisms are involved in the development of hepatic insulin resistance and hepatic steatosis induced by high-fructose or high-fat feeding.

Taken together, it is clear that both nutrients in excessive amounts have profound effects on hepatic insulin sensitivity and glucose metabolism. However, most of the aforementioned clamp studies were conducted under euglycemic conditions, in which the liver is only a minor contributor to whole-body glucose disposal. Thus, a defect in hepatic glucose uptake might have gone undetected. In addition, previous studies have generally utilized supraphysiological quantities of fructose (e.g. $\approx 60\%$ of kcal as fructose) to investigate its physiologic and cellular effects [126, 151, 171, 179]. As a result, the combined effects of dietary fat and fructose, in quantities that mimic a Western diet, on the temporal development of glucose intolerance and impaired hepatic glucose flux in vivo are incompletely understood. Thus, one of the overarching goals of this dissertation is to shed light on the pathogenesis of impaired hepatic glucose flux under conditions that mimic the postprandial state after chronic consumption of dietary fat and fructose in quantities that mimic a Western diet.

Regulation of Hepatic Glucose Uptake

The liver plays an integral role in maintaining whole-body glucose homeostasis. It consumes glucose in the postprandial state and stores it as glycogen, while in the post absorptive state it supplies glucose to the blood by breaking down glycogen and by converting gluconeogenic precursors into glucose. The ability of the liver to act as a dynamic regulator of glucose homeostasis is due in part to its proximity to the portal vein, the vessel into which the two main hormonal regulators of glucose metabolism, insulin and glucagon, are secreted. Thus, the liver is the first tissue to be exposed to secreted insulin and glucagon, and is extremely sensitive to subtle changes in the concentrations of

these hormones. Likewise, the liver is uniquely equipped with the ability to sense the route by which glucose is delivered to it. In contrast to intravenous glucose infusion by way of a peripheral vein, hepatic portal venous glucose delivery (by means of oral glucose ingestion or intraduodenal/portal vein glucose infusion) markedly amplifies HGU and GSYN in the rat [180, 181], dog [181-189], and human [190, 191]. amplifies HGU and glycogen synthesis (GSYN) in the rat [180, 181], dog [181-189], and human [190, 192]. The augmentation of HGU elicited by the intraportal route of glucose delivery has been attributed to a unique, neurally-mediated signal generated in the presence of a negative arterial-portal venous glucose gradient, termed the “portal glucose signal” [26, 182-184, 193-199]. In response to ingestion of a glucose-containing meal, the portal signal works in concert with increased plasma glucose and insulin to orchestrate a coordinated response favoring enhanced HGU and GSYN, thereby buffering perturbations in postprandial glycemia. Although the metabolic effects of intraportal glucose delivery have been studied in animal models and in the human, the molecular events linking the pleiotropic actions of the portal glucose signal to increased HGU and GSYN in vivo have not been clearly defined.

The clinical significance of investigating the regulation of hepatic glucose flux is underscored by the finding that individuals with diabetes display a marked impairment not only in the ability of hyperinsulinemia and hyperglycemia to suppress hepatic glucose production, but also in the ability of those postprandial stimuli to activate HGU and GSYN [200-204]. As a result, diabetic individuals experience frequent bouts of postprandial hyperglycemia, which contributes to the elevation of their hemoglobin A₁C and pre-disposes them to many of the complications associated with the disease.

However, the molecular events associated with a diminished response of the liver to hyperinsulinemia, hyperglycemia, and portal glucose delivery are incompletely understood.

Regulation of NHGU by Hyperglycemia

Previously, Shulman et al. [205] investigated the effect of hyperglycemia per se on the net hepatic glucose balance independent of changes in plasma insulin and glucagon levels in 36-h-fasted, conscious dogs. A pancreatic clamp was performed during which somatostatin was infused to inhibit endogenous insulin and glucagon secretion. Insulin and glucagon were replaced into the portal venous circulation at basal rates (0.3 mU/kg/min and 1.0 ng/kg/min, respectively), while saline or glucose was infused into a peripheral vein at the beginning of the experimental period. In contrast to the saline-infused group, hyperglycemia per se induced a significant decline (56%) in net hepatic glucose output (NHGO) (from 2.2 ± 0.1 to 0.9 ± 0.1 mg/kg/min) in the presence of basal insulin and glucagon concentrations, but net hepatic glucose uptake (NHGU) did not occur during the 2 hour experimental period [205]. Similar results were reported by Cherrington et al. [206] in the presence of a 2-fold increase in the hepatic glucose load (HGL) brought about by intravenous glucose infusion during euinsulinemic and euglucagonemic conditions. Furthermore, hyperglycemia per se was not associated with an increase in terminal liver glycogen levels over those of saline-infused dogs [205], consistent with the lack of NHGU in the presence of basal insulin and glucagon concentrations [205, 206]. In accord with this, Sacca et al. [207] reported that hyperglycemia had an inhibitory effect on glucose production in the presence of fixed

basal pancreatic hormone concentrations in the overnight-fasted human.

Interestingly, acute removal of glucagon in the presence of similar hyperglycemia and euinsulinemia induced a switch from just reduced NHGO to NHGU (0.9 ± 0.2 to 1.5 ± 0.2 mg/kg/min, respectively), suggesting that glucagon is a powerful modulator of NHGB during hyperglycemia and euinsulinemia [205]. On the other hand, acute removal of glucagon in presence of basal glucose and insulin concentrations partially suppressed NHGO in dogs (approximately 35% reduction) [208], and net splanchnic glucose production in humans (approximately 75% reduction) [209].

A decline in NHGO in the presence of hyperglycemia can be the consequence of a decrease in net hepatic gluconeogenesis, net hepatic glycogenolysis, or both. Rossetti and colleagues [210] investigated the mechanisms by which hyperglycemia per se regulates hepatic glucose production in vivo. Pancreatic clamp studies were performed in conscious rats during which somatostatin was infused to disable the endocrine pancreas, and insulin and glucose were replaced at basal and 2-fold basal rates, respectively, into the peripheral circulation. Consistent with previous studies [205, 206], hyperglycemia per se under euinsulinemic conditions was associated with a 58% decrease in hepatic glucose production, nearly all of which was accounted for by a decline (89%) in hepatic glycogenolysis [210]. These changes were accompanied by an increase in the activation of glycogen synthase coupled with a decrease in glycogen phosphorylase *a* activity, whereas the activities of glucose-6-phosphatase and glucokinase were unaffected by acute hyperglycemia [210]. However, a significant increase in the contribution of plasma-derived glucose carbons to the hepatic glucose-6-phosphate pool and total glucose-6-

phosphatase flux (as a reflection of glucose cycling) was indicative of a substrate-mediated increase in glucokinase flux in response to an acute elevation of plasma glucose [210]. Interestingly, infusion of a glucokinase inhibitor, glucosamine, significantly impaired the ability of hyperglycemia per se to suppress hepatic glucose production in rats, suggesting that activation of glucokinase is also a key component in facilitating hepatic glucose effectiveness [211].

The metabolic findings of Rossetti et al. [210] were confirmed in the conscious dog by Sindelar and colleagues [212], in which hyperglycemia was shown to inhibit glucose production through suppression of hepatic glycogenolysis. Likewise, Petersen et al. [213] demonstrated in humans that hyperglycemia per se suppressed net hepatic glycogenolysis primarily through inhibition of glycogen phosphorylase flux. Thus, in normal individuals, hyperglycemia alone can suppress NHGO and HGP by affecting the regulation of enzymes involved in glucose phosphorylation and glycogen metabolism in the absence of a change in glucose-6-phosphatase activity or flux. However, hyperglycemia alone is inadequate to stimulate HGU in the presence of basal insulin and glucagon levels.

Regulation of NHGU by Hyperinsulinemia

McGuinness and colleagues [89] performed four-step hyperinsulinemic euglycemic clamp experiments in conscious dogs following an overnight fast. Insulin was infused into a peripheral (cephalic) vein at 1, 2, 10, and 15 mU/kg/min for 100 minutes each, which corresponded to steady state plasma insulin levels of 58 ± 3 , 120 ± 18 , 1134 ± 102 , and 2044 ± 293 $\mu\text{U}/\text{ml}$. In addition, glucose was infused through the saphenous

vein in order to maintain euglycemia throughout the study. Physiologic hyperinsulinemia in the presence of euglycemia and basal glucagon concentrations resulted in complete suppression of NHGO, with only marginal stimulation of NHGU (from 2.38 ± 0.66 to -0.1 ± 0.29 or -0.55 ± 0.26 mg/kg/min with 1 or 2 mU/kg/min of exogenous insulin infusion, respectively) [89]. In contrast, pharmacologic hyperinsulinemia in the presence of euglycemia stimulated a significant increase in NHGU (-1.83 ± 0.13 or -2.89 ± 0.96 mg/kg/min with 10 or 15 mU/kg/min of exogenous insulin infusion, respectively) [89]. Nevertheless, supraphysiologic levels of circulating insulin were still insufficient to elicit peak rates of NHGU seen in response to physiologic hyperinsulinemia, hyperglycemia, and portal vein glucose delivery.

Recently, Ramnanan et al. [214] described the time course of the physiologic and hepatocellular changes associated with suppression of NHGO in response to an 8-fold elevation in hepatic sinusoidal insulin concentrations during euglycemia and euglucagonemia in 24-h-fasted conscious dogs. Indeed, hyperinsulinemia resulted in rapid suppression (within the first 30 min) of NHGO, which was attributable to a robust decline in net hepatic glycogenolysis and gluconeogenesis, with only a transient decrease in net hepatic gluconeogenic flux. Despite complete inactivation of hepatic glucose production, however, 4 hours of hyperinsulinemia was associated with only marginal stimulation of NHGU (-0.8 ± 0.1 mg/kg/min) [214].

Molecular markers in the liver that changed within the first 30 min of hyperinsulinemia concomitant with suppression of hepatic glucose production included activation of insulin signaling intermediates (Akt and GSK3 β), nuclear exclusion of FOXO1, activation of glycogen synthase, inhibition of glycogen phosphorylase, and

increased fructose-2,6-bisphosphate concentrations [214]. In humans, hyperinsulinemia per se was also shown to inhibit hepatic glycogenolysis primarily through stimulation of liver glycogen synthase flux [213]. Collectively, the aforementioned studies demonstrate that a physiologic rise in insulin in the presence of euglycemia and basal glucagon concentrations is inadequate to stimulate NHGU to any large extent.

Regulation of NHGU by Hyperglycemia and Hyperinsulinemia

In 36-h-fasted dogs, Cherrington and colleagues [206] investigated whether a physiologic, four-fold increase in plasma insulin (from 12 ± 1 to 36 ± 2 $\mu\text{U/ml}$) brought about by intraportal infusion of the hormone would augment the response of the liver to hyperglycemia (from 112 ± 12 to 244 ± 11 mg/dl) brought about by intravenous infusion of glucose. Indeed, the combination of hyperglycemia and hyperinsulinemia caused a robust switch from NHGO (2.8 ± 3 mg/kg/min) to NHGU (peak rate of 3.7 ± 1.2 mg/kg/min), but 2 hours of hyperinsulinemia and hyperglycemia was required to elicit peak rates of NHGU. Consistent with the stimulation of NHGU, terminal liver glycogen levels were significantly greater in the hyperinsulinemic-hyperglycemic group (44.0 ± 4.2 mg/g liver) compared to the euinsulinemic-hyperglycemic group (19.4 ± 2.2 mg/g liver). Pagliassotti et al. [198] reported a similar time course and magnitude of change in NHGB in 42-h-fasted dogs in the presence of a four-fold elevation in insulin and a two-fold increase in the hepatic glucose load brought about by intravenous (peripheral) glucose infusion, in which a peak rate of NHGU (approximately 3.0 mg/kg/min) was achieved after ninety minutes of hyperinsulinemia and hyperglycemia (approximately 35 $\mu\text{U/ml}$ and 235 mg/dl , respectively, in arterial plasma) [198]. Augmented NHGU in the presence of a

combined elevation in glucose and insulin was associated with rapid (30 min) activation of liver glycogen synthase, and a significant increase in liver glycogen levels relative to control animals with hyperglycemia alone [198]. Likewise, physiologic elevations of glucose and insulin in humans led to high rates of net hepatic glycogen synthesis secondary to stimulation of glycogen synthase flux and suppression of glycogen phosphorylase flux [213].

Numerous other studies have also demonstrated rates of NHGU in the dog ranging from 1.0 to 2.9 mg/kg/min in the presence of plasma glucose concentrations of 160 to 290 mg/dl and plasma insulin levels of 35 to 384 μ U/ml [215]. In humans, splanchnic glucose uptake (comprising glucose disposal by the gut and liver) ranged from 1.0 to 1.6 mg/kg/min in the presence of plasma glucose concentrations of 175 to 225 mg/dl and plasma insulin levels of 40 to 55 μ U/ml [215].

Altogether, the aforementioned studies indicate that physiologic changes in glucose, insulin, or glucagon individually are insufficient to stimulate NHGU. In addition, although NHGU is significantly increased in the presence of a four-fold rise in insulin and a two-fold increase in glucose by way of intravenous glucose infusion, these factors still cannot account for the peak rates of NHGU that are evident following an oral glucose challenge [27, 190]. Thus, factors in addition to hyperglycemia and the concentrations of pancreatic hormones must be involved in the regulation of NHGU in response to ingestion of a glucose-containing meal.

Regulation of NHGU by Portal Glucose Delivery

It has been known for some time now that in the presence of matched blood glucose profiles, oral glucose ingestion results in a plasma insulin response that is nearly double that seen in the same individuals when glucose is infused intravenously [216]. The unique hormonal response to oral versus intravenous glucose delivery was attributed to the release of insulinotropic factors by the gut in the presence of oral glucose ingestion, and thus termed the “incretin effect.” In addition, DeFronzo and colleagues [190] assessed the influence of the route of glucose administration (oral versus intravenous) on splanchnic (which includes the gut and liver tissues) glucose uptake in humans. During the first hour of their experiment, glucose was infused intravenously to elevate the plasma glucose concentration at 125 mg/dl above basal. Afterwards, participants ingested 1.2 g of glucose per kilogram of body weight, and the variable intravenous (“peripheral”) glucose infusion rate was adjusted to clamp the plasma glucose concentration at 125 mg/dl above basal for the remaining 3 hours of the study. Net splanchnic glucose uptake during the first 60 min of intravenous glucose infusion was 1.0 mg/kg/min. In response to oral glucose ingestion, net splanchnic glucose uptake increased six-fold (to approximately 6.0 mg/kg/min) despite unchanged plasma glucose levels. Likewise, oral glucose ingestion was associated with a 50% increase in the mean plasma insulin response compared to that reached with intravenous glucose infusion alone [190]. Thus, the route of glucose administration had a significant impact not only on the beta cell, as reported previously, but also on glucose uptake by splanchnic tissues.

The findings of DeFronzo and colleagues [190] in humans were tested in the dog model in a study by Abumrad et al. [27], in which conscious dogs were administered an

oral glucose load of 1.63 g/kg body weight. In response to the oral glucose challenge, the arterial blood glucose concentration nearly doubled, while the arterial plasma insulin concentration increased approximately 5-fold, with minimal changes in plasma glucagon levels. Under these hormonal and glycemic conditions, there was a rapid switch from NHGO (2.0 mg/kg/min) to NHGU (approximately 4.5 mg/kg/min), demonstrating that the increase in glucose uptake by splanchnic tissues following oral glucose ingestion was predominantly attributable to augmented hepatic glucose uptake. Furthermore, the magnitude of the increase in splanchnic [190] or hepatic [27] glucose uptake following oral glucose ingestion was greater than what would have been predicted based on the accompanying plasma insulin and glucose levels, suggesting that the normal response of the liver to an oral glucose challenge requires a signal in addition to glucose and insulin to ensure adequate storage of glucose by the liver in the postprandial state.

Initially, DeFronzo and colleagues [190] speculated that ingestion of glucose triggers the release of a gastrointestinal factor that enhances splanchnic glucose uptake, but other changes also accompanied oral versus intravenous glucose delivery. For example, there was an increase in insulin secretion, and there was a shift in the blood glucose gradient between the hepatic artery and the portal vein. Oral glucose delivery resulted in portal venous glucose concentrations that were higher than those in the arterial circulation (negative arterial-portal [A-P] glucose gradient), whereas arterial glucose concentrations were higher with intravenous (peripheral) glucose infusion (positive A-P glucose gradient). As a result, it was not clear how much of the enhanced response of splanchnic tissues to oral glucose delivery was attributable to augmented insulin secretion, the secretion of a gut factor, or the generation of a negative A-P gradient. Thus,

our laboratory carried out a series of pancreatic clamp experiments in the conscious dog in which NHGU was assessed during peripheral versus intraportal glucose infusion, thereby bypassing the gut. In addition, somatostatin was infused to inhibit endogenous insulin and glucagon secretion, and both hormones were replaced intraportally at a fixed rate. Adkins and colleagues [182] demonstrated that under conditions of basal insulinemia, basal glucagonemia, and hyperglycemia by way of peripheral glucose infusion (mean arterial and portal venous plasma glucose concentrations of 217 and 213 mg/dl, respectively), there was no stimulation of NHGU. However, when some of that glucose was switched from a peripheral to an intraportal infusion (arterial and portal plasma glucose concentrations of 200 and 220 mg/dl, respectively), NHGU was significantly increased (1.4 mg/kg/min), even though the hepatic glucose load and the plasma insulin and glucagon concentrations were the same as those in the peripheral glucose infusion protocol [182]. Altogether, these data and others [186, 187] ruled out the involvement of a gut factor in the enhanced response of the liver to oral glucose ingestion, and suggested that augmented NHGU in the presence of intraportal glucose infusion was attributable to the generation of a "portal glucose signal." Subsequent studies [183, 197, 198] demonstrated that when hyperinsulinemia (four-fold increase) was combined with hyperglycemia, NHGU was consistently 2.5 to 3-fold greater in the presence versus absence of the portal signal, suggesting that hyperinsulinemia and portal glucose delivery have an additive effect in augmenting NHGU. Furthermore, Holste et al. [217] demonstrated that a selective decrease in glucagon does not further enhance the response of the liver to hyperglycemia, hyperinsulinemia, and portal glucose delivery, whereas an increase in glucagon reduces NHGU due to impaired suppression of hepatic

glucose uptake. Thus, in diabetic individuals, hyperglucagonemia may antagonize splanchnic glucose uptake in response to a meal.

Interaction between the Portal Glucose Signal, Insulin, and the Hepatic Glucose Load

Myers and colleagues [196, 197] further investigated the relationship between portal glucose delivery, the hepatic sinusoidal insulin level, and the hepatic glucose load in 2 separate studies using the conscious dog model. In the first study [197], the pancreatic clamp technique was employed to fix plasma glucagon levels at a basal concentration, while insulin was infused intraportally at two-, four-, or eight-fold basal in two separate groups. One group received a portal glucose infusion (approximately 4-5 mg/kg/min) in order to activate the portal glucose signal, while the other group received an intraportal saline infusion. In both groups, a variable peripheral glucose infusion was utilized to double the hepatic glucose load in both protocols. In the presence of hyperinsulinemia and hyperglycemia without the portal glucose signal, NHGU was 0.6 ± 0.3 , 1.5 ± 0.4 , 3.0 ± 0.8 mg/kg/min with a two-, four-, and eight-fold rise in insulin, respectively. However, infusion of a portion of that glucose into the portal vein in order to activate the portal signal triggered an increase in NHGU at all 3 insulin infusion rates, which corresponded to NHGU rates of 2.0 ± 0.5 , 3.7 ± 0.7 , and 5.5 ± 0.9 mg/kg/min in the 3 insulin infusion periods, respectively [197]. Thus, although insulin is a clear determinant of NHGU in both the absence and presence of portal glucose delivery, the effect of the portal glucose signal on NHGU is at least equal to the effect of insulin, even across wide range of insulin concentrations [26, 197]. Likewise, the effects of portal glucose delivery and hyperinsulinemia on hepatic glycogen accumulation are additive under physiologic

conditions [198], demonstrating that the two signals efficiently couple glucose uptake and storage by the liver in the postprandial state [208, 219]. Indeed, the permissive effect of insulin on the response of the liver to portal glucose delivery was exemplified in a study by Pagliassotti et al [218], in which acute or chronic removal of insulin by way of somatostatin infusion or pancreatectomy, respectively, resulted in the loss of an increase in NHGU in the presence of the portal glucose signal.

In a second study, Myers and colleagues [196] again utilized the pancreatic clamp to fix the glucagon concentration at a basal level while elevating the plasma insulin concentration four-fold. In one group, the hepatic glucose load was increased by approximately 65%, 140%, and 220% by means of a peripheral glucose infusion. In another group, glucose was infused intraportally (approximately 10 mg/kg/min), while the peripheral glucose infusion was adjusted as necessary to match the hepatic glucose loads to those of the first group. In the absence of portal glucose delivery, NHGU was 1.2 ± 0.4 , 2.8 ± 0.8 , and 5.1 ± 1.2 mg/kg/min, which corresponded to graded increases in the hepatic glucose load. However, NHGU at the three different hepatic glucose loads was magnified in the presence of portal glucose delivery (3.8 ± 0.4 , 4.8 ± 0.6 , and 9.6 ± 1.4 mg/kg/min, respectively) [196]. Thus, analogous to insulin, the hepatic glucose load is also a determinant of NHGU in both the absence and presence of portal glucose delivery, but the portal signal substantially augments NHGU across a wide range of hepatic glucose loads [26, 196]. Likewise, the rate of NHGU is directly related to the magnitude of the negative A-P gradient across the range of physiologic gradients under conditions of hyperglycemia and physiologic hyperinsulinemia [199]. Altogether, these data provide

sufficient evidence to indicate that NHGU is dependent upon the hepatic glucose load, the hepatic sinusoidal insulin level, and the portal glucose signal [26].

Mechanism of Portal Signaling

The mechanism(s) by which a negative A-P glucose gradient is sensed, a portal glucose signal generated, and NHGU increased has been the focus of numerous studies. Several lines of evidence suggest that the portal glucose signal is neurally-mediated. For example, Adkins-Marshall et al. [184] demonstrated in dogs that surgical denervation of the liver ablates its response to portal glucose delivery (NHGU was 2.1 ± 0.5 and 2.2 ± 0.7 mg/kg/min during peripheral and portal glucose infusion, respectively) under conditions of basal glucagonemia, hyperinsulinemia (four-fold basal), and hyperglycemia (hepatic glucose load two-fold basal). In addition, Pagliassotti and colleagues [198] compared the time course of the effect of insulin and the portal glucose signal on NHGU in conscious dogs, the idea being that a neurally-mediated signal generated by portal glucose infusion should result in rapid stimulation of NHGU as opposed to peripheral glucose delivery. The pancreatic clamp was used to fix plasma glucagon at a basal level, and to vary the plasma insulin level as desired. Hyperglycemia preceded the experimental period in order to suppress NHGO to zero. In one group (Control), hyperglycemia via peripheral infusion was sustained for the duration for the study. In a second group (Portal Signal), insulin was fixed at a basal level while glucose was infused intraportally to activate the portal glucose signal, and the peripheral glucose infusion rate was adjusted as necessary to match the hepatic glucose load to that of the control group. In a third group (Insulin), the insulin level was increased four-fold in the presence of hyperglycemia, but in the absence

of portal glucose delivery, while in the fourth group (Insulin + Portal Signal), all stimuli were present (hyperglycemia, hyperinsulinemia, and portal glucose delivery). In the control group, NHGU was 0.4 mg/kg/min, and there was little accumulation of liver glycogen during the study. In the Portal Signal group, NHGU was markedly (approximately 3.0 mg/kg/min) and rapidly (15 min) increased despite the same experimental conditions as the Control group. This resulted in a robust increase in liver glycogen levels in association with rapid activation of liver glycogen synthase, even in the absence of a rise in insulin [198]. These data lend support to the notion that the portal signal is in part, neurally-mediated. Furthermore, when hyperglycemia and hyperinsulinemia were combined in the Insulin group, NHGU eventually approached the rate observed in the Portal Signal group alone, but it required nearly 90 min to achieve this rate. On the other hand, hyperglycemia, hyperinsulinemia, and portal glucose delivery increased NHGU to a maximum rate of approximately 4.3 mg/kg/min after only 60 min, demonstrating that the portal signal activates the liver much more quickly than would otherwise be the case in its absence [208, 219]. Likewise, dissipation of the hepatic response to portal glucose delivery is equally as rapid (\approx 15 min) upon removal of the portal glucose signal [194].

Further evidence supporting the involvement of the nervous system in the effect of portal glucose delivery on NHGU was provided by Shiota and colleagues [219], in which they conducted a study to shed light on which branch of the autonomic nervous system (sympathetic or parasympathetic) was associated with the response of the liver to the portal glucose signal. Under conditions of hyperglycemia and hyperinsulinemia, pharmacologic blockade of α,β -adrenergic receptors by means of intraportal infusion of

phentolamine and propranolol did not result in an increase in NHGU. On the other hand, the combination of adrenergic blockade and cholinergic stimulation by means of intraportal infusion of acetylcholine resulted in an increase in NHGU of 1.8 mg/kg/min in the presence of hyperinsulinemia and hyperglycemia, but not portal glucose delivery [219]. These data imply a role for the parasympathetic nervous system in mediating the effects of portal glucose delivery on NHGU. However, Cardin et al. [220] and DiCostanzo et al. [221] later found that halting electrical transmission in the vagus nerves by vagal cooling had no effect on NHGU in the presence of hyperinsulinemia, hyperglycemia, and portal glucose delivery. Thus, the afferent limb of the vagus nerve is not likely to be involved in the response of the liver to portal glucose delivery. Other studies have highlighted a potential role for changes in nitric oxide [222-224] and serotonin [225-227] signaling in mediating the effects of the portal glucose signal on NHGU. Nevertheless, the precise mechanism(s) by which portal glucose delivery coordinates changes in hepatic glucose metabolism in the postprandial state are incompletely understood.

Mechanism of Action of the Portal Glucose Signal

Given that the metabolic response of the liver to portal glucose delivery is rapid (NHGU is maximally stimulated 15 min after initiation of intraportal glucose infusion), its biochemical mechanism of action cannot be explained by changes in gene expression. Pagliassotti et al. [198] demonstrated rapid activation of liver glycogen synthase in response to portal glucose delivery, even in the presence of basal insulin concentrations. Rapid stimulation of NHGU in the presence of portal glucose infusion might result in an

increase in hepatocellular glucose-6-phosphate concentrations, which is a potent allosteric activator of phosphorylated glycogen synthase. Thus, the portal signal increases the provision of substrate needed for glycogen synthesis, and directs a significant proportion of that substrate into glycogen by activating glycogen synthase, with the remaining carbon leaving the liver as lactate [198]. Rapid activation of liver glycogen synthase by portal glucose delivery might also be neurally-mediated. Afferent fibers in the hepatic branch of the vagus nerve can detect the glucose concentration in the hepatic portal vein, and previous studies have demonstrated that electrical stimulation of the efferent limb of the vagus nerve activates liver GS [215, 228-230]. Thus, the biochemical mechanism of action of the portal glucose signal might also be neurally-mediated.

Given the magnitude of the increase in NHGU in response to portal glucose delivery, it is likely that other mechanisms in addition to rapid activation of glycogen synthase are involved. One potential target through which the portal signal might exert its effects is hepatic glucokinase (GK). Indeed, phosphorylation of glucose by GK is thought to be rate-limiting for HGU [231, 232]. Under basal conditions, GK is sequestered in the nucleus in a catalytically inactive, super-open conformation via binding by its regulatory protein, GKRP; under hyperglycemic and/or hyperinsulinemic conditions, GK dissociates from GKRP and translocates to the cytoplasm where it catalyzes the phosphorylation of glucose [122, 123, 162, 233-235]. In addition, hyperglycemia stimulates the transition of GK from a super-open conformation to a closed conformation, corresponding to the high affinity, catalytically active form of GK [122, 234-237]. Given that GLUT2 is a high capacity, low affinity glucose transporter that is expressed at a high level in the liver, the transport step for glucose into the hepatocyte is not rate-limiting [238]. As a result,

fluctuations in extracellular blood glucose levels are immediately followed by parallel changes in intracellular glucose levels, which are monitored by GK [122]. Thus, the rapid effects of portal glucose delivery on NHGU might also be mediated by stimulation of the translocation of GK from the nucleus to the cytosol secondary to a rise in the portal vein blood glucose level [26, 233]. In Specific Aim III, one of our goals is to identify the acute molecular changes associated with increased HGU and GSYN in response to portal glucose delivery per se in normal dogs.

Impaired Regulation of Splanchnic Glucose Uptake with Diabetes

Postprandial hyperglycemia is one of the sequelae of diabetes that contributes to the elevation of hemoglobin A1c associated with the disease [24, 25]. It is due in part to inappropriate suppression of hepatic glucose production (HGP) coupled with inadequate stimulation of HGU, highlighting the key role of the liver in regulating postprandial glucose metabolism [200, 202-204, 239-243]. Indeed, splanchnic (which comprises the gut and liver tissues) glucose uptake (SGU) and hepatic GSYN through the direct pathway were markedly diminished in type 2 diabetic subjects compared to non-diabetic controls despite equivalent elevations in plasma insulin and glucose during a clamp experiment [200, 201, 244]. Furthermore, delivery of glucose into the portal venous circulation (by way of enteral glucose infusion) in the presence of hyperinsulinemia was ineffective in normalizing the diminished rates of SGU and GSYN in diabetic subjects [200]. Given that type 2 diabetic subjects displayed a decrease in the contribution of extracellular glucose to the UDP-glucose pool, the authors [200, 201] speculated that that a defect in GK was linked to the aberrant hepatic response in type 2 diabetic individuals.

Indeed, a reduction in hepatic GK expression has been reported previously in morbidly obese type 2 diabetic humans [245] and in genetic rodent models of obese, type 2 diabetes [246]. The critical role of GK in maintaining whole-body glucose homeostasis is exemplified in subjects with autosomal dominant mutations on one or two alleles of the GK gene, resulting in a moderate to severe form of diabetes, respectively, called maturity-onset diabetes of the young, Type 2 (MODY) [247-250]. These individuals display fasting hyperglycemia, and impaired glucose uptake and hepatic GSYN in response to hyperinsulinemia and hyperglycemia [250]. Likewise, animal models with a liver specific deletion of GK have mild fasting hyperglycemia, markedly impaired glucose tolerance, and significantly decreased hepatic GSYN under hyperglycemic conditions [251]. On the other hand, transgenic overexpression of hepatic GK lowers postprandial hyperglycemia in normal rats [252], improves hepatic glucose flux and fasting plasma glucose levels in 20-week-old Zucker diabetic fatty (ZDF) rats [246], and renders mice resistant to the development of obesity-induced type 2 diabetes when fed a high-fat diet [253].

Altogether, these data indicate that the diabetic liver is resistant to the hormonal and glycemc cues that are characteristic of the postprandial state, and suggest that impaired regulation of hepatic GK might be a common pathogenic factor underlying disturbances in postprandial hepatic glucose flux and glycogen synthesis with diabetes. However, the temporal manifestation of impaired HGU along the continuum of worsening insulin action that occurs with type 2 diabetes is poorly understood. Likewise, the cellular events associated with a diminished response of the liver to hyperinsulinemia, hyperglycemia, and portal glucose delivery under insulin resistant conditions have not

been clearly defined.

Specific Aims

The overall objective of this body of work is to elucidate the metabolic and hepatocellular consequences associated with chronic consumption of a high-fat and/or high-fructose diet, focusing on perturbations in the regulation of hepatic glucose uptake and disposition by hyperglycemia, hyperinsulinemia, and portal vein glucose delivery – the primary determinants of hepatic glucose uptake in vivo [26]. The following Specific Aims were designed to investigate these issues.

Specific Aim I: To determine the temporal impact of high-fat/high-fructose feeding – with or without partial pancreatic resection – on glucose tolerance, whole-body insulin sensitivity, and net hepatic glucose uptake (NHGU).

The objective of Specific Aim I was to investigate the influence of a high-fat/high-fructose diet (HFFD; 52% of energy from fat / 17% of energy from fructose) on, 1) the temporal development of insulin resistance and impaired glucose tolerance in the presence or absence of a compromised endocrine pancreas, and 2) the ability of the liver to take up glucose under conditions that mimic the postprandial state (e.g. hyperinsulinemia, hyperglycemia, and portal vein glucose delivery). Partial pancreatectomies (\approx 65% resection) were carried out with the intent to develop a large animal model of type 2 diabetes when coupled with a HFFD, thereby mimicking the natural progression and metabolic characteristics of the human disease. Prior to initiation

of the HFFD or chow control diet (CTR), baseline metabolic assessments of glucose tolerance and whole-body insulin sensitivity were acquired by performing oral glucose tolerance tests (OGTTs) and hyperinsulinemic euglycemic (HIEG) clamps, respectively. The OGTTs were repeated after 4 and 8 weeks of HFFD or CTR feeding, whereas the HIEG clamps were repeated after 10 weeks of feeding. Finally, hyperinsulinemic hyperglycemic clamps with portal vein glucose delivery were performed after 13 weeks of HFFD or CTR feeding in order to assess NHGU and net glycogen synthesis during conditions that mimic the postprandial state. Specific Aim I enabled us to characterize the temporal manifestation of perturbations in glucose metabolism and whole-body insulin sensitivity in a large animal model upon exposure to a HFFD, which mimics a typical Western diet.

Specific Aim II: To delineate the impact of a HFFD on the response of the gastrointestinal tract, endocrine pancreas, liver, and peripheral tissues to an orally-administered, liquid mixed meal.

In Specific Aim I, the metabolic consequences associated with HFFD feeding were detected in response to a glucose challenge, which lacked other meal-associated factors that can influence the gastric emptying rate, insulin and glucagon secretion, and NHGU. Administration of a standard mixed meal has been proposed as a more physiological challenge to the system. In view of these considerations, experiments were conducted in the conscious dog to determine if 8 weeks of HFFD feeding, 1) impairs NHGU in a non-clamped, mixed meal setting, 2) impairs insulin secretion in the presence of other insulin secretagogues (e.g. amino and fatty acids), 3) affects the acute lipid

response to a mixed meal and, 4) alters gastrointestinal function and/or meal macronutrient absorption. Specific Aim II enabled us to expose defects in hepatic and extrahepatic tissues in response to a more physiological mixed meal challenge, which contributed to our understanding of the mechanisms responsible for impaired glucose tolerance after chronic consumption of a HFFD.

Specific Aim III: To elucidate the physiologic and hepatocellular effects of the portal glucose signal per se during conditions that mimic the postprandial state, following short-term exposure to a HFFD or chow control (CTR) diet.

Specific Aim I revealed impaired glucose tolerance after only 4 weeks of HFFD feeding. Hepatic glucose uptake was not measured at 4 weeks, but was impaired when measured after longer-term (i.e. 13 weeks) consumption of a HFFD. Given the vital role of the liver in the disposition of an oral glucose load, we hypothesized that impaired HGU was already present at 4 weeks of HFFD feeding, and was responsible in part for the exaggerated glycemic response to an oral glucose challenge. Thus, one of the objectives of Specific Aim III was to determine if 4 weeks of HFFD feeding is sufficient to impair HGU under hyperinsulinemic hyperglycemic conditions. In addition, Specific Aim I revealed that portal glucose delivery was incapable of stimulating a switch from net hepatic glucose output (NHGO) to NHGU after 13 weeks of HFFD feeding. Thus, we hypothesized that HFFD feeding precipitated the loss of an intact portal signaling mechanism, but the cellular changes associated with portal glucose delivery in normal dogs have not been clearly defined, and the cellular changes associated with resistance to the stimulatory effects of hyperinsulinemia, hyperglycemia, and portal glucose delivery in

HFFD-fed dogs are not known. Thus, another objective of Specific Aim III was to identify the molecular “signature” of the portal glucose signal per se in the presence of a physiologic rise in glucose and insulin. Furthermore, we wanted to elucidate the cellular explanation for the defect in HGU associated with HFFD feeding, and whether that cellular defect persists in the presence of the portal glucose signal after only 4 weeks of HFFD feeding. Specific Aim III enabled us to delineate the molecular changes associated with hyperinsulinemia, hyperglycemia, and portal glucose delivery per se in CTR-fed and HFFD-fed dogs.

Specific Aim IV: To compare the physiologic and hepatocellular effects of high dietary fat vs. fructose on HGU and glycogen synthesis (GSYN) during conditions that mimic the postprandial state.

The observation that HFFD feeding significantly impaired HGU posed the question of whether excess dietary fat, fructose, or both are required to elicit aberrant hepatic glucose flux under conditions that mimic the postprandial state. We hypothesized that their individual effects on hepatic glucose flux would be additive. Thus, the objective of Specific Aim IV was to delineate the relative contribution (when consumed isoenergetically) of high dietary fat vs. fructose (17% of total energy) to impaired HGU and GSYN after 4 weeks of feeding.

CHAPTER II

MATERIALS AND METHODS

Animal Care and Surgical Procedures

Animal Care

Experiments were conducted on 18- (Specific Aims I, III, and IV) or 24-h (Specific Aims I and II) fasted conscious male mongrel dogs that had been fed once daily a specific experimental diet (see Table 2.1). Water was available *ad libitum*, whereas a fixed quantity of food was provided each day. All facilities met the standards published by the American Association for the Accreditation of Laboratory Animal Care, and the Vanderbilt University Medical Center Animal Care and Use Committee approved all protocols.

Surgical Procedures

Hepatic Catheterization

Approximately 16 days prior to the hyperinsulinemic hyperglycemic pancreatic clamp study, a sterile laparotomy was performed on each dog under general anesthesia. A surgical plane of anesthesia was induced with propofol (5.0 mg/kg, intravenous or I.V.) preceded 30 minutes by Glycopyrolate/Buprenex (0.01/0.02 mg/kg subcutaneous or S.C.). A S.C. injection of Cephazolin (10 mg/kg) was also administered to the dog pre-operatively. Following induction, the animal was immediately intubated with an 8.5 mm

inner diameter (ID) endotracheal tube (Concord/Portex, Kennebec, NH), and ventilated with a tidal volume of 400 ml at a rate of 14 breaths per minute. The plane of anesthesia was maintained by inhalation of 1.5-2.0% isoflurane with oxygen. A laparotomy was performed by making a midline incision 1.5 cm caudal to the xyphoid process through the skin, subcutaneous layers, and linea alba, and extending caudally 15-20 cm. A portion of the jejunum was exposed and a branch of a jejunal vein was selected for cannulation. A small section of the vessel was exposed by blunt dissection and ligated with 4-0 silk (Ethicon, Inc, Sommerville, NJ). A silastic infusion catheter (0.04 in ID; HelixMedical, Carpinteria, CA) was inserted into the vessel through a small incision and advanced antegrade until the tip of the catheter lay approximately 1 cm proximal to the coalescence of two jejunal veins. A portion of the spleen was retracted and another silastic catheter (0.04 in ID) was inserted into a distal branch of the splenic vein and advanced until the tip of the catheter lay 1 cm beyond the bifurcation of the main splenic vein. The catheters were secured in place with 4-0 silk, filled with saline (Baxter Healthcare Corp, Deerfield, IL) containing 200 U/ml heparin (Abbott Laboratories, North Chicago, IL), knotted and placed in a subcutaneous pocket prior to closure of the skin. These catheters were used for intraportal infusion of pancreatic hormones (insulin and glucagon).

The central and left lateral lobes of the liver were retracted cephalically and caudally, respectively. The left common hepatic vein and the left branch of the portal vein were exposed. A 14-gauge angiocath (Benton Dickinson Vascular Access, Sandy, UT) was inserted in the left branch of the portal vein 2 cm from the central lobe of the liver. A silastic catheter (0.04 in ID) for blood sampling was inserted into the hole created

by the angiocath, advanced retrograde about 4 cm into the portal vein so that the tip of the catheter lay 1 cm beyond the bifurcation of the main portal vein. It was then secured with three ties of 4-0 silk through the adventitia of the vessel and around the catheter. Another angiocath was inserted into the left common hepatic vein 2 cm from its exit from the left lateral lobe. A silastic sampling catheter was inserted into the hole and advanced antegrade 2 cm and secured into place with three ties of 4-0 silk. The sampling catheters were filled with heparinized saline, knotted and placed in a subcutaneous pocket, with excess catheter looped within the peritoneum. These catheters were used for the acquisition of blood samples from the hepatic portal vein and hepatic vein, respectively.

An arterial sampling catheter was inserted into the left femoral artery following a cut-down in the left inguinal region. A 2 cm incision was made parallel to the vessel. The femoral artery was isolated and ligated distally, and a sampling catheter (0.04 in ID) was inserted and advanced 16 cm in order to place the tip of the catheter in the abdominal aorta. The arterial catheter was secured and filled with a mixture of heparin and glycerin (1000 U/ml in a 1:1 ratio), while its free end was knotted and placed in a subcutaneous pocket prior to closure of the skin. This catheter was used for the sampling of arterial blood.

Sections of the portal vein and hepatic artery were exposed by retracting the duodenum laterally. A small section of the portal vein was exposed by blunt dissection taking care not to disturb the nerve bundle located on the vessel. A 6 or 8 mm ID ultrasonic flow probe (Transonic Systems Inc, Ithaca, NY) was placed around the vessel. A small portion of the common hepatic artery was also carefully exposed and a 3 mm ID ultrasonic flow probe was secured around the vessel. The flow probes were used to

determine portal vein and hepatic artery blood flow during experiments. To prevent blood from entering the portal vein beyond the site of the flow probe, the gastroduodenal vein was isolated and ligated. Blood that would normally flow through the gastroduodenal vein was shunted through the caudal pancreatoduodenal vein draining the tail of the pancreas. The ultrasonic flow probe leads were positioned in the abdominal cavity, secured to the abdominal wall, and placed in a subcutaneous pocket prior to closure of the abdominal skin.

The subcutaneous layer was closed with a continuous suture of 3-0 Vicryl (Ethicon, Inc). The skin was closed with horizontal mattress sutures of 3-0 Ethilon (Ethicon, Inc.). Metacam (0.2 mg/kg S.C.) was administered 30 minutes prior to surgical recovery for acute pain relief. Animals awoke from surgery within 2 h, were active, and ate normally approximately 8 h after surgery. For 3 post-operative days, dogs received 10 mg/kg Simplicef (Pfizer Animal Health, New York City, NY) orally, once a day.

Partial Pancreatectomy

Prior to commencing the HFFD in Specific Aims I and II, each dog underwent a laparotomy in which a sham operation (Sh; $n=13$) or a partial pancreatectomy (Px, approximately 65% removal; $n=11$) was performed. The Px was utilized as a surgical tool to compromise endocrine pancreatic function in the hope that, when coupled with a dietary insult, a diabetic phenotype would emerge that mimicked the metabolic characteristics of type 2 diabetes. Briefly, the pancreatic-duodenal artery and vein were isolated along with isolation of the right lobe of the pancreas from its mesenteric connections. The right lobe was ligated and transected at the union of the right lobe caudal extremity and the distal duodenum while preserving the venous and arterial

vasculature of the duodenum. The pancreatico-duodenal artery and vein were ligated and transected at the distal end of the lobe and the right pancreatic lobe was removed. Next, the pancreatico-splenic arteries and veins were identified and isolated. The left lobe was ligated and transected at the union with the pylorus in the apical portion of the pancreas. The mesenteric and omental connections and the arterial and venous vasculature supplying the left lobe were ligated and transected, and the left pancreatic lobe was removed. Approximately 35% of the pancreas remained in place with intact exocrine and biliary tree function.

All dogs studied had: 1) leukocyte count $<18,000/\text{mm}^3$, 2) a hematocrit $>35\%$, 3) a good appetite, and 4) normal stools at the time of study. On the morning of the clamp experiment, the free ends of the catheters and ultrasonic leads were removed from their subcutaneous pockets under local anesthesia (2% lidocaine; Abbott Laboratories, North Chicago, IL). The contents of each catheter were aspirated, and flushed with saline. Blunt needles (18 gauge; Monoject, St. Louis, MO) were inserted into the catheter ends, and stopcocks (Medex, Inc, Hilliard, OH) were attached to prevent the backflow of blood between sampling times. Twenty gauge Angiocaths (Beckton Dickson) were inserted percutaneously into the left and right cephalic and saphenous veins for the infusion of labeled (3- ^3H)-glucose; left cephalic) and unlabeled (50% dextrose; right cephalic) glucose, para-aminohippuric acid (Specific Aims I, III, and IV; PAH; right saphenous), and somatostatin (SRIF; left saphenous). A continuous infusion of heparinized saline was started via the femoral artery at a rate to prevent blood clotting in the line. For oral glucose tolerance tests and hyperinsulinemic euglycemic clamp experiments (OGTTs and HIEGs, respectively; Specific Aim I), deep venous sampling catheters (19 ga catheter,

adjustable up to 18 in; MILA International Inc., Erlanger, KY) were inserted into the left or right saphenous vein and advanced 30 cm to reach inferior vena cava. Animals were allowed to rest quietly in a Pavlov harness for 30 min before commencing the experiment.

Experimental Diets

Table 2.1: Macronutrient compositions of experimental diets utilized in Specific Aims I-IV.

Macronutrient	Percentage of Total Energy			
	CTR	HFFD	HFA	HFR
Fat	26.0	52.0	52.0	26.0
Protein	31.0	22.0	22.0	26.0
Carbohydrate	43.0	26.0	26.0	48.0
Starch	41.0	8.5	21.0	24.0
Glucose	<1.0	<0.1	<0.1	<0.1
Fructose	<1.0	17.0	<0.1	17.0
Sucrose	1.3	<1.0	<1.0	<1.0
Lactose	<1.0	<1.0	<1.0	<1.0
Mean Daily Energy Intake (kcal/day)	2000 ± 30	3200 ± 70	2800 ± 50	2800 ± 20

Dogs were fed once daily a pre-determined quantity (to match daily energy intake in HFFD, HFA, and HFR) of one of the following diets: 1) meat (Kal Kan, Franklin, TN) and laboratory chow diet (Laboratory Canine Diet 5006, chunk form; Control or CTR); 2) high-fat/high-fructose diet (5A4J, short cut pellet form; HFFD); 3) high-fat diet (modification of 5A4J with cornstarch replacing fructose, short cut pellet form; HFA); 4) high-fructose diet (modification of 5A4J with lower fat content, short cut pellet form; HFR). PMI Nutrition TestDiet in St. Louis, MO produced each diet. The feeding paradigms for each Specific Aim are outlined in Table 2.2.

Table 2.2: Experimental diet assignment, feeding duration (weeks), and sample size (*n*) for Specific Aims I-IV.

Diet	Specific Aim			
	I	II	III	IV
CTR	13 weeks (Sh, <i>n</i> =4)	8 weeks (<i>n</i> =5)	4 weeks (<i>n</i> =15)	4 weeks (<i>n</i> =5)
HFFD	13 weeks	8 weeks (<i>n</i> =5)	4 weeks (<i>n</i> =16)	-----
	(Sh, <i>n</i> =4; Px, <i>n</i> =6)			
HFA	-----	-----	-----	4 weeks (<i>n</i> =5)
HFR	-----	-----	-----	4 weeks (<i>n</i> =5)

Collection and Processing of Samples

Blood Samples

Before the start of the experiment, a blood sample was drawn and used for the preparation of PAH standards and hormone infusions when applicable. During the study, blood samples were drawn from the femoral artery and portal and hepatic veins at the predetermined sampling points indicated in the experimental protocols. Prior to acquisition of the blood sample, the respective sampling catheter was cleared of saline by withdrawing 5 ml of blood into a syringe. The blood sample was then drawn using a separate syringe, after which the cleared blood was re-infused into the animal, and the catheter was flushed with heparinized saline (1U/ml; Abbott Laboratories, North Chicago, IL). In addition, whenever the experimental design required a glucose clamp, small (~0.5 ml) arterial or deep venous blood samples were drawn every 5 min for

assessment of the plasma glucose concentration. When samples were taken from all three vessels, the arterial and portal blood samples were collected simultaneously ~30 s before the collection of the hepatic venous sample in an attempt to compensate for the transit time through the liver, and thus allow the most accurate estimates of net hepatic substrate balance [254]. The total volume of blood withdrawn did not exceed 20% of the animal's blood volume, and two volumes of saline were given for each volume of blood withdrawn. No significant decrease in hematocrit occurred with this procedure.

Immediately following sample collection, the blood was processed. A small arterial aliquot (20 μ l) was used for the assessment of hematocrit in duplicate using capillary tubes (0.4 mm ID; Drumond Scientific Co., Broomall, PA). The remaining blood was quickly placed into tubes containing potassium ethylenediaminetetraacetate (EDTA, 1.6 mg EDTA/ml; Sarstedt, Newton, NC), inverted and mixed gently. One-half ml of whole blood was removed from the above tube and lysed with 1.5 ml of 4% perchloric acid (PCA; Fisher Scientific, Fair Lawn, New Jersey). The solution was vortexed, centrifuged, and the supernatant was stored for later determination of whole-blood metabolites (alanine, glycerol, and lactate). For Specific Aim II, 1 ml of whole blood was added to a tube containing 10 μ l of DPP-IV inhibitor (Linco Research, St. Charles, MO) to ensure the integrity of the GLP-1. This aliquot was then centrifuged, and the supernatant was stored on dry ice for later determination of plasma GLP-1 levels. The remainder of the whole blood containing EDTA was centrifuged at 3000 rpm for 6 minutes at 4°C to obtain plasma.

Four to eight 10 μ l aliquots of plasma from each sample were immediately analyzed for glucose using the glucose oxidase technique in a glucose analyzer (Analox

Instruments, London, U.K.) A 1 ml aliquot of plasma received 50 μ l of 10,000 KIU/ml Trasylol (aprotinin; FBA Pharmaceuticals, New York, NY), a protease inhibitor, and was stored for analysis of immunoreactive glucagon and c-peptide. A 10 μ l aliquot of tetrahydrolipstatin (THL, Xenical; Roche Pharmaceuticals, Nutley, NJ) was added to a 0.5 ml aliquot of plasma for the measurement of non-esterified free fatty acid (NEFA) concentrations. To ensure that the assessment of portal venous plasma insulin concentrations was on the linear range of the insulin assay standard curve, 400 μ l of portal vein plasma was mixed with 400 μ l of insulin assay buffer for a 1:1 dilution. The remainder of the plasma was used for analysis of 3-[³H]-glucose (in triplicate), total triglycerides, and cortisol. All samples were kept in an ice bath during the experiment and were then stored at -80°C until the assays were performed. Plasma samples for the assessment of 3-[³H]-glucose were deproteinized according to the method of Somogyi-Nelson [255-257]. Briefly, 1 ml aliquots of saline and plasma (0.5 ml saline + 0.5 ml plasma) were mixed with 5 ml of 0.067 N Ba(OH)₂ and 5 ml of 0.067 N ZnSO₂ (Sigma Chemical). Samples were shaken and stored at 4°C for 1-3 days prior to processing.

Tissue Samples

Immediately after the final sample was attained, each animal was anesthetized with an I.V. injection of sodium pentobarbital (390 mg/ml Fatal-Plus; Vortech Pharmaceutical Inc., Dearborn, MI) at 125 mg/kg. The animal was then removed from the Pavlov harness while the tracers, hormones, and glucose continued to infuse. A midline laparotomy incision was made, the liver was exposed, and clamps cooled in liquid nitrogen were used to simultaneously freeze portions of the left central, left lateral,

and right central hepatic lobes *in situ*. The hepatic tissue was immediately immersed in liquid nitrogen, and stored at -80°C. Approximately two minutes elapsed between the time of anesthesia and the time of tissue sampling. All animals were then euthanized.

Sample Analysis

Whole Blood Metabolites

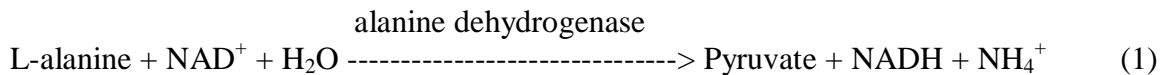
Whole blood metabolite concentrations were determined using the methods developed by Lloyd *et al.* [258] for the Technicon Autoanalyzer (Tarrytown, NY) and were modified to the Packard Multi Probe Robotic Liquid Handline System (Perkin Elmer; Shelton, CT). Enzymes and coenzymes for metabolic analyses were obtained from Boehringer-Mannheim Biochemicals (Germany) and Sigma Chemicals. These assays rely upon a reaction in which NAD (oxidized) is reduced to NADH. In contrast to the oxidized form, NADH has a native fluorescence; as the reaction proceeds and NADH is produced, the system detects changes in fluorescence via a fluorometer incorporated in the system. Thus, the concentration of the metabolite in a given sample is proportional to the amount of NADH produced.

Metabolites were measured in the PCA-treated blood samples as described under *Collection and Processing of Samples*. A standard curve was constructed for each metabolite using known concentrations of the analyte prepared in 3% PCA. The Packard Multi Probe Robotic Liquid Handling System pipettes the sample into one well of a 96 well plate. For the analysis of alanine and glycerol, an initial reading is taken, after which the system pipettes enzyme solution into each well, shakes the plate to ensure adequate

mixing of the sample and enzyme, and the reaction then proceeds. After a designated period of time, the change in absorbance is recorded. When lactate is assayed, an intermediate reading is taken half way through the run, and then another reading is obtained at the end. Excluding glycerol kinase, all assay reactions are reversible. However, the NAD and enzyme are in excess compared to the substrate, thus the reactions are essentially taken to completion with the substrate being the rate-limiting component. As a result, all reactions written below are presented with a single direction arrow. All reactions were carried out at 23°C.

Alanine

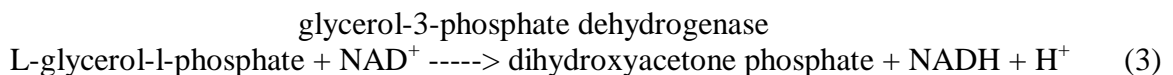
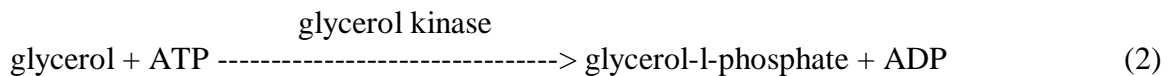
The alanine assay involved the reaction:



The enzyme buffer used was 0.05 M trizma base, 2 mM EDTA and 1 mM hydrazine hydrate, pH 10. To 10 ml of enzyme buffer, 4.6 mg of NAD and 3.4 Units (U) of alanine dehydrogenase were added.

Glycerol

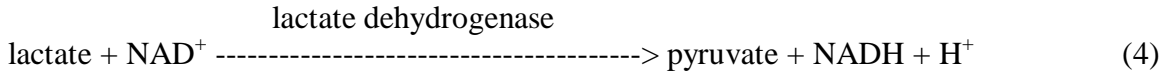
The glycerol assay involved the following reactions:



The enzyme buffer was 0.09 M glycine, 1 mM hydrazine, and 0.01 M MgCl₂, pH 9.5. To 10 ml of the enzyme buffer, 15.4 g NAD, 15.4 mg ATP, 0.3 U glycerokinase, and 0.6 U glycerol-3-phosphate dehydrogenase were added.

Lactate

The lactate assay involved the following reaction:

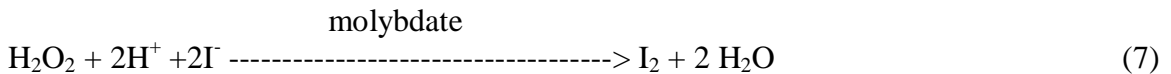
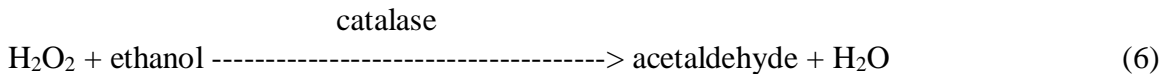
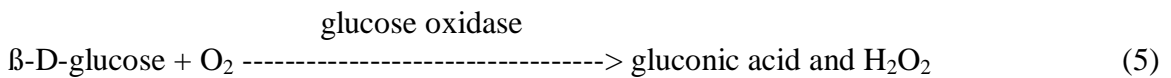


The enzyme buffer used was 0.24 M glycine and 0.25 M of hydrazine dihydrochloride and 7 mM disodium EDTA, pH 9.6. To 10 ml of enzyme buffer, 4.6 mg NAD and 0.1 U lactate dehydrogenase were added.

Plasma Metabolites

Plasma Glucose

Plasma glucose concentrations were determined using the glucose oxidase method [259] with a glucose analyzer (Analox Instruments, Lunenburg, MA). The reaction sequence was as follows:



The plasma glucose concentration is proportional to the rate of oxygen consumption, and the glucose level in a plasma sample is determined by comparison of the oxygen

consumption in the samples with the rate of oxygen consumption by a standard solution. The second and third reactions quickly remove all hydrogen peroxide so that there is no end-product inhibition of the process. Glucose was measured 4 times at each sampling time point for each vessel and a minimum of 2 times for samples drawn to clamp glucose. The glucose analyzer is accurate to 450 mg/dl.

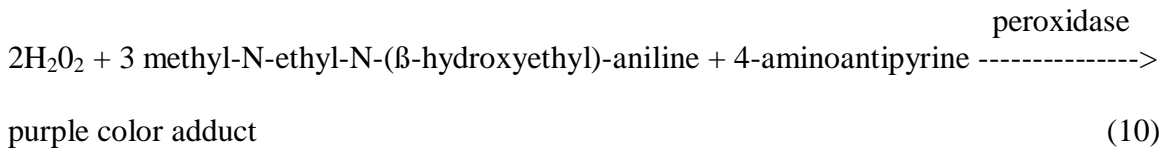
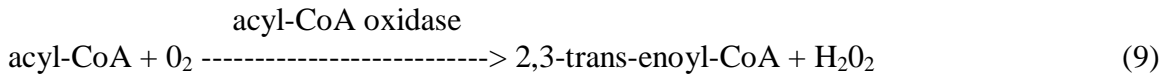
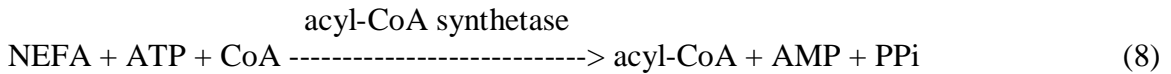
Plasma 3-[³H]-glucose

For determination of plasma 3-[³H]-glucose, samples were deproteinized according to the method of Somogyi-Nelson [255-257]. Immediately following each experiment, three 1 ml aliquots of plasma + saline (1:1) from each sample were mixed with 5 ml of 0.067 N Ba(OH)₂ and 5 ml of 0.067 N ZnSO₂ (Sigma Chemical). These samples were kept at 4°C for 1-3 days, after which they were centrifuged at 3000 rpm for 30 min. A 5 ml aliquot of the supernatant was pipetted into a glass scintillation vial and placed in a heated vacuum oven to evaporate ³H₂O. The residue was reconstituted in 1 ml of deionized water and 10 ml liquid scintillation fluid (EcoLite (+); Research Product Division, Costa Mesa, CA), and placed in Beckman LS 9000 Liquid Scintillation Counter (Beckman Instruments Inc, Irvine, CA). The counter was programmed so that the processor corrected the counts per minute (cpm) for quenching of the radioactivity in the sample, and presented the data as disintegrations per minute (dpm). To assess for the loss of labeled glucose during the deproteinization step, a recovery standard was created. The 3-[³H]-glucose infusate was diluted 1:250 (v:v) with saturated benzoic acid. Six, 1 ml aliquots of this diluted ³H infusate were placed into 2 sets of glass scintillation vials and were labeled as chemical standard evaporated (CSE) or chemical standard (CS). The diluted infusate aliquots in the CSE vials were evaporated to dryness in a heated vacuum

oven, reconstituted with 1 ml of deionized water plus 10 ml of scintillation fluid and counted. The diluted infusate aliquots in the CS vials were not evaporated, but had scintillation fluid added and were counted. Three additional 1 ml aliquots of diluted ^3H infusate were treated in a manner identical to the plasma samples and labeled chemical recovery standard (CRS). Comparison of the CS and CSE provided an evaluation of the loss of ^3H counts in the evaporation process. The ratio of radioactivity in the CSE samples compared to the CRS samples generated a recovery factor that was used to determine the final radioactivity by accounting for the loss during sample processing.

Non-esterified fatty acids

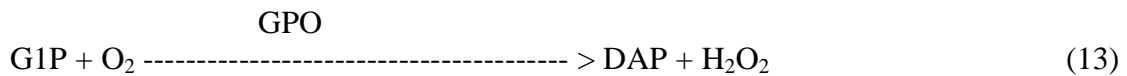
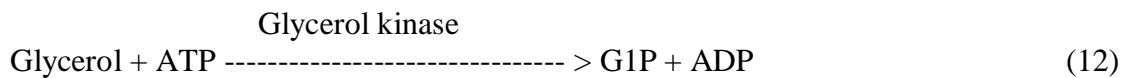
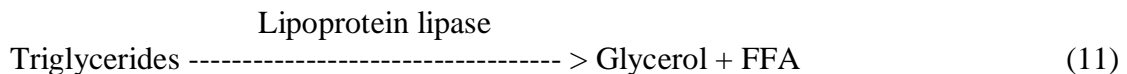
Plasma non-esterified fatty acids were determined spectrophotometrically using the Packard Multi probe Robotic Liquid Handling System (Perkin Elmer; Shelton, CT) and a kit from Wako Chemicals (Richmond, VA). The following reactions were used in the analysis:



The purple colored adduct optical density was measured at 550 nm and is proportional to the NEFA concentration in the sample. The NEFA values were then obtained from a calibration curve with known amounts of oleic acid. This reaction was run at 37°C.

Triglycerides

Plasma triglyceride levels were assessed by the enzymatic measurement of glycerol, true triglycerides, and total triglycerides in plasma using the Spectramax Plus 384 (Molecular Device Corp. Sunnyvale, CA) and the Serum Triglyceride Determination Kit (Sigma, St. Louis, MI). The assay was performed in a 96 well plate. The procedure involves enzymatic hydrolysis of triglycerides by lipoprotein lipase to free fatty acids (FFA) and glycerol. Glycerol is then phosphorylated by glycerol kinase and adenosine-5'-triphosphate (ATP) resulting in the production of glycerol-1-phosphate (G1P) and adenosine-5'-diphosphate (ADP). G1P is then oxidized by glycerol phosphate oxidase (GPO) to dihydroxyacetone phosphate (DAP) and hydrogen peroxide (H₂O₂). H₂O₂ is then coupled with 4-aminoantipyrine(4-AAP) and sodium N-ethyl-N-(3-sulfopropyl)-anisiden (ESPA) producing quinoneimine dye (absorbance 540 nm). The increase in absorbance is directly proportional to the triglyceride levels of the plasma sample. The assay was run at 37°C. The triglyceride concentrations were calculated using a calibration curve of known amounts of glycerol. The specific reactions were as follows:



Hormones

The plasma hormone levels of insulin, glucagon, cortisol, and c-peptide were measured using radioimmunoassay (RIA) techniques [260]. Briefly, a plasma sample

containing an unknown amount of hormone was incubated with an antibody specific for that hormone. A known amount of radiolabeled hormone was added to the mixture to compete with the antibody binding sites. A double antibody procedure (single antibody procedure for cortisol), which caused precipitation of the bound complex, was used to separate unbound hormone from the antibody-hormone complexes. The radioactivity of the precipitate was measured via a Cobra II Gamma Counter (Packard Instrument Co, Meriden, CT). The binding of the radiolabeled hormone was inversely proportional to the amount of unlabeled hormone present. A standard curve was constructed using known concentrations of the unlabelled hormone.

Insulin

Immunoreactive plasma insulin was measured using a double-antibody RIA procedure [261]. Insulin antibodies and ^{125}I tracers were obtained from Linco Research Inc. (St. Charles, MO). A 100 μl aliquot of the plasma sample was incubated 18h at 4°C with 200 μl of ^{125}I -labeled insulin and 100 μl guinea pig specific antibody to insulin. The sample was then treated with 100 μl goat anti-guinea pig IgG (2nd antibody) and 100 μl IgG carrier and incubated for 30 min at 4°C. One ml of a wash buffer was added, and the tubes were centrifuged at 3000 rpm. The liquid portion of the samples was decanted and the remaining pellet containing the total radioactivity bound to the antibody was counted in a Cobra II Gamma Counter. The log of the amount of hormone in the samples was inversely proportional to the log (bound label/free label). The insulin concentration in each sample was determined by comparison to a standard curve constructed using known amounts of unlabeled hormone. The samples were corrected for non-specific binding. The sample detection range was 1-150 $\mu\text{U/ml}$. The specificity of the antibody is 100% to

porcine, canine, and human insulin, but cross-reacts with bovine insulin (90%), human proinsulin (38%), and the split proinsulin products Des 31,32 (47%) and Des 64,65 (72%). In general, less than 15% of the basal insulin level is due to non-insulin material. The antibody has no cross-reactivity with glucagon, pancreatic polypeptide, C-peptide, or somatostatin. The recovery for the assay was between 90-100% and the interassay CV was approximately 7-8% for the entire range of the dose response curve.

Glucagon

Immunoreactive glucagon was measured using a double antibody insulin RIA [262]. The protocol utilized primary and secondary antibodies specific for glucagon. Glucagon antibodies and ^{125}I tracers were obtained from Linco Research (St. Louis, MO). A 100 μl aliquot of the plasma sample was incubated for 24 hours at 4°C with 100 μl of guinea pig specific antibody to glucagon. Next, 100 μl of ^{125}I -labeled glucagon was added to the solution and incubated for 24 h at 4°C. Afterwards, the samples were incubated for 2 h at 4°C with 100 μl of both goat anti-guinea pig IgG (2nd antibody) and IgG carrier. One ml of a wash buffer was added and the tubes were centrifuged at 3000 rpm. The samples were decanted and the portion of total radioactivity bound to the antibody (pellet) was counted in a Cobra II Gamma Counter. The log of the amount of hormone in the sample was inversely proportional to the log (bound label/free label). The glucagon concentration in each sample was determined by comparison to a standard curve constructed using known amounts of unlabeled hormone. The samples were corrected for non-specific binding. The sample detection range was 20-400 ng/l. The antibody is 100% specific to glucagon with only slight (0.01 %) cross reactivity to oxyntomodulin, and no cross reactivity with human insulin, human proinsulin, human C-

peptide, glucagon-like peptide-1, somatostatin or pancreatic polypeptide. However, due to a cross-reacting protein effect, this assay reads 15-20 pg/ml above the actual glucagon level, representing a stable, constant background in all samples. The recovery for the assay was between 80-100%, and the interassay CV was approximately 6-10% for the entire range of the dose response curve.

C-peptide

Canine C-peptide was measured using a double antibody disequilibrium procedure similar to that used for glucagon [263]. Kits containing canine C-peptide antibody and ^{125}I tracer were obtained from Linco Research (St. Louis, MO). A 100 μl aliquot of the plasma sample was incubated for 24 h at 4°C with 100 μl of guinea pig-specific antibody to canine C-peptide. Then, 100 μl of ^{125}I -labeled canine C-peptide was added and incubated for 24 h at 4°C , after which the sample was incubated with 1 ml of precipitating agent containing anti-guinea pig IgG (2nd antibody) and IgG carrier for 30 min at 4°C . Tubes were centrifuged, decanted, and the portion of total radioactivity bound to the antibody (pellet) was counted in a Cobra II Gamma Counter. The log of the amount of hormone in the sample was inversely proportional to the log (bound label/free label). The C-peptide concentration in each sample was determined by comparison to standards dissolved in plasma using known amounts of unlabeled hormone. Samples were corrected for non-specific binding. The sample detection range was 0.1-10 ng/ml. The antibody is 100% specific for canine C-peptide with no cross-reactivity to rat C-peptide, human C-peptide, human proinsulin, bovine proinsulin, porcine proinsulin, or glucagon. The recovery of the assay was approximately 90%.

Glucagon-like Peptide-1 (GLP-1)

For Specific Aim II, plasma GLP-1 levels were determined using an enzyme-linked immunosorbent assay (ELISA) kit (Linco Research, Inc.) A 100 µl aliquot of plasma (pretreated with DPP-IV inhibitor as described in *Collection and Processing of Samples*) and 100 µl of assay buffer were manually pipetted into a well of a 96-well plate, bound with monoclonal antibodies specific to the N-terminal region of active GLP-1 molecules, and incubated at 4°C overnight. After a series of washes, 200 µl of methyl umbelliferyl phosphate (MUP) was added and incubated in the dark for 25 min at room temperature. MUP, in the presence of alkaline phosphatase, forms the fluorescent product umbelliferone. This reaction was stopped with 50 µl of stop buffer. Immediately after stop solution was added, excitation/emission wavelength was read at 365/450 nm on a fluorescence plate reader (Packard Fusion, PerkinElmer, Waltham, MA).

All samples were pipetted in duplicate, and read by the plate reader three times. The amount of fluorescence generated was directly proportional to the concentration of active GLP-1 in the sample. Quantification of plasma GLP-1 levels was derived from a standard curve run on the same plate as the samples. This assay is highly specific for active forms of GLP-1 [GLP-1 (7-36) amide and GLP-1 (7-37)], with no cross-reactivity to other forms of GLP-1 (e.g., 1-36 amide, 1-37, 9-36 amide, 9-37), and is reliable in a range of 2-100 pM.

Acetaminophen

For Specific Aim II, arterial plasma acetaminophen levels were measured using a modified protocol designed for high performance liquid chromatography (HPLC) [264]. A

500 ml aliquot of plasma was spiked with 20 μ l of 2-acetaminophenol (40 μ g/ml) to serve as an internal standard [265]. Equal volumes of spiked plasma, 0.3 N barium hydroxide, and 0.3 N zinc sulfate were mixed and incubated on ice for 5 min. The sample was then spun at 4°C at 3000 rpm for 10 min. The decanted supernatant was dried using vacuum centrifugation (Speedvac Concentrator, Savant SVC 200H, Thermo Scientific, Waltham, MA). The sample was then reconstituted with 200 μ l of a 10% methanol/water solution (v:v). A 50 μ l aliquot was injected for delivery into the HPLC column (uBondapak C18 3.9x30 w/guard), at a temperature of 45°C. The mobile phase A (5% methanol/water, v:v) and B (15% methanol/water, v:v) were set at a combined flow rate of 0.4 ml/min for the entire duration of the assay. With the profile curve indicating the type of transition from one setting to the next, the gradient for the mobile phase was set as follows: initial setting at 100% A, 0 profile curve; t=4 min at 100% A, 11 profile curve; t=20 min at 75% A, 25% B, 6 profile curve; t=30 min at 100% B, 7 profile curve; t=40 min at 100% A, 11 profile curve. The total run time was 64 min, with an 18 min acquisition delay. Fluorescence was measured with variable wavelength UV detector (Waters 481, Millipore, Billerica, MA) set at 240 nm at 0.5 AUFS.

Peak area as identified by the ESA 500 Chromatograph and data station are representative of acetaminophen concentration. Peak area increases in a linear fashion, proportional to acetaminophen concentration. Thus, sample concentration is determined as a ratio of acetaminophen peak area in the sample to internal standard peak area. This assay has been validated up to concentrations of 40 μ g/ml.

Hepatic Blood Flow

Total hepatic blood flow in the hepatic artery and portal vein was measured by use of ultrasonic flow probes (Transonic Systems Inc, Ithaca, NY) that were implanted during surgery, as described in *Surgical Procedures*. Ultrasonic flow measurements demonstrated instantaneous variations in velocity and provided blood flow in individual vessels. This method determines the mean transit time of an ultrasonic signal passed back and forth between two transducers within a probe that are located upstream and downstream of the direction of blood flow in the vessel. The transducers are made of piezoelectric material, which is both capable of receiving and transmitting the ultrasonic signal. The downstream transducer emits an ultrasonic pulse into the blood vessel that is received upstream by a second transducer. After the upstream transducer receives the ultrasonic signal, it re-emits the ultrasonic pulse signal back to the downstream transducer. The transit time of each ultrasonic beam, as measured by the upstream and downstream transducers (ΔT_{up} and ΔT_{down} , respectively) is defined by the following relationships:

$$\Delta T_{up} = D / (v_o - v_x) \quad (14)$$

$$\Delta T_{down} = D / (v_o + v_x) \quad (15)$$

where D is the distance traveled by the ultrasonic beam within the acoustic window of the probe, v_o is the phase velocity, or the speed of sound, in blood, and v_x is the component of fluid velocity that is parallel or antiparallel to the phase velocity. The parallel component augments the phase velocity when the signal is traveling in the same direction of blood flow, while the antiparallel component subtracts from phase velocity if the

ultrasonic signal is moving against the flow of blood in the vessel. Combining the two expressions for transit time yields the following equation:

$$\Delta T_{\text{up}} - \Delta T_{\text{down}} = [D / (v_0 - v_x)] - [D / (v_0 + v_x)] \quad (16)$$

Since the transit times measured by both transducers, the distance traveled by the beam, and the speed of sound in blood are all known quantities, this equation can be used to calculate v_x . Once v_x is attained, the transit velocity (V) of blood traveling through the vessel can be determined according to the following equation:

$$V \cos \theta = v_x \quad (17)$$

where θ is the angle between the centerline of the vessel and the ultrasonic beam axis.

Finally, the product of the transit velocity and the cross-sectional area of the vessel determine blood flow. The cross-sectional area of the vessel is pre-determined by the size of the acoustic window according the probe model. Since transit time is sampled at all points across the diameter of the vessel, volume flow is independent of the flow velocity profile.

Liver Tissue Analysis

Liver Glycogen Content

Liver glycogen content was determined using a modification of the method of Keppler and Decker [266]. Frozen liver tissue was ground and weighed (180-200 mg) while kept chilled with liquid nitrogen. The tissue weight (mg) was multiplied by 5 to determine the volume (ml) of 0.6 N PCA to be used. The tissue was combined with the PCA then thoroughly homogenized. A 200 μ l aliquot was then combined with 100 μ l

KHCO₃ to neutralize the sample. A 500µl aliquot of amyloglucosidase in sodium acetate solution (2 mg amyloglucosidase / ml 0.4 M sodium acetate buffer) was incubated in a shaker bath at 40°C for 2 hrs. Glycogen concentration was calculated by subtracting the glucose concentration in duplicate samples not treated with the enzyme from samples incubated with amyloglucosidase. [³H]-glycogen counts were determined in the supernatant after evaporation, reconstitution, and counting as discussed previously for determination of plasma 3-[³H]-glucose.

Liver Total Triglyceride Content

Approximately 100 mg of tissue was homogenized in chloroform/methanol (2:1 v/v) and the lipids were extracted using a modified method of Folch-Lees [267]. The homogenates were then filtered through sharkskin filter paper. 0.1 M potassium chloride was added to separate the chloroform and methanol layers. The chloroform phase was removed, dried down, and the individual classes of lipids were separated by thin layer chromatography using a Silica Gel 60 A plate developed in acetic acid (80:20:1), ethyl ether, and petroleum ether, and visualized by rhodamine 6G. Phospholipids and acylglycerol bands were scraped from the plates and methylated using boron trifluoride/methanol as described by Morrison and Smith [268]. Methylated fatty acids were extracted and analyzed by gas chromatography. Gas chromatographic analysis was carried out on an HP 5890 gas chromatograph equipped with flame ionization detectors, an HP 3365 Chemstation, and a capillary column (SP2380, 0.25 mm x 30 m, 0.25 µm film, Supelco, Bellefonte, PA). Helium was used as a carrier gas. Fatty acid methyl esters were identified by comparing the retention times to those of known standards. Inclusion

of lipid standards with odd chain fatty acids permitted quantification of the amount of lipid in the sample. Standards used were dipentadecanoyl phosphatidylcholine (C15:0) and triicosenoin (C20:1).

RNA Extraction, cDNA Synthesis, and Real-Time PCR

Total RNA was extracted by homogenizing 50 mg of canine liver in 1 mL of Tri-reagent (Sigma, St. Louis, MO) following the manufacturer's instructions. The RNA pellet was dissolved in nuclease-free TE buffer (where from). The purity of the RNA in solution was verified based on A260/A280 ratios greater than 1.8, whereas the integrity of the RNA was verified using ethidium bromide-stained agarose gels. First strand cDNA was synthesized from 1 µg of total RNA using the High Capacity reverse transcription kit (ABI, Foster City, CA) as per manufacturer's directions, and cDNA was stored at -80°C until use. Primers were designed and analyzed using Premier Biosoft International Beacon Designer Software (Palo Alto, CA). Real-time PCR primer specificity was determined by BLAST analysis. Primer efficiencies were validated to be between 91-96%, and primer specificity was confirmed by melt curve analysis. The sequences of canine primer pairs were as follows: *GK*, 5'-CAGAGGGGACTTTGAAATG-3' and 5'-ATGAATCCTTACCCACAATC-3'; *RPL13*, 5'-GCCGGAAGGTTGTAGTCGT-3' and 5'-GGAGGAAGGCCAGGTAATTC-3'. Real-time PCR analysis was performed using a BioRad iCycler Detection System (CFX96) with iQ SYBR Green Supermix fluorophore (BioRad) and the following protocol: step 1, 95°C for 3 min (1x); step 2, 95°C for 10 s; step 3, 55°C for 30 s (steps 2 and 3 were repeated 39 x). Reactions were initiated by adding 100 ng of cDNA template to 25 µL total reaction mix, which consisted of the

following: 12.5 μ L iQ SYBR Green Supermix, 2 μ L of 5 μ M forward primer (0.4 μ M final concentration), 2 μ L of 5 μ M reverse primer (0.4 μ M final concentration), 6.5 μ L nuclease free water, and 2 μ L cDNA template. Target genes were normalized to RPL13 (reference gene) using the Livak method [269], and expressed relative to basal CTR animals. Melt curve analysis was performed after every run and samples were run in duplicate. Relative gene expression data comprise the average of 2 to 3 runs per target gene. In addition, gene expression analysis was performed on liver tissue from the left central and left lateral lobes because they represent approximately 50% of the total liver mass of the dog.

Western Blotting

Frozen liver tissue (~50 mg) was combined with 1 ml of homogenizing buffer (pH 7.2; 20 mM Tris, 200 mM NaCl, 50 mM NaF, 1 mM EDTA, 1 mM EGTA, 10% v:v glycerol, 10 μ l/ml buffer of phosphatase inhibitor cocktail 1 and 2, and protease inhibitor cocktail [Sigma; St. Louis, MO]) and thoroughly homogenized. Tissue homogenates were centrifuged at 12,000 g for 15 min, after which the supernatants were removed and soluble protein concentration was determined using the BioRad Protein Assay (BioRad; Hercules, CA). Aliquots of supernatant were mixed 1:1 (v:v) with freshly prepared 2X SDS-PAGE loading buffer (100 mM Tris-HCl pH 6.8, 4% w:v SDS, 20% v:v glycerol, 0.2% w:v bromophenol blue, 10% v:v 2-mercaptoethanol), and denatured at ~85-90°C for 10 min. Samples were subjected to SDS-PAGE (4-12% resolving gel) for ~ 2 hrs at 180 V, followed by transfer to nitrocellulose membranes for 1.5 hrs at 60 V. Nitrocellulose membranes, SDS-PAGE, and wet-transfer reagents were supplied by

Invitrogen (Carlsbad, CA). Membranes were blocked for 1 hr at room temperature in 5% (w:v) bovine serum albumin in Tris-buffered saline containing Tween 20 (TBS-T: 10 mM Tris-base pH 7.0, 150 mM NaCl, 0.2% v:v Tween 20). Upon blocking, membranes were incubated overnight with the appropriate primary antibody at 4°C. After 3 x 5 min washes with TBS-T, membranes were incubated with HRP-conjugated secondary antibody (Promega, Madison, WI) for 1 hr at room temperature, followed by 3 x 5 min washes in TBS-T. Proteins were visualized using ECL Plus Western detection reagents (GE Healthcare, Piscataway, NJ), and the ECL signals were detected after brief (1-60 sec) exposure to X-ray film (BioMax Light X-ray films, Kodak, Chalon-sur-Saone, France). Bands were quantified via densitometric analysis using ImageJ software (<http://rsb.info.nih.gov/ij/>), and the intensity of the target protein signal was normalized against that of β -Actin. Antibodies specific for phosphorylated Akt (Ser473), GSK3 β (Ser9), and GS (Ser641) were purchased from Cell Signaling Technology, Inc. (Danvers, MA), whereas the GGRP and actin antibodies were purchased from Santa Cruz Biotechnology Inc. (Santa Cruz, CA). The GK antibody was a gift from Dr. Masakazu Shiota (Vanderbilt University School of Medicine, Molecular Physiology & Biophysics Department). The following antibody dilutions were used: GK and GGRP, 1:10,000; Akt (Ser473), GSK3 β (Ser9), GS (Ser 641), and Actin, 1:5000. Relative protein data comprise the average of 2 to 3 western blots per test protein. In addition, western blotting experiments were performed on liver tissue from the left central and left lateral lobes because they represent approximately 50% of the total liver mass of the dog.

Glucokinase Activity

To assess the catalytic activity of hepatic glucokinase (GK) [270], 200 mg of freeze-clamped liver was homogenized in 2 ml of buffer containing 50 mmol/l HEPES, 100 mmol/l KCl, 1 mmol/l EDTA, 5 mmol/l MgCl₂, and 2.5 mmol/l dithioerythritol. Homogenates were centrifuged at 100,000g for 45 min to sediment the microsomal fraction. The post-microsomal fraction (10 µl) was assayed in 1 ml of incubation buffer (37°C, pH 7.4) containing 50 mmol/l HEPES, 100 mmol/l KCl, 7.5 mmol/l MgCl₂, 5 mmol/l ATP, 2.5 mmol/l dithioerythritol, 10 mg/ml albumin, 0.5, 8, and 100 mmol/l glucose, 0.5 mmol/l NAD⁺, and 4 units/ml of G-6-P dehydrogenase (*Leuconostoc mesenteroides*). The reaction was initiated by the addition of ATP, and the rate of NAD⁺ reduction was recorded at 340 nm for 30 min. Glucose phosphorylation by GK was determined as the absorbance change in the presence of 8 or 100 mmol/l glucose minus the absorbance change in the presence of 0.5 mmol/l glucose under conditions in which the absorbance was increasing linearly between 10 and 30 min. This assay is not reflective of the subcellular compartmentation of GK or its association with GK regulatory protein.

Glycogen Synthase and Phosphorylase Activity

Hepatic glycogen synthase (GS) activity was determined by measuring the incorporation of [¹⁴C]-glucose from UDP-[¹⁴C]-glucose into glycogen in the absence or presence of 7.2 mM glucose-6-phosphate [271]. Glycogen phosphorylase (GP) activity was assayed by measuring the incorporation of [¹⁴C]-glucose from [¹⁴C]-glucose-1-phosphate into glycogen in the absence or presence of 2 mM AMP [272]. Activity ratios

represent the activity measured in the absence divided by that in the presence of the allosteric effectors glucose-6-phosphate for GS or AMP for GP, and are indicative of the phosphorylation state of the enzyme.

Calculations

Net Hepatic Substrate Balance

The net hepatic balance of a substrate (NHSB) was calculated as:

$$\text{NHSB} = \text{Load}_{\text{out}} - \text{Load}_{\text{in}} \quad (18)$$

or the difference between the substrate load leaving the liver (Load_{out}) and the substrate load reaching the liver (Load_{in}). The Load_{in} was calculated according to the equation:

$$\text{Load}_{\text{in}} = ([S]_{\text{A}} \times \text{HABF}) + ([S]_{\text{PV}} \times \text{PVBF}) \quad (19)$$

where $[S]_{\text{A}}$ and $[S]_{\text{PV}}$ are arterial and portal venous blood substrate concentrations, respectively, and HABF, PVBF are hepatic artery and the portal vein blood/plasma flows, respectively. The Load_{out} was calculated according to the equation:

$$\text{Load}_{\text{out}} = [S]_{\text{HV}} \times \text{HBF} \quad (20)$$

where $[S]_{\text{HV}}$ is the substrate concentration in the hepatic vein blood, and HBF is the total hepatic blood flow. Blood flows were used for all substrate balance calculations except NEFA balances, for which plasma flows were used.

Net Gut Substrate Balance

Net gut substrate balance (NGSB) was calculated as:

$$\text{NGSB} = \text{Load}_{\text{outgut}} - \text{Load}_{\text{ingut}} \quad (21)$$

or the difference between the substrate load leaving the gut ($\text{Load}_{\text{outgut}}$) and the substrate load entering the gut ($\text{Load}_{\text{ingut}}$). The $\text{Load}_{\text{ingut}}$ was calculated according to the equation:

$$\text{Load}_{\text{ingut}} = [\text{S}]_{\text{A}} \times \text{PVBF} \quad (22)$$

$$\text{Load}_{\text{outgut}} = [\text{S}]_{\text{PV}} \times \text{PVBF} \quad (23)$$

Net Hepatic Substrate Fractional Extraction

Net substrate fractional extraction across the liver (NHSFE) was calculated as:

$$\text{NHSFE} = \text{NHSU} / \text{Load}_{\text{in}} \quad (24)$$

where NHSU is the net hepatic substrate uptake.

Hepatic Sinusoidal Substrate Concentration

Hepatic sinusoidal substrate level (HSSL) was calculated as:

$$\text{HSSL} = ([\text{S}]_{\text{A}} \times \text{HABF}/\text{HBF}) + ([\text{S}]_{\text{PV}} \times \text{PVBF}/\text{HBF}) \quad (25)$$

where $[\text{S}]_{\text{A}}$ and $[\text{S}]_{\text{PV}}$ are arterial and portal venous blood substrate concentrations, respectively, and HABF, PVBF, and HBF are hepatic artery, portal vein, and total hepatic blood flows, respectively.

Glucose Mixing in the Portal Vein

Technical issues associated with assessment of the responsiveness of the liver to portal glucose delivery, as well as our rationale for using a tracer-based method to quantify ‘committed’ unidirectional hepatic glucose uptake (HGU) for Specific Aims III and IV warrant discussion. When glucose is infused into the laminar flow of the hepatic portal vein, poor mixing of the blood with the portal glucose infusate can occur.

Streaming of glucose in the portal vein results in random under- or over-recovery of the portal glucose infusate in the portal and hepatic vein blood samples, leading to variation in the estimate of *net* hepatic glucose uptake (NHGU). Historically, we have utilized the para-aminohippuric acid (PAH) method to assess for errors associated with poor mixing, given that PAH is not extracted by the liver or red blood cells and thus, should be quantitatively recovered in the portal and hepatic veins. Briefly, PAH is mixed with the portal glucose infusate such that the PAH infusion rate is 0.4 mg/kg/min. The concentration of PAH is then measured on whole-blood samples from arterial, portal venous, and hepatic venous blood [273]. The assay involves a 1:5 dilution (200 μ l of metabolite sample + 800 μ l of PAH reagent solution) of the blood sample in a reagent solution (10 g p-dimethylamino-benzaldehyde, 600 ml 95% ethanol, 40 ml 2N HCl, deionized H₂O up to 1000 ml). Light absorbance of the diluted samples is then measured on a spectrophotometer at 465 nm, and compared with a standard curve containing increasing concentrations of PAH in blood drawn from the animal prior to the start of PAH infusion. The ratio between the recovery of PAH in portal and hepatic veins, and the actual intraportal PAH infusion rate is then used as an index of mixing of the intraportal glucose infusate with the blood entering and exiting the liver. A ratio of 1.0 would represent perfect mixing.

Our laboratory established criteria to define studies as “poorly mixed” if recovery of the infused PAH in the portal and/or hepatic veins was < 60% or > 140%. This does not necessarily mean that all studies that fit within those inclusion criteria were mixed; it just meant that we could not prove that they were not mixed. Historically, we lost 1 in 3 studies due to poor mixing. In my experiments for Specific Aims III and IV, however,

mixing in the portal vein was poor such that, based on our own exclusion criteria by means of the PAH method, I would have lost 2 in 3 studies. Given the expense of each experiment, the fact that we knew we were going to have several diet groups with a relatively small sample size in each ($n=5-6/\text{group}$), and the fact that our primary endpoint was the calculation of ‘committed’ (because this method does not account for glucose cycling within the liver and thus, underestimates total HGU) unidirectional HGU, we wanted to develop a method that would, to the best of our ability, overcome errors in the assessment of HGU associated with poor mixing and thus, utilize our resources most effectively. Given that 3- ^3H -glucose (labeled) can be infused into a peripheral vein, it circulates through the heart before reaching peripheral tissues. As a result, labeled and unlabeled plasma glucose mix completely by the time they reach the liver. Thus, unidirectional HGU was calculated in Specific Aims III and IV using a tracer-based hepatic fractional extraction method. It should be noted that this method yields HGU rather than NHGU; however, values derived from either method will be equal when HGP is zero.

Unidirectional Hepatic Glucose Uptake (Specific Aims III and IV)

Unidirectional HGU (mg/kg/min) was calculated by multiplying the hepatic fractional extraction of ^3H -glucose (HFrExG^*) by the hepatic glucose load (HGL; mg/kg/min). HFrExG^* (unitless) was determined by dividing the hepatic ^3H -glucose balance by the hepatic ^3H -glucose load according to the following equation,

$$G_H^* \times \text{BF}_H - [(G_A^* \times \text{BF}_A) + (G_P^* \times \text{BF}_P)] / [(G_A^* \times \text{BF}_A) + (G_P^* \times \text{BF}_P)], \quad (26)$$

where G_A^* , G_P^* , and G_H^* represent [^3H]-glucose values (dpm/ml) in the artery, portal, and hepatic veins, respectively, and BF_A , BF_P , and BF_H represent blood flow (ml/kg/min as determined by the ultrasonic flow probes) in the hepatic artery, portal vein, and total liver, respectively. HGL was calculated according to the following equation,

$$\text{HGL} = G_A \times \text{BF}_H - \text{GUG}, \quad (27)$$

where G_A represents the unlabeled blood glucose concentration in the artery (mg/ml), BF_H represents total hepatic blood flow (ml/kg/min), and GUG represents the uptake of glucose by the gut (mg/kg/min). GUG was calculated as follows,

$$([\text{G}_A^* - \text{G}_P^*] / \text{G}_A^*) \times (G_A \times \text{BF}_P), \quad (28)$$

where $([\text{G}_A^* - \text{G}_P^*] / \text{G}_A^*)$ represents the fractional extraction (unitless) of [^3H]-glucose across the gut, G_A represents the unlabeled blood glucose concentration (mg/ml) in the artery, and BF_P represents blood flow (ml/kg/min) in the portal vein, respectively.

Samples drawn for the measurement of [^3H]-glucose in the arterial, portal, and hepatic vein plasma were assayed in triplicate to allow for precise determination of HFrExG^* throughout the study.

One of the assumptions of this method is that the characteristics of glucose entry into the erythrocyte are the same for labeled and unlabeled glucose. Based on this assumption, plasma [^3H]-glucose was converted to blood [^3H]-glucose by applying the same corrections factors (the mean of the ratio of the blood value to the plasma concentration [187, 279]) to labeled glucose as we do to unlabeled glucose (0.74 for all values because [^3H]-glucose was infused peripherally). Nevertheless, calculation of HGU using plasma [^3H]-glucose or whole blood-converted [^3H]-glucose yielded very similar results.

Another assumption of this method is that HGU in response to portal glucose delivery would be similar in well mixed and poorly mixed studies. In other words, the rate of HGU would be similar whether all of the HGL was delivered to half the liver or to the whole liver. This assumption holds true as long as HGU does not become saturated in any one part of the liver. Given that previous studies [116] have reported NHGU rates as high as 12.0 mg/kg/min in the presence of intraportal fructose infusion, we believe this assumption is valid.

Hepatic Glucose Production

Upon calculation of unidirectional HGU, hepatic glucose production (HGP) can then be determined by taking the difference between NHGB and HGU according to the following equation:

$$\text{HGP} = \text{NHGB} - \text{HGU}, \quad (29)$$

where NHGB and HGU represent net hepatic glucose balance and tracer-determined unidirectional hepatic glucose uptake, respectively, as described under *Net Hepatic Substrate Balance* and *Unidirectional Hepatic Glucose Uptake*. One of the advantages of this method is that it provides an estimate of hepatic glucose production, as opposed to tracer-determined R_a , which provides an estimate of whole-body glucose production.

Glucose Turnover

The rates of glucose production (R_a) and glucose utilization (R_d) were calculated using Steele's steady-state equation [274]. The glucose pool was initially primed with an injection of 3- ^3H -glucose, followed by a constant infusion of the tracer. By the

beginning of the control period the tracer (3-[³H]-glucose) and tracee (cold glucose) were in equilibrium so that the specific activity of glucose (SA = dpm glucose/mg glucose) was in a steady state. R_a and R_d were calculated according to the following equations:

$$R_a = [I - N (dSA/dt)]/SA, \text{ and} \quad (30)$$

$$R_d = R_a - (dN/dt) \quad (31)$$

where I is infusion rate of tracer (dpm/min), N is the pool size of glucose (mg) and t is time (min) [275]. In a steady state, when $dSA/dt = 0$, the R_a equation is simplified to:

$$R_a = I/SA \quad (32)$$

Only values obtained during the steady-state period of the clamp (during which the specific activities were constant) were used for the determination of glucose turnover. In Specific Aim I, endogenous glucose production (endo R_a) was calculated as $R_a -$ (peripheral glucose infusion rate + [portal glucose infusion rate x 1-net hepatic fractional glucose extraction]) [220]. Hepatic glucose uptake was estimated (est HGU) by subtracting NHGU from endo R_a (Specific Aim 1).

There are two major assumptions when using the isotope dilution method to determined whole-body glucose turnover: 1) labeled and unlabeled glucose molecules are assumed to be metabolized in the same manner, and 2) the label is assumed to be irreversibly lost [276]. It should also be noted that tracer-determined glucose production is slightly higher than hepatic glucose release, given that both the liver and the kidneys produce glucose. Although net kidney glucose balance in the postabsorptive state is near zero, the kidney has been estimated to contribute 5-15% to whole body endogenous glucose production [277].

Net Hepatic Carbon Retention

Net hepatic carbon retention, an estimate of hepatic glycogen accretion, was calculated as the sum of the hepatic balances of glucose, lactate, alanine x 2 (to account for the contribution of amino acids other than alanine), and glycerol, with all factors in glucose equivalents as described and validated previously [222, 278-281]. It has the advantage of not being dependent upon an estimate of the pre-study glycogen content, which must be obtained from a separate set of fasted dogs.

The direct contribution of plasma glucose to hepatic glycogen stores was estimated by dividing ³H-glycogen counts/g liver by the average arterial plasma ³H-glucose specific activity present during the experimental period (dpm/g ÷ dpm/mg).

Nonhepatic Glucose Uptake

Nonhepatic glucose uptake (Non-HGU) was calculated over time intervals by the following formula:

$$\text{Non-HGU} = \text{average total glucose infusion rate between T1 and T2} + (\text{T1}_{\text{NHGB}} + \text{T2}_{\text{NHGB}})/2 - \text{glucose mass change in the pool between T1 and T2} \quad (33)$$

where T1 and T2 represent the time points for which Non-HGU is begin measured. Note that the $((\text{T1}_{\text{NHGB}} + \text{T2}_{\text{NHGB}})/2)$ term will be negative when the liver is taking up glucose in a net sense. The glucose mass change in the pool is calculated using the following equation:

$$\text{Glucose mass change in the pool} = \left(\frac{([G_A]_{T2} - [G_A]_{T1})}{100} \right) * \left(\frac{(0.22 * \text{body wt in kg} * 1000 * 0.65)}{\text{body wt in kg}} \right) / (T2 - T1), \quad (34)$$

where $[G_A]$ is the blood glucose concentration, T1 and T2 are the two end time points of the interval, 0.22 represents the volume of extracellular fluid (the volume of distribution) or 22% of the dog's weight [282], and 0.65 represents the pool fraction [283].

Statistical Analysis

All data are expressed as means \pm standard error (SE). Time course data were analyzed with two-way repeated measures ANOVA (group x time), and one-way ANOVA was used for comparisons of other mean data. Post-hoc analysis was performed with Student-Newman-Keuls method. When only two values were compared, an independent student t-test was used. Statistical significance was accepted at $P < 0.05$.

CHAPTER III

CHRONIC CONSUMPTION OF A HIGH-FAT/HIGH-FRUCTOSE DIET RENDERS THE LIVER INCAPABLE OF NET HEPATIC GLUCOSE UPTAKE

(Adapted from Coate et al. *Am J Physiol Endocrinol Metab* 299:E887-E898, 2010)

Aim

Chronic consumption of a western diet, characterized by foods rich in sugar and abundant in total and saturated fat, has been suggested to play a role in the development of type 2 diabetes [28, 29, 143]. While the effects of high dietary fat or fructose on insulin's ability to suppress hepatic glucose production have been extensively studied, their effects on hepatic glucose uptake and disposition have not been delineated. In addition, the combined effects of dietary fat and fructose, in quantities that mimic a western diet, on the temporal development of glucose intolerance and hepatic and/or peripheral insulin resistance are incompletely understood. Lastly, it is not known if high-fat, high-fructose feeding coupled with an experimental reduction in beta cell mass (partial pancreatectomy) augments glucose intolerance to a larger extent than diet alone. Thus, the objective of Specific Aim I was to investigate how the combination of high dietary fat and fructose influences, 1) the temporal development of insulin resistance and impaired glucose tolerance in the presence or absence of a compromised endocrine pancreas, and 2) the ability of the liver to take up glucose under conditions that mimic the postprandial state (hyperinsulinemia, hyperglycemia and the portal glucose feeding

signal).

Experimental Timeline (Figure 3.1)

Prior to initiation of experimental diets (as described in Tables 2.1 and 2.2), baseline metabolic assessments of glucose tolerance and whole-body insulin sensitivity were attained by performing oral glucose tolerance tests (OGTTs) and hyperinsulinemic euglycemic (HIEG) clamps, respectively. The following week, each dog underwent a laparotomy in which a sham operation (Sh; $n=8$) or a partial pancreatectomy (Px; $n=6$) was performed, as described under *Surgical Procedures* in Chapter II. Post-operatively, dogs were randomly assigned to either the control (CTR; $n=4$) or high-fat, high-fructose diet (HFFD-Sh; $n=4$; HFFD-Px; $n=6$). OGTTs were repeated after 4 and 8 weeks of CTR or HFFD feeding, and HIEGs after 10 weeks of feeding. At week 11, dogs underwent a second laparotomy for hepatic catheterization and flow cuff placement, as described under *Surgical Procedures* in Chapter II. At week 13, hyperinsulinemic hyperglycemic clamps (HIHG) were performed, and net hepatic substrate balance was measured.

Experimental Design

Oral glucose tolerance tests (OGTTs)

The OGTTs were conducted in 24-h-fasted dogs that had been fed 1 can of meat immediately prior to fasting. Following a 10 min basal control period, Polycose (0.9 g/kg body weight; Polycose, Abbott Nutrition; Columbus, OH) was administered orally and

plasma glucose, insulin, c-peptide and glucagon concentrations were monitored over the following 180 min.

Hyperinsulinemic-euglycemic clamp (HIEG)

The HIEGs were conducted in 18-h-fasted dogs that had been fed 1 can of meat just prior to initiation of the fast. The HIEGs consisted of a 90 min equilibration period (-120 to -30 min), a 30 min basal control period (-30 to 0 min) and a 120 min experimental period (0 to 120 min). At time 0, a constant infusion of somatostatin (0.8 $\mu\text{g}/\text{kg}/\text{min}$; Bachem, Torrance, CA) was started in a peripheral vein in order to suppress endogenous insulin and glucagon secretion. Insulin (2.0 mU/kg/min; Lilly, Indianapolis, IN) and glucagon (0.7 ng/kg/min; Novo Nordisk, Princeton, NJ) were then replaced via infusion into a peripheral vein with a goal of increasing arterial insulin 10-fold while clamping glucagon at a basal value. In addition, at time 0, a variable IV infusion of 50% dextrose was started in a leg vein in order to maintain euglycemia (~ 100 mg/dl) throughout the study.

Hyperinsulinemic-hyperglycemic clamp (HIHG)

The HIHGs were conducted in 18-h-fasted adult male mongrel dogs that had been fed 1 can of meat just prior to initiation of the fast. Each experiment consisted of a 100 min equilibration period (-120 to -20 min), a 20 min basal control period (-20 to 0 min), and a 180 min experimental period divided into 2 sub-periods (P1, 0 to 90 min; P2, 90 to 180 min). At -120 min, a priming dose of 3- ^3H -glucose (38 μCi) was given, followed by a constant infusion of 3- ^3H -glucose (0.38 $\mu\text{Ci}/\text{min}$). At time 0, a constant infusion of

somatostatin (0.8 $\mu\text{g}/\text{kg}/\text{min}$) was started in a peripheral vein, and insulin and glucagon were then replaced intraportally at threefold basal (1.2 mU/kg/min) and basal (0.55 ng/kg/min) rates, respectively. In addition, a variable infusion of 50% dextrose was started in a leg vein in order to double the arterial plasma glucose concentration (~ 220 mg/dl) and the hepatic glucose load (HGL). In P2, 20% dextrose (4.0 mg/kg/min) was infused intraportally, and the peripheral glucose infusion rate was adjusted as necessary to clamp the HGL to that in P1.

Results

Oral glucose tolerance tests. In the CTR group, glucose tolerance (assessed by the delta AUC for glucose over 180 min), insulin secretion (assessed by the delta AUC for c-peptide over 180 min) and plasma insulin levels (assessed by the delta AUC for insulin over 180 min) seen in response to an oral glucose challenge were not different at baseline, or after 4 or 8 weeks of feeding (Figure 3.2), demonstrating the reproducibility of normal glucose tolerance in dogs maintained on a standard meat and chow diet. On the other hand, the glycemic response to an oral glucose challenge was significantly increased after HFFD feeding, as indicated by a 123% and 113% increase in the delta AUC for glucose in the HFFD-Sh and HFFD-Px groups, respectively, after 4 weeks of feeding, and a 106% and 147% increase in the HFFD-Sh and HFFD-Px groups, respectively, after 8 weeks of feeding (Figures 3.3A and 3.4A). The deterioration of glucose tolerance in the HFFD groups was attributable in part to a beta cell defect, given that a compensatory increase in insulin secretion, as indicated by c-peptide levels, failed to occur whether or not the pancreas was compromised (Figures 3.3B and 3.4B). As a

result, the delta AUC for insulin at 4 and 8 weeks was not significantly different from that observed in the baseline OGTT (Figures 3.3C and 3.4C) despite increased plasma glucose. In addition, while fasting plasma glucagon concentrations were similar between diet groups at BL, 4 and 8 weeks, the magnitude of the decrease in plasma glucagon during the 8 week OGTT was significantly less in both HFFD groups compared to CTR (pg/ml; HFFD-Px: 7 ± 3 and HFFD-Sh: 13 ± 5 vs. CTR: 29 ± 8 , $P < 0.05$) (Table 3.1), suggestive of impaired alpha cell function after HFFD feeding.

Hyperinsulinemic-euglycemic clamps. Hyperinsulinemic-euglycemic (HIEG) clamp studies were performed at baseline (BL) and after 10 weeks of feeding. Plasma glucagon concentrations were clamped at basal levels while plasma insulin concentrations were elevated 10-fold from basal (Table 3.2). Plasma c-peptide levels fell to zero in each group secondary to somatostatin infusion. In the CTR group, the average (90-120 min) glucose infusion rate (GIR) required to maintain euglycemia was 19.9 ± 3.4 and 17.6 ± 1.3 mg/kg/min during the BL- and 10wk-HIEGs, respectively (Figure 3.5A and C). On the other hand, the average GIR (mg/kg/min) required to maintain euglycemia in the HFFD group was decreased by approximately 30% (BL: 18.9 ± 0.9 , 10wk: 13.9 ± 0.7 , $P < 0.05$ vs. BL) after 10 weeks of HFFD feeding (Figure 3.5B and C). Because the reduction in GIR after HFFD feeding was similar between the HFFD-Sh and HFFD-Px groups, the data from both groups were combined in Figure 3.5 (see figure legend 3.5). Despite use of the same insulin infusion rate (2.0 mU/kg/min), the steady-state plasma insulin concentration was higher in the HFFD group at week 10 compared to BL ($\mu\text{U/ml}$; BL: 112 ± 16 , 10wk: 128 ± 10) (Table 3.2). As a result, a 33% decrease in the GIR to insulin ratio was evident in the HFFD group after 10 weeks of feeding (Figure 3.5D). As expected, the elevation in

insulin elicited a rapid reduction in plasma NEFA levels, while plasma TGs tended to drift down throughout the experiment in each group at BL and 10 weeks (Table 3.2).

There were no differences in plasma lipid levels between the CTR and HFFD groups at any time point.

Hyperinsulinemic-hyperglycemic clamps.

Hormone concentrations

After 13 weeks of HFFD feeding, the fasting plasma arterial insulin ($\mu\text{U/ml}$; CTR: 8 ± 2 , HFFD: 11 ± 1 , $P = 0.06$) and glucagon (pg/ml ; CTR: 33 ± 4 , HFFD: 48 ± 5 , $P = 0.06$) concentrations tended to be elevated relative to those in the CTR group (Figure 3.6A and C and Table 3.3). During the HIHG clamp, glucagon was maintained at a basal level while insulin was increased 3-4 fold (Figure 3.6 A-D).

Plasma glucose concentrations and hepatic glucose load

During the control period, arterial plasma glucose concentrations were 108 ± 1 and 106 ± 1 mg/dl in the CTR and HFFD groups, respectively (Figure 3.7A). During P1, arterial plasma glucose was increased to 218 ± 3 mg/dl in both groups in order to double the hepatic glucose load. The arterial plasma glucose concentrations were reduced slightly in both groups during P2 (mg/dl; CTR: 205 ± 4 , HFFD: 199 ± 6) to maintain a doubling of the hepatic glucose load in the presence of portal glucose infusion. As a result, the hepatic glucose loads (mg/kg/min; CTR: 36 ± 3 , HFFD: 40 ± 3) were similar throughout the experiment in both groups (Figure 3.7C).

Net hepatic glucose balance (NHGB)

Net hepatic glucose output in the control period (NHGO, mg/kg/min; CTR: 1.6 ± 0.2 , HFFD: 1.8 ± 0.3) was unaffected by diet (Figure 3.7D). Since NHGB after 13

weeks of HFFD feeding was similar in the HFFD-Px and HFFD-Sh groups (see figure legend 3.7), the data from both groups were combined in Figures 3.6 and 3.7. When challenged with hyperinsulinemia and hyperglycemia (P1), the CTR group switched from net glucose output to net glucose uptake (NHGU), reaching an average NHGU rate of -1.8 ± 0.8 mg/kg/min (last 30 min of P1, Figure 3.7D). The livers of dogs in the HFFD group, on the other hand, displayed an inability to consume glucose in the presence of hyperinsulinemia and hyperglycemia, as indicated by an average NHGO rate of 0.4 ± 0.1 mg/kg/min (last 30 min of P1, $P < 0.05$ vs. CTR, Figure 3.7D). When glucose was infused into the portal vein to activate the portal glucose signal (P2), there was a doubling of NHGU in the CTR group (-3.5 ± 1.0 mg/kg/min during the last 30 min of P2, Figure 3.7D). In contrast, portal glucose delivery in the HFFD group was unable to cause significant NHGU (-0.2 ± 0.8 mg/kg/min during the last 30 min of P2, $P < 0.05$ vs. CTR, Figure 3.7D).

Glucose turnover, glucose infusion rates, and nonhepatic glucose uptake

In the CTR group during hyperinsulinemia and hyperglycemia (P1), the tracer-determined rate of endogenous glucose appearance (endo R_a) decreased (mg/kg/min; Basal: 2.2 ± 0.2 , P1: 0.6 ± 0.5 , $P < 0.05$ vs. basal period) and the estimated rate of hepatic glucose uptake (est HGU) increased (mg/kg/min; Basal: 0.6 ± 0.3 , P1: 2.5 ± 1.2) relative to the basal period (Table 3.4). In the presence of the portal glucose signal (P2), there was no further suppression of endo R_a (mg/kg/min; P2: 0.8 ± 0.6), but the rate of est HGU significantly increased (mg/kg/min; P2: 4.3 ± 1.3 , $P < 0.05$ vs. basal). However, in the HFFD group, a significant decline in endo R_a was not observed until P2 (mg/kg/min; Basal: 2.4 ± 0.2 , P1: 1.7 ± 0.2 , P2: 0.4 ± 0.2 , $P < 0.05$ vs. basal period). Despite the presence

of the portal glucose signal, est HGU did not increase significantly (mg/kg/min; Basal: 0.8 ± 0.3 , P1: 1.4 ± 0.3 , P2: 1.3 ± 0.7 , not significant [NS]) (Table 3.4).

The GIR and the rate of nonhepatic glucose uptake (non-HGU) increased over time in both groups in response to hyperinsulinemia, hyperglycemia, and portal glucose delivery (Table 3.5 and Figure 3.7B). Given that NHGU was reduced by ≈ 3.0 mg/kg/min in the HFFD group compared to the CTR group, one might have expected a comparable decrease ($\approx 30\%$) in the GIR in the HFFD group if peripheral insulin sensitivity was unchanged. However, the decrease in GIR was somewhat less than that (1.9 mg/kg/min or $\approx 20\%$ reduction) indicating that a small increase occurred in the average non-HGU rate (mg/kg/min; CTR: 6.6 ± 1.1 , HFFD: 7.9 ± 0.8). Furthermore, the rate of glucose disappearance (R_d) did not differ significantly among the CTR and HFFD groups during either experimental period (mg/kg/min; CTR, P1: 7.3 ± 0.8 , P2: 10 ± 1.5 ; HFFD, P1: 7.0 ± 0.9 , P2: 8.7 ± 1.3) (Table 3.4). In fact, the difference in R_d between groups in P2 (1.3 mg/kg/min) was similar to the difference in GIR in P2 (1.9 mg/kg/min). These data thus clearly indicate that the defect in glucose uptake occurred in the liver and not peripheral tissues.

Lactate, net hepatic carbon retention and glycogen metabolism

During the control period, arterial blood lactate concentrations and net hepatic lactate uptake were similar in both groups (Table 3.5). However, in response to hyperinsulinemia, hyperglycemia and portal glucose delivery, there was a significant increase in the arterial blood lactate concentrations in the CTR group that resulted from a switch in net hepatic lactate balance from uptake to output (Table 3.5). In contrast, a switch from net hepatic lactate uptake to output did not occur at any time in the HFFD

group (Table 3.5). Likewise, net hepatic carbon retention (mg glucose equivalents/kg/min), an index of glycogen accretion, was lower in the HFFD group compared to the CTR group during P1 (CTR: 1.2 ± 0.7 ; HFFD: -0.1 ± 0.1 [net glycogen breakdown]). In response to portal glucose delivery, there was an increase in net hepatic carbon retention (mg glucose equivalents/kg/min) in the CTR group (1.9 ± 0.3) coincident with a doubling in NHGU; however, this was not evident in the HFFD group (0.6 ± 0.8), consistent with an inability of the portal signal to activate NHGU (Table 3.5). Although the terminal hepatic glycogen content was not significantly lower in the HFFD group (mg glycogen/g liver, CTR: 46 ± 2 ; HFFD: 38 ± 5 [data not shown]), glycogen synthesis via the direct pathway was (mg/kg/min; CTR: 1.5 ± 0.4 , HFFD: 0.5 ± 0.2 , $P < 0.05$ [data not shown]), consistent with a decrease in NHGU and net hepatic carbon retention in the HFFD group.

Fat metabolism

Arterial plasma free fatty acid (NEFA) and glycerol concentrations were similar between the HFFD and CTR groups during the basal control period (Table 3.5). In response to an elevation in arterial insulin (P1 and P2), an equivalent decrease in arterial plasma NEFA and blood glycerol concentrations was observed in the two groups. The net hepatic uptake rates of NEFA and glycerol were reduced in parallel to the changes in the levels of NEFA and glycerol in the blood (Table 3.5).

Discussion

The purpose of this study was to investigate, in a large animal model, how consumption of a high-fat, high-fructose diet (HFFD), coupled with a compromised

pancreatic mass, influences the temporal development of impaired glucose tolerance, whole-body insulin resistance, and the ability of the liver to take up and store glucose in the presence of conditions that mimic the postprandial state. Utilization of the canine model enabled the longitudinal assessment of perturbations in glucose metabolism and insulin sensitivity at the whole-body and organ level, including the measurement of NHGU. Herein we report that 13 weeks of HFFD feeding rendered the liver incapable of NHGU despite the presence of hyperinsulinemia, hyperglycemia, and the portal glucose feeding signal.

HFFD and the Liver

The chow-fed control (CTR) group displayed normal glucose tolerance, as well as a rapid induction of NHGU in the presence of hyperinsulinemia and hyperglycemia, a response that was augmented even further in the presence of the portal glucose signal. Coincident with stimulation of NHGU, a significant increase in net hepatic carbon retention was observed. On the other hand, consumption of a HFFD resulted in impaired glucose tolerance (IGT) in a relatively short period of time (4 weeks) as indicated by more than a doubling in the delta AUC for glucose in response to an oral glucose challenge in both the HFFD-Sh and HFFD-Px groups. Given the vital role of the liver in the disposition of an oral glucose load [184], these data raise the possibility that a reduction in hepatic insulin sensitivity and/or hepatic glucose effectiveness (GE) contributed to the attenuation in glucose tolerance after 4 weeks of HFFD feeding. This is supported by our data from the hyperinsulinemic-hyperglycemic clamps which demonstrated that 13 wks of HFFD feeding rendered the liver incapable of switching from net glucose output to net glucose uptake in response to a combined increase in

glucose and insulin. Glucose tracer kinetics indicated that this was attributable to a defect in both the suppression of glucose production and in the augmentation of hepatic glucose uptake. Consequently, net hepatic carbon retention and glycogen synthesis through the direct pathway were markedly diminished relative to the rates evident in the CTR group. Altogether, these data demonstrate that HFFD feeding elicits adverse metabolic effects characterized by a diminished ability of hyperinsulinemia and hyperglycemia to suppress hepatic glucose production, as well as an inability of the liver to consume glucose and synthesize glycogen under conditions that mimic the postprandial state.

HFFD and Non-hepatic Tissues (Adipose and Skeletal Muscle)

It was evident from the OGTTs that some degree of whole-body insulin resistance or reduced GE contributed to the attenuation in glucose tolerance, given that greater hyperglycemia existed in the HFFD group compared to the CTR group even though their insulin levels were virtually equivalent. Thus, hyperinsulinemic-euglycemic clamp (HIEG) experiments were conducted to assess changes in whole-body insulin sensitivity more precisely. Consistent with IGT, whole-body insulin resistance was evident in the HFFD group as indicated by a significant decrease (≈ 5.0 mg/kg/min) in the GIR required to maintain euglycemia after 10 weeks of feeding. Since tracers were not infused during the HIEG clamps, it is not known if the reduction in GIR was due to an impairment in the ability of insulin to suppress hepatic glucose production, stimulate glucose uptake in the liver and/or peripheral tissues (skeletal muscle and adipose tissue), or some combination of the two. The possibility exists that the reduction in GIR may have been accounted for solely by a decrease in hepatic, not peripheral, insulin sensitivity. For example, the GIR decreased by ≈ 5.0 mg/kg/min in the HFFD group, and by ≈ 2.0 mg/kg/min in the CTR

group after 10 weeks of feeding. The decrease in GIR in the CTR group was not statistically significant and did not impact glucose tolerance, whole-body insulin sensitivity or NHGU. If the decrease in GIR in the HFFD group was adjusted for the decrease observed in the CTR group, the signal size of the reduction in whole-body glucose utilization in the HFFD group would be ≈ 3.0 mg/kg/min. Given that hepatic glucose production under basal conditions is ≈ 2.5 mg/kg/min, and that the liver can take up a small amount of glucose even under euglycemic conditions (≈ 1.0 mg/kg/min), we think it is likely that the reduction in GIR seen after 10 weeks of HFFD feeding was explained primarily by a defect at the liver.

Consistent with this notion, as stated earlier, the ability of hyperinsulinemia and hyperglycemia to suppress endo R_a and stimulate hepatic glucose uptake was significantly impaired after 13 weeks of HFFD feeding. On the other hand, the ability of insulin to stimulate skeletal muscle glucose uptake was normal if not improved, given that non-HGU was modestly elevated (20%) in the HFFD group compared to CTR during the HIHG clamps. The increase in non-HGU was likely related to the fact that the arterial insulin concentration was slightly higher in the HFFD group compared to the CTR group during insulin infusion. Indeed, when non-HGU was expressed relative to the arterial insulin concentration, the ratios were similar in the HFFD and CTR groups (HFFD: 0.25 ± 0.03 ; CTR: 0.28 ± 0.08). Furthermore, although NHGU during P2 was decreased by 3.3 mg/kg/min in the HFFD group compared to the CTR group, the reductions in whole-body glucose R_d (1.3 mg/kg/min) and GIR (1.9 mg/kg/min) were nearly equivalent in magnitude and less than the change in NHGU, indicating that the ability of insulin and/or

glucose to stimulate non-HGU was enhanced despite a marked impairment in hepatic glucose uptake.

Previous studies have suggested that diet-induced impairments in insulin action during euglycemia can be compensated for by enhanced glucose effectiveness during hyperglycemia. For example, Commerford et al [284] demonstrated in rodents that consumption of a high-fat or high-sucrose diet resulted in a decrease in insulin's ability to suppress hepatic glucose production and stimulate whole-body glucose uptake during a hyperinsulinemic-euglycemic clamp, but during a hyperinsulinemic-hyperglycemic clamp, these parameters were restored to the rates observed in chow-fed controls. This was also demonstrated to be the case in insulin resistant, normoglycemic relatives of type 2 diabetic patients, in which glucose disposal was increased during a hyperglycemic pancreatic clamp due in part to enhanced glucose effectiveness in the skeletal muscle [285]. Thus, it is possible that increased non-HGU in the HFFD group during the HIHG clamps was reflective of enhanced glucose effectiveness in the skeletal muscle in the presence of hyperglycemia. The absence of a defect in Non-HGU might be related to the fact that the dog does not develop fasting hyperglycemia or dyslipidemia when fed a HFFD. As a result, the dog does not develop gluco- or lipotoxicity. It is possible that these pathogenic processes need to be present in order to elicit a defect in skeletal muscle glucose uptake.

With regard to adipose tissue, the ability of insulin to suppress lipolysis after 13 weeks of HFFD feeding was also similar between the HFFD and CTR groups, as demonstrated by rapid and comparable reductions in arterial NEFA and glycerol concentrations in the presence of a 4-fold rise in plasma insulin. As a result, net hepatic

NEFA uptake was similar between groups and did not provide an explanation for the deficit in NHGU in the HFFD group.

HFFD and the Endocrine Pancreas

Consumption of a HFFD resulted in significantly augmented glycemia in response to an oral glucose challenge in both the HFFD-Sh and HFFD-Px groups after 4 and 8 weeks of feeding. Based on the delta AUCs for c-peptide and insulin, it appeared as if the impairment in glucose tolerance was due in part to a beta cell defect given that insulin secretion was not enhanced relative to baseline studies despite a greater than 2-fold increase in glucose. To lend support to the observation that HFFD feeding impaired glucose tolerance due in part to a beta cell defect, a meta-analysis of all OGTTs performed over the last 3 years in our lab was conducted. Consistent with the findings of the current paper, HFFD feeding increased the delta AUC for glucose in response to an oral glucose challenge by 121% in sham pancreatectomized (n=5; $P < 0.05$ vs. baseline OGTT) and 130% in pancreatectomized (n=10; $P < 0.05$ vs. baseline OGTT) dogs. On the other hand, the rise in insulin secretion (as indicated by the delta AUC for c-peptide following HFFD feeding vs. that observed during the baseline OGTT) was virtually unchanged in the either group (7% decrease in the sham group; 5% increase in pancreatectomized group). Although a decrease in beta cell mass and/or function could explain insufficient glucose-stimulated insulin secretion (GSIS) in response to an oral glucose challenge, the beta cell responses were similar in both HFFD groups regardless of partial pancreatic resection, suggesting that a defect in beta cell function, not mass, was associated with the lack of hyperinsulinemic compensation. In fact, it appears as though the surgical reduction ($\approx 65\%$) in pancreatic mass was without significant effect,

which is consistent with earlier data. For example, Frey and colleagues [286] suggested that the development of diabetes following a partial pancreatectomy was directly related to the extent of pancreatic resection. In patients with otherwise normal pancreatic function, up to 80% of the pancreatic parenchyma could be removed without a change in metabolic status. On the other hand, near-total (80-95%) or total pancreatectomy resulted in 100% of the patients developing diabetes post-operatively [286, 287]. Studies conducted in rodents demonstrated that removal of 85-95% of the pancreas was required before hyperglycemia ensued, and even then, there was a heterogeneous hyperglycemic response, which correlated with the extent of pancreatic resection [288, 289]. Our hope was that the dietary insult might trigger a further reduction in beta cell function in HFFD-fed dogs leading to the development of a diabetic phenotype, but that did not occur.

Recently, Ionut et al. [290] characterized the development of IGT in a canine model of high-fat diet-induced obesity before and after streptozotocin [STZ]-induced beta cell destruction. In the absence of STZ, glucose tolerance was retained during high-fat feeding due to a compensatory increase in insulin secretion, whereas high-fat feeding coupled with an intermediate dose of STZ (18.5 mg/kg) resulted in impaired glucose tolerance due to a 77-93% reduction in beta cell function secondary to beta cell destruction [290]. In the present study, however, insulin secretion following an oral glucose challenge was impaired in both the HFFD-Sh and -Px groups, resulting in augmented glycemia. There are some key differences between the studies conducted by Ionut et al. [290] and those presented here. First, we utilized a surgical (partial pancreatectomy) rather than chemical (STZ) approach to create a pure model of compromised pancreatic mass so that any toxic, off-target effects of STZ could be

avoided (e.g. generation of highly reactive ions and DNA strand break within the beta cells) [291, 292]. In addition, after the initial hypercaloric phase, dogs in the present study consumed approximately 1600-2100 kcal/day, whereas caloric consumption by dogs in the study of Ionut et al. [290] exceeded 5000 kcal/day. Lastly, we utilized a high-fat and high-fructose feeding paradigm to emulate consumption of a Western diet. High fructose feeding has been associated with a reduction in beta cell mass and an increase in the percentage of apoptotic cells, whereas high-fat feeding has been associated with a reduction in beta cell glucose oxidation and insufficient GSIS [293, 294]. It is possible that an interaction with the fructose component of the diet modified the impact of high dietary fat on whole-body insulin sensitivity and beta cell function in the current study. Just as STZ precipitated the development of impaired glucose tolerance secondary to beta cell destruction [290], so might an increase in dietary fructose impair beta cell function and glucose tolerance in the context of high-fat feeding.

In addition, the composition of dietary fat has been shown to directly influence beta cell function in that unsaturated fat impairs, whereas saturated fat enhances, GSIS [69]. Although the composition of dietary fat was not described in the paper by Ionut et al. [290], it is possible that their diet contained a higher concentration of saturated fat and/or a lower concentration of unsaturated fat than that used in the current study (22% saturated / 28% unsaturated as a % of total energy), which might have altered beta cell responses in the presence of a glucose challenge [69]. Altogether, the phenotypic differences amongst our models are likely related to differences in dietary constituents and caloric consumption.

In conclusion, a defect in the ability of the liver to transition from glucose

production to glucose uptake has been implicated in the development of IGT and hyperglycemia with type 2 diabetes[200-204]. Likewise, a marked reduction in splanchnic glucose uptake and hepatic glycogen synthesis following a meal has been observed in individuals with either type 1 or type 2 diabetes [203, 204]. In the present study, we utilized a large animal model to demonstrate that chronic consumption of a HFFD diminishes the sensitivity of the liver to hormonal (insulin) and glycemic (hyperglycemia and the portal glucose signal) cues, and results in a marked impairment in NHGU and glycogen synthesis. Thus, consumption of dietary fat and fructose in excess might play a role in the etiology of IGT, insulin resistance and diabetes through their hepatospecific effects.

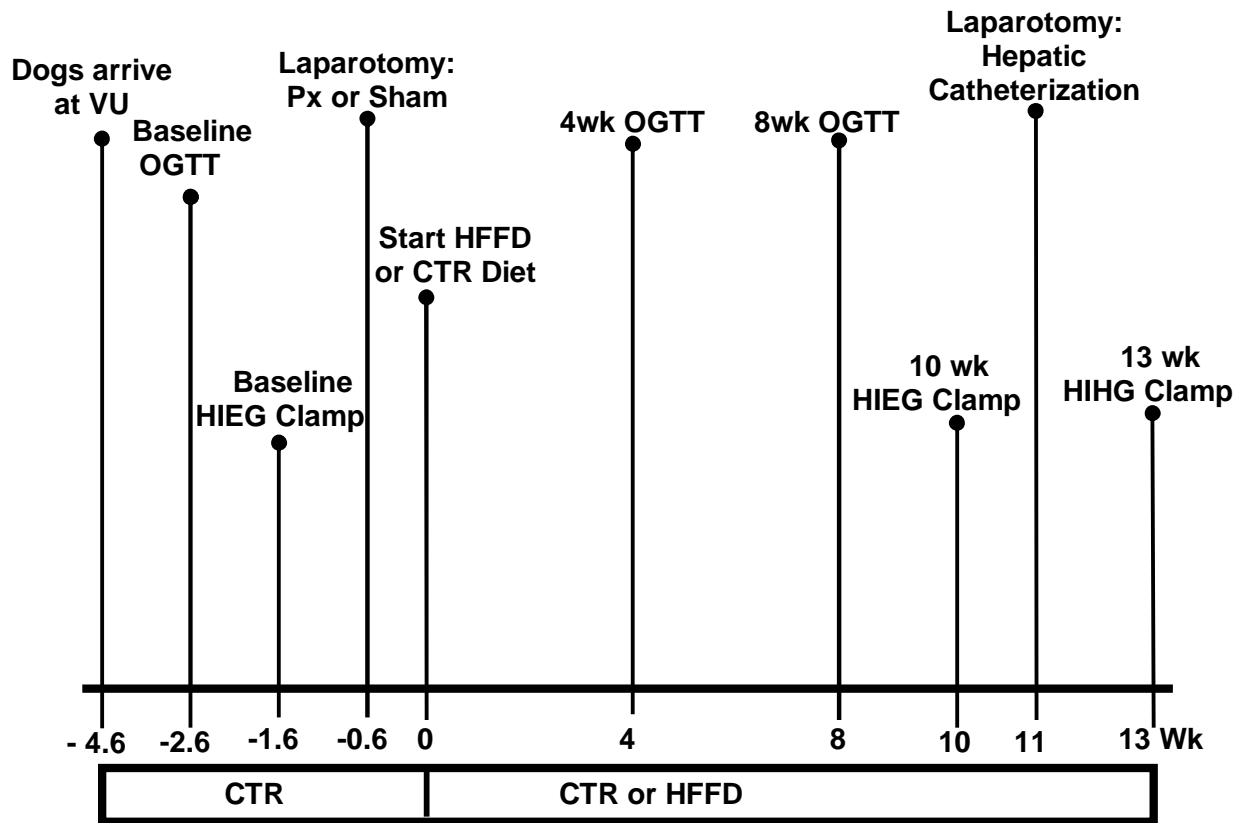


Figure 3.1: Experimental timeline. Numbers below the horizontal line indicate the week in which an experiment or surgery was conducted relative to initiation of the experimental diets (CTR or HFFD). CTR, standard meat and laboratory chow diet; HFFD, high-fat, high-fructose diet; VU, Vanderbilt University; OGTT, oral glucose tolerance test; HIEG, hyperinsulinemic-euglycemic clamp; Px, partial pancreatectomy; HIHG, hyperinsulinemic-hyperglycemic clamp.

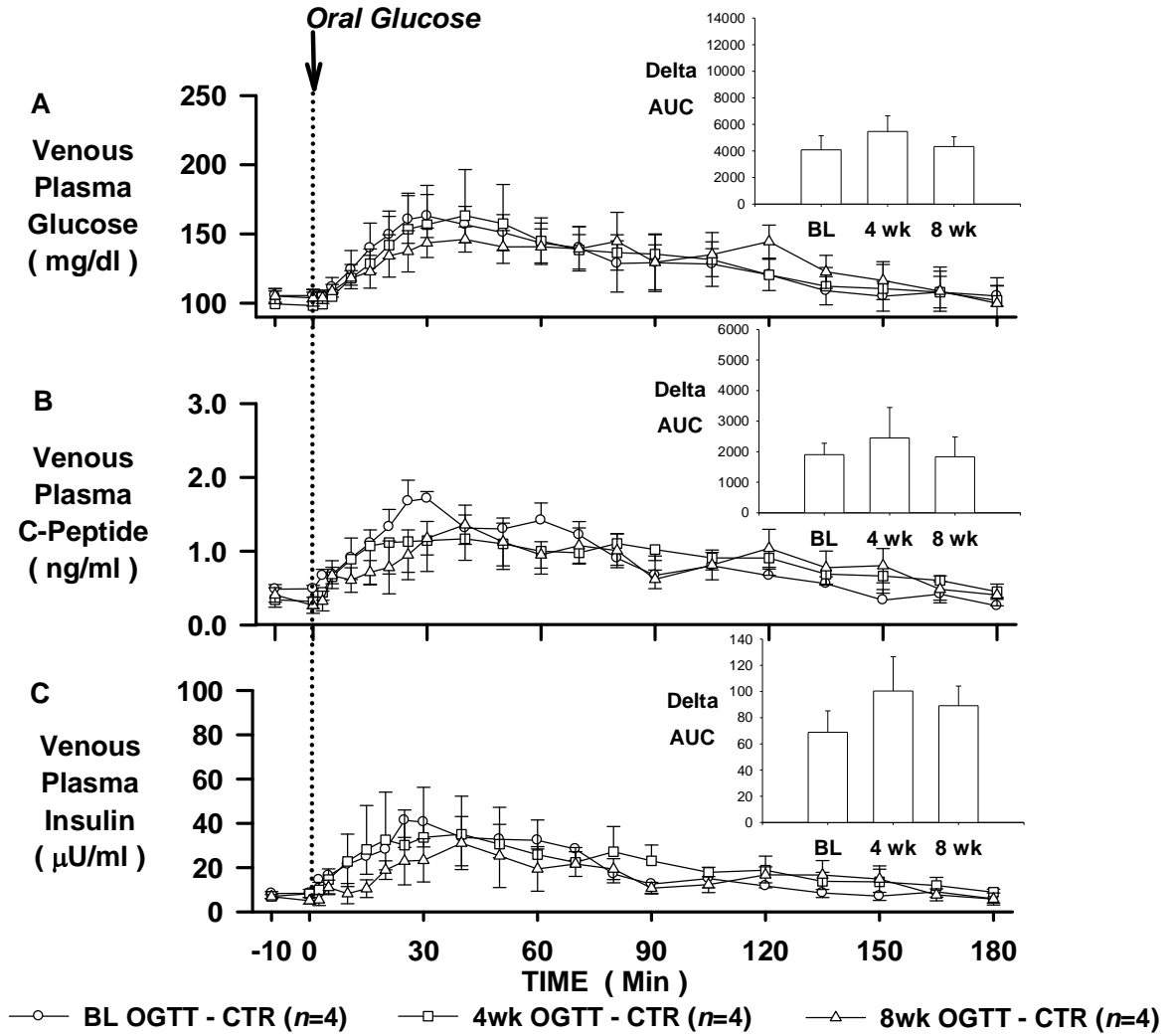


Figure 3.2: OGTTs in CTR group. OGTTs were conducted in 24-h-fasted dogs at baseline (BL; ○), and after 4 (□) and 8 (△) weeks of feeding a CTR diet ($n = 4$). Polycose was administered orally (0.9 g/kg), and plasma glucose (A), c-peptide (B), and insulin (C) concentrations were measured over 180 min. *Insets:* Delta AUCs over 180 min for glucose (A), c-peptide (B), and insulin (C). Data are means \pm SE.

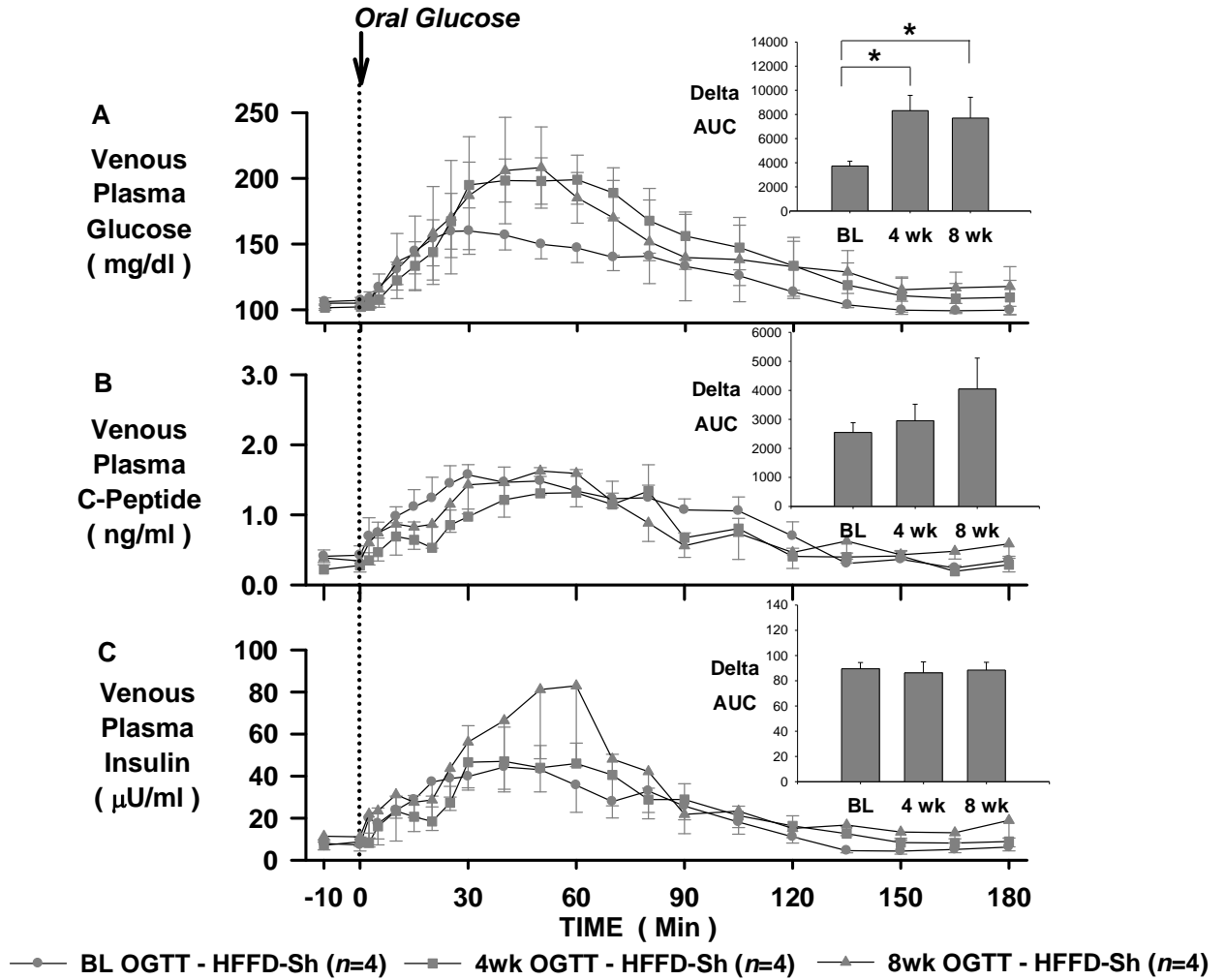


Figure 3.3: OGTTs in HFFD-Sh group. OGTTs were conducted in 24-h-fasted dogs at baseline (BL; ●), and after 4 (■) and 8 (▲) weeks of feeding a HFFD to sham-operated dogs (HFFD-Sh; $n = 4$). Polycose was administered orally (0.9 g/kg), and plasma glucose (A), c-peptide (B), and insulin (C) concentrations were measured over 180 min. *Insets:* Delta AUCs over 180 min for glucose (A), c-peptide (B), and insulin (C). Data are means \pm SE. * $P < 0.05$ vs. baseline Δ AUC.

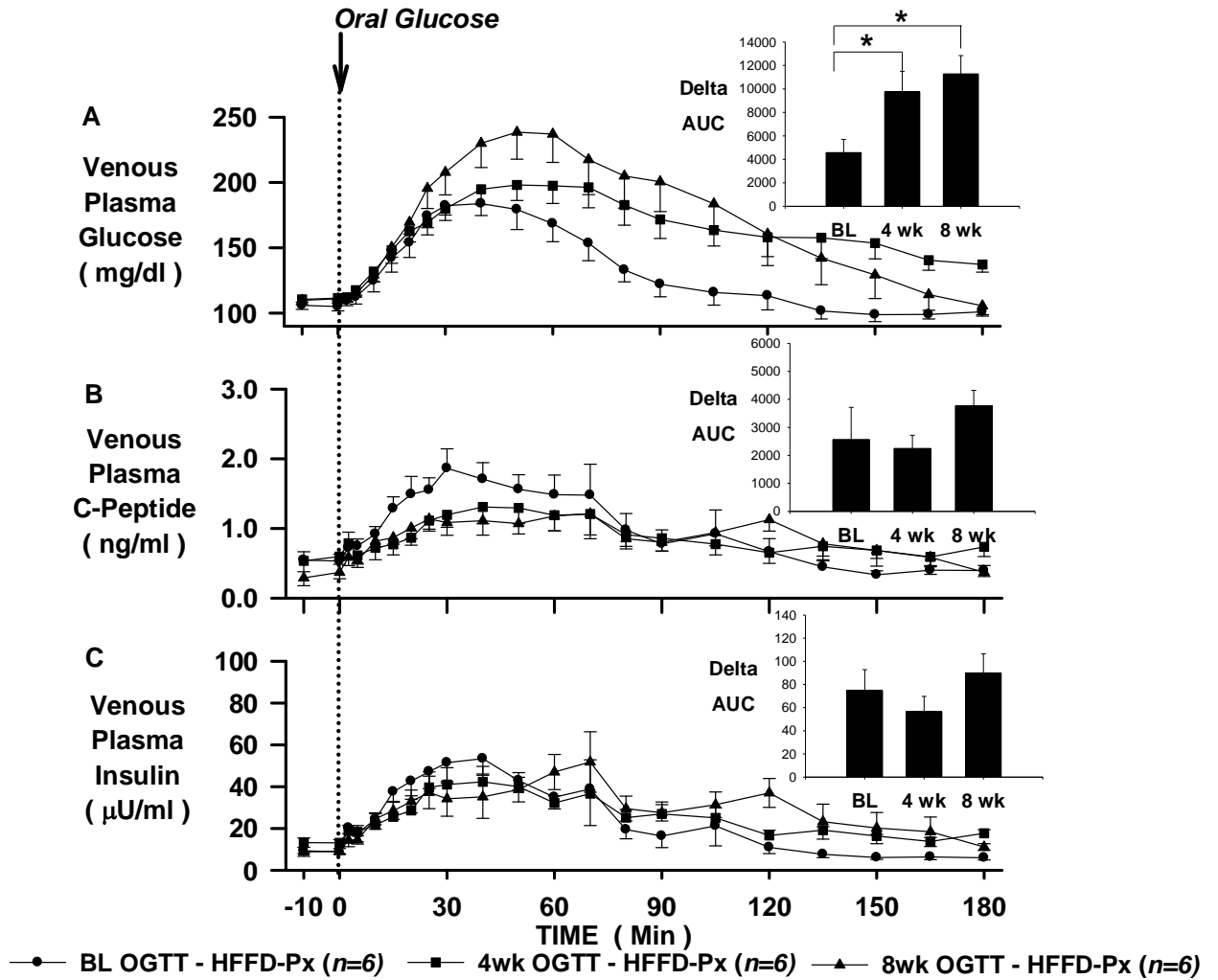


Figure 3.4: OGTTs in HFFD-Px group. OGTTs were conducted in 24-h-fasted dogs at baseline (BL; ●), and after 4 (■) and 8 (▲) weeks of feeding a HFFD to partially pancreatectomized dogs (HFFD-Px; $n = 6$). Polycose was administered orally (0.9 g/kg), and plasma glucose (A), c-peptide (B), and insulin (C) concentrations were measured over 180 min. *Insets:* Delta AUCs over 180 min for glucose (A), c-peptide (B), and insulin (C). Data are means \pm SE. * $P < 0.05$ vs. baseline Δ AUC.

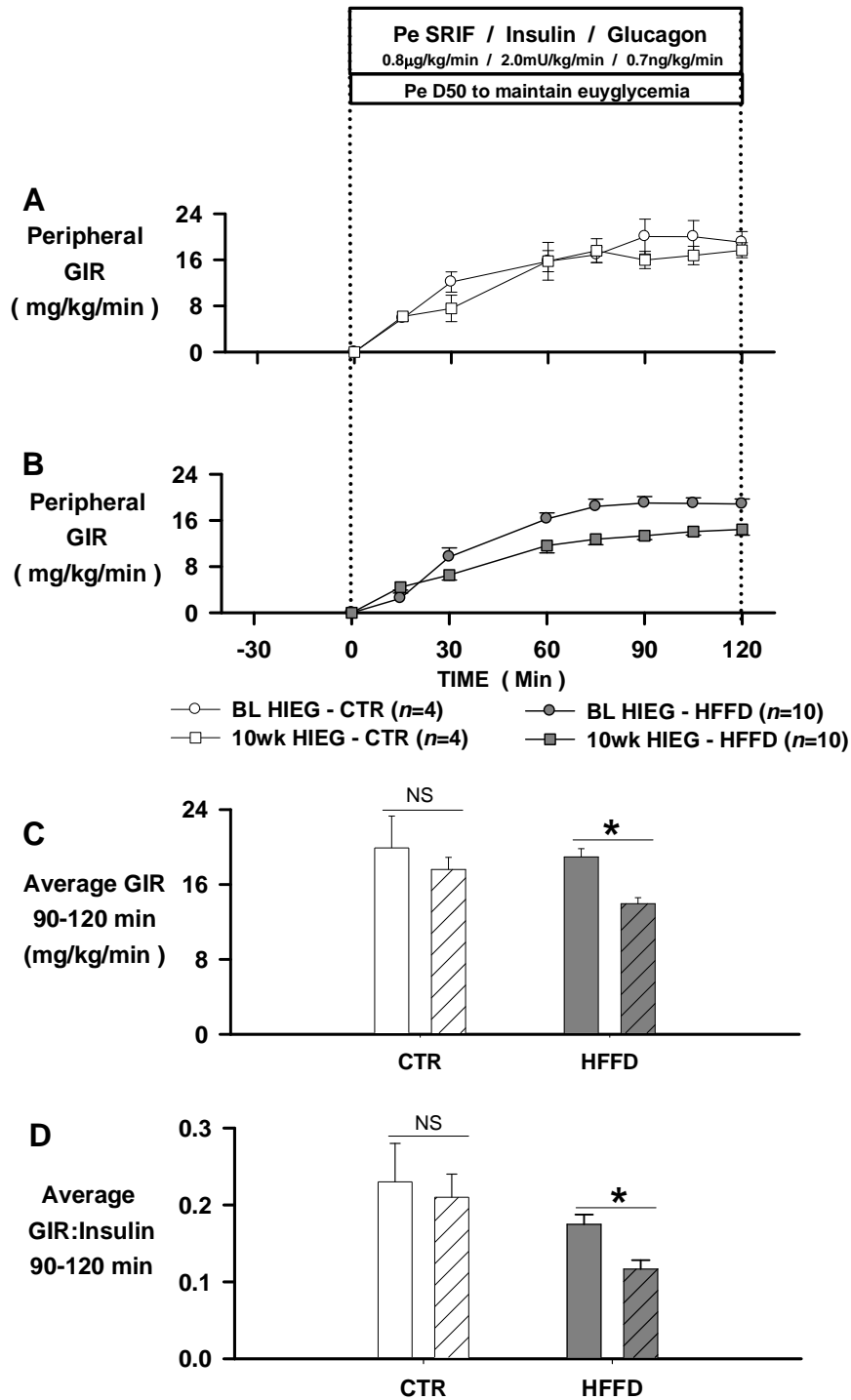


Figure 3.5: Hyperinsulinemic euglycemic clamps in CTR and HFFD groups. Mean glucose infusion rates (GIR; A and B) during HIEG clamps conducted in 18-h-fasted dogs at baseline (BL; CTR, ○; HFFD, ●) and after 10 weeks (CTR, □; HFFD, ■) of feeding a CTR ($n = 4$; A) or a HFFD to Sh or Px ($n = 10$; B) dogs. Average GIR (C) and GIR-to-insulin ratios (D) during 90-120 min of HIEGs conducted at BL (filled bars) and after 10 weeks (patterned bars) of feeding. Data from the HFFD-Sh and HFFD-Px groups were combined in B-D because the reduction in GIR (mg/kg/min) after 10 weeks of HFFD feeding was similar between groups (HFFD-Sh, BL: 18.5 ± 1.7 , 10wk: 13.9 ± 0.7 ; HFFD-Px, BL: 19.2 ± 1.3 , 10wk: 14.1 ± 1.1). Data are means \pm SE. * $P < 0.05$ vs. baseline; NS, not significant.

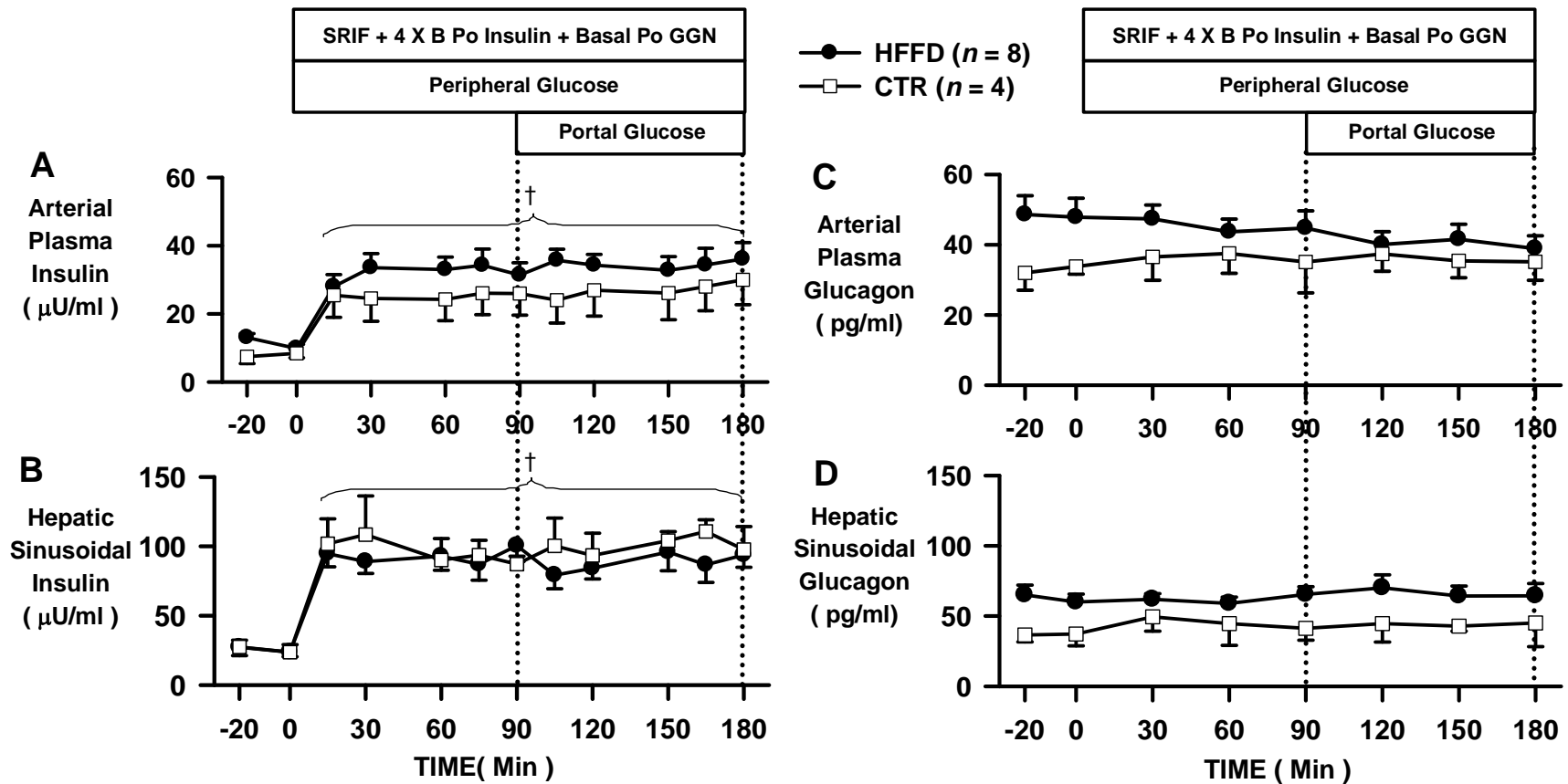


Figure 3.6: Plasma hormone concentrations during hyperinsulinemic hyperglycemic clamps in CTR and HFFD groups. Arterial plasma insulin (A) and glucagon (C), and hepatic sinusoidal insulin (B) and glucagon (D) during the basal (-20 to 0 min) and experimental periods (0 to 180 min) of HIHG clamps conducted in 18-h-fasted dogs after 13 weeks of feeding a CTR diet ($n = 4$; □) or a HFFD ($n = 8$; ●). Data from the HFFD-Sh and HFFD-Px groups were combined in this figure because there were no differences between groups for these clamped parameters. Two dogs in the HFFD-Px group had to be dropped from the cohort, one because of catheter failure and one because of an infusion error. Data are means \pm SE. † $P < 0.05$ vs. basal period (HFFD and CTR groups).

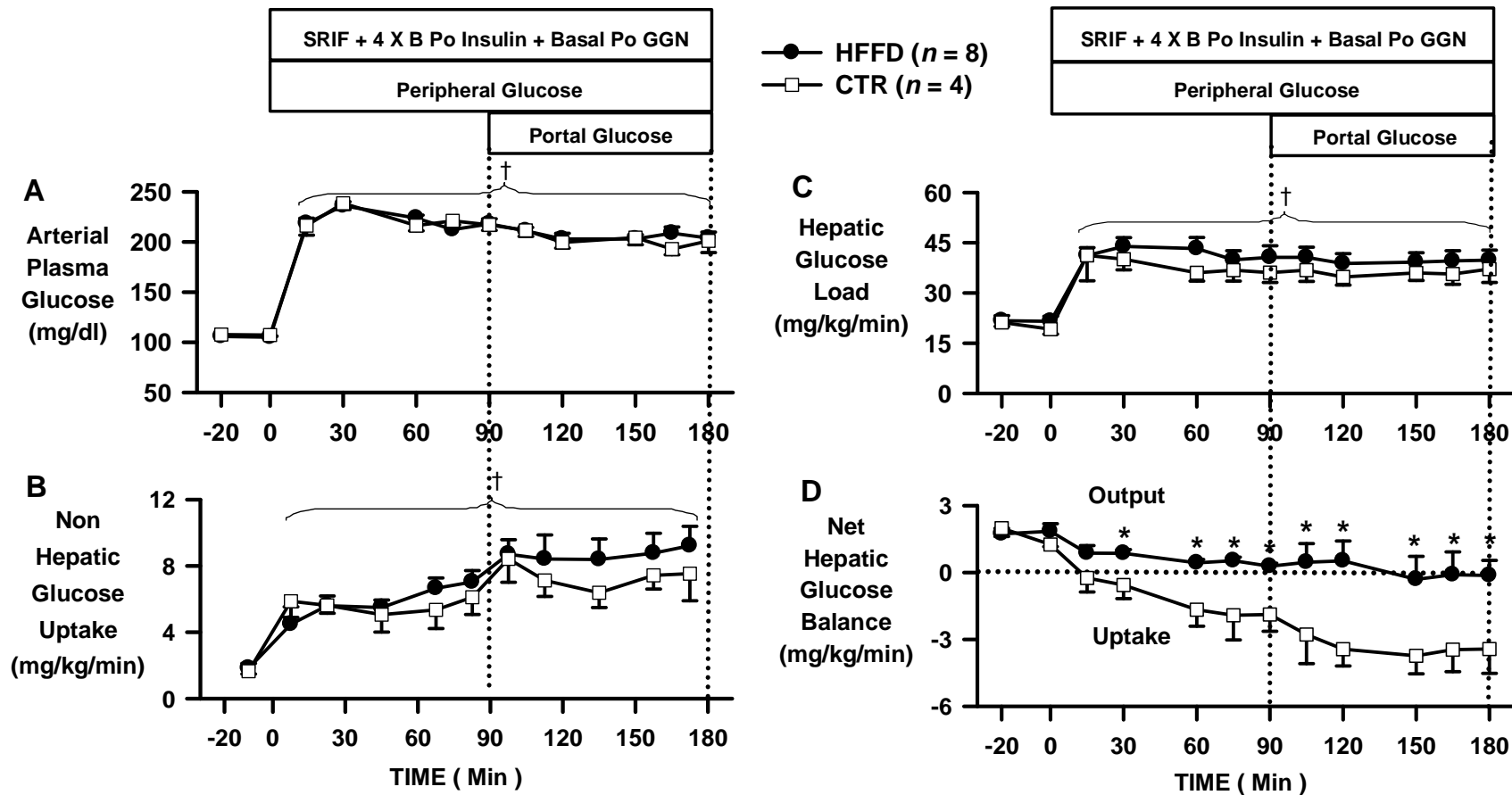


Figure 3.7: Hyperinsulinemic hyperglycemic clamps in CTR and HFFD groups. Arterial blood glucose (A), nonhepatic glucose uptake (B), hepatic glucose load (C) and net hepatic glucose balance (NHGB; D) during the basal (-20 to 0 min) and experimental periods (0 to 180 min) of HIHG clamps conducted in 18-h-fasted dogs after 13 weeks of feeding a CTR diet ($n = 4$; \square) or a HFFD ($n = 8$; \bullet). Negative values for NHGB indicate net hepatic uptake; positive values indicate net hepatic production. Data from the HFFD-Sh and HFFD-Px groups were combined for HIHG analyses because there was no difference in NHGB (mg/kg/min) between the two groups (average during last 30 min of the 2 subperiods; HFFD-Sh: -0.1 ± 0.5 ; HFFD-Px: 0.3 ± 0.8). Data are means \pm SE. † $P < 0.05$ vs. basal period (HFFD and CTR groups); * $P < 0.05$ vs. CTR group.

TABLE 3.1.
Venous plasma glucagon concentrations during OGTTs

Group	Basal Period,	Experimental Period, min					
	-10 to 0 min	30	60	90	120	150	180
<i>Plasma Glucagon (pg/ml)</i>							
CTR							
BL	38 ± 11	34 ± 9	31 ± 7	29 ± 8	29 ± 7	35 ± 6	31 ± 8
4wk	40 ± 4	37 ± 3	39 ± 3	33 ± 5	30 ± 4	32 ± 4	35 ± 3
8wk	65 ± 7	58 ± 8	55 ± 14	52 ± 8	57 ± 9	46 ± 2	50 ± 4
HFFD-Sh							
BL	46 ± 11	54 ± 12	43 ± 7	45 ± 12	44 ± 14	47 ± 11	43 ± 10
4wk	42 ± 9	41 ± 11	43 ± 9	40 ± 11	42 ± 11	47 ± 11	42 ± 10
8wk	46 ± 5	38 ± 4	47 ± 14	44 ± 12	47 ± 12	41 ± 12	42 ± 12
HFFD-Px							
BL	42 ± 9	42 ± 10	44 ± 13	41 ± 9	37 ± 9	41 ± 9	39 ± 7
4wk	47 ± 9	38 ± 10	44 ± 13	43 ± 8	38 ± 8	39 ± 8	40 ± 7
8wk	43 ± 10	45 ± 10	46 ± 9	48 ± 11	48 ± 9	46 ± 8	48 ± 11

Values are means ± S.E.; CTR, $n = 4$; HFFD-Sh, $n = 4$; HFFD-Px, $n = 6$. Dogs were 24-h-fasted prior to study. BL, baseline.

TABLE 3.2.

Venous plasma glucose, insulin, glucagon, free fatty acid, and triglyceride concentrations during hyperinsulinemic euglycemic clamps

Group	Basal Period, -30 to 0 min	Experimental Period, min			
		30	60	90	120
<i>Plasma glucose, mg/dl</i>					
CTR					
BL	102 ± 3	102 ± 1	101 ± 6	105 ± 7	104 ± 2
10wk	104 ± 4	93 ± 8	90 ± 5	113 ± 5	99 ± 3
HFFD					
BL	108 ± 2	99 ± 4	97 ± 2	106 ± 3	104 ± 3
10wk	110 ± 2	104 ± 4	103 ± 2	101 ± 2	105 ± 3
<i>Plasma insulin, μU/ml</i>					
CTR					
BL	8 ± 1	76 ± 5 [†]	82 ± 8 [†]	84 ± 7 [†]	85 ± 6 [†]
10wk	7 ± 1	87 ± 13 [†]	83 ± 6 [†]	85 ± 6 [†]	83 ± 8 [†]
HFFD					
BL	10 ± 1	104 ± 7 [†]	110 ± 7 [†]	113 ± 7 [†]	114 ± 5 [†]
10wk	11 ± 1	122 ± 9 [†]	125 ± 10 [†]	128 ± 10 [†]	126 ± 11 [†]
<i>Plasma glucagon, pg/ml</i>					
CTR					
BL	34 ± 5	42 ± 8	41 ± 3	42 ± 3	40 ± 3
10wk	47 ± 11	44 ± 6	45 ± 5	44 ± 3	48 ± 9
HFFD					
BL	41 ± 5	49 ± 5	48 ± 6	50 ± 6	48 ± 6
10wk	43 ± 5	52 ± 4	49 ± 5	48 ± 6	46 ± 6
<i>Plasma free fatty acids, μmol/l</i>					
CTR					
BL	821 ± 49	166 ± 30 [†]	56 ± 7 [†]	48 ± 10 [†]	39 ± 13 [†]
10wk	775 ± 113	127 ± 26 [†]	97 ± 21 [†]	71 ± 21 [†]	62 ± 19 [†]
HFFD					
BL	758 ± 97	168 ± 52 [†]	105 ± 13 [†]	71 ± 11 [†]	54 ± 9 [†]
10wk	751 ± 72	146 ± 21 [†]	113 ± 27 [†]	80 ± 10 [†]	61 ± 8 [†]
<i>Plasma triglycerides, μmol/l</i>					
CTR					
BL	1195 ± 81	1202 ± 107	1044 ± 104	937 ± 106	841 ± 96 [†]
10wk	1244 ± 239	1304 ± 188	1122 ± 142	979 ± 146	958 ± 182
HFFD					
BL	870 ± 100	858 ± 105	779 ± 117	669 ± 75 [†]	625 ± 58 [†]
10wk	1021 ± 77	979 ± 89	812 ± 75 [†]	736 ± 58 [†]	700 ± 72 [†]

Values are means ± SE; CTR, *n* = 4; HFFD, *n* = 10. Dogs were 18-h-fasted prior to study. [†]*P* < 0.05 vs. basal period.

TABLE 3.3.
Body weight, fasting plasma glucose, and insulin

Group	Week of CTR or HFFD Feeding			
	BL	4 wk	8 wk	13 wk
Body weight, kg				
CTR	25 ± 2	24 ± 1	25 ± 2	26 ± 1
HFFD	26 ± 1	28 ± 1	29 ± 1	29 ± 1
Plasma glucose, mg/dl				
CTR	106 ± 5	99 ± 9	105 ± 6	108 ± 1
HFFD	106 ± 2	107 ± 3	108 ± 2	106 ± 1
Plasma insulin, µU/ml				
CTR	8 ± 2	8 ± 1	6 ± 1	8 ± 2
HFFD	8 ± 1	11 ± 1*	10 ± 1	11 ± 1*

Values are means ± SE; CTR, *n* = 4; HFFD, *n* = 10. Data from the HFFD-Sh and HFFD-Px groups were combined because there was no difference between groups for each parameter. Dogs were 24-h-fasted prior to plasma collection. **P* < 0.05 vs. baseline (BL; paired *t*-test).

TABLE 3.4.

Tracer-determined rate of endogenous glucose appearance (Endo R_a), net hepatic glucose balance (NHGB), estimated hepatic glucose uptake (Est HGU = Endo R_a - NHGB), and rate of glucose disappearance (Glucose R_d) during hyperinsulinemic hyperglycemic clamps in a subset of dogs

Group	Basal Period		Experimental Period			
			Period 1		Period 2	
Endo R_a						
CTR	2.2	± 0.2	0.6	± 0.5 [†]	0.8	± 0.6 [†]
HFFD	2.4	± 0.2	1.7	± 0.2	0.4	± 0.2 [†]
NHGB						
CTR	1.6	± 0.2	-1.9	± 0.8 [†]	-3.5	± 0.9 [†]
HFFD	1.6	± 0.1	0.3	± 0.1 ^{†*}	-0.9	± 0.9 [†]
Est HGU						
CTR	0.6	± 0.3	2.5	± 1.2	4.3	± 1.3 [†]
HFFD	0.8	± 0.3	1.4	± 0.3	1.3	± 0.7
Glucose R_d						
CTR	2.2	± 0.2	7.3	± 0.8 [†]	10.0	± 1.5 [†]
HFFD	2.4	± 0.2	7.0	± 0.9 [†]	8.7	± 1.3 [†]

Values are means ± SE in mg/kg/min; CTR, $n = 4$; HFFD, $n = 4$. Negative values for balance data indicate net hepatic uptake; positive values indicate net hepatic output. Dogs were 18-h-fasted prior to study. [†] $P < 0.05$ vs. basal period; * $P < 0.05$ vs. CTR.

TABLE 3.5.

Total hepatic blood flow, total glucose infusion rate, arterial blood lactate and glycerol concentrations, arterial plasma NEFA concentration, net hepatic lactate, glycerol and NEFA balance, and net hepatic carbon retention during hyperinsulinemic hyperglycemic clamps

Group	Basal Period		Experimental Period					
			Period 1			Period 2		
Total hepatic blood flow, ml/kg/min								
CTR	23	± 3	21	± 3	22	± 3		
HFFD	27	± 2	25	± 2	26	± 1		
Total glucose infusion rate, mg/kg/min								
CTR	0.0	± 0.0	7.7	± 0.9 [†]	11.0	± 1.2 [†]		
HFFD	0.0	± 0.0	6.0	± 0.6 [†]	9.1	± 1.0 [†]		
Arterial blood lactate, μmol/l								
CTR	295	± 10	703	± 113 [†]	829	± 58 [†]		
HFFD	296	± 17	469	± 35 ^{†*}	731	± 72 [†]		
Net hepatic lactate balance, μmol/kg/min								
CTR	-6.4	± 0.9	5.3	± 2.8 [†]	6.2	± 2.3 [†]		
HFFD	-6.9	± 0.8	-3.6	± 1.1 ^{†*}	-4.1	± 0.8 ^{†*}		
Arterial blood glycerol, μmol/l								
CTR	81	± 17	33	± 5 [†]	34	± 7 [†]		
HFFD	96	± 7	42	± 7 [†]	44	± 9 [†]		
Net hepatic glycerol balance, μmol/kg/min								
CTR	-1.6	± 0.5	-0.6	± 0.1	-0.7	± 0.1		
HFFD	-2.3	± 0.3	-0.8	± 0.1	-1.0	± 0.2		
Arterial plasma NEFA, μmol/L								
CTR	828	± 117	122	± 22 [†]	62	± 10 [†]		
HFFD	813	± 81	127	± 34 [†]	101	± 38 [†]		
Net hepatic NEFA balance, μmol/kg/min								
CTR	-2.4	± 0.9	-0.4	± 0.1 [†]	-0.1	± 0.1 [†]		
HFFD	-3.0	± 0.4	-0.2	± 0.1 [†]	-0.2	± 0.1 [†]		
Net hepatic carbon retention, mg glucose equivalents/kg/min								
CTR	-1.0	± 0.1	0.7	± 0.7 [†]	2.6	± 0.9 [†]		
HFFD	-1.2	± 0.2	-0.1	± 0.1 [†]	0.5	± 0.8 [†]		

Values are means ± SE; CTR, *n* = 4; HFFD, *n* = 8. Negative values for balance data indicate net hepatic uptake; positive values indicate net hepatic production; negative values for carbon retention indicate net hepatic glycogen breakdown; positive values indicate net hepatic glycogen synthesis. Dogs were 18-h-fasted prior to study. [†]*P* < 0.05 vs. basal period; **P* < 0.05 vs. CTR.

CHAPTER IV

A HIGH-FAT, HIGH-FRUCTOSE DIET ACCELERATES NUTRIENT ABSORPTION AND IMPAIRS NET HEPATIC GLUCOSE UPTAKE IN RESPONSE TO A MIXED MEAL IN PARTIALLY PANCREATECTOMIZED DOGS

(Adapted from Coate et al. *J Nutr* 141:1-9, 2011)

Aim

The liver serves as one of the principal buffers of perturbations in postprandial glycemia; however, individuals with diabetes display a marked impairment not only in the ability of hyperinsulinemia and hyperglycemia to suppress hepatic glucose production, but also in the ability of those postprandial stimuli to activate splanchnic glucose uptake and hepatic glycogen synthesis in response to a mixed meal [200, 201, 203, 204]. In Specific Aim I, we found that chronic consumption of a high-fat, high-fructose diet renders the liver incapable of switching from net glucose output to net glucose uptake. However, this defect was identified in response to a glucose challenge, which lacked other meal-associated factors that can influence the gastric emptying rate, insulin and glucagon secretion, and net hepatic glucose uptake (NHGU) [295-304]. Thus, the goal of Specific Aim II was to investigate whether high-fat, high-fructose (HFFD) feeding impairs NHGU during a more physiological mixed meal test. Experiments were conducted to assess the response of the liver and extrahepatic tissues to an orally-

administered liquid mixed meal after consumption of a HFFD or a chow control diet (CTR) for 8 weeks.

Experimental Design

Ten adult male mongrel dogs were randomly assigned to either a CTR diet ($n = 5$) or a HFFD ($n = 5$) for 8 weeks (Table 4.1). Dogs in CTR or HFFD underwent a sham or partial pancreatectomy (PPx; $\approx 65\%$ resection), respectively, at wk 0, as described under *Surgical Procedures* in Chapter II. Approximately 2 weeks before the meal test (week 6 of feeding), dogs underwent a second laparotomy for hepatic catheterization and flow cuff placement, as described under *Surgical Procedures* in Chapter II. After 8 weeks of feeding, dogs were challenged with a liquid mixed meal, and net gut/hepatic substrate balance was measured.

Oral mixed meal tests were carried out in dogs that had been feed-deprived for 24-h. On the morning of the study, a liquid mixed meal was drawn up into two 60 mL syringes. Following the control period, it was delivered directly into the dog's mouth over the course of 2 minutes in order to activate the cephalic response to a meal. Experiments consisted of consecutive 60 min equilibration (0 to 60 min) and control (60 to 120 min) periods, followed by oral administration of a defined liquid mixed meal, and then a 270 min postprandial sampling period (120 to 390 min). The test meal consisted of 20% protein (26.9g Beneprotein [96 kcal]; Nestle Healthcare Nutrition, Inc., Minneapolis, MN), 56% carbohydrate (67.2g Polycose [255 kcal]; Abbott Nutrition, Columbus, OH) and 24% fat (25.3 ml Microlipid [114 kcal]; Nestle Healthcare Nutrition, Inc., Minneapolis, MN). Beneprotein and Polycose were dissolved in 60 mL of water along

with Microlipid. Each meal was spiked with acetaminophen (500 mg) in order to measure the gastric emptying rate during mixed meal testing [305]. Blood was drawn every 10 min during the early postprandial period (120 to 150 min), and every 30 min thereafter (180 to 390 min).

Results

Glucose metabolism and hormone levels

In CTR, arterial plasma glucose levels tended to rise in response to the meal and tended to remain elevated for the duration of the study, albeit not significantly greater than their glucose concentrations during the basal period (Figure 4.1A). A significant increase from basal in net gut output of glucose was evident 1 h after the meal which coincided with an increase in the gastric emptying rate, as indicated by a significant elevation from basal in arterial plasma acetaminophen concentration in CTR (Figure 4.1B and C). Glucose output by the gut and arterial plasma acetaminophen levels eventually plateaued 3 h post-meal delivery in CTR (Figure 4.1B and C). In HFFD, on the other hand, arterial plasma glucose levels increased more rapidly from basal following meal consumption, and were significantly elevated from basal and CTR for 2.5 h post-meal delivery (Figure 4.1A). Glucose output by the gut also increased more rapidly from basal in HFFD, albeit for a shorter duration, peaking 1.5 h post-meal administration ($P < 0.05$ vs. basal period and CTR), and then falling such that during the last hour of the experiment, it was significantly lower in HFFD than in CTR (Figure 4.1B). In agreement with their gut glucose absorption profile, arterial plasma acetaminophen levels were significantly increased in HFFD vs. CTR during the early postprandial period (Figure

4.1C).

In response to the meal, there was a 4- and 5-fold increase from basal in arterial plasma c-peptide ($P < 0.05$) and insulin concentrations, respectively, in CTR, as well as a significant elevation from basal in arterial and portal vein plasma GLP-1 (active form) concentrations 3 h post-meal administration (Figure 4.2 A-C and Table 4.2). In agreement with a sustained rate of gastric emptying and delivery of nutrients to the gut, plasma GLP-1 levels tended to remain elevated from basal throughout the experiment in CTR (Figure 4.2C and Table 4.2). In contrast, there was a 5- and 7-fold increase from basal ($P < 0.05$) in arterial plasma c-peptide and insulin concentrations, respectively, in HFFD, which were significantly greater than those in CTR during the experiment (Figure 4.2A and B). Likewise, arterial and portal vein plasma GLP-1 levels were significantly greater in HFFD vs. CTR 1 h post-meal delivery, but returned to basal levels by the end of the study (Figure 4.2C and Table 4.2). There were no significant changes from basal or between groups in arterial or hepatic sinusoidal plasma glucagon concentrations following meal consumption (Table 4.2).

During the basal period, net hepatic glucose output (NHGO) was comparable between CTR and HFFD groups (Figure 4.3A). In response to meal consumption, the livers of dogs in CTR rapidly switched from net glucose output to net glucose uptake ($P < 0.05$ vs. basal period and HFFD), and remained in an uptake mode for the duration of the study (Figure 4.3A). In contrast, NHGU was nearly absent in HFFD, as evidenced by the lack of a significant change from basal in net hepatic glucose balance following meal consumption (Figure 4.3A). As a result, NHGU was significantly lower in HFFD vs. CTR during the last 2 h of the experiment (Figure 4.3A). On the other hand, non-hepatic

glucose uptake (non-HGU) in response to meal consumption was markedly amplified in HFFD compared to CTR ($P < 0.05$ vs. basal period and CTR) (Figure 4.3C). Given that the ratios of non-HGU to arterial insulin (CTR: 0.15 ± 0.04 , HFFD: 0.10 ± 0.01) and non-hepatic glucose clearance to arterial insulin (CTR: 0.15 ± 0.04 , HFFD: 0.09 ± 0.01) were similar between groups, these data indicate that the muscle was able to compensate for impaired NHGU in HFFD, but at the expense of increased postprandial plasma insulin and glucose.

Lactate metabolism

In both CTR and HFFD, arterial blood lactate levels increased from basal following meal consumption (Figure 4.4A). In CTR, this was consistent with a robust switch from net hepatic lactate uptake to output, and a significant increase from basal in net hepatic carbon retention, an index of net hepatic glycogen synthesis (GSYN) (Figure 4.4B and Figure 4.3B, respectively). Net hepatic lactate output and GSYN continued for the remainder of the study in CTR. In HFFD, on the other hand, there was only a transient switch from net hepatic lactate uptake to output following meal consumption, and the rate was significantly lower in HFFD than in CTR during the experiment (Figure 4.4B). This was consistent with a significantly diminished rate of net hepatic carbon retention in HFFD compared to CTR (Figure 4.3B). These data suggest that in the absence of meal-associated glucose uptake, the livers of dogs in the HFFD group produced significantly less lactate and synthesized significantly less glycogen.

Glycerol, non-esterified fatty acid (FFA), and triglyceride metabolism

During the basal period, arterial blood glycerol levels were significantly elevated in HFFD vs. CTR (Table 4.3). Although arterial blood glycerol and plasma FFA levels

fell rapidly in both groups following meal consumption, glycerol concentrations remained significantly higher in HFFD vs. CTR for the duration of the study (Table 4.3). Likewise, arterial plasma FFA concentrations began to rise in HFFD 3 h post-meal delivery such that by the end of the study, they were similar to basal values and significantly greater than those in CTR (Table 4.3). Changes in net hepatic glycerol uptake paralleled those in arterial blood glycerol; by the end of the study, net hepatic glycerol uptake was significantly greater in HFFD compared to CTR (Table 4.3). Arterial plasma triglyceride (TG) concentrations declined in both groups over the first 3 postprandial hours, after which they remained low in CTR but returned to basal levels in HFFD (Table 4.3).

Alanine metabolism

Arterial blood alanine levels rose to a significantly greater extent in HFFD than in CTR 2 h post-meal administration (Table 4.4). This was partly attributable to a 5- vs. 3-fold increase from basal in alanine output from the gut in HFFD vs. CTR, respectively, 1 h post-meal delivery, coupled with a lower hepatic fractional extraction of alanine during the mid- to late postprandial period in HFFD vs. CTR (Table 4.4).

Discussion

The objective of the present study was to investigate whether chronic consumption of a HFFD, in combination with partial ($\approx 65\%$) pancreatic resection, alters the response of the liver and extrahepatic tissues to an orally-delivered, liquid mixed meal under non-clamped experimental conditions. A HFFD was utilized because it reflects the macronutrient composition of a western diet, which contains foods that are replete with

fat and fructose, and when consumed in increasing quantities, has been associated with a heightened risk for the development of type 2 diabetes [28, 306]. We report herein that 8 weeks of HFFD feeding elicited: 1) excessive postprandial hyperglycemia due to accelerated gastric emptying and glucose absorption, as well as diminished NHGU, and 2) a reduction in the ability of insulin to suppress lipolysis.

Several factors probably contributed to postprandial hyperglycemia in HFFD-fed animals. For example, the rates of gastric emptying and glucose absorption can influence the timing and magnitude of postprandial glucose excursions in healthy and diabetic individuals [307, 308]. Previously, Davis et al. [309] demonstrated that glucose absorption (and presumably, gastric emptying) occurs very slowly in the overnight fasted dog when fed a test meal of the same composition as their normal diet. In the present study, a sustained rate of glucose output by the gut occurred in the CTR group following meal consumption, consistent with the observations of Davis et al. [309]. In contrast, the rates of gastric emptying and glucose output by the gut were significantly increased in HFFD vs. CTR during the early postprandial period, consistent with excessive postprandial hyperglycemia in the former. Furthermore, there was a tendency for alanine production by the gut to be greater in HFFD vs. CTR 1 h post-meal delivery, suggesting that accelerated nutrient absorption in HFFD was not exclusive to glucose. By the end of the study, however, temporal differences in gastric emptying and nutrient absorption between groups were reversed such that net glucose and alanine output by the gut were significantly greater in CTR vs. HFFD, indicative of accelerated meal macronutrient absorption in the latter.

In addition, there was a doubling in arterial and portal vein plasma GLP-1 levels

10 min post-meal delivery in HFFD, whereas there was virtually no change 10 min post-meal in CTR. GLP-1 is an incretin hormone secreted by the L-cells cells of the distal small intestine primarily in response to nutrient ingestion [310, 311]. GLP-1 is thought to delay gastric emptying and potentiate glucose-dependent insulin secretion, thus limiting postprandial hyperglycemia [312-321]. Previous studies conducted in our laboratory, however, have demonstrated that a physiologic rise in endogenous GLP-1 is without significant effect on insulin secretion, gastric emptying, and glucose utilization in dogs [322-324]. Thus, we believe that the temporal changes in GLP-1 levels in the current study are a reflection of the differential gastric emptying rates in HFFD vs. CTR.

Previous studies conducted in individuals in the early stages of type 2 diabetes or those without autonomic neuropathy have also reported an accelerated gastric emptying rate following consumption of a glucose solution or liquid mixed meal [325-332]. Although the mechanisms that mediate differential gastric emptying rates in healthy and diabetic individuals remain poorly defined, one study [327] attributed augmented gastric emptying to increased phasic contractility of the proximal stomach in patients with asymptomatic (no autonomic neuropathy) type 2 diabetes. It is also possible that the HFFD induced perturbations in the gut microbiota, which might have elicited an increase in intestinal permeability as a consequence of endotoxemia, as reported previously [333-338]. Future studies will need to be conducted to explore the mechanism(s) responsible for accelerated gastric emptying in HFFD-fed animals.

Another factor that contributed to meal-associated glucose intolerance in HFFD was inadequate stimulation of NHGU. Under normal conditions, the liver is highly responsive to the route of glucose delivery (peripheral vs. enteral/intraportal), the hepatic

glucose load, and the hepatic sinusoidal insulin level [183, 196, 197]. However, NHGU was markedly diminished in HFFD vs. CTR despite 1.6- and 2.4-fold greater increases in peak plasma glucose and insulin levels, respectively. These data suggest that HFFD feeding rendered the liver insensitive to the stimulatory effects of glucose, insulin, and portal glucose delivery on NHGU in the context of a physiologic mixed meal challenge, consistent with our previous findings with a glucose challenge [339].

In agreement with impaired NHGU, net hepatic lactate production, an index of net glycolytic flux, and net hepatic carbon retention, an index of net GSYN, were markedly diminished in HFFD vs. CTR following meal consumption. Previously, Basu et al. [200, 201] reported that decreased hepatic UDP-glucose flux in type 2 diabetic individuals during hyperinsulinemia and hyperglycemia is entirely accounted for by a decrease in the contribution of extracellular glucose to the UDP-glucose pool, suggestive of reduced hepatic glucokinase (HGK) activity with diabetes. Moreover, restoration of HGK expression in 20-week-old Zucker diabetic fatty rats, a genetic model of obese type 2 diabetes, normalized their hepatic glucose flux and the incorporation of glucose into glycogen during a hyperglycemic clamp [246]. Thus, it is possible that HFFD feeding impaired HGK activity, which resulted in diminished NHGU and GSYN in response to a mixed meal challenge.

Interestingly, Non-HGU, which is primarily reflective of glucose uptake in the skeletal muscle [340], was augmented in HFFD vs. CTR in response to meal ingestion. This was due in part to the fact that the skeletal muscle of dogs in the HFFD group was exposed to a much higher concentration of glucose and insulin postprandially. Thus, through a mass action effect of glucose as well as through the pleiotropic effects of

insulin on muscle glucose uptake [340-343], the skeletal muscle responded accordingly by increasing its consumption of glucose. Indeed, when Non-HGU or clearance was expressed relative to the arterial plasma insulin level in HFFD and CTR, the ratios were similar between groups, suggesting that augmented Non-HGU in HFFD was secondary to elevated insulin and glucose. These data also underscore the predominance of the defect in hepatic glucose uptake.

Eight weeks of HFFD feeding was also associated with a remarkable resistance to insulin at the level of triglyceride hydrolysis within the adipose tissue. This was evident from the fact that postprandial blood glycerol concentrations were significantly elevated in HFFD vs. CTR despite peak arterial plasma insulin concentrations that were 100% greater in HFFD. Conversely, plasma FFA concentrations were similar between groups, indicative of a selective impairment in the ability of insulin to suppress lipolysis, whereas the ability of hyperinsulinemia and hyperglycemia to stimulate re-esterification of FFA into TG remains intact. The latter is exemplified by the fact that plasma FFA concentrations began to increase in HFFD towards the end of the study as plasma insulin and glucose concentrations waned.

We cannot ascertain from these data whether relative beta cell failure contributed to meal-associated glucose intolerance in HFFD because we do not know how much insulin would have been secreted in CTR had their plasma glucose concentrations been matched to those of HFFD. What we now know that was not evident at the time in which we designed these experiments is that resection of 65% of the pancreas is insufficient to exacerbate the glucose intolerance induced by HFFD feeding [339]. This is consistent with previous studies conducted in rodents in which removal of 85-95% of the pancreas

was required before diabetes ensued, and even then, there was a heterogeneous hyperglycemic response, which correlated with the extent of pancreatic resection [288, 289]. Nevertheless, the possibility cannot be excluded that in the context of a mixed meal, factors associated with a PPx might have influenced the results in the present study.

This study revealed novel metabolic consequences of a HFFD on the function of the gastrointestinal tract, liver, and adipose tissue in response to a mixed meal. These data highlight the need for additional studies aimed at elucidating the mechanism(s) by which a HFFD per se perturbs the coordinated response of the aforementioned tissues in the postprandial state.

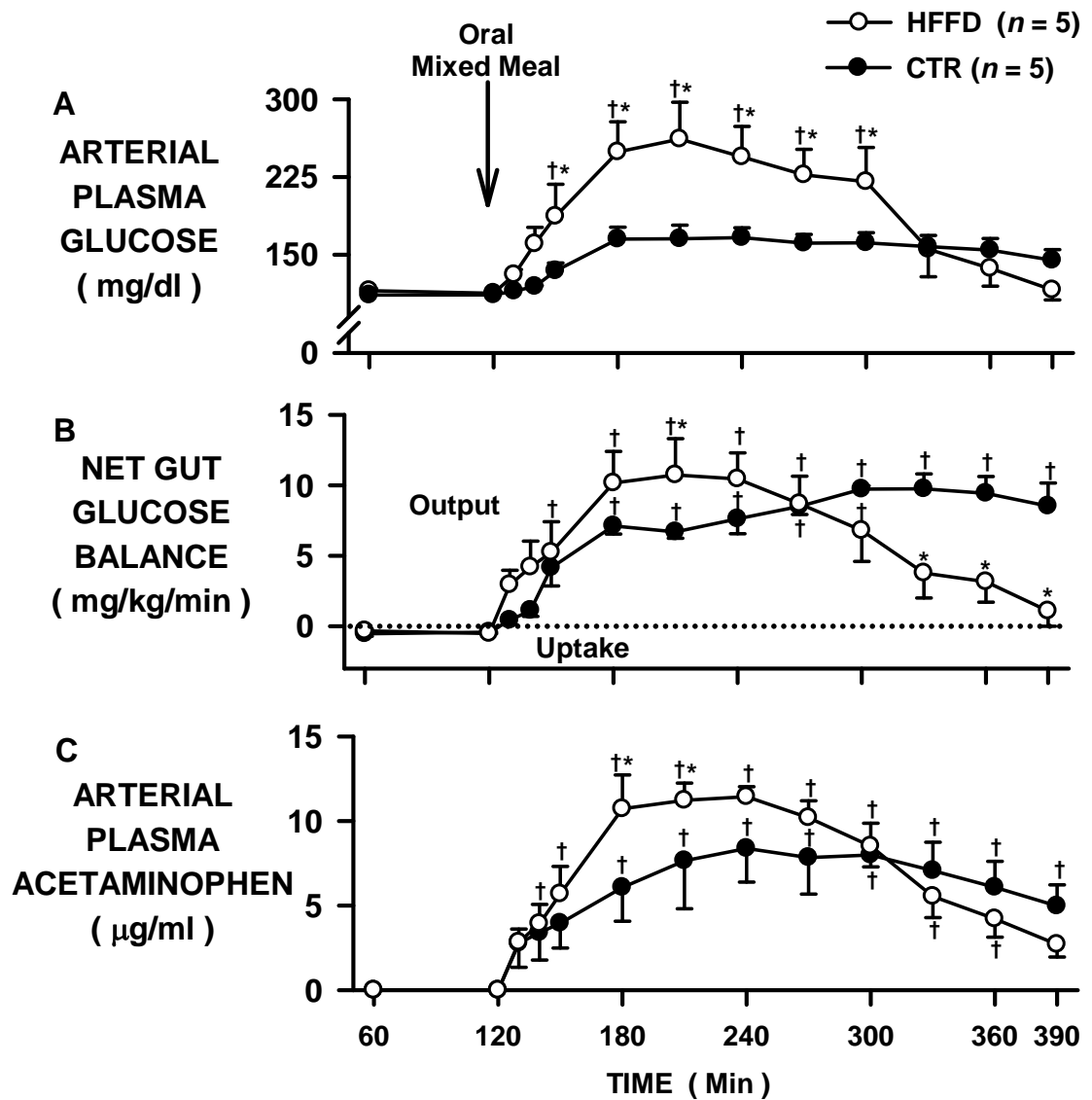


Figure 4.1: Arterial plasma glucose (A), net gut glucose balance (B), and arterial plasma acetaminophen (C) concentrations during the basal (60 to 120 min) and experimental (120 to 390 min) periods following oral administration of a liquid mixed meal to 24-h-fasted dogs that had been fed a CTR ($n = 5$; \bullet) or HFFD ($n = 5$; \circ) for 8 weeks. Data are means \pm SE. † $P < 0.05$ vs. basal period; * $P < 0.05$ vs. CTR group.

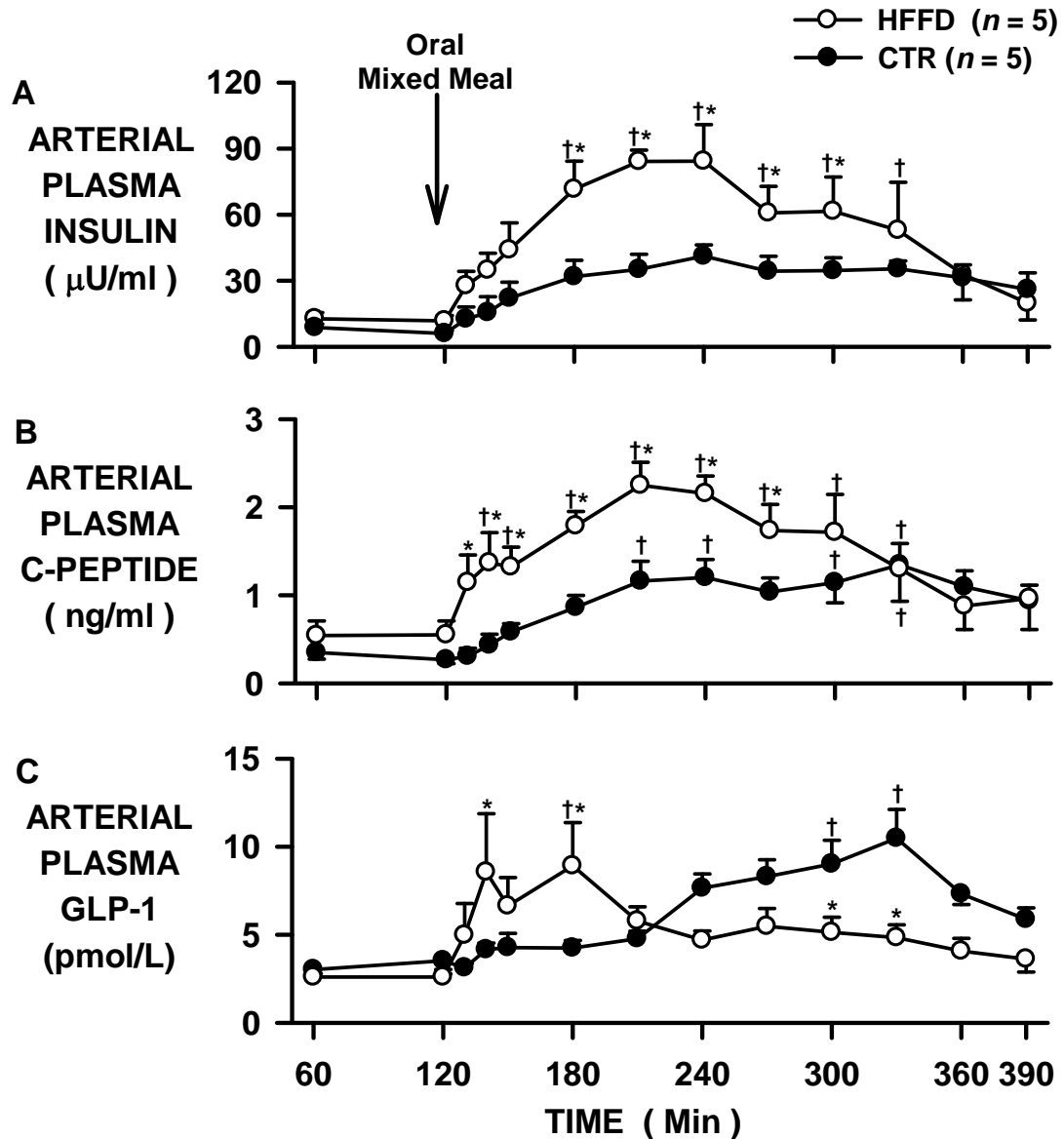


Figure 4.2: Arterial plasma insulin (A), c-peptide (B), and glucagon like peptide-1 (GLP-1, active) (C) concentrations during the basal (60 to 120 min) and experimental (120 to 390 min) periods following oral administration of a liquid mixed meal to 24-h-fasted dogs that had been fed a CTR ($n = 5$; ●) or HFFD ($n = 5$; ○) for 8 weeks. Data are means \pm SE. † $P < 0.05$ vs. basal period; * $P < 0.05$ vs. CTR group.

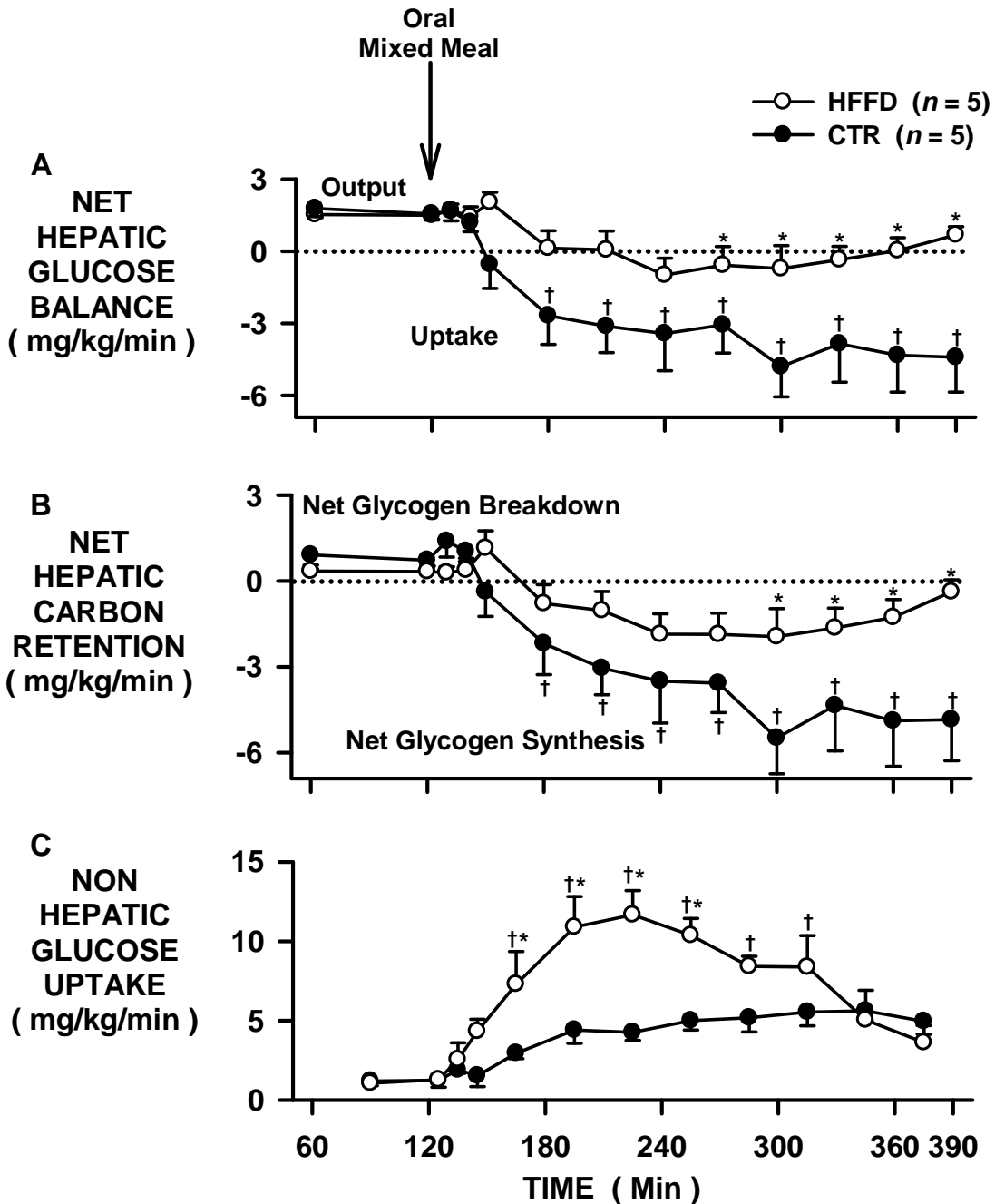


Figure 4.3: Net hepatic glucose balance (NHGB) (A), net hepatic carbon retention (NHCR; mg of glucose equivalents) (B), and nonhepatic glucose uptake (C) during the basal (60 to 120 min) and experimental (120 to 390 min) periods following oral administration of a liquid mixed meal to 24-h-fasted dogs that had been fed a CTR ($n = 5$; ●) or HFFD ($n = 5$; ○) for 8 weeks. Negative values for NHGB or NHCR indicate net hepatic glucose uptake or glycogen synthesis, respectively; positive values indicate net hepatic glucose output or glycogen breakdown, respectively. Data are means \pm SE. † $P < 0.05$ vs. basal period; * $P < 0.05$ vs. CTR group.

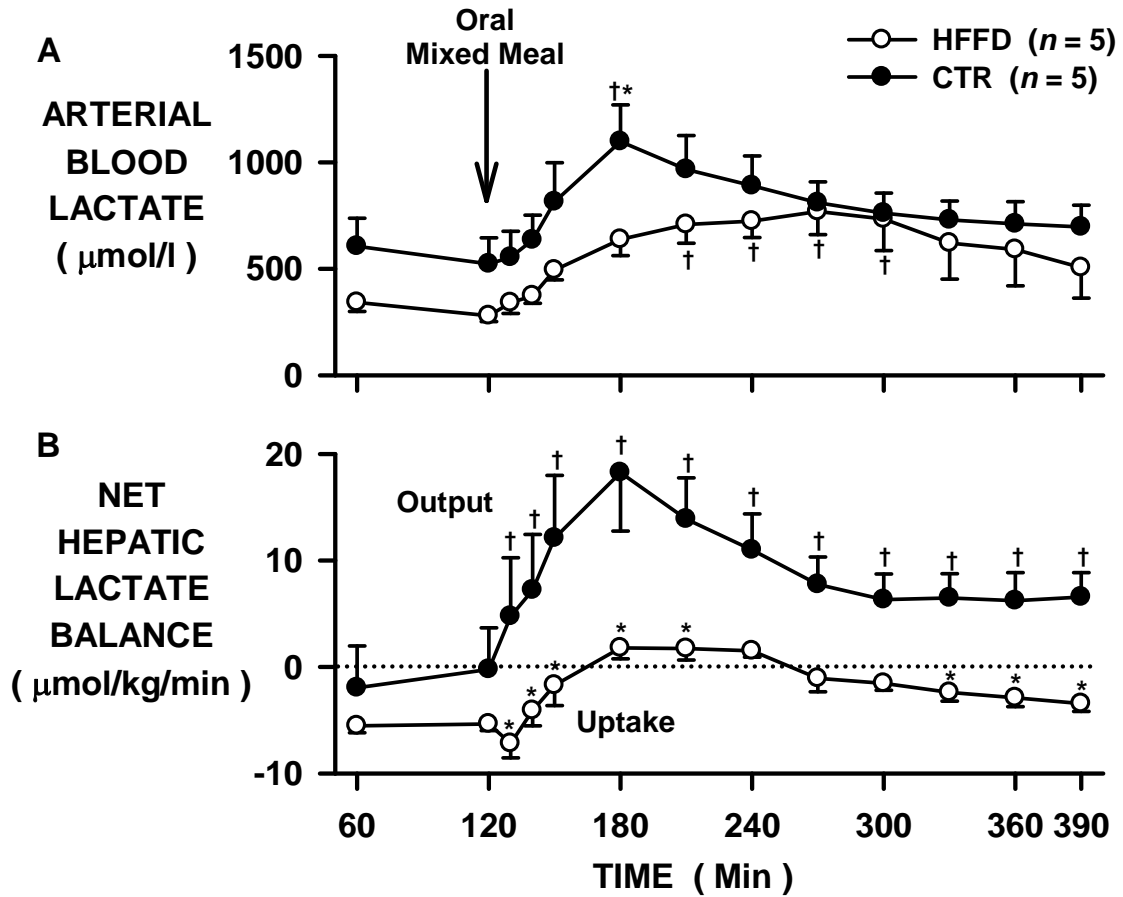


Figure 4.4: Arterial blood lactate (A) and net hepatic lactate balance (B) during the basal (60 to 120 min) and experimental (120 to 390 min) periods following oral administration of a liquid mixed meal to 24-h-fasted dogs that had been fed a CTR ($n = 5$; ●) or HFFD ($n = 5$; ○) for 8 weeks. Negative values for net hepatic lactate balance indicate net hepatic lactate uptake; positive values indicate net hepatic lactate output. Data are means \pm SE. † $P < 0.05$ vs. basal period; * $P < 0.05$ vs. CTR group.

TABLE 4.1.*Composition of the experimental diets*

Nutrient	High-Fat, High-Fructose Diet (HFFD) Composition	Meat + Chow Control Diet (CTR) Composition
	g/kg diet	g/kg diet
Protein ¹	247	289
Fat ²	252	98
Saturated Fat	110.9	36.6 ³
Monounsaturated Fat	104.2	34.0 ³
Polyunsaturated Fat	34.2	13.3 ³
Total Carbohydrate	298	355
Starch ⁴	95.9	335
Glucose	0.1	2.3
Fructose	189.3	2.3
Sucrose	7.4	10.8
Lactose	5.6	4.6
Crude Fiber ⁵	22	28
Moisture	100	100
Vitamins ⁶	1.7	1.7
Minerals ⁷	73	73
Percentage of Energy:	%	%
Protein	21.8	30.7
Fat	52.0	25.8
Total Carbohydrate	26.2	43.5
Starch	8.5	41.0
Glucose	<0.01	0.3
Fructose	16.7	0.3
Sucrose	0.6	1.3
Lactose	0.5	0.6
Energy Density	18.9 kJ/g	17.3 kJ/g

¹Protein sources include porcine meat meal, dehulled soybean meal, corn gluten meal, wheat middlings, and dried whey

²Fat sources include lard, porcine animal fat, vegetable shortening, and/or unsalted butter

³Corresponds to saturated, mono- and polyunsaturated fat content of non-purified diet only; these data are not provided by the manufacturer for the can of meat

⁴Starch sources include wheat germ and middlings

⁵Fiber sources include wheat, beat pulp, and corn

⁶Vitamin mix, mg/kg prepared diet: provitamin A carotenoids, 1.0; retinol, 12.0; cholecalciferol, 0.11; α -tocopherol, 29.4; menadione, 0.3; thiamin hydrochloride, 8.9; riboflavin, 4.5; niacin, 78; pantothenic acid, 20; folic acid, 2.8; pyridoxine, 13; biotin, 0.2; vitamin B-12, 27; choline chloride, 1492

⁷Mineral mix, g/kg (unless otherwise specified) prepared diet: calcium, 19.2; phosphorus, 10.6; phosphorus (available), 9.1; potassium, 7.0; magnesium, 1.7; sulfur, 2.0; sodium, 4.5; chloride, 7.1; fluorine, 48 mg/kg; iron, 390 mg/kg; zinc, 160 mg/kg; manganese, 55 mg/kg; copper, 14 mg/kg; cobalt, 0.5 mg/kg; iodine, 1.7 mg/kg; chromium, 2.3 mg/kg; selenium, 0.36 mg/kg

TABLE 4.2.

Portal vein plasma glucagon like peptide-1 (GLP-1), arterial plasma glucagon, and hepatic sinusoidal plasma glucagon concentrations during the basal (60 to 120 min) and experimental (120 to 390 min) periods following oral administration of a liquid mixed meal to 24-h-fasted dogs that had been fed a control diet (CTR) or a high-fat, high-fructose diet (HFFD) for 8 weeks

	Basal Period			Experimental Period														
	<i>min</i>			<i>min</i>														
	60 to 120			180	240	300	360	390										
	<i>Portal vein plasma GLP-1, pmol/l</i>																	
CTR	3.9	±	0.5	5.6	±	0.7	12.7	±	1.8	15.6	±	2.8 [†]	13.5	±	1.4	9.6	±	1.1
HFFD	3.1	±	0.3	14.4	±	4.7 ^{†*}	9.8	±	1.4	9.4	±	2.8	9.7	±	3.8	6.5	±	3.0
	<i>Arterial plasma glucagon, ng/l</i>																	
CTR	47.4	±	6.4	40.6	±	4.3	40.9	±	4.2	43.2	±	4.5	45.2	±	5.2	43.8	±	3.4
HFFD	31.9	±	6.0	34.4	±	4.1	36.2	±	6.0	35.5	±	6.4	36.1	±	4.0	36.4	±	4.2
	<i>Hepatic sinusoidal plasma glucagon, ng/l</i>																	
CTR	51.0	±	7.7	43.5	±	6.8	45.2	±	4.6	49.1	±	10.9	47.3	±	8.6	49.1	±	7.5
HFFD	40.1	±	6.1	43.4	±	4.0	40.6	±	3.3	41.2	±	5.2	41.2	±	4.0	42.2	±	6.4

Values are means ± SE; CTR, *n* = 5; HFFD, *n* = 5. [†]*P* < 0.05 vs. basal period; **P* < 0.05 vs. CTR.

TABLE 4.3.

Arterial blood glycerol, net hepatic glycerol uptake, and arterial plasma FFA and TG concentrations during the basal (60 to 120 min) and experimental (120 to 390 min) periods following oral administration of a liquid mixed meal to 24-h-fasted dogs that had been fed a control diet (CTR) or a high-fat, high-fructose diet (HFFD) for 8 weeks

	Basal Period		Experimental Period					
	<i>min</i>		<i>min</i>					
	60 to 120	180	240	300	360	390		
	<i>Arterial blood glycerol, $\mu\text{mol/l}$</i>							
CTR	87 \pm 7	29 \pm 4 [†]	27 \pm 3 [†]	31 \pm 3 [†]	29 \pm 3 [†]	32 \pm 3 [†]		
HFFD	113 \pm 10 [*]	55 \pm 14 ^{†*}	56 \pm 13 ^{†*}	60 \pm 15 ^{†*}	83 \pm 9 ^{†*}	80 \pm 6 ^{†*}		
	<i>Net hepatic glycerol uptake, $\mu\text{mol/kg/min}$</i>							
CTR	1.9 \pm 0.2	0.7 \pm 0.1 [†]	0.6 \pm 0.1 [†]	0.6 \pm 0.1 [†]	0.5 \pm 0.1 [†]	0.5 \pm 0.1 [†]		
HFFD	1.9 \pm 0.3	1.3 \pm 0.4 [†]	1.2 \pm 0.4 [†]	1.4 \pm 0.5 [*]	1.6 \pm 0.2 [*]	1.6 \pm 0.2 [*]		
	<i>Arterial plasma FFA, $\mu\text{mol/l}$</i>							
CTR	926 \pm 122	144 \pm 7 [†]	123 \pm 5 [†]	104 \pm 12 [†]	81 \pm 4 [†]	92 \pm 8 [†]		
HFFD	914 \pm 43	137 \pm 34 [†]	92 \pm 21 [†]	137 \pm 59 [†]	280 \pm 104 ^{†*}	402 \pm 110 ^{†*}		
	<i>Arterial plasma TG, mmol/l</i>							
CTR	0.22 \pm 0.03	0.20 \pm 0.03	0.18 \pm 0.11	0.16 \pm 0.03	0.14 \pm 0.02 [†]	0.16 \pm 0.03 [†]		
HFFD	0.20 \pm 0.02	0.19 \pm 0.02	0.16 \pm 0.01	0.15 \pm 0.01	0.18 \pm 0.01	0.19 \pm 0.03		

Values are means \pm SE; CTR, $n = 5$; HFFD, $n = 5$. [†] $P < 0.05$ vs. basal period; $*$ $P < 0.05$ vs. CTR.

TABLE 4.4.

Arterial blood alanine, gut production of alanine, net hepatic alanine uptake, and hepatic fractional extraction of alanine during the basal (60 to 120 min) and experimental (120 to 390 min) periods following oral administration of a liquid mixed meal to 24-h-fasted dogs that had been fed a control diet (CTR) or a high-fat, high-fructose diet (HFFD) for 8 weeks

	Basal Period		Experimental Period				
	<i>min</i>		<i>min</i>				
	60 to 120	180	240	300	360	390	
	<i>Arterial blood alanine, $\mu\text{mol/l}$</i>						
CTR	284 \pm 46	350 \pm 20	321 \pm 9	313 \pm 17	307 \pm 20	311 \pm 19	
HFFD	318 \pm 35	442 \pm 25 [†]	452 \pm 29 ^{†*}	452 \pm 46 ^{†*}	409 \pm 46 [†]	374 \pm 63 [†]	
	<i>Gut production of alanine, $\mu\text{mol/kg/min}$</i>						
CTR	1.1 \pm 0.2	3.5 \pm 0.4 [†]	3.6 \pm 0.5 [†]	3.7 \pm 0.3 [†]	3.9 \pm 0.4 [†]	3.8 \pm 0.6 [†]	
HFFD	0.9 \pm 0.1	4.4 \pm 0.5 [†]	3.7 \pm 0.4 [†]	2.8 \pm 0.4 [†]	3.4 \pm 1.0 [†]	1.1 \pm 0.4 [*]	
	<i>Net hepatic alanine uptake, $\mu\text{mol/kg/min}$</i>						
CTR	3.0 \pm 0.1	5.8 \pm 0.6 [†]	5.4 \pm 0.6 [†]	6.5 \pm 0.1 [†]	5.8 \pm 0.6 [†]	5.3 \pm 0.6 [†]	
HFFD	1.9 \pm 0.3	4.9 \pm 0.7 [†]	4.5 \pm 0.6 [†]	4.6 \pm 0.5 ^{†*}	3.9 \pm 0.5 ^{†*}	2.5 \pm 0.5 [*]	
	<i>Hepatic fractional extraction of alanine</i>						
CTR	0.29 \pm 0.04	0.32 \pm 0.02	0.33 \pm 0.02	0.41 \pm 0.02 [†]	0.37 \pm 0.03 [#]	0.35 \pm 0.03	
HFFD	0.22 \pm 0.02	0.25 \pm 0.02	0.27 \pm 0.03	0.32 \pm 0.04 ^{†*}	0.32 \pm 0.04 [†]	0.25 \pm 0.03 [*]	

Values are means \pm SE; CTR, $n = 5$; HFFD, $n = 5$. [†] $P < 0.05$ vs. basal period; ^{*} $P < 0.05$ vs. CTR.

CHAPTER V

PORTAL VEIN GLUCOSE ENTRY TRIGGERS A COORDINATED MOLECULAR RESPONSE THAT ACTIVATES HEPATIC GLUCOSE UPTAKE AND GLYCOGEN SYNTHESIS IN NORMAL, BUT NOT HIGH-FAT, HIGH- FRUCTOSE-FED, DOGS

(Manuscript in preparation)

Aim

Neither hyperinsulinemia (physiologic) nor hyperglycemia alone is sufficient to stimulate hepatic glucose uptake (HGU) [182, 190, 205-207]. Likewise, a physiologic elevation in plasma insulin concomitant with hyperglycemia resulting from the infusion of glucose into a peripheral vein is insufficient to elicit the peak rates of HGU and glycogen synthesis (GSYN) that occur in response to oral glucose ingestion [27, 182, 183, 185, 190, 192, 198, 206, 344]. On the other hand, hyperinsulinemia and hyperglycemia in the presence of hepatic portal venous glucose delivery (by means of oral glucose ingestion or intraduodenal/portal vein glucose infusion), markedly amplifies HGU and GSYN in the rat [180, 181], dog [181-189], and human [190, 191]. The augmentation of HGU elicited by the intraportal route of glucose delivery has been attributed to a unique, neurally-mediated signal generated in the presence of a negative arterial-portal venous glucose gradient, termed the “portal glucose signal” [26, 182-184, 193-199]. In response to ingestion of a glucose-containing meal, the portal signal works

in concert with increased plasma glucose and insulin to orchestrate a coordinated response favoring enhanced HGU and GSYN [26, 198]. Although the metabolic effects of intraportal glucose delivery have been studied in experimental animal models and in the human, the molecular events linking the pleiotropic actions of the portal glucose signal to increased HGU and GSYN in vivo have not clearly defined. Thus, the first objective of Specific Aim III was to identify the molecular “signature” of the portal glucose signal per se in the presence of a physiologic rise in glucose and insulin.

Postprandial hyperglycemia is one of the sequelae of diabetes that contributes to the elevation of hemoglobin A1c associated with the disease [24, 25]. It is due in part to inappropriate suppression of hepatic glucose production coupled with inadequate stimulation of HGU, highlighting the key role of the liver in regulating postprandial glucose metabolism [200, 202-204, 239-243]. Indeed, splanchnic glucose uptake (SGU) and hepatic GSYN through the direct pathway were markedly diminished in type 2 diabetic subjects compared to non-diabetic controls despite equivalent elevations in plasma insulin and glucose during a clamp experiment [200, 201, 244]. Furthermore, delivery of glucose into the portal venous circulation (by way of enteral glucose infusion) in the presence of hyperinsulinemia was ineffective in normalizing the diminished rates of SGU and GSYN in diabetic subjects [200]. The authors [200, 201] conjectured that a defect in glucokinase was linked to the aberrant hepatic response in type 2 diabetic individuals, but cellular evidence supporting their supposition was not provided. In Specific Aims I and II, we demonstrated that HFFD feeding is also associated with a significant impairment in NHGU and GSYN in response to a glucose challenge or a mixed-meal challenge, but the cellular events associated with a diminished hepatic

response to hyperinsulinemia, hyperglycemia, and portal glucose delivery were not identified. Thus, the second objective of Specific Aim III was to elucidate the molecular explanation for the defect in HGU caused by HFFD feeding, and whether it persists in the presence of the portal glucose signal.

Experimental Design (Figure 5.1)

Adult male mongrel dogs were randomly assigned to either a standard meat and laboratory chow diet (CTR, $n=15$), or to a high-fat, high-fructose diet (HFFD, $n=16$) for 4 weeks. The specific macronutrient compositions of the CTR and HFFD diets are listed in Table 2.2 under *Experimental Diets*, and also in more detail in Table 4.1. After 4 weeks of feeding, a subset of dogs (CTR, $n = 5$; HFFD, $n = 5$) was euthanized following an 18-h fast for the acquisition of liver biopsies under basal conditions. In the remaining dogs, hyperinsulinemic hyperglycemic (HIHG) clamp experiments with (+) or without (-) portal vein glucose (PoG) infusion were conducted following an 18-h-fasted dogs. Just prior to the fast, each dog was fed a can of meat as their meal to ensure equivalent energy and macronutrient consumption among groups the day before the study. There were four groups total: HIHG-PoG CTR, $n = 5$; HIHG-PoG HFFD, $n = 5$; HIHG +PoG CTR, $n = 5$; and HIHG+PoG HFFD, $n = 6$. As described in Figure 5.1, each experiment consisted of a 100 min equilibration period (-120 to -20 min), a 20 min basal control period (-20 to 0 min), and a 180 min experimental period divided into 2 sub-periods (P1, 0 to 90 min; P2, 90 to 180 min). At -120 min, a priming dose of [$3\text{-}^3\text{H}$] glucose (38 μCi) was given, followed by a constant infusion of [$3\text{-}^3\text{H}$] glucose (0.38 $\mu\text{Ci}/\text{min}$). At time 0, a constant infusion of somatostatin (0.8 $\mu\text{g}/\text{kg}/\text{min}$) was started in a peripheral vein, and insulin and

glucagon were then replaced intraportally at 3-fold basal (1.2 mU/kg/min) and basal (0.55 ng/kg/min) rates, respectively. In addition, a variable infusion of 50% dextrose was started in a leg vein in order to double the hepatic glucose load (HGL). In P2, normal saline (HIHG-PoG) or 20% dextrose (HIHG+PoG; 4.0 mg/kg/min) was infused intraportally. In the HIHG+PoG groups, the peripheral glucose infusion rate was adjusted as necessary to clamp the HGL to that in P1. For this study, unidirectional hepatic glucose uptake was calculated using a tracer-determined hepatic fractional extraction method, as described in detail under *Calculations* in Chapter II. At the end of the study, each animal was anaesthetized with sodium pentobarbital and a laparotomy was performed. The hormone, cold glucose, and [^3H] glucose infusions were continued while liver sections from the left central, left lateral, and right central lobes were freeze-clamped in situ and stored at -80°C until tissue analysis. Glucokinase relative expression (mRNA and protein) and activity, glucokinase regulatory protein content, phosphorylation of Akt, GSK3 β , and glycogen synthase, glycogen synthase and phosphorylase activity ratios, and terminal liver glycogen levels were determined in liver biopsies obtained at the end of the clamp experiment in all four groups (as described in detail under *Liver Tissue Analysis* in Chapter II). These values were compared to values from liver biopsies obtained under basal conditions (see above) in dogs that had been fed the CTR or HFFD 4 weeks, but were not clamped.

Results

Plasma hormone concentrations and hepatic blood flow

HFFD feeding was associated with 43% and 47% increases in fasting arterial

plasma insulin ($\mu\text{U/ml}$; CTR: 6.9 ± 0.9 , HFFD: 9.8 ± 1.1 , $P = 0.05$) and c-peptide (ng/ml ; CTR: 0.30 ± 0.05 , HFFD: 0.45 ± 0.07 , $P = 0.13$) concentrations, respectively, during the basal period, but there was no effect of diet on arterial plasma glucagon levels. During the HIHG clamp, arterial and hepatic sinusoidal insulin concentrations ($\mu\text{U/ml}$; HIHG-PoG CTR: 22 ± 1 and 68 ± 6 , HIHG-PoG HFFD: 23 ± 1 and 67 ± 3 , HIHG+PoG CTR: 23 ± 4 and 78 ± 10 , HIHG+PoG HFFD: 27 ± 1 and 81 ± 11 ; $P < 0.05$ vs. basal period) were increased to similar levels in all 4 groups, whereas arterial and hepatic sinusoidal glucagon concentrations were kept at a basal level throughout the study (Figure 5.2 A-D). Total hepatic blood flow was similar among the 4 groups under basal conditions and throughout the HIHG clamp (Table 5.1).

Blood glucose, hepatic glucose load, and total glucose infusion rate

Fasting blood glucose concentrations did not differ between groups during the basal period. During P1, arterial blood glucose concentrations were increased to a similar level in all 4 groups (mg/dl ; HIHG-PoG CTR: 159 ± 3 , HIHG-PoG HFFD: 161 ± 3 , HIHG+PoG CTR: 161 ± 4 , HIHG+PoG HFFD: 166 ± 2 ; $P < 0.05$ vs. basal period) in order to double the hepatic glucose load (mg/kg/min ; HIHG-PoG CTR: 37 ± 3 , HIHG-PoG HFFD: 36 ± 3 , HIHG+PoG CTR: 37 ± 2 , HIHG+PoG HFFD: 37 ± 4 ; $P < 0.05$ vs. basal period) (Figure 5.3A and B). During P2, arterial blood glucose concentrations were clamped at a slightly reduced concentration in the HIHG+PoG groups (mg/dl ; CTR: 147 ± 3 , HFFD: 152 ± 2) to maintain a doubling of the hepatic glucose load in the presence of intraportal glucose infusion (Figure 5.3A). The total glucose infusion rates (GIR) required to maintain hyperglycemia in CTR and HFFD groups did not differ significantly from one another throughout the HIHG clamp (Table 5.1).

Hepatic glucose uptake, hepatic glucose production, and net hepatic glucose balance

Hepatic glucose uptake (HGU) and hepatic glucose production (HGP) (mg/kg/min; HIHG-PoG CTR: 0.3 ± 0.1 and 1.4 ± 0.1 , HIHG-PoG HFFD: 0.3 ± 0.1 and 1.8 ± 0.3 , HIHG+PoG CTR: 0.4 ± 0.1 and 2.1 ± 0.4 , and HIHG+PoG HFFD: 0.4 ± 0.1 and 1.9 ± 0.3 , respectively) were similar among all 4 groups during the basal period (Figure 5.3C and D and Table 5.2). In response to hyperinsulinemia and hyperglycemia, HGU increased to a similar rate in both CTR groups during P1, reaching a peak of 1.5 ± 0.3 and 1.8 ± 0.3 mg/kg/min in the HIHG-PoG CTR and HIHG+PoG CTR groups, respectively ($P < 0.05$ vs. basal period) (Figure 5.3C and D and Table 5.2). When coupled with near complete suppression of HGP during P1, a robust switch from net hepatic glucose output (NHGO) to uptake (NHGU) occurred in both CTR groups (Table 5.2). In the absence of portal glucose delivery during P2 in the HIHG-PoG CTR group, mean rates of HGU and NHGU (1.6 ± 0.1 and 1.5 ± 0.2 mg/kg/min, respectively) were similar to that in P1 (Figure 5.3C and Table 5.2). On the other hand, delivery of glucose into the portal vein in the presence of a sustained rise in glucose and insulin rapidly augmented HGU in the HIHG+PoG CTR group, with a significant increase occurring 15 min after the start of intraportal glucose infusion (HGU, mg/kg/min; HIHG-PoG CTR: 1.4 ± 0.2 vs. HIHG+PoG CTR: 2.2 ± 0.3 , $P < 0.05$), and eventually reaching a peak of 3.0 ± 0.3 mg/kg/min (Figure 5.3D and Table 5.2). Given that HGP was already suppressed, the significant increase in NHGU in response to portal glucose delivery in the HIHG+PoG CTR group was accounted for by an increase in HGU (Table 5.2).

In contrast to the response observed in CTR animals, 4 weeks of HFFD feeding rendered the liver resistant to the stimulatory effects of hyperinsulinemia, hyperglycemia,

and portal glucose delivery on HGU. As a result, mean rates of HGU in HFFD-fed animals during P1 and P2 (mg/kg/min; 0.4 ± 0.1 and 0.6 ± 0.2 in HIHG-PoG HFFD, and 0.5 ± 0.1 and 0.6 ± 0.2 in HIHG+PoG HFFD, respectively) changed minimally from those observed during the basal period, and were significantly diminished relative to rates observed in the corresponding CTR groups (Figure 5.3C and D and Table 5.2). Furthermore, HGP was incompletely suppressed in both HFFD groups during P1, resulting in sustained NHGO despite the presence of hyperinsulinemia and hyperglycemia (Table 5.2). In the absence of portal glucose delivery during P2, there was no further suppression of HGP in the HIHG-PoG HFFD group. Thus, mean rates of HGU and HGP remained similar to those in P1, and as a result, the liver failed to take up glucose in net sense for the duration of the experiment (Figure 5.3C and D and Table 5.2). In contrast, portal glucose delivery suppressed HGP further in the HIHG+PoG HFFD group ($P < 0.05$, P2 vs. P1), although it did not augment HGU (Table 5.2). As a result, NHGB fell to a value not significantly different from zero (Table 5.2).

Lactate metabolism

All groups exhibited net hepatic lactate uptake under basal conditions (Table 5.3). Coincident with the increase in HGU during P1, there was a significant increase in arterial blood lactate concentrations in both CTR groups that resulted from a switch from net hepatic lactate uptake to output in the presence of hyperinsulinemia and hyperglycemia (Table 5.3). Net hepatic lactate output waned during P2 in the absence of portal vein glucose infusion, while in its presence, it was sustained at an elevated rate, consistent with augmented HGU in response to the portal glucose signal (Table 5.3). On the other hand, both HFFD groups exhibited net hepatic lactate uptake for the duration of

the study, although it was somewhat reduced during both P1 and P2 (Table 5.3).

Glycerol, nonesterified fatty acid, and triglyceride metabolism

During the basal period, arterial blood glycerol and plasma NEFA concentrations were similar among the 4 groups. During P1 and P2, their levels declined in response to hyperinsulinemia, but the steady state values were slightly lower in the two CTR groups (Table 5.3). The net hepatic uptake rates of glycerol and NEFA decreased in parallel to the changes in their circulating concentrations, and were not different between groups (Table 5.3). Fasting plasma total triglyceride concentrations also did not differ between groups ($\mu\text{mol/l}$; 904 ± 116 , 1084 ± 65 , 1156 ± 220 , and 1089 ± 163 in HIHG-PoG CTR, HIHG-PoG HFFD, HIHG+PoG CTR, and HIHG+PoG HFFD, respectively; data not shown).

Hepatic glucokinase and glucokinase regulatory protein

Under basal conditions, GK mRNA levels were similar between CTR and HFFD groups (Figure 5.4A). Hyperinsulinemia in the presence of hyperglycemia stimulated a 6- and 7-fold increase in GK expression in HIHG-PoG CTR and HFFD groups, respectively ($P < 0.05$ vs. basal CTR) (Figure 5.4A). Strikingly, delivery of glucose into the portal vein in the presence of hyperinsulinemia and hyperglycemia stimulated a significantly greater increase in GK expression in the HIHG+PoG CTR and HFFD groups (26- and 24-fold increase above basal CTR animals, respectively; $P < 0.05$ vs. basal CTR and corresponding HIHG-PoG group) (Figure 5.4A). Likewise, portal glucose delivery was associated with a significant increase in the amount of GK protein and its activity in the HIHG+PoG CTR group relative to the HIHG-PoG CTR group (Figure 5.4B and C). In contrast, hepatic GK protein levels and its catalytic activity were markedly reduced in

HFFD-fed animals under basal conditions and during the HIHG clamp ($P < 0.05$ vs. corresponding CTR group), in agreement with impaired stimulation of HGU (Figure 5.4B and C). Further, portal glucose delivery failed to augment GK protein or activity. Interestingly, glucokinase regulatory protein (GKRP) levels were also significantly reduced in HFFD-fed animals under basal conditions and during the HIHG clamp (Figure 5.4D).

Hepatic insulin signaling and glycogen metabolism

Under basal conditions, the phosphorylation of Akt (P-Akt on Ser473) and GSK3 β (P- GSK3 β on Ser9) did not differ significantly between groups (Figure 5.5A and B). In CTR liver biopsies obtained at the end of the HIHG clamp, P-Akt on Ser473 was significantly increased from basal in both the absence and presence of portal glucose infusion (34% and 50% in HIHG-PoG and HIHG+PoG CTR, respectively; NS between the two groups) (Figure 5.5A). In contrast, P-Akt on Ser473 in the livers of HFFD-fed animals was significantly lower than in the corresponding CTR group under both experimental conditions, and did not change from basal in response to hyperinsulinemia and hyperglycemia (Figure 5.5A). P-GSK3 β on Ser9 did not change from basal in any of the groups, but tended to be reduced in HFFD-fed animals relative to CTR (Figure 5.5B).

Under basal conditions, the phosphorylation of GS (P-GS on Ser641) and the activity ratios of GS and GP were not different between CTR and HFFD groups (Figure 5.6 A-D). Likewise, total GS activity was similar between groups under basal conditions (data not shown). In the HIHG-PoG CTR group, hyperinsulinemia in the presence of hyperglycemia produced a significant decrease (35%) in P-GS on Ser641, consistent with stimulation of Akt phosphorylation (Figure 5.6A). Likewise, the activity ratio of GS

increased approximately 5-fold ($P < 0.05$ vs. basal), whereas that of GP was reduced by 40% (Figure 5.6B and C). Thus, when GS and GP were themselves expressed as a ratio (GS/GP), there was an 8-fold increase from basal ($P < 0.05$) concomitant with an increase in liver glycogen levels (Figure 5.6D and E). In the HIHG+PoG CTR group, delivery of glucose into the portal vein in the presence of hyperinsulinemia and hyperglycemia did not produce a further decrement in P-GS on Ser641, but did stimulate a further increase in the GS activity ratio (approximately 40%, $P < 0.05$ vs. HIHG-PoG CTR), and an additional small decrease in that of GP (Figure 5.6 A-C). As a result, the GS/GP activity ratio was elevated 12-fold in the presence of intraportal glucose infusion ($P < 0.05$ vs. HIHG-PoG CTR), and liver glycogen levels were increased significantly more than in the HIHG-PoG CTR group (Figure 5.6D and E).

In the HIHG-PoG HFFD group, on the other hand, hyperinsulinemia in the presence of hyperglycemia did not produce a decrease in P-GS on Ser641, consistent with lack of stimulation of Akt phosphorylation (Figure 5.6A). Although the activity ratio of GS increased approximately 3-fold ($P < 0.05$ vs. basal), it was significantly reduced relative to the corresponding CTR group, whereas the activity ratio of GP changed minimally from basal (Figure 5.6B and C). As a result, the GS/GP activity ratio and the change in liver glycogen were significantly lower in the HIHG-PoG HFFD group relative to the corresponding CTR group (Figure 5.6D and E). Portal glucose delivery in the presence of hyperinsulinemia and hyperglycemia produced no further change in P-GS on Ser641, or in the GS, GP, or GS/GP activity ratios (Figure 5.6 A-E). Total GS activity did not differ between groups during the HIHG clamp (data not shown). Although liver glycogen levels were slightly increased in the HIHG+PoG HFFD group, the change in

glycogen induced by portal glucose delivery was markedly less in HFFD-fed dogs than in CTR-fed dogs (Figure 5.6E). Lastly, HFFD-feeding was associated with a significant decrease (approximately 70% in HIHG-PoG and HIHG+PoG HFFD groups vs. the corresponding CTR group; $P < 0.05$) in the incorporation of glucose into glycogen through the direct synthetic pathway (glucose \rightarrow glucose 6-phosphate \rightarrow glucose 1-phosphate \rightarrow UDP-glucose \rightarrow glycogen), in agreement with diminished HGU and GK activity, and impaired activation of GS in response to hyperinsulinemia, hyperglycemia, and intraportal glucose infusion (Figure 5.6F).

Total Liver Triglyceride

There was no effect of diet or experimental condition on total liver triglyceride levels ($\mu\text{g}/\text{mg}$ liver; Basal CTR: 2.5 ± 0.4 , Basal HFFD: 1.6 ± 0.1 , HIHG-PoG CTR: 1.3 ± 0.2 , HIHG-PoG HFFD: 1.8 ± 0.4 , HIHG+PoG CTR: 1.4 ± 0.2 ; HIHG+PoG HFFD: 1.1 ± 0.2 ; data not shown).

Discussion

The first aim of this study was to identify the molecular “signature” of the portal glucose signal per se in the presence of a physiologic rise in glucose and insulin - experimental conditions that mimic the postprandial state. The second aim of this study was to elucidate the molecular explanation for the defect in HGU caused by HFFD feeding, and whether it persists in the presence of the portal glucose signal. To this end, we performed hyperinsulinemic hyperglycemic (HIHG) clamp experiments in the absence or presence (HIHG-PoG or HIHG+PoG, respectively) of portal vein glucose infusion in dogs that were fed a CTR or HFFD for 4 weeks. Liver biopsies were obtained

under basal conditions and at the end of the experiment for biochemical analyses. To date, the molecular events linking the pleiotropic actions of the portal glucose signal to increased HGU and GSYN have not been clearly defined. Likewise, the molecular changes associated with a diminished response of the liver to hyperinsulinemia, hyperglycemia, and portal glucose delivery in the insulin resistant individual are incompletely understood. Herein we demonstrated that delivery of glucose into the portal vein in the presence of a physiologic rise in glucose and insulin triggered a coordinated cellular response involving an increase in the activity of hepatic GK and GS, which occurred in association with further augmentation in HGU and GSYN. In contrast, 4 weeks of HFFD feeding impaired HGU and GSYN in association with a marked decrease in GK activity, and impaired activation of Akt and GS in the presence of hyperinsulinemia and hyperglycemia. Furthermore, intraportal glucose infusion was ineffective in stimulating GK and GS activity in HFFD-fed animals, and these defects were associated with a loss of the stimulatory effects of the portal glucose signal. Altogether, these data provide novel mechanistic insight into the molecular physiology of the portal glucose signal under normal conditions, and to the pathophysiology of aberrant postprandial hepatic glucose disposition evident under an insulin resistant condition.

Metabolic and cellular response of the liver to hyperglycemia and hyperinsulinemia in CTR-fed animals.

Consistent with previous observations [182, 183, 188], a physiologic rise in glucose (2x basal) and insulin (3x basal) in the absence of intraportal glucose infusion resulted in a dynamic switch from net hepatic glucose output to uptake (1.1 to -1.5 mg/kg/min, respectively). This was due to near complete suppression of HGP

concomitant with significant stimulation of HGU (mean rate of 1.6 mg/kg/min during the last 30 min of the study). A 6-fold increase in hepatic GK expression accompanied hyperinsulinemia in the HIHG-PoG CTR group, but this did not result in an increase in the functional amount of hepatic GK protein or its enzymatic activity within the 3-hour observation period. Previously, Ramnanan et al. [214] reported a 12-fold increase in hepatic GK expression after 2 hours of hyperinsulinemia (8-fold basal) and euglycemia, which was associated with an approximate 2-fold increase in GK protein. In the present study, insulin levels were increased only 3-fold basal, resulting in hepatic sinusoidal insulin concentrations of approximately 70 μ U/ml vs. 160 μ U/ml in the study of Ramnanan et al. [214]. Given that insulin is a potent inducer of hepatic GK expression [345-347], differences in GK mRNA levels and protein content between the two studies are most likely related to widely differing insulin concentrations during both experiments. In addition, Iynedjian and colleagues [238, 345] demonstrated that there is substantial lag in the time course of GK protein accumulation relative to induction of GK mRNA expression, which was attributed to the fairly long half-life of liver GK (approximately 30 h in the rat). Thus, it is possible that a similar lag in GK protein accumulation existed in the present study under conditions of acute physiologic hyperinsulinemia, but in the absence of portal glucose delivery. Nevertheless, a substrate-mediated increase in GK flux can occur in the absence of an increase in GK activity. Indeed, Rossetti and colleagues [210] reported that hyperglycemia per se suppressed HGP in rats by decreasing glycogen phosphorylase *a* activity and increasing GK flux, while GK activity was unaffected. Given the sigmoidal kinetic properties of liver GK and its high K_m for glucose relative to other hexokinases [122, 348], a 2-fold increase in the arterial plasma

glucose concentration (from 6 to 12 mM), as occurred in the present study, increased HGU and undoubtedly increased GK flux in the HIHG-PoG CTR group.

Hyperinsulinemia in the presence of hyperglycemia resulted in a significant decrease in P-GS on Ser 641, consistent with activation of insulin signal transduction to Akt. Likewise, the activity ratio of GS, a reflection of its phosphorylation state *in vivo*, increased approximately 5-fold, whereas that of GP was reduced by 40%. This resulted in an 8-fold increase in the GS/GP activity ratio. Thus, in addition to activation of HGU, hyperglycemia and hyperinsulinemia stimulated the dephosphorylation and *activation* of GS, while triggering the dephosphorylation and *inactivation* of GP, which culminated with an increase in the deposition of carbon as glycogen within the liver. These data are in agreement with previous observations by Pagliassotti et al. [198] in dogs, and Petersen et al. [213] in humans.

Activation of the PI3-kinase/Akt arm of the insulin signaling pathway usually stimulates the phosphorylation and inactivation of GSK3 β (Ser9), a negative regulator of GS activity [349]. Ser641 is one of four residues on GS that is phosphorylated by GSK3 β [349, 350]. In the present study, hyperinsulinemia in the presence of hyperglycemia stimulated the phosphorylation of Akt on Ser473, the dephosphorylation of GS on Ser641, and an increase in GS activity, in the absence of an increase in GSK3 β phosphorylation on Ser9. Although the explanation for this finding is not clear, it is possible that other kinases sensitive to inhibition by hyperinsulinemia and/or hyperglycemia are capable of phosphorylating GS on Ser641. In addition, Patel and colleagues [351] demonstrated previously that the dephosphorylation of hepatic GS on Ser641, and the increase in GS activity in response to insulin, glucose, or a meal, was not

enhanced in mice with a liver-specific deletion of GSK3 β . These data suggest that factors independent of hepatic GSK3 β are also involved in the regulation of GS activity by insulin and glucose. In addition, loss of Akt activation in IRS 1/2 null mice had no impact on the ability of insulin to stimulate the phosphorylation of GSK3 β on Ser9 [352], indicating that factors independent of Akt can regulate the phosphorylation state of GSK3 β .

Metabolic and cellular response of the liver to portal glucose delivery in CTR-fed animals.

Delivery of glucose into the portal vein in the presence of equivalent (see above) hyperinsulinemia and hyperglycemia at the liver triggered a significantly greater increase in *net* hepatic glucose uptake, which was solely attributable to further augmentation of HGU (peak rate of 3.0 mg/kg/min), given that HGP was already suppressed. Intriguingly, portal glucose delivery also resulted in a dramatic induction of hepatic GK mRNA expression over that of the HIHG-PoG group, despite the fact that insulin concentrations were equivalent between the two. Previously, Iynedjian and colleagues [346] reported that there was no effect of hyperglycemia (up to 40 mM glucose) on the induction of GK expression by insulin in cultured liver cells. However, the response of the liver to portal vein glucose delivery is thought to be neurally-mediated [26, 184, 193, 195, 219, 353]. Thus, it is possible that the ability of the portal glucose signal to augment hepatic GK expression is also under neural control. In such a case, its effect would only be detected in the intact organism. Afferent fibers in the hepatic branch of the vagus nerve can detect the glucose concentration in the portal vein [195, 215, 228, 354], and delivery of glucose into the portal vein results in a decrease in the firing rate of these afferent fibers [195,

355, 356]. Thus, changes in parasympathetic tone to the liver, or changes in the abundance of other biological mediators of NHGU (e.g. nitric oxide or serotonin [5-HT]) might be involved in the induction of GK expression by portal glucose delivery. Recently, Ramnanan et al. [357] demonstrated that a selective rise in insulin in the brain under euglycemic conditions induces a 3-fold increase in hepatic GK expression, whereas icv delivery of a PI3-kinase inhibitor (LY294002) ablates the effect. These data raise the possibility that the induction of hepatic GK expression by insulin and/or the portal glucose signal is in part, neurally-mediated.

Interestingly, hyperinsulinemia and hyperglycemia in the absence of portal glucose infusion produced a 6-fold increase in GK mRNA without an increase in GK protein over a 3-hour observation period. In contrast, portal glucose delivery during the last 90 min of the study produced a further 4-fold increase in GK mRNA concomitant with a significant increase GK protein and activity relative to the HIHG-PoG CTR group. One possibility for this observation is that the portal glucose signal might reduce the lag time for GK protein accumulation (see previous section) by stimulating more efficient coupling between GK transcription and GK translation, thereby ensuring the appropriate amount of glucose uptake and storage by the liver in response to a meal. Another possibility is that the portal glucose signal prevents the degradation of GK protein in addition to stimulating its expression. Indeed, previous studies [358-360] have suggested that binding of GK in the cytosol by the bifunctional enzyme, 6-phosphofructo-2-kinase (PFK-2) / fructose-2,6-bisphosphatase (BIF), protects GK from degradation and increases its catalytic activity. Furthermore, Wu and colleagues [360, 361] demonstrated that increasing the levels of hepatic fructose-2,6-bisphosphate, a metabolite synthesized by

PFK-2 secondary to an increase in glycolytic flux, increases the gene expression and protein content of GK. In the present study, net hepatic lactate output during P2 was significantly lower in the absence than in the presence of intraportal glucose infusion, suggesting that net hepatic glycolysis was increased in the latter. Thus, it is possible that the portal glucose signal increased the activity of PFK-2 and the abundance of fructose-2,6-bisphosphate, thereby preventing the degradation of GK protein and facilitating an increase in GK expression and activity. Given that phosphorylation of glucose by GK is thought to be rate-limiting for HGU [231, 232], our data suggest that activation of GK by intraportal glucose delivery is one of the mechanisms through which the portal glucose signal stimulates a further increase in HGU over that observed in the presence of hyperglycemia and hyperinsulinemia alone. The present data do not shed light on the issue of whether portal glucose delivery stimulates the translocation of hepatic GK *in vivo*, as we have conjectured previously [26, 180, 233], but they clearly demonstrate that at least one additional regulatory mechanism exists through which the portal glucose signal *per se* can augment GK expression and activity. Altogether, our findings indicate that the portal glucose signal regulates hepatic GK acutely by increasing its activity, and chronically by inducing its expression, thus priming the liver for increased glucose uptake and storage at a subsequent meal.

In agreement with the findings of Pagliassotti et al [198], portal glucose delivery triggered a significantly greater increase GS activity than the same hyperglycemia and hyperinsulinemia alone. Although this was not associated with further diminution in the phosphorylation of GS on Ser641, GS contains several other phosphorylation sites that regulate its activity [349, 350, 362]. Thus, the effect of the portal glucose signal on the

phosphorylation state of liver GS could have been mediated by dephosphorylation of sites distinct from that of Ser 641. In addition, it is possible that there was an increase in hepatocellular glucose-6-phosphate levels in response to the portal signal-induced increase in GK activity and HGU, which made GS a better substrate for dephosphorylation by protein phosphatase-1 [363, 364]. Lastly, it is also possible that there was neural modulation of liver GS activity in the presence of intraportal glucose infusion, as postulated earlier for GK mRNA. Indeed, previous studies have demonstrated that electrical stimulation of the efferent limb of the vagus nerve activates liver GS [215, 228-230]. The coupling of an increase in GS activity and a smaller decrease in GP activity resulted in a 12-fold increase from basal in the GS/GP activity ratio in the presence of the portal glucose signal, and a robust increase in liver glycogen levels relative to that observed in the absence of the portal glucose signal.

Collectively, these data suggest that the portal glucose signal triggers a significantly greater increase in HGU and GSYN by augmenting the activity of hepatic GK and GS. In addition, they support the concept that the intraportal route of glucose delivery generates a unique signal that serves as one of the primary determinants of HGU and GSYN in vivo [182, 183, 188, 189, 365].

Metabolic and cellular response of the liver to hyperglycemia and hyperinsulinemia in HFFD-fed animals.

Previously [366], we demonstrated that 4 weeks of HFFD feeding was associated with significantly impaired glucose tolerance. Given that the contribution of the liver to the disposition of a moderately-sized oral glucose load is at least as great as that of skeletal muscle [27, 184], that observation prompted us to assess whether 4 weeks of

HFFD feeding was associated with a decrease in HGU in the presence of a physiologic rise in glucose and insulin, and in the presence of portal glucose delivery. In addition, we wanted to compare the molecular changes associated with hyperinsulinemia, hyperglycemia, and portal glucose delivery in CTR and HFFD-fed animals in an attempt to shed light on the early cellular defects associated with impaired regulation of hepatic glucose flux in an insulin resistant model.

In stark contrast to the response observed in CTR-fed dogs, the combination of hyperinsulinemia and hyperglycemia was associated with impaired suppression of HGP, and virtually no stimulation of HGU in HFFD-fed dogs. In accord with this finding, livers of dogs in the HFFD group continued in net hepatic lactate uptake for the duration of the study, despite the presence of hyperglycemia and hyperinsulinemia. Although a 7-fold increase in hepatic GK expression accompanied hyperinsulinemia in the HIHG-PoG HFFD group, this did not result in an increase in the functional amount of GK protein. In fact, hepatic GK protein content and activity were markedly reduced in HFFD-fed dogs under basal conditions and during the HIHG clamp, consistent with impaired activation of HGU. Furthermore, the phosphorylation of Akt on Ser473 was significantly lower in HFFD-fed animals, indicative of biochemical insulin resistance after 4 weeks of HFFD feeding. As a result, the phosphorylation of GS on Ser641 was not reduced from basal, and the activity ratio of GS in the presence of hyperinsulinemia and hyperglycemia was only modestly increased, and was significantly lower in HFFD-fed dogs relative to the corresponding CTR group. When coupled with attenuated suppression of GP activity, there was a 4-fold increase in the GS/GP activity ratio in HFFD-fed dogs compared to an 8-fold increase in CTR-fed dogs under the same experimental conditions. Consequently,

the change in liver glycogen levels in response to hyperinsulinemia and hyperglycemia was barely detectable, consistent with a marked decrease in direct glycogen synthesis compared to the corresponding CTR group. Thus, impaired activation of HGU in HFFD-fed dogs in the presence of hyperinsulinemia and hyperglycemia was associated with decreased GK protein content and activity, impaired activation of Akt and glycogen synthase activity, and reduced suppression of glycogen phosphorylase activity.

Metabolic and cellular response of the liver to portal glucose delivery in HFFD-fed animals.

Interestingly, delivery of glucose into the portal vein in the presence of hyperinsulinemia and hyperglycemia triggered suppression of residual HGP in the HIHG+PoG HFFD group, but did not stimulate HGU. As a result, net hepatic glucose balance decreased to a rate not significantly different from zero, so that in a net sense, the liver did not take up any glucose. Although the mechanism by which portal glucose delivery suppressed HGP in HFFD-fed dogs is not clear, studies conducted by Newgard et al. [367] and Mithieux et al. [368] have suggested that inhibition of G6Pase activity plays a role in the suppression of HGP and in liver glycogen repletion after refeeding in rodents. Thus, a similar mechanism might be involved in the present study. Nevertheless, portal glucose delivery had no impact on net hepatic lactate balance in HFFD-fed dogs, consistent with lack of stimulation of HGU. These data are in agreement with those of Basu and colleagues [200], who demonstrated that impaired splanchnic glucose uptake (SGU) in type 2 diabetic individuals is not dependent on the route of glucose delivery, given that intraduodenal glucose infusion was incapable of restoring their diminished rates of SGU during an HIHG clamp.

There are several possibilities for why the livers of dogs fed a HFFD did not switch from net lactate uptake to net lactate output, despite the presence of hyperinsulinemia, hyperglycemia, and portal glucose delivery. One possibility is that HFFD-feeding produced hepatic insulin resistance and thus, might have led to impaired insulin-mediated activation of rate-limiting enzymes involved in the glycolytic pathway (phosphofructokinase-1/2 and pyruvate kinase). It is also possible that a decrease in the amount of substrate available for catabolism through the glycolytic pathway secondary to impaired HGU might have limited net hepatic lactate output during the clamp experiment. Another possibility relates to the difference in suppression of lipolysis in CTR and HFFD groups. Chu and colleagues [369] demonstrated previously that elevation of plasma NEFA levels brought about using intralipid and heparin infusion completely eliminated the ability of hyperglycemia per se to cause net hepatic lactate output. This was attributed to stimulation of hepatic gluconeogenic flux and inhibition of glycolysis [177, 369]. In the present study, there was a tendency for arterial plasma NEFA and glycerol concentrations to be higher in HFFD-fed dogs than in CTR-fed dogs throughout the experiment, which might have contributed to aberrant net hepatic lactate balance in the former. These data also suggest that insulin resistance was present in adipose tissue after only 4 weeks of HFFD feeding. This raises the possibility that endocrine factors (adipokines) and/or inflammatory cytokines secreted from insulin resistant adipose tissue might have played a role in reducing hepatic GK activity and HGU.

Portal glucose delivery also stimulated a dramatic increase in hepatic GK mRNA expression in the HIHG+PoG HFFD group as it did in the CTR group, suggesting that the mechanism(s) through which hyperglycemia, hyperinsulinemia, and portal glucose

delivery bring about an increase in GK expression are intact in HFFD-fed animals. In contrast, the increase in GK protein content and activity seen in CTR animals in response to the portal glucose signal was abolished in HFFD-fed animals, as their GK protein levels were reduced by more than 50% relative to the corresponding CTR group. Likewise, there was no effect of intraportal glucose infusion on GS and GP activity ratios in the HIHG+PoG HFFD group, which was associated with a minimal increase in their liver glycogen levels. Thus, 4 weeks of HFFD feeding abrogated the stimulatory effects of hyperglycemia, hyperinsulinemia, and portal glucose delivery on GK and GS activity, which manifested as diminished HGU and GSYN.

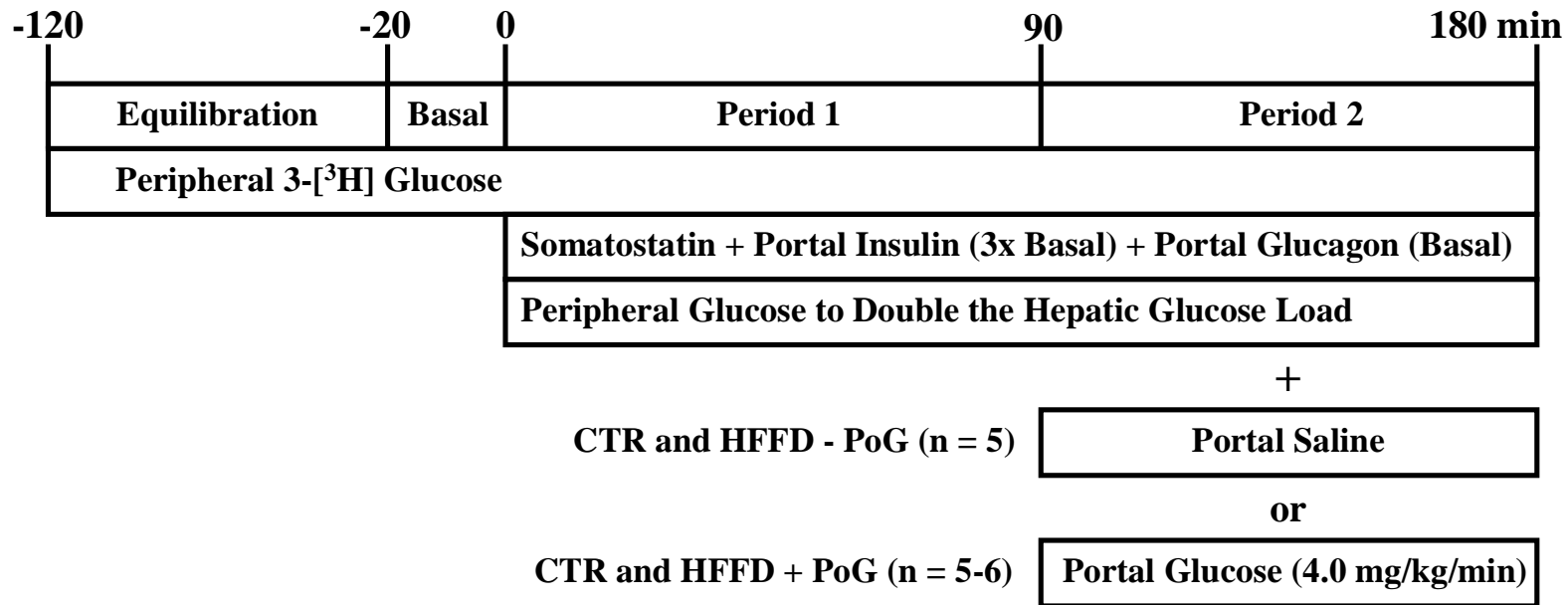
Normal GK mRNA expression concomitant with significantly diminished GK protein content suggests that the HFFD-induced decrease in GK protein occurred post-transcriptionally. Studies conducted in GKRP-deficient mice demonstrated that they also have significantly reduced GK immunoreactive protein despite normal basal and insulin-stimulated GK mRNA expression, suggesting that GKRP exerts a permissive effect on the level of GK protein through a post-transcriptional mechanism [370, 371]. Interestingly, GKRP protein levels were significantly reduced in the HFFD group under basal conditions and during the HIHG clamp, suggesting that reduced levels of hepatic GKRP in HFFD-fed animals may have contributed to the post-transcriptional decline in GK protein. However, the mechanism(s) through which HFFD feeding elicits a decrease in hepatic GKRP and GK protein content is currently unknown.

In obese rodent models of insulin resistance and type 2 diabetes, activation of the unfolded protein response and induction of endoplasmic reticulum (ER) stress have been shown to halt the translation of proteins by phosphorylating and inactivating eIF2 α

{Thomas, #4940}; however, there was no difference between diet groups in the phosphorylation of PERK on Thr980, its downstream target, eIF2 α on Ser51, or in the protein level of the ER chaperone, Bip, in the present study (data not shown). Likewise, there was no difference between diet groups in the hepatic expression of genes involved in the production of reactive oxygen and nitrogen species (NADPH oxidase [Nox2 and Nox4] and iNOS, respectively; data not shown). Furthermore, HFFD feeding induced a marked impairment in HGU and GSYN in the absence of an increase in liver triglyceride levels. In agreement with this finding, long-chain acyl Co-A, diacylglycerol, and ceramide levels were also not different between CTR and HFFD-fed animals in a smaller cohort of dogs (data not shown). These data suggest that diet-induced impairments in GK and hepatic glucose flux can occur independently of liver lipid accumulation. Future studies will need to be conducted to elucidate the mechanism(s) through which a HFFD impairs the regulation of hepatic GK in a post-transcriptional fashion.

In conclusion, we demonstrated that delivery of glucose into the hepatic portal vein in the presence of hyperinsulinemia and hyperglycemia triggered a coordinated molecular response involving an increase in the catalytic activity of hepatic GK, and stimulation of GS activity, which collectively augmented HGU and GSYN in vivo. In contrast, HFFD-feeding abrogated the stimulatory effects of hyperinsulinemia, hyperglycemia, and portal glucose delivery on GK, Akt, and GS activation, and as a result, HGU and GSYN were impaired. These data provide novel mechanistic insight into the molecular physiology of the portal signaling mechanism under normal conditions, and suggest that impaired regulation of hepatic GK under insulin resistant conditions is one of the early molecular defects that contribute to the deterioration of glucose tolerance and

development of postprandial hyperglycemia secondary to diminished HGU.



Performed in 18-h-fasted conscious dogs.

CTR = Chow control group; HFFD = High-Fat, High-Fructose group; PoG = Portal Glucose

Figure 5.1: Schematic representation of the hyperinsulinemic hyperglycemic clamp protocol. The protocol consisted of basal (-20 to 0 min) and experimental periods (1: 0-90 min; 2: 90-180 min). Somatostatin and 3-[³H] glucose were infused peripherally, insulin (3-fold basal) and glucagon (basal) were infused intraportally, and glucose was infused peripherally at a variable rate to increase the hepatic glucose load 2-fold basal during periods 1 and 2. During period 2, glucose was also infused intraportally to activate the portal glucose signal.

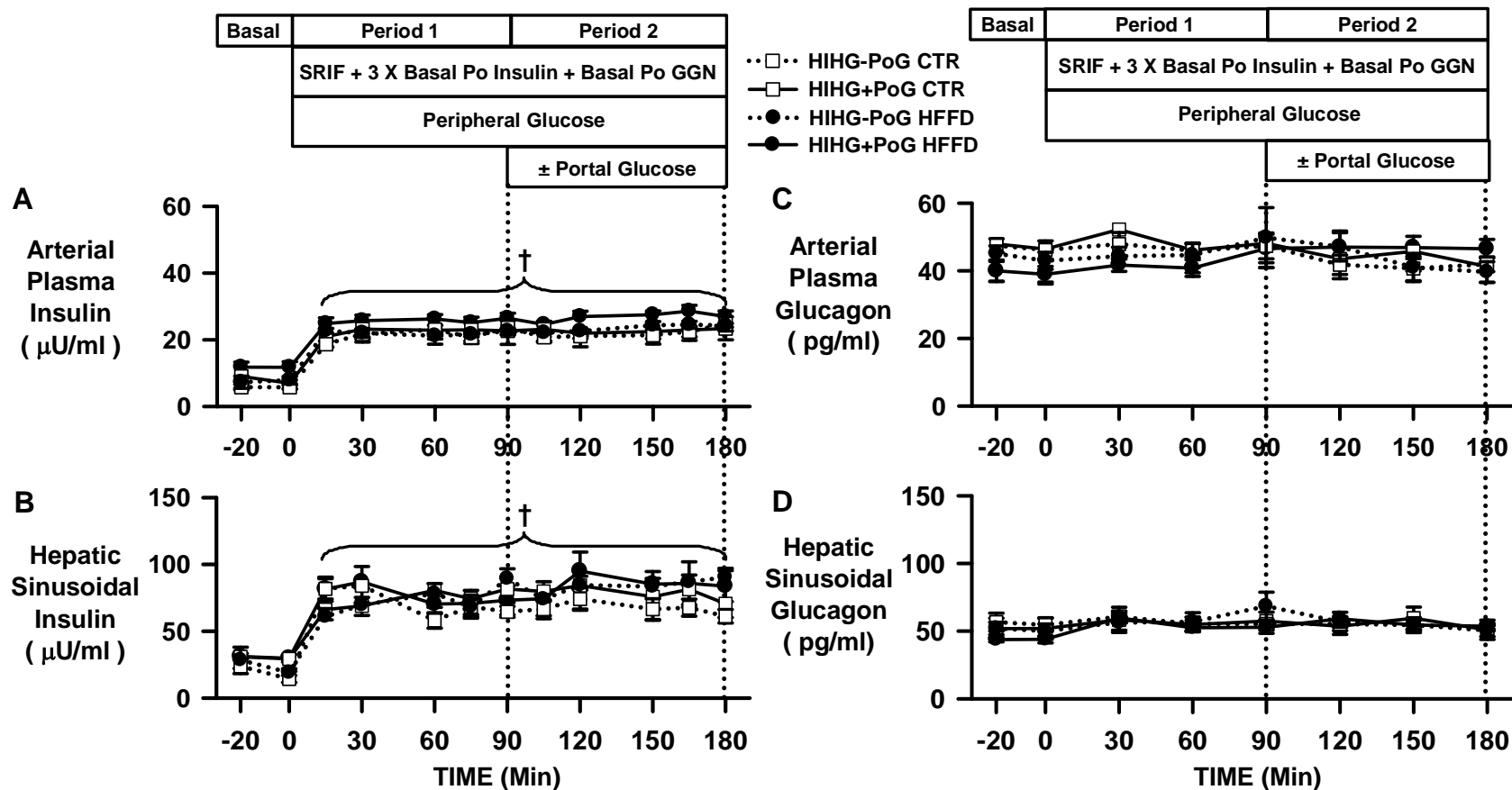


Figure 5.2: Plasma hormone concentrations during hyperinsulinemic hyperglycemic clamps in CTR and HFFD groups. Arterial plasma insulin (A) and glucagon (C), and hepatic sinusoidal insulin (B) and glucagon (D) during basal (-20 to 0 min) and experimental periods (0 to 180 min) of HIHG clamps conducted in 18-h-fasted dogs after 4 weeks of feeding a CTR (HIHG-PoG CTR, $n = 5$; HIHG+PoG CTR, $n = 5$; \square) or HFFD (HIHG-PoG HFFD, $n = 5$; HIHG+PoG HFFD, $n = 6$; \bullet). Data are means \pm SE. $\dagger P < 0.05$ vs. basal period.

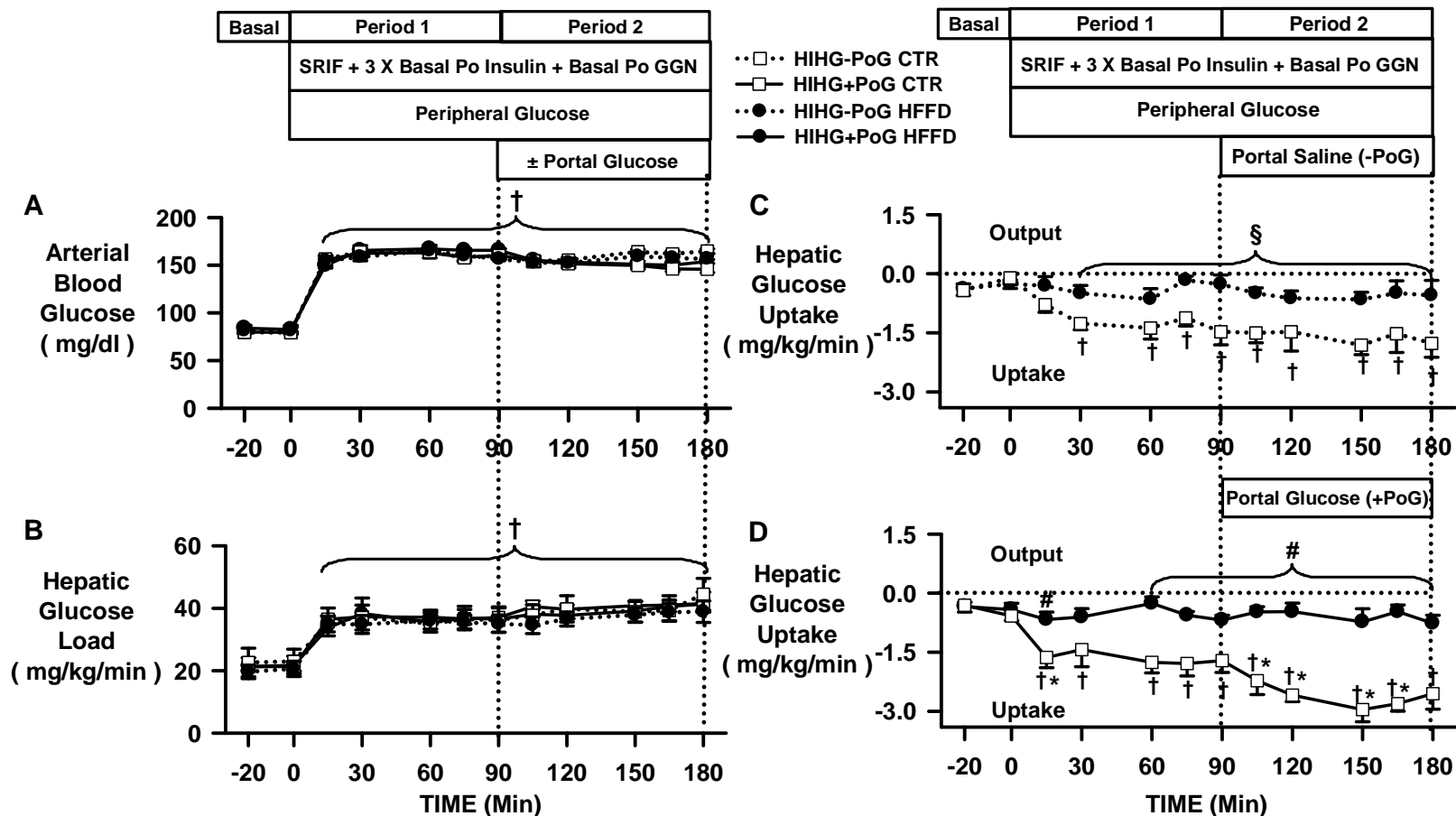


Figure 5.3: Arterial blood glucose, hepatic glucose load, and hepatic glucose uptake during hyperinsulinemic hyperglycemic clamps in CTR and HFFD groups. Arterial blood glucose (A), hepatic glucose load (B), and hepatic glucose uptake in the portal saline (C) and portal glucose (D) groups during the basal (-20 to 0 min) and experimental periods (0 to 180 min) of HIHG clamps conducted in 18-h-fasted dogs after 4 weeks of feeding a CTR (HIHG-PoG CTR, $n = 5$; HIHG+PoG CTR, $n = 5$; □) or HFFD (HIHG-PoG HFFD, $n = 5$; HIHG+PoG HFFD, $n = 6$; ●). Data are means \pm SE. † $P < 0.05$ vs. basal period; * $P < 0.05$ vs. corresponding CTR group; § $P < 0.05$, HIHG-PoG HFFD vs. CTR; # $P < 0.05$, HIHG+PoG HFFD vs. CTR.

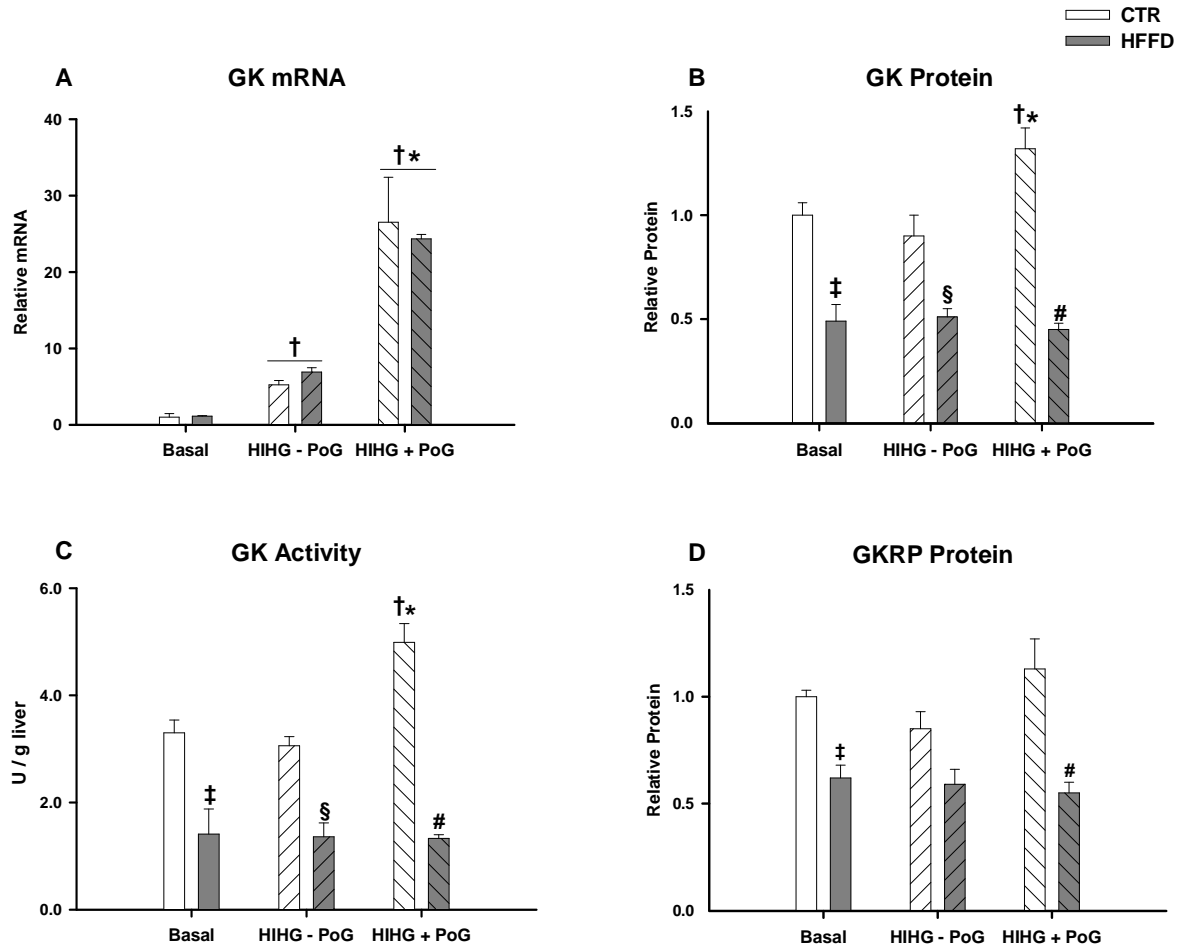


Figure 5.4: Hepatic glucokinase (GK) and glucokinase regulatory protein (GKRP) in CTR and HFFD groups. Levels of GK mRNA (A) and protein (B), GK activity (C), and levels of GKRP protein (D). A, B, and D are expressed relative to levels observed in basal CTR animals. Data are means \pm SE; $n = 5-6$ per group. ‡ $P < 0.05$, basal HFFD vs. CTR; † $P < 0.05$ vs. basal CTR; * $P < 0.05$ vs. corresponding CTR group; § $P < 0.05$, HIHG - PoG HFFD vs. CTR; # $P < 0.05$, HIHG + PoG HFFD vs. CTR.

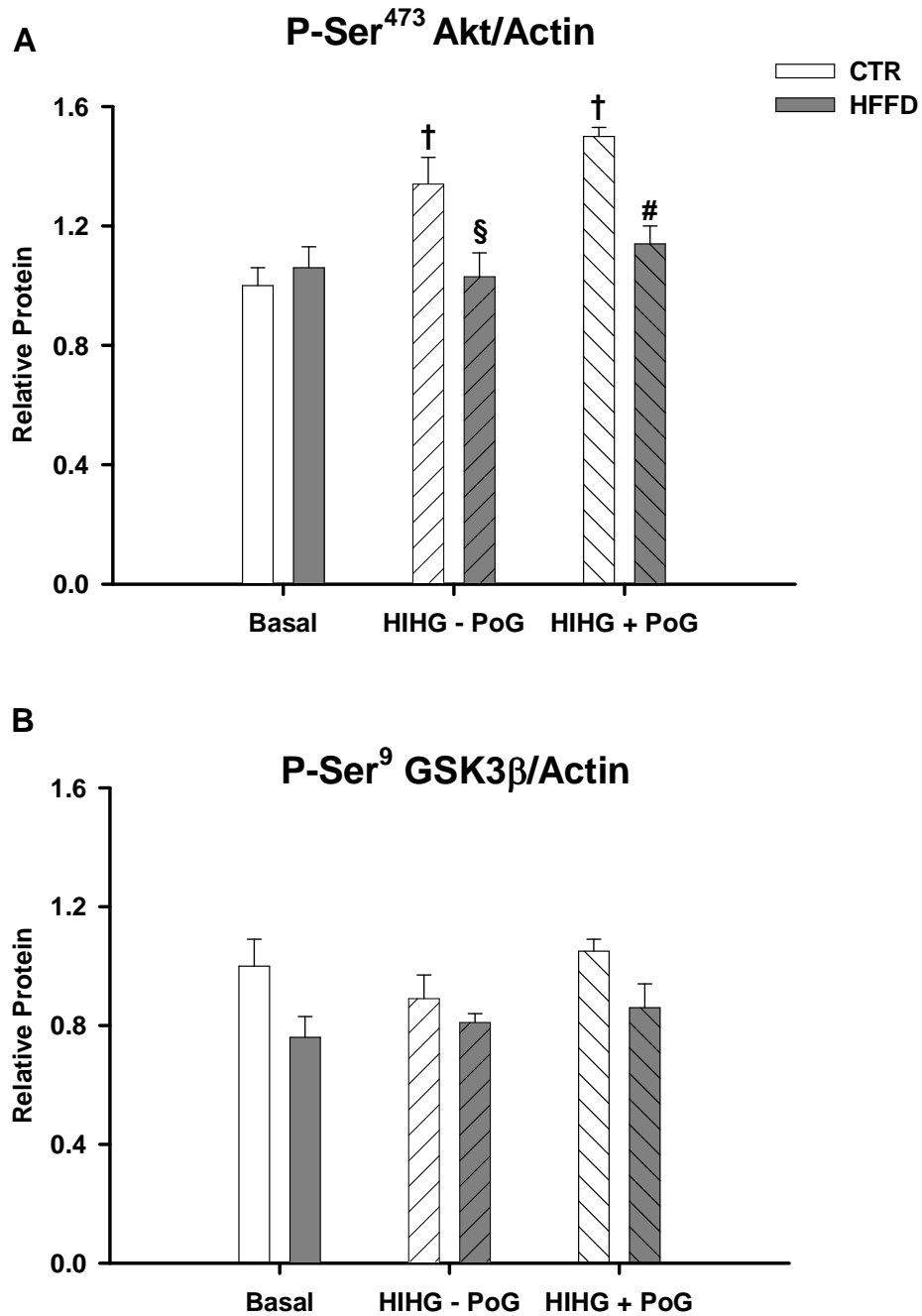


Figure 5.5: Markers of hepatic insulin signaling in CTR and HFFD groups. Phosphorylation of Akt on Ser473 (A) and GSK3β on Ser9 (B) relative to levels observed in basal CTR animals. Data are means ± SE; *n* = 5-6 per group. †*P* < 0.05 vs. basal CTR; §*P* < 0.05, HIHG - PoG HFFD vs. CTR; # *P* < 0.05, HIHG + PoG HFFD vs. CTR.

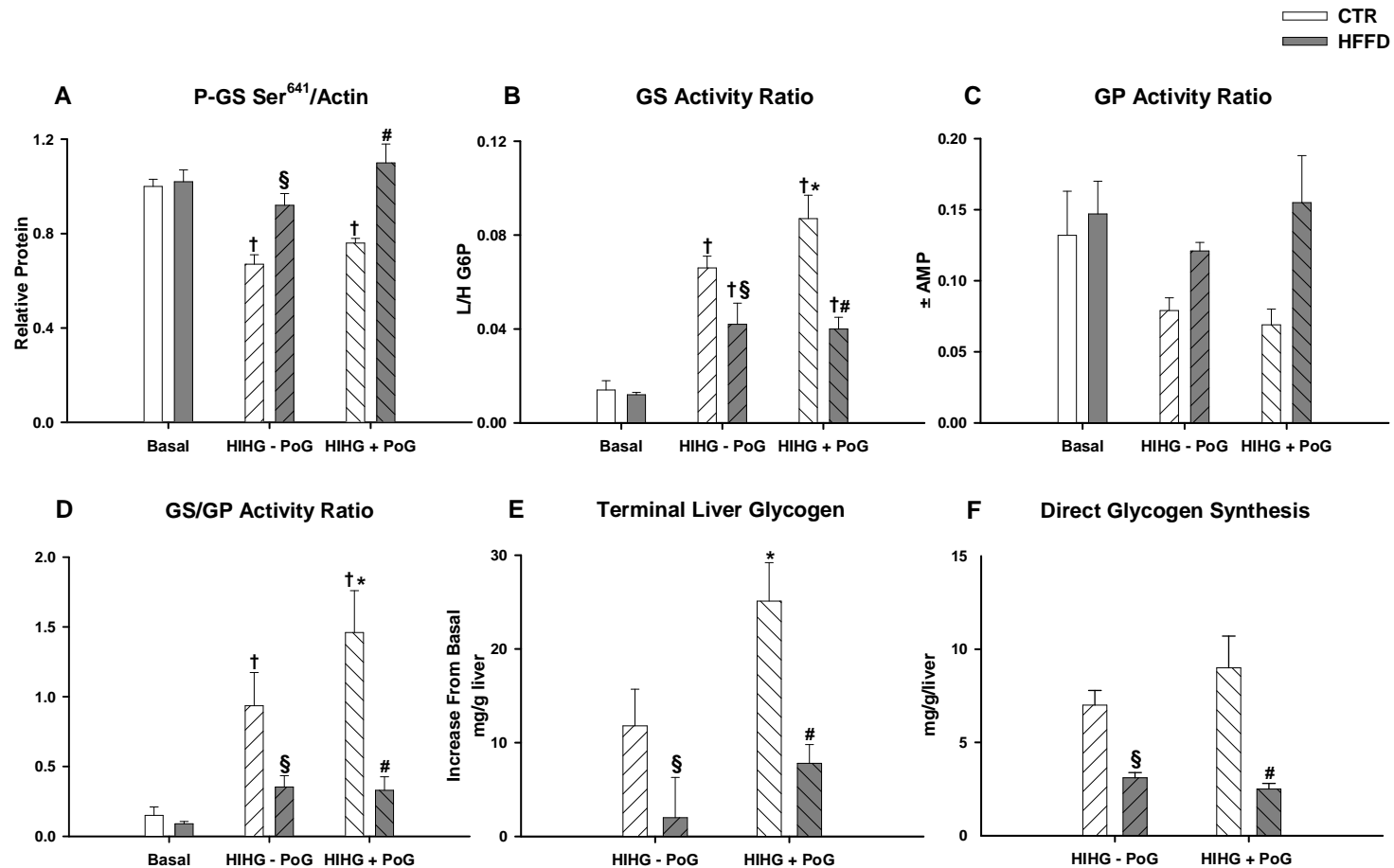


Figure 5.6: Markers of hepatic glycogen metabolism in CTR and HFFD groups. Phosphorylation of glycogen synthase (GS) on Ser641 (A) relative to levels observed in basal CTR animals. Activity ratios of GS (B), glycogen phosphorylase (GP) (C), and GS/GP (D). Calculated increment in liver glycogen from basal (E). Glycogen synthesized through the direct pathway (F). Data are means \pm SE; $n = 5-6$ per group. † $P < 0.05$ vs. basal CTR; * $P < 0.05$ vs. corresponding CTR group; § $P < 0.05$, HIHG - PoG HFFD vs. CTR; # $P < 0.05$, HIHG + PoG HFFD vs. CTR.

TABLE 5.1.

Mean values for total hepatic blood flow and glucose infusion rate during the basal (-20 to 0 min) and experimental periods (P1, 60 to 90 min; P2, 150-180 min) of a hyperinsulinemic hyperglycemic clamp

Group	Experimental Period										
	Basal Period			Period 1			Period 2				
Total hepatic blood flow, ml/kg/min											
CTR	-	PoG	29	±	5	23	±	2	26	±	2
HFFD	-	PoG	25	±	1	22	±	1	25	±	2
CTR	+	PoG	25	±	3	21	±	2	23	±	3
HFFD	+	PoG	25	±	3	22	±	3	24	±	2
Total glucose infusion rate, mg/kg/min											
CTR	-	PoG	0.0	±	0.0	7.3	±	0.8 ^A	10.4	±	1.3 ^A
HFFD	-	PoG	0.0	±	0.0	8.4	±	1.6 ^A	12.7	±	1.6 ^A
CTR	+	PoG	0.0	±	0.0	9.0	±	3.0 ^A	10.2	±	2.4 ^A
HFFD	+	PoG	0.0	±	0.0	5.8	±	0.7 ^A	7.6	±	1.1 ^A

Values are means ± SE; CTR-PoG, *n* = 5; HFFD-PoG, *n* = 5; CTR+PoG, *n* = 5; HFFD+PoG, *n* = 6. Dogs were 18h-fasted prior to study. A, *P* < 0.05 vs. basal period.

Table 5.2.

Mean values for unidirectional hepatic glucose uptake, hepatic glucose production, and net hepatic glucose balance during the basal (-20 to 0 min) and experimental (P1, 30 to 90 min; P2, 120 to 180 min) periods of a hyperinsulinemic hyperglycemic clamp in the CTR - PoG, HFFD - PoG, CTR + PoG, and HFFD + PoG groups

Group	Basal Period	Period 1	Period 2
Hepatic glucose uptake, mg/kg/min			
CTR - PoG	-0.27 ± 0.12	-1.31 ± 0.17 ^A	-1.64 ± 0.13 ^{AB}
HFFD - PoG	-0.32 ± 0.11	-0.35 ± 0.07 ^D	-0.58 ± 0.21 ^D
CTR + PoG	-0.44 ± 0.11	-1.67 ± 0.29 ^A	-2.73 ± 0.22 ^{ACF}
HFFD + PoG	-0.38 ± 0.10	-0.53 ± 0.05 ^E	-0.61 ± 0.17 ^E
Hepatic glucose production, mg/kg/min			
CTR - PoG	1.35 ± 0.14	0.04 ± 0.36 ^A	0.10 ± 0.22 ^A
HFFD - PoG	1.78 ± 0.29	0.90 ± 0.21 ^A	0.79 ± 0.39 ^A
CTR + PoG	2.11 ± 0.36	0.21 ± 0.26 ^A	0.31 ± 0.29 ^A
HFFD + PoG	1.94 ± 0.30	1.33 ± 0.18 ^{AE}	0.47 ± 0.42 ^{AC}
Net hepatic glucose balance, mg/kg/min			
CTR - PoG	1.09 ± 0.06	-1.27 ± 0.21 ^A	-1.54 ± 0.17 ^A
HFFD - PoG	1.46 ± 0.23	0.55 ± 0.24 ^{AD}	0.21 ± 0.24 ^{AD}
CTR + PoG	1.66 ± 0.26	-1.47 ± 0.14 ^A	-2.42 ± 0.36 ^{ACF}
HFFD + PoG	1.57 ± 0.25	0.80 ± 0.16 ^{AE}	-0.14 ± 0.38 ^{ACE}

Values are means ± SE; CTR-PoG, *n* = 5; HFFD-PoG, *n* = 5; CTR+PoG, *n* = 5; HFFD+PoG, *n* = 6. Dogs were 18-h-fasted prior to study. A, *P* < 0.05 vs. basal period; B, *P* < 0.05, P1 vs. P2; C, *P* < 0.01, P1 vs. P2; D, *P* < 0.05, HFFD-PoG vs. CTR-PoG; E, *P* < 0.05, HFFD+PoG vs. CTR+PoG; F, *P* < 0.05 vs. corresponding -PoG group. Negative values for balance data indicate net hepatic uptake; positive values indicate net hepatic production.

Table 5.3.

Mean values for lactate, glycerol, and NEFA concentrations, and their net hepatic balance during the basal (-20 to 0 min) and experimental (P1, 60 to 90 min; P2, 150-180 min) periods of the hyperinsulinemic hyperglycemia clamp in the CTR - PoG, HFFD - PoG, CTR + PoG, and HFFD + PoG groups.

Group	Basal Period, min	Period 1, min			Period 2, min		
	-20 to 0	60	75	90	150	165	180
Arterial blood lactate, $\mu\text{mol/l}$							
CTR - PoG	325 \pm 43	1000 \pm 71 ^A	972 \pm 22 ^A	970 \pm 39 ^A	850 \pm 45 ^A	873 \pm 79 ^A	853 \pm 66 ^A
HFFD - PoG	472 \pm 154	504 \pm 54 ^C	579 \pm 65 ^C	658 \pm 87	811 \pm 132 ^C	762 \pm 83 ^C	783 \pm 85 ^C
CTR + PoG	397 \pm 111	663 \pm 87 ^A	628 \pm 74 ^{AB}	642 \pm 88 ^A	643 \pm 78 ^A	689 \pm 87 ^A	693 \pm 121 ^A
HFFD + PoG	318 \pm 42	422 \pm 44	386 \pm 45	394 \pm 50	444 \pm 57 ^B	452 \pm 59 ^{BD}	466 \pm 45 ^B
Net hepatic lactate balance, $\mu\text{mol/kg/min}$							
CTR - PoG	-6.6 \pm 0.6	7.2 \pm 1.6 ^A	6.9 \pm 1.9 ^A	3.8 \pm 2.3 ^A	2.7 \pm 0.9 ^A	1.9 \pm 1.0 ^A	1.2 \pm 1.0 ^A
HFFD - PoG	-7.3 \pm 2.0	-4.1 \pm 1.4 ^{AC}	-3.4 \pm 1.3 ^{AC}	-3.8 \pm 1.4 ^{AC}	-4.0 \pm 1.0 ^{AC}	-4.6 \pm 0.3 ^C	-4.7 \pm 0.3 ^C
CTR + PoG	-5.3 \pm 0.3	8.3 \pm 1.9 ^A	7.0 \pm 1.7 ^A	6.3 \pm 1.3 ^A	5.1 \pm 0.6 ^{AB}	4.4 \pm 0.8 ^{AB}	5.0 \pm 0.8 ^{AB}
HFFD + PoG	-6.3 \pm 1.1	-3.6 \pm 0.9 ^D	-2.8 \pm 0.9 ^{AD}	-2.5 \pm 0.9 ^{AD}	-3.3 \pm 0.7 ^{AD}	-3.6 \pm 1.0 ^D	-3.6 \pm 0.7 ^D
Arterial blood glycerol, $\mu\text{mol/l}$							
CTR - PoG	81 \pm 12	27 \pm 6 ^A	31 \pm 11 ^A	27 \pm 6 ^A	23 \pm 10 ^A	31 \pm 12 ^A	29 \pm 10 ^A
HFFD - PoG	92 \pm 15	62 \pm 18 ^A	62 \pm 15 ^A	57 \pm 15 ^A	68 \pm 19 ^{AC}	51 \pm 17 ^A	53 \pm 18 ^A
CTR + PoG	72 \pm 6	32 \pm 4 ^A	27 \pm 3 ^A	23 \pm 1 ^A	29 \pm 3 ^A	29 \pm 5 ^A	29 \pm 3 ^A
HFFD + PoG	98 \pm 12	56 \pm 6 ^A	51 \pm 7 ^A	45 \pm 4 ^A	55 \pm 6 ^A	49 \pm 6 ^A	50 \pm 7 ^A
Net hepatic glycerol balance, $\mu\text{mol/kg/min}$							
CTR - PoG	-1.7 \pm 0.4	-0.5 \pm 0.2 ^A	-0.4 \pm 0.1 ^A	-0.4 \pm 0.1 ^A	-0.3 \pm 0.1 ^A	-0.6 \pm 0.2 ^A	-0.6 \pm 0.2 ^A
HFFD - PoG	-1.7 \pm 0.4	-1.0 \pm 0.4 ^A	-1.1 \pm 0.3 ^A	-1.0 \pm 0.4 ^A	-1.2 \pm 0.4 ^A	-1.0 \pm 0.3 ^A	-0.9 \pm 0.5 ^A
CTR + PoG	-1.7 \pm 0.1	-0.7 \pm 0.2 ^A	-0.5 \pm 0.1 ^A	-0.5 \pm 0.1 ^A	-0.7 \pm 0.1 ^A	-0.6 \pm 0.1 ^A	-0.8 \pm 0.1 ^A
HFFD + PoG	-2.0 \pm 0.4	-1.0 \pm 0.2 ^A	-1.0 \pm 0.3 ^A	-0.8 \pm 0.2 ^A	-1.0 \pm 0.3 ^A	-0.8 \pm 0.2 ^A	-0.9 \pm 0.2 ^A
Arterial plasma NEFA, $\mu\text{mol/l}$							
CTR - PoG	924 \pm 127	99 \pm 25 ^A	116 \pm 26 ^A	114 \pm 42 ^A	63 \pm 10 ^A	103 \pm 33 ^A	89 \pm 28 ^A
HFFD - PoG	791 \pm 119	212 \pm 61 ^A	203 \pm 64 ^A	152 \pm 44 ^A	146 \pm 56 ^A	117 \pm 38 ^A	107 \pm 33 ^A
CTR + PoG	831 \pm 73	154 \pm 30 ^A	136 \pm 27 ^A	118 \pm 33 ^A	84 \pm 17 ^A	109 \pm 30 ^A	102 \pm 20 ^A
HFFD + PoG	852 \pm 115	261 \pm 51 ^A	207 \pm 46 ^A	168 \pm 31 ^A	169 \pm 43 ^A	139 \pm 25 ^A	174 \pm 39 ^A
Net hepatic NEFA balance, $\mu\text{mol/kg/min}$							
CTR - PoG	-2.7 \pm 0.5	-0.1 \pm 0.1 ^A	-0.2 \pm 0.1 ^A	-0.2 \pm 0.1 ^A	-0.1 \pm 0.1 ^A	-0.3 \pm 0.2 ^A	-0.2 \pm 0.1 ^A
HFFD - PoG	-2.3 \pm 0.3	0.0 \pm 0.3 ^A	-0.5 \pm 0.3 ^A	-0.3 \pm 0.1 ^A	-0.5 \pm 0.4 ^A	-0.3 \pm 0.1 ^A	-0.3 \pm 0.1 ^A
CTR + PoG	-2.5 \pm 0.2	-0.2 \pm 0.2 ^A	-0.1 \pm 0.1 ^A	-0.2 \pm 0.1 ^A	-0.2 \pm 0.1 ^A	-0.3 \pm 0.1 ^A	-0.3 \pm 0.1 ^A
HFFD + PoG	-2.9 \pm 0.5	-0.9 \pm 0.2 ^A	-0.7 \pm 0.1 ^A	-0.5 \pm 0.2 ^A	-0.7 \pm 0.2 ^A	-0.3 \pm 0.1 ^A	-0.5 \pm 0.2 ^A

Values are means \pm SE; CTR-PoG, $n = 5$; HFFD-PoG, $n = 5$; CTR+PoG, $n = 5$; HFFD+PoG, $n = 6$. Dogs were 18-h-fasted prior to study. A, $P < 0.05$ vs. basal period; B, $P < 0.05$ vs. corresponding HIHG-PoG group; C, $P < 0.05$, HIHG-PoG HFFD vs. CTR; D, $P < 0.05$, HIHG+PoG HFFD vs. CTR. Negative values for balance data indicate net hepatic uptake; positive values indicate net hepatic production.

CHAPTER VI

THE EFFECT OF SHORT-TERM HIGH-FAT VS. HIGH-FRUCTOSE FEEDING ON HEPATIC GLUCOSE UPTAKE AND DISPOSITION

(Manuscript in Preparation)

Aim

In Specific Aim III, we demonstrated that 4 weeks of high-fat, high-fructose feeding is associated with diminished hepatic glucokinase (GK) and glycogen synthase (GS) activity, decreased insulin-mediated activation of Akt, and impaired hepatic glucose uptake (HGU) and glycogen synthesis (GSYN) when a dog is challenged with physiologic hyperinsulinemia (approximately 3-fold basal), hyperglycemia (hepatic glucose load that is 2-fold basal), and portal glucose delivery. However, we cannot ascertain from these data whether excess dietary fat, fructose, or both are required to elicit aberrant hepatic glucose flux under conditions that mimic the postprandial state. Thus, the objective of Specific Aim IV was to elucidate which macronutrient (fat or fructose) is driving metabolic dysfunction at the liver after 4 weeks of feeding.

Experimental Design

Adult male mongrel dogs were fed once daily a pre-determined quantity of a meat/laboratory chow diet (control or CTR; $n=5$), a high-fat diet (HFA; $n=5$), or a high-fructose diet (HFR; $n=5$) for 4 weeks. The specific macronutrient compositions of the

experimental diets utilized in Specific Aim IV are described in Chapter II under *Experimental Diets*, Table 2.2. Energy consumption of dogs in HFA and HFR was matched, but both groups were hypercaloric relative to CTR (mean daily energy intake [kcal/d] over 4 weeks: CTR, 1982±94; HFA, 2695±232; HFR, 2790±219) (Figure 6.1).

After 4 weeks of experimental diet feeding, hyperinsulinemic hyperglycemic (HIHG) clamp experiments with portal vein glucose infusion were conducted on 18-h-fasted, conscious dogs. Just prior to the fast, each dog was fed a can of meat as their meal to ensure equivalent energy and macronutrient consumption among groups the day before the study. Each experiment consisted of a 100 min equilibration period (-120 to -20 min), a 20 min basal control period (-20 to 0 min), and a 180 min experimental period divided into 2 sub-periods (P1, 0 to 90 min; P2, 90 to 180 min). At -120 min, a priming dose of [3-³H]-glucose (38 µCi) was injected, followed by a constant infusion of [3-³H]-glucose (0.38 µCi/min). At time 0, a constant infusion of somatostatin (0.8 µg/kg/min) was initiated in the left saphenous vein, and insulin and glucagon were replaced intraportally at 3-fold basal (1.2 mU/kg/min) and basal (0.55 ng/kg/min) rates, respectively. In addition, a variable infusion of 50% dextrose was started in the right cephalic vein in order to double the hepatic glucose load (HGL). In P2, 20% dextrose (4.0 mg/kg/min) was infused intraportally, and the peripheral glucose infusion rate was adjusted as necessary to clamp the HGL to that in P1. For this study, unidirectional hepatic glucose uptake was calculated using a tracer-determined hepatic fractional extraction method, as described in detail under *Calculations* in Chapter II. At the end of the study, each animal was anaesthetized with sodium pentobarbital and a laparotomy was performed. The hormone, 3-[³H]-glucose, and unlabeled glucose infusions were continued while liver

sections from the left central, left lateral, and right central lobes were freeze-clamped in situ and stored at -80°C for tissue analysis.

Results

Plasma hormone concentrations and hepatic blood flow

Fasting arterial plasma insulin levels were increased 45% and 70% in HFA and HFR, respectively, relative to CTR ($\mu\text{U/ml}$; CTR: 8.0 ± 1.6 , HFA: 11.6 ± 1.2 , HFR: 13.6 ± 1.2 ; $P < 0.05$ CTR vs. HFR), whereas arterial plasma c-peptide concentrations (data not shown) were elevated 79% and 50% in HFA and HFR, respectively, relative to CTR (ng/ml ; CTR: 0.24 ± 0.03 , HFA: 0.43 ± 0.08 , HFR: 0.36 ± 0.0 ; NS between groups). There was no effect of diet on fasting arterial plasma glucagon levels. During the HIHG clamp, arterial and hepatic sinusoidal insulin concentrations ($\mu\text{U/ml}$; CTR: 23 ± 4 and 78 ± 10 , HFA: 26 ± 2 and 89 ± 6 , HFR: 25 ± 2 and 90 ± 7 , respectively; $P < 0.05$ vs. basal period) were increased to similar levels in all 3 groups, whereas arterial and hepatic sinusoidal glucagon concentrations were kept at a basal level throughout the study (Figure 6.2 A-D). Total hepatic blood flow was similar among groups under basal conditions and throughout the HIHG clamp (Table 6.1).

Blood glucose, hepatic glucose load, and hepatic glucose uptake

Fasting blood glucose concentrations did not differ between groups during the basal period. During P1, arterial blood glucose concentrations were increased to a similar level in all 3 groups (mg/dl ; CTR: 161 ± 4 , HFA: 164 ± 1 , HFR: 163 ± 1 ; $P < 0.05$ vs. basal period) in order to double the hepatic glucose load (mg/kg/min ; CTR: 37 ± 2 , HFA: 39 ± 2 , HFR: 38 ± 3 ; $P < 0.05$ vs. basal period) (Figure 6.3A and B). During P2, arterial blood

glucose levels were clamped at a slightly reduced concentration (mg/dl; CTR: 147 ± 3 , HFA: 150 ± 2 , HFR: 149 ± 2) to maintain a doubling of the hepatic glucose load in the presence of intraportal glucose infusion (Figure 6.3A and B).

Hepatic glucose uptake (HGU) was similar among groups during the basal period (mg/kg/min; CTR: 0.4 ± 0.1 , HFA: 0.5 ± 0.3 , HFR: 0.4 ± 0.2) (Figure 6.3C and D). During P1, hyperinsulinemia and hyperglycemia stimulated an increase in HGU in CTR, reaching a peak of 1.8 ± 0.3 mg/kg/min ($P<0.05$ vs. basal period). Delivery of glucose into the portal vein during P2 in the presence of a sustained rise in glucose and insulin augmented HGU even further in CTR, eventually reaching a peak of 3.0 ± 0.3 mg/kg/min (Figure 6.3C or D). In contrast, both high-fat and high-fructose feeding for 4 weeks rendered the liver resistant to the stimulatory effects of hyperinsulinemia, hyperglycemia, and portal glucose delivery on HGU. Thus, mean rates of HGU in HFA and HFR during P1 (1.0 ± 0.4 and 0.6 ± 0.2 mg/kg/min, respectively) and P2 (0.9 ± 0.3 and 0.7 ± 0.1 mg/kg/min, respectively) were not significantly increased from their corresponding rates during the basal period (Figure 6.3C and D). However, the mean rate of HGU in high-fat-fed dogs during P1 (average during the last 30 min of P1) did not differ significantly from that of CTR, whereas it did in the high-fructose-fed dogs (Figure 6.3C and D). In the presence of portal glucose delivery (P2), on the other hand, both groups displayed significantly lower rates of HGU relative to CTR. This was due to further stimulation of HGU during P2 in CTR, and the lack of such an effect in both HFA and HFR (Figure 6.3C and D).

Although the total glucose infusion rate (GIR) required to maintain hyperglycemia did not significantly differ among groups, it tended to be lower in HFA

and HFR vs. CTR throughout the entire HIHG clamp (Table 6.1).

Lactate metabolism

All groups exhibited net hepatic lactate uptake (NHLU) under basal conditions (Table 6.2). In CTR and HFA, hyperinsulinemia and hyperglycemia elicited an increase in arterial blood lactate levels coincident with a switch from NHLU to output (NHLO), although NHLO was significantly reduced in HFA vs. CTR (Table 6.2). In contrast, arterial blood lactate levels were not significantly elevated from basal during either test period in HFR, and these animals exhibited NHLU for the duration of the study ($P < 0.05$ vs. CTR and HFA) (Table 6.2).

Glycerol, nonesterified fatty acid, and triglyceride metabolism

During the basal period, arterial blood glycerol concentrations were significantly elevated in HFA and HFR vs. CTR, whereas net hepatic glycerol uptake was significantly higher only in HFR (Table 6.2). Fasting arterial plasma NEFA concentrations were similar among the 3 groups. During P1 and P2, their levels declined in response to hyperinsulinemia, but the steady state values were slightly lower in CTR than in HFA or HFR (Table 6.2). The net hepatic uptake rates of glycerol and NEFA decreased in parallel to the changes in their circulating concentrations (Table 6.2).

Fasting plasma total triglyceride concentrations (data not shown) did not differ between diet groups (1139 ± 137 , 1148 ± 28 , and 1156 ± 284 $\mu\text{mol/l}$ in HFA, HFR, and CTR, respectively). Likewise, terminal liver triglyceride levels (data not shown) were not significantly different among groups ($\mu\text{g/mg}$ liver; HFA: 2.0 ± 0.3 , HFR: 1.7 ± 0.2 , CTR: 1.4 ± 0.2).

Hepatic glucokinase (GK) and glucokinase regulatory protein (GKRP)

Molecular parameters ($n=5/\text{group}$) in liver biopsies obtained at the end of the HIHG clamp experiment were compared amongst CTR, HFA, and HFR groups. Although relative hepatic GK mRNA expression was similar among groups (Figure 6.4A), GK protein content and its catalytic activity were reduced by 35% and 56%, respectively, in HFA vs. CTR ($P < 0.05$) (Figure 6.4B and C). In HFR, on the other hand, GK protein content and activity were reduced even further (53% and 74%, respectively; $P < 0.05$ vs. CTR and HFA), and there was a significant decrease, albeit not to the same extent, in GKRP content (Figure 6.4 B-D).

Hepatic insulin signaling and glycogen metabolism

The phosphorylation of Akt was significantly lower (21%) in HFA compared to CTR, whereas there was only a minor (9%) and nonsignificant decline in HFR (Figure 6.5A). There was no difference between groups in GSK3 β phosphorylation. In support of impaired activation of Akt, the activity ratio of glycogen synthase (GS) was reduced by 50% in HFA vs. CTR ($P < 0.05$), whereas that of glycogen phosphorylase (GP) tended to be elevated (Figure 6.6A and B). When the activity ratios of GS and GP were themselves expressed as a ratio (GS/GP), they were significantly lower in both HFA and HFR vs. CTR (Figure 6.6C). Total GS activity was similar among groups (Figure 6.6D). In agreement with diminished GK activity and impaired regulation of enzymes involved in glycogen metabolism, terminal liver glycogen levels were significantly lower in HFR vs. CTR, and tended to be lower in HFA (Figure 6.6E). Likewise, the incorporation of glucose into glycogen through the direct synthetic pathway (glucose \rightarrow glucose 6-phosphate \rightarrow glucose 1-phosphate \rightarrow UDP-glucose \rightarrow glycogen) was markedly decreased

in both HFR and HFA (78% and 62%, respectively; $P < 0.05$ vs. CTR) compared to CTR, but the reduction was significantly greater in HFR than in HFA (Figure 6.5F).

Discussion

Excess consumption of dietary fat and fructose in what has been commonly referred to as a “Western” diet, has been suggested to play a role in the obesity and diabetes epidemic within the U.S. [12, 28, 29]. Our previous studies (Specific Aims I and III) demonstrated that 4 weeks of high-fat, high-fructose (52%, 17% of total energy) feeding impairs glucose tolerance and renders the liver resistant to the stimulatory effects of hyperinsulinemia, hyperglycemia, and portal glucose delivery on HGU and GSYN [339]. The molecular correlates to these phenotypic observations included diminished hepatic GK and GS activity, impaired activation of Akt, and a decrease in GKRP protein content (Specific Aim III). The objective of the present study was to delineate the relative contribution of high dietary fat (52% of total energy) vs. fructose (17% of total energy) to impaired HGU and GSYN. Herein we demonstrate that both a high-fat (HFA) and a high-fructose (HFR) diet significantly impair HGU, direct GSYN, and GK activity in the presence of hyperinsulinemia, hyperglycemia, and portal glucose delivery; however, the magnitude of the decrease in GK activity was significantly greater in HFR than in HFA. In addition, the sum of their individual effects on HGU, GSYN, and GK activity exceeded those observed previously in response to consumption of a combination high-fat/high-fructose diet (HFFD; Specific Aim III). These data indicate that the relative contributions of fat and fructose to aberrant hepatic glucose metabolism in vivo are not additive, and suggest that either the HFA and HFR diets utilize the same pathway to

impair HGU, or they signal through separate pathways which converge at the same rate-limiting, saturable step.

Numerous studies have described the adverse metabolic effects of high dietary fat [16, 17, 23, 95] or fructose [18, 19, 150] on whole-body insulin action and hepatic glucose metabolism; however, most of those studies were conducted under hyperinsulinemic euglycemic conditions. Under euglycemic conditions, however, the liver is only a minor contributor to whole-body glucose disposal. Thus, the effects of a HFA or HFR diet on HGU and disposition under conditions that mimic the postprandial state are poorly understood. In view of this consideration, we performed hyperinsulinemic, hyperglycemic clamps with portal glucose delivery after 4 weeks of HFA or HFR feeding. In the presence of hyperinsulinemia and hyperglycemia, there was a tendency for HGU to be reduced in HFA vs. CTR during P1, but mean rates of HGU did not differ significantly between the two groups. When glucose was infused intraportally in the presence of elevated insulin and glucose, HGU was augmented even further in CTR, but not HFA. As a result, HGU was significantly lower in HFA than in CTR throughout P2. On the other hand, HGU was markedly reduced in HFR vs. CTR throughout the entire clamp study, suggesting that a selective increase in dietary fructose has a greater impact on HGU than that caused by an isocalorically-equivalent increase in dietary fat. Given that rates of HGU under the same experimental conditions in dogs fed a combination HFFD (Specific Aim III) were similar to those observed in the present study, these data suggest that the adverse effects of high dietary fat or fructose on the response of the liver to hyperinsulinemia, hyperglycemia, and portal glucose delivery are not additive.

Although HGU only statistically differed between the HFR and HFA diet groups at 2 time points, it tended to be lower in HFR than in HFA throughout the entire HIHG clamp. In support of this observation, the livers of dogs in the HFR group remained in NHLU for the duration of the experiment, despite the presence of hyperinsulinemia, hyperglycemia, and intraportal glucose infusion. On the other hand, livers of dogs in the HFA group rapidly switched from NHLU to NHLO upon initiation of hyperinsulinemia and hyperglycemia, although the rate was significantly reduced relative to CTR. Nevertheless, these data suggest that net hepatic glycolytic flux was increased in HFA in response to a physiologic rise in glucose and insulin, but it is not clear whether the source of carbon for the increase NHLO was glycogenolytically-derived or derived from extracellular glucose. In our previous study [339], and in Specific Aim III, dogs fed the combination HFFD did not switch from NHLU to NHLO under identical experimental conditions. In light of that observation and the present results, it would appear that a selective and physiologic increase in dietary fructose elicits greater impairment in net hepatic glycolytic flux than a selective increase in dietary fat. However, net hepatic lactate balance was significantly reduced in both groups relative to CTR. This might be due to impaired insulin-mediated activation of rate-limiting enzymes involved in the glycolytic pathway (phosphofructokinase-1/2 and pyruvate kinase), or a decrease in the amount of substrate available for catabolism through the glycolytic pathway secondary to impaired HGU. Previously, Chu and colleagues [369] demonstrated that elevation of plasma NEFA levels brought about by using intralipid and heparin infusion completely eliminated the ability of hyperglycemia per se to cause NHLO. This was attributed to stimulation of hepatic gluconeogenic flux and presumably, inhibition of glycolysis [177,

369]. In the present study, there was a tendency for arterial plasma NEFA and glycerol concentrations to be higher in HFA and HFR than in CTR, which might have contributed to aberrant net hepatic lactate balance in response to hyperinsulinemia and hyperglycemia.

In support of the notion that hepatic GK is rate limiting for glucose utilization by the liver [231], there was a significant post-transcriptional decrease in GK protein content and activity in both the HFA and HFR groups vs. CTR. However, GK activity was significantly lower in HFR-fed than in HFA-fed animals. In fact, the decrease in GK activity in HFR was equivalent in magnitude to the decrease observed previously in dogs fed the combination HFFD (Specific Aim III). Thus, in accord with HGU, the effects of high dietary fat and fructose per se on hepatic GK activity are also not additive, and appear to be saturable in the presence of a selective increase in dietary fructose. Furthermore, the differences in GK protein between HFA, HFR, and CTR correlated with the differences in HGU and net hepatic lactate balance between groups, indicating that GK serves a critical function in facilitating the normal response of the liver to elevated glucose and insulin.

A significant decline in GK protein content and activity in HFA and HFR vs. CTR in the absence of a difference between groups in relative GK expression suggests that either the translation of GK mRNA was impaired, or that the turnover (degradation) of GK protein was enhanced after 4 weeks of HFA or HFR feeding. The inhibitory effect of a high-fat diet on hepatic GK activity has been shown previously in rodents. For example, Oakes and colleagues [22] reported that three weeks of high-fat feeding (59% of energy from fat) in rats resulted in a significant impairment in the ability of insulin to

suppress hepatic glucose production during a hyperinsulinemic-euglycemic clamp, which was associated with elevated glucose-6-phosphatase activity, and significantly reduced glucokinase activity. Likewise, Collier et al. [20] reported that 3 weeks of high-fat feeding (66% of energy from fat) resulted in a more pronounced impairment of oral than intravenous glucose tolerance in rats, which was associated with a marked decrease (> 50% reduction compared to low-fat-fed rats) in hepatic GK activity. Given the vital role of the liver in the disposition of an oral glucose load [26, 190, 215], these data suggest that impaired oral glucose tolerance was linked to a decrease in HGU secondary to a reduction in GK activity, as speculated by the authors [20]. In agreement with these findings, Minassian et al. [373] reported a greater than 50% decrease in GK activity after 3 weeks of high-fat feeding in rats. Thus, it is clear from the literature that HFA feeding is associated with a decline in GK activity, and our findings in the present study in the HFA group are in accord with previous observations.

The effect of high-fructose or high-sucrose feeding on hepatic GK activity is less clear. For example, Bizeau and colleagues [14] demonstrated a significant decrease in GK activity in primary cultures of periportal hepatocytes isolated from rats that were fed a high-sucrose diet (in which 35% of the energy was derived from fructose) for 1 week as opposed to a high-starch diet. On the other hand, liver GK activity was increased in rats that were administered 10% fructose in their drinking water for 3 weeks [374, 375], despite the fact that they had impaired glucose tolerance. However, fasting hyperglycemia, hyperinsulinemia, hypertriglyceridemia, and increased liver triglyceride content accompanied the impaired glucose tolerance associated with 3 weeks of fructose consumption. Thus, it is difficult to isolate the effect of excess fructose per se on liver

GK activity in the presence of all the other metabolic changes that occurred. In the present study, excess consumption of dietary fat or fructose per se induced a significant decrease in GK activity in the dog in the absence of coincident gluco- or lipotoxicity when fed a HFA or HFR diet for 4 weeks. These data are intriguing when considering that the dog only eats one meal per day, and the absorption of that meal is very slow such that the dog does not experience significant postprandial hyperglycemia [309]. In contrast, humans spend most of their day in the fed (postprandial) state. Thus, chronic consumption of a Western diet, replete with foods high in fat and fructose, might have an even greater detrimental impact on hepatic glucose flux and glucose tolerance in humans, and might precipitate the development of type 2 diabetes in susceptible individuals.

In our previous study (Specific Aim III), there was also a marked decrease in the amount of hepatic GKRP content in response to HFFD feeding. Given that GKRP is thought to exert a permissive effect on GK protein expression by protecting it from degradation [370, 371], reduced levels of hepatic GKRP in HFFD-fed animals may have contributed to the post-transcriptional decline in GK protein. In the present study, GKRP was significantly reduced only in high-fructose-fed dogs, albeit not to the same extent as in our previous study (Specific Aim III). Although it raises the possibility that the combination of fat and fructose might synergize to drive a decline in GKRP when consumed in excess quantities, the implication of this decline with regard to GK protein levels is not clear, given that GK was equivalently reduced in high-fructose-fed and high-fat, high-fructose fed (Specific Aim III) dogs.

Hepatic GK expression is hormonally and nutritionally regulated by insulin and fasting-refeeding, respectively [345-347]. This is exemplified by the fact that hepatic GK

activity falls during fasting, and is restored by refeeding in association with robust induction of GK expression [376-380]. In addition, 90% pancreatectomy [210] or streptozotocin administration [175] in rats results in a significant decrease in hepatic GK mRNA and activity, whereas insulin treatment is accompanied by a prompt overshoot of GK mRNA levels [238, 345]. Given the putative role of insulin in the regulation of hepatic GK expression, one might expect a decrease in GK mRNA with hepatic insulin resistance. Indeed, rats fed a HFA diet for 8 weeks displayed a significant decrease in GK mRNA and activity relative to chow-fed CTR rats, despite the fact that their fasting insulin levels were increased by 74%. On the other hand, hepatic GK activity was significantly elevated in insulin-resistant, hyperinsulinemic Zucker *fa/fa* rats [381], which are homozygous for a mutation in the leptin receptor gene. Thus, the impact of insulin resistance on hepatic GK expression and activity appears to be dependent upon the manner in which insulin resistance was induced (e.g. by high-fat diet or by single gene mutations).

Interestingly, there was dissociation among diet groups in the present study with regard to biochemical insulin resistance, with HFA-feeding resulting in a significant decrease in insulin-stimulated phosphorylation of Akt during the HIHG clamp. In agreement with this finding, the activity ratio of glycogen synthase, a reflection of its phosphorylation state *in vivo*, was also significantly reduced in HFA vs. CTR, whereas that of GP tended to be increased. In HFR, on the other hand, Akt phosphorylation, and the individual GS and GP activity ratios did not differ significantly from CTR, although there was a tendency for GS and GP to be aberrantly regulated. Thus, when GS and GP were themselves expressed as a ratio, there was a significant decrease in both HFA and

HFR vs. CTR, although it was greater in HFA. Conversely, terminal liver glycogen levels were reduced in both HFA and HFR vs. CTR, but the reduction was significantly greater in HFR, as was the decrease in direct glycogen synthesis. Thus, high-fat feeding was associated with greater impairment in Akt phosphorylation and in the covalent regulation of GS and GP, whereas high-fructose feeding was associated with greater impairment in GK activity and hepatic GSYN. This was perhaps due to insufficient provision of substrate required for the synthesis of liver glycogen secondary to markedly impaired HGU. Nevertheless, the combination of fat and fructose in Specific Aim III under similar experimental conditions did not result in a further decline in the activity ratio of GS, a further increase in the activity ratio of GP, or a greater impairment in hepatic GSYN. Thus, the relative contributions of fat and fructose to aberrant hepatic GSYN are also not additive.

Furthermore, the presence or absence of biochemical insulin resistance did not appear to have an impact on relative GK expression in HFA and HFR vs. CTR at the end of the clamp. Thus, mechanisms in addition to insulin action must be involved in the regulation of hepatic GK expression in HFA and HFR. Given the dramatic effect of portal glucose delivery on GK expression in Specific Aim III, it is possible that the portal signal also induced an equivalent increase in GK expression in the present study, but was insufficient to drive an increase in GK protein in HFA and HFR.

At this time, the mechanism by which HFA or HFR diets decrease HGK activity and HGU is unclear. Previous studies have implicated liver lipid accumulation in the pathogenesis of hepatic insulin resistance induced by HFA or HFR feeding, in which HFA diets increase the delivery of dietary fat to the liver, whereas HFR diets activate de

novo lipogenesis within the liver [23, 146, 171]. In the present study, however, total liver TG levels did not significantly differ among groups, suggesting that the mechanism linking HFA and HFR feeding to impaired regulation of HGK and HGU was independent of liver lipid accumulation. Asterholm and Scherer [382] demonstrated previously that dynamic changes in liver lipid levels occur upon exposure to a HFD, with peak concentrations appearing after only 48 hours of HFD feeding. This is followed by a significant and rapid decline in liver lipid levels, referred to as an “adaptation phase”, and then a gradual increase thereafter [382]. Thus, it is possible that the HFA or HFR diets augmented liver lipid levels within the first few days of feeding, after which the liver underwent an adaptation phase to cope with the dietary challenge. Nevertheless, the defect in HGK and HGU was sustained after 4 weeks of feeding, suggesting that processes other than hepatic lipid accumulation were associated with aberrant hepatic glucose flux in the presence of a hyperinsulinemic, hyperglycemic challenge. Future studies would need to be conducted to assess the early metabolic and hepatocellular changes that occur upon exposure to a HFA or HFR diet.

In summary, both HFA and HFR diets significantly impair hepatic GK activity, HGU, and direct GSYN after 4 weeks of feeding, but the magnitude of the decrease in GK activity was significantly greater in HFR than in HFA. Whereas removal of the fructose component of the diet in the presence of high dietary fat ameliorated the severity of the defect in GK activity, HGU, and hepatic glucose disposition, removal of excess fat in the presence of high dietary fructose attenuated the severity in biochemical insulin resistance. Nevertheless, the sum of their individual effects on HGU, GK, and GSYN exceeded those observed after consumption of a combination high-fat/high-fructose diet,

suggesting that their relative contributions to aberrant hepatic glucose disposition are not additive.

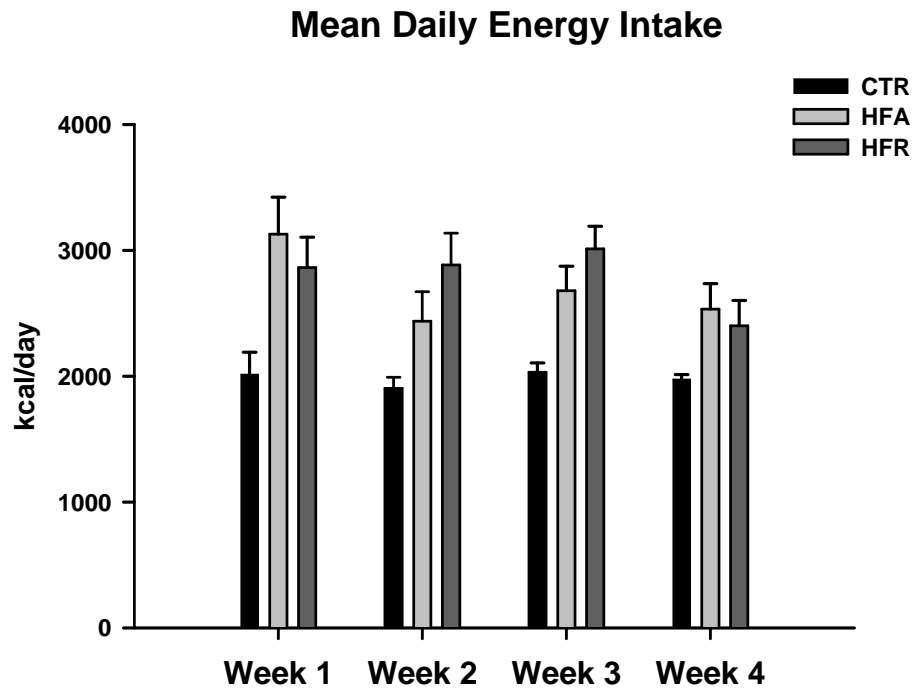


Figure 6.1: Mean daily energy intake. Mean daily energy intake was recorded in dogs fed control diet (CTR, $n = 5$), a high-fat diet (HFA, $n = 5$), or a high-fructose diet (HFR, $n = 5$) for 4 weeks. Dogs fed the HFA or HFR diet were provided isoenergetic quantities of their respective diets over the course of 4 weeks, but both were hypercalorically-fed relative to CTR dogs.

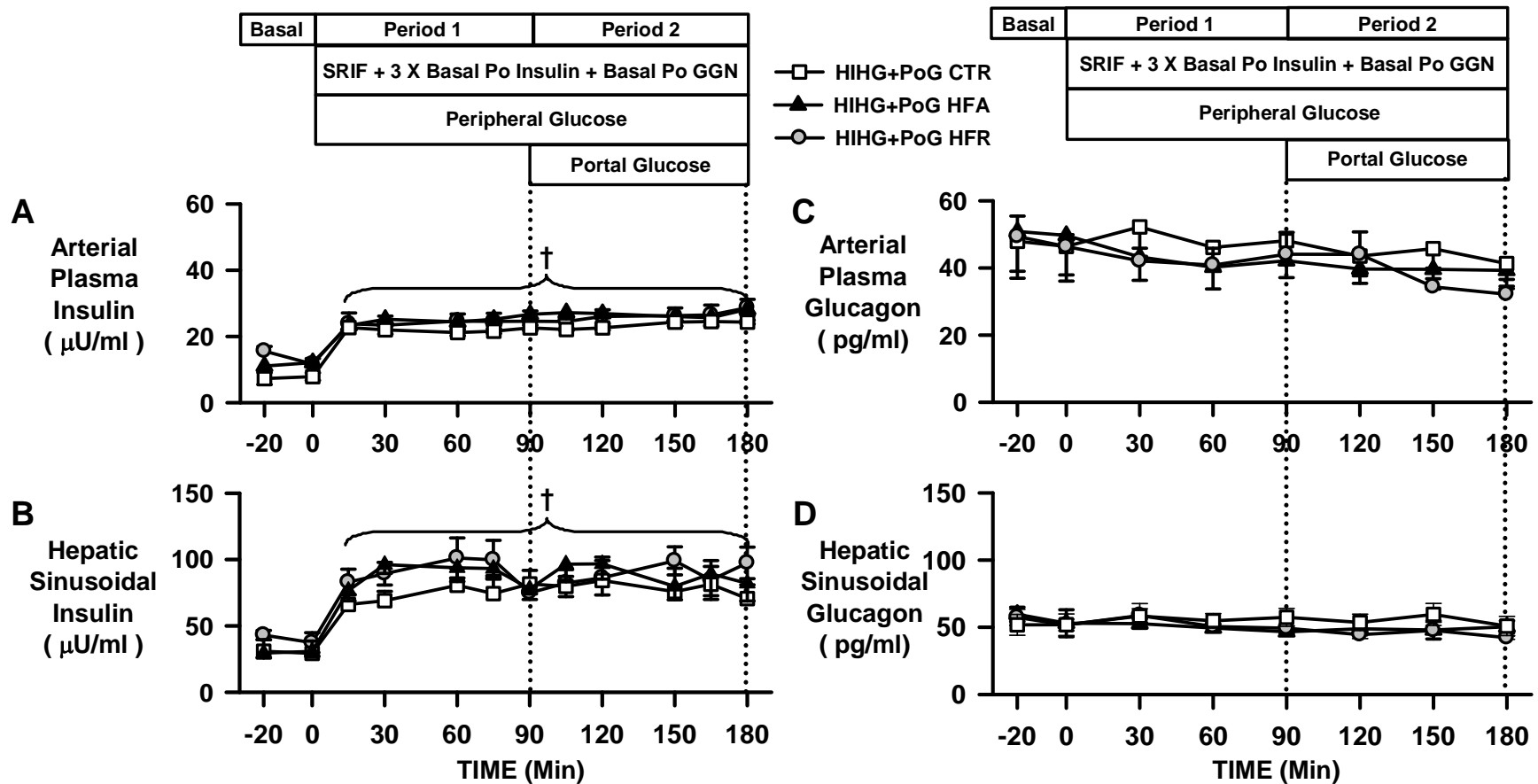


Figure 6.2: Plasma hormone concentrations during hyperinsulinemic hyperglycemic clamps in CTR, HFA, and HFR groups. Arterial plasma insulin (A) and glucagon (C), and hepatic sinusoidal insulin (B) and glucagon (D) during basal (-20 to 0 min) and experimental periods (0 to 180 min) of HIHG clamps conducted in 18-h-fasted dogs after 4 weeks of feeding a CTR (HIHG+PoG, $n = 5$; \square), HFA (HIHG+PoG, $n = 5$; \blacktriangle), or HFR (HIHG+PoG HFR, $n = 5$; \bullet) diet. Data are means \pm SE. † $P < 0.05$ vs. basal period.

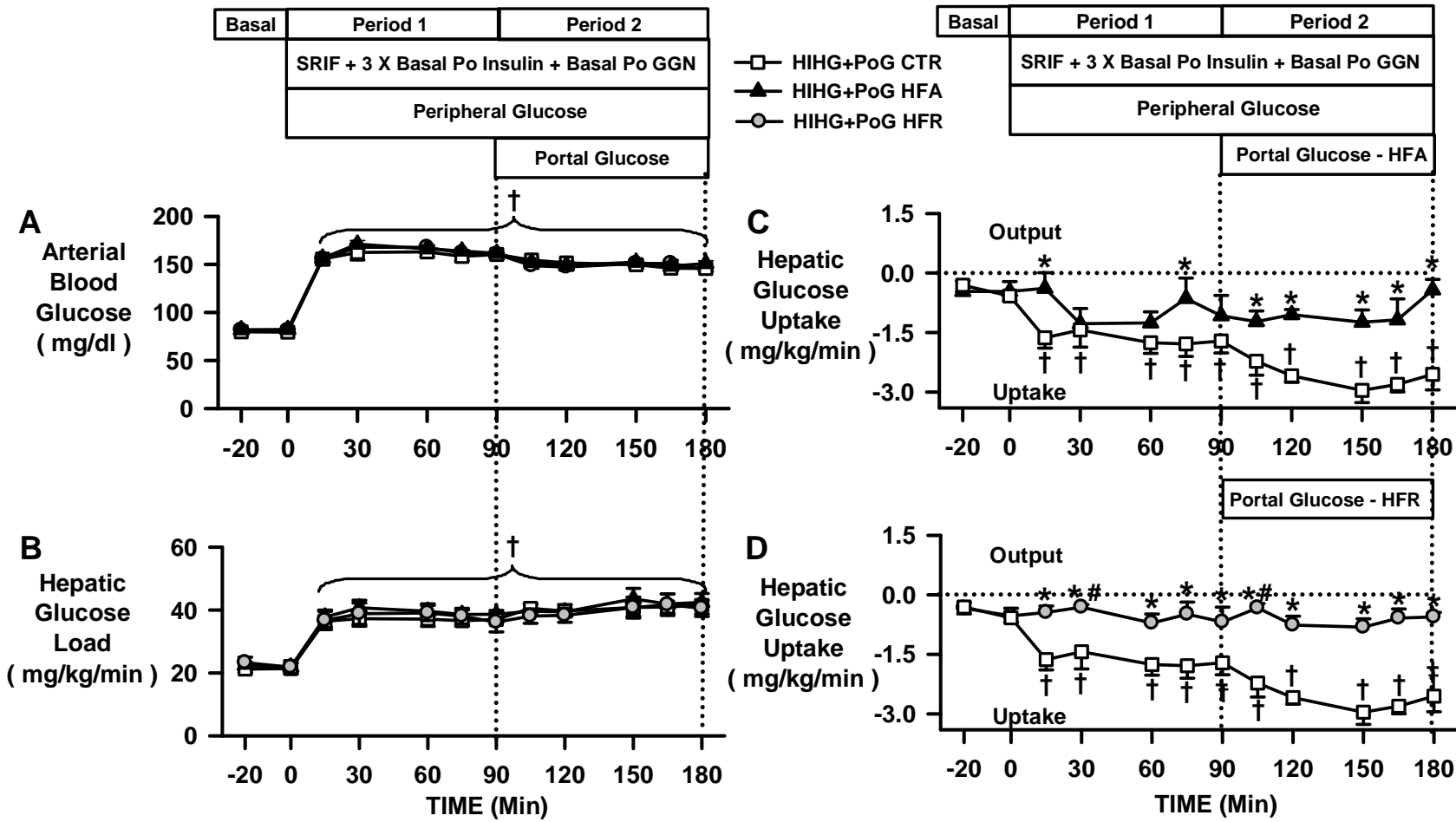


Figure 6.3: Arterial blood glucose, hepatic glucose load, and hepatic glucose uptake during hyperinsulinemic hyperglycemic clamps in CTR, HFA, and HFR groups. Arterial blood glucose (A), hepatic glucose load (B), and hepatic glucose uptake in the portal saline (C) and portal glucose (D) groups during the basal (-20 to 0 min) and experimental periods (0 to 180 min) of HIHG clamps conducted in 18-h-fasted dogs after 4 weeks of feeding a CTR (HIHG+PoG, $n = 5$; \square), HFA (HIHG+PoG, $n = 5$; \blacktriangle), or HFR (HIHG+PoG HFR, $n = 5$; \bullet) diet. Data are means \pm SE. $\dagger P < 0.05$ vs. basal period; $*P < 0.05$ vs. CTR; $\# P < 0.05$, HFR vs. HFA.

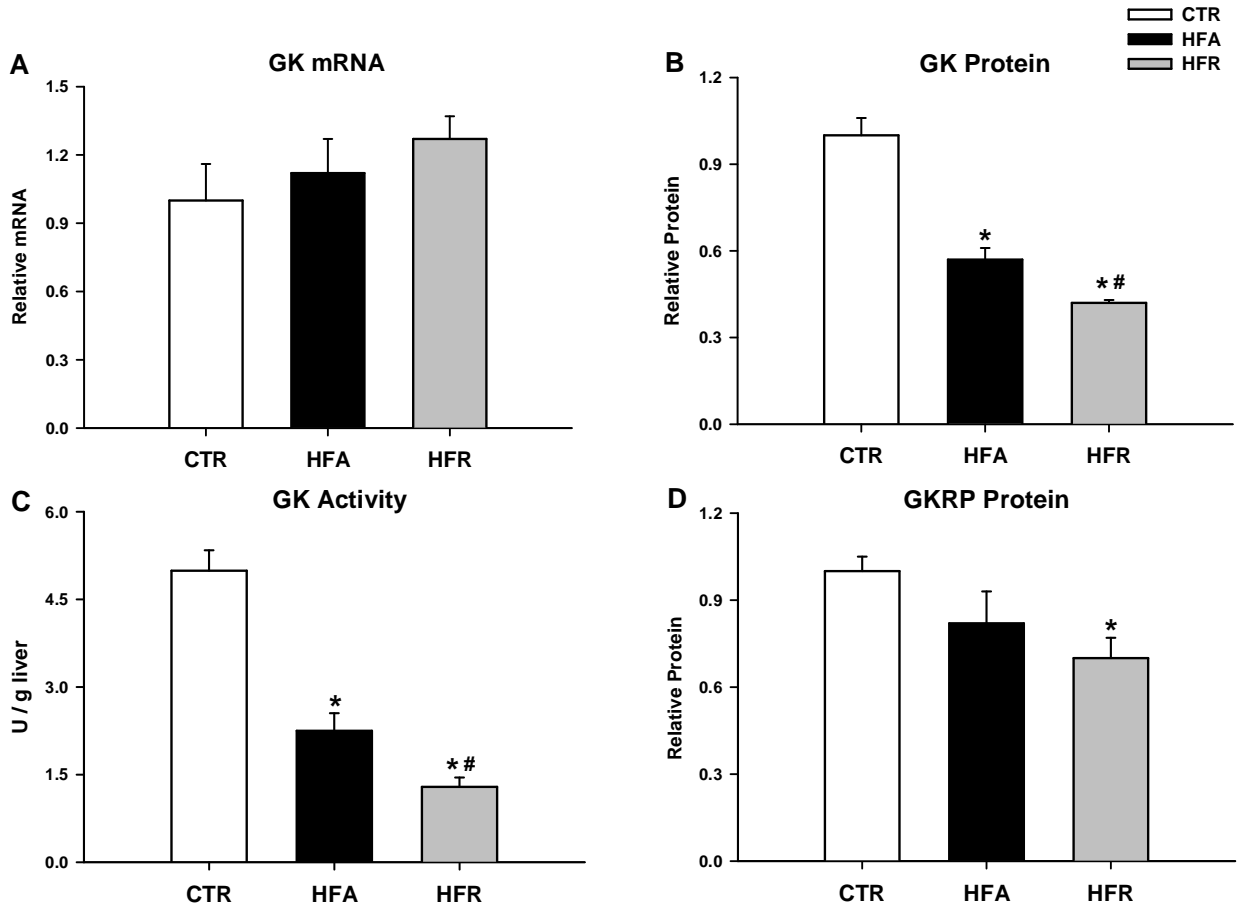


Figure 6.4: Hepatic glucokinase (GK) and glucokinase regulatory protein (GKR) in CTR, HFA, and HFR groups. Levels of GK mRNA (A) and protein (B), GK activity (C), and levels of GKR protein (D). A, B, and D are expressed relative to levels observed in CTR animals. Data are means \pm SE; $n = 5$ per group. * $P < 0.05$ vs. CTR; # $P < 0.05$, HFR vs. HFA.

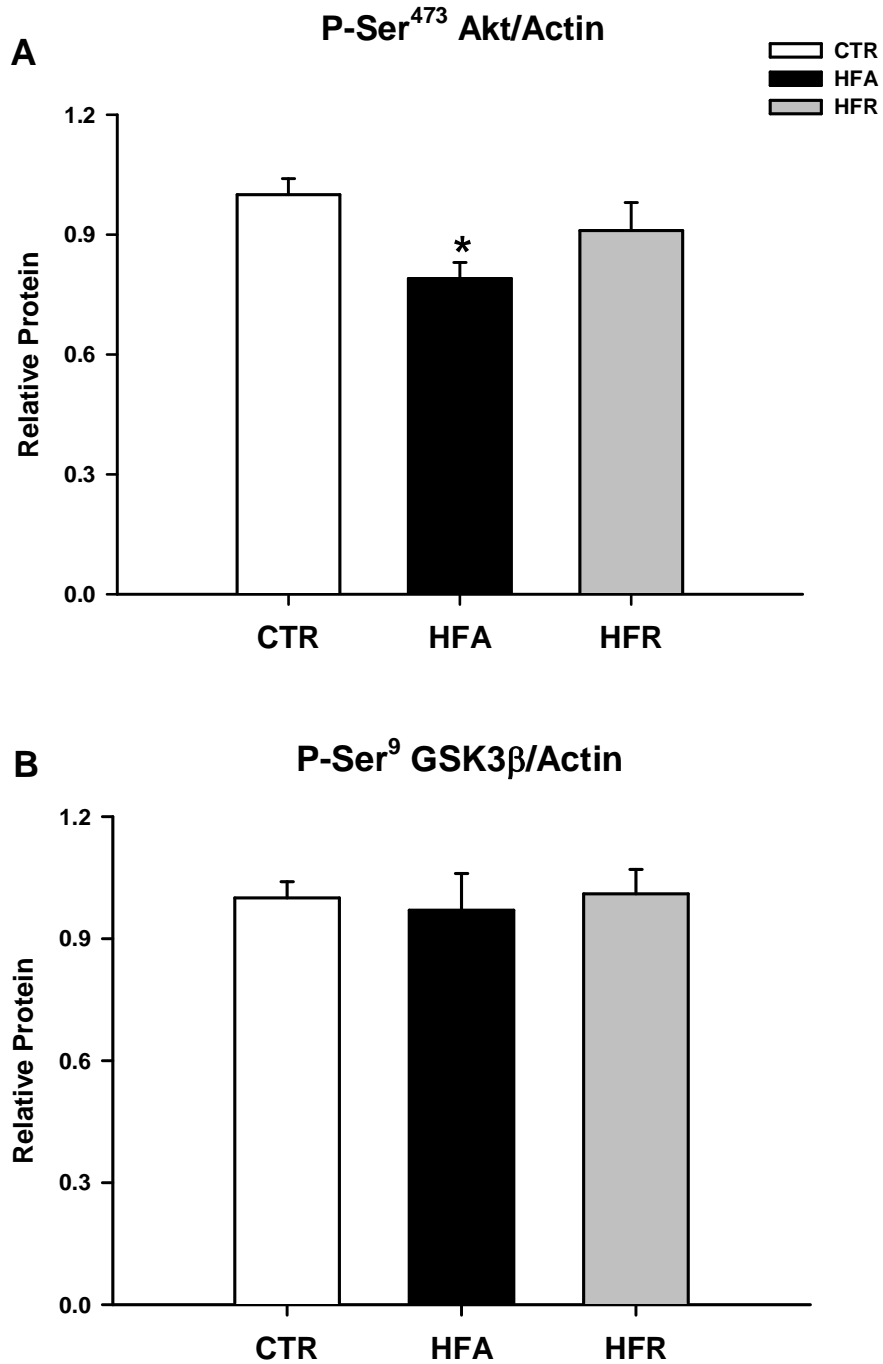


Figure 6.5: Markers of hepatic insulin signaling in CTR, HFA, and HFR groups. Phosphorylation of Akt on Ser473 (A) and GSK3β on Ser9 (B) relative to levels observed in CTR animals. Data are means ± SE; *n* = 5 per group. **P* < 0.05 vs. CTR.

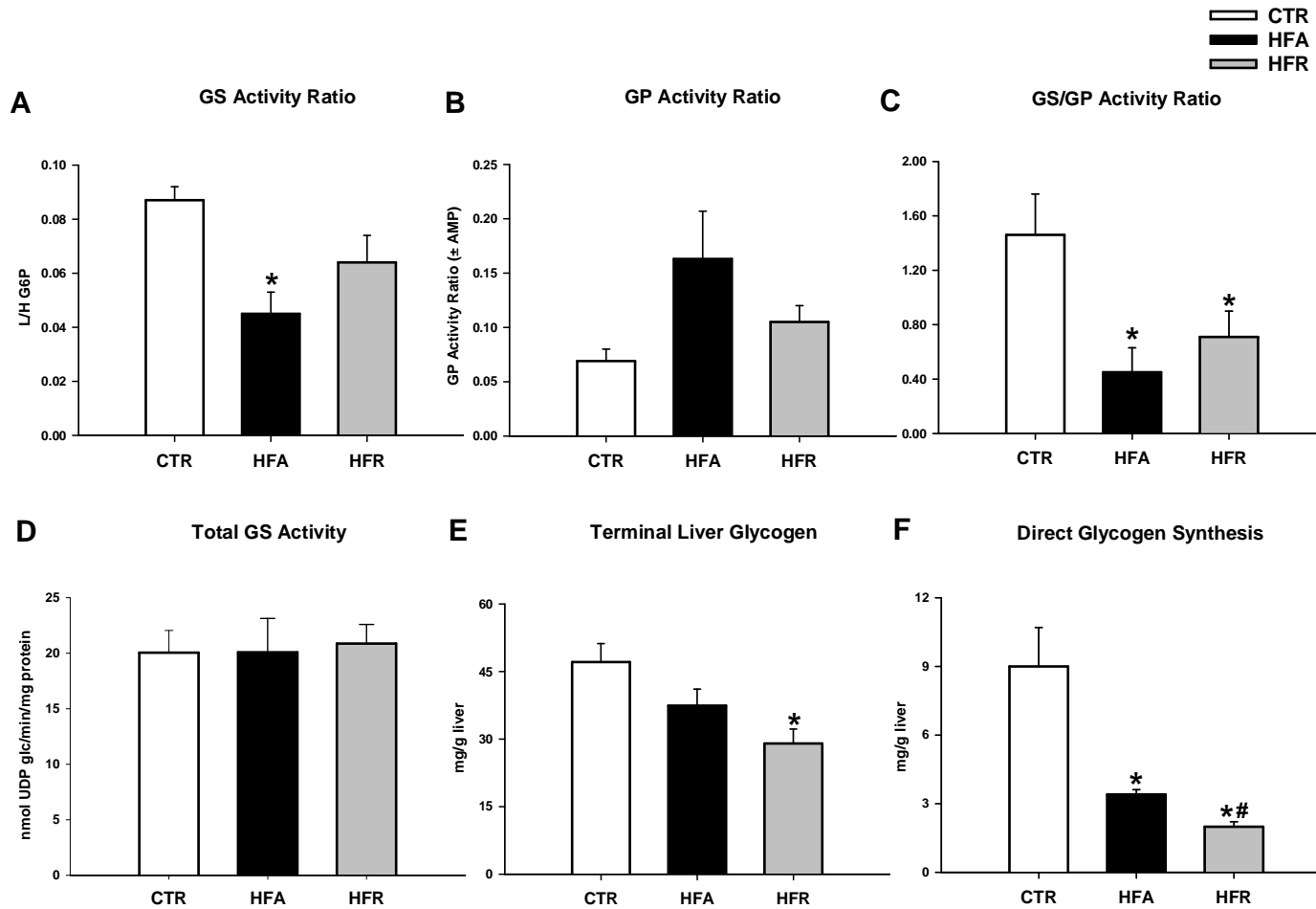


Figure 6.6: Markers of hepatic glycogen metabolism in CTR, HFA, and HFR groups. Activity ratios of glycogen synthase (GS) (A), glycogen phosphorylase (GP) (B), GS/GP (C), and total GS activity (D). Terminal liver glycogen levels (E), and glycogen synthesized through the direct pathway (F). Data are means \pm SE; $n = 5$ per group. * $P < 0.05$ vs. CTR; # $P < 0.05$, HFR vs. HFA.

TABLE 6.1.

Mean values for hepatic arterial and portal venous blood flow, as well as total glucose infusion rate during the basal (-20 to 0 min) and experimental periods (P1, 60 to 90 min; P2, 150 to 180 min) of a hyperinsulinemic hyperglycemic clamp

Group	Experimental Period					
	Basal Period		Period 1 – PoG		Period 2 + PoG	
Hepatic artery blood flow, ml/kg/min						
CTR	4.2	± 0.5	5.4	± 0.4	5.8	± 0.8
HFA	4.7	± 0.7	5.3	± 0.8	6.0	± 1.0
HFR	3.9	± 0.2	4.2	± 0.2	4.4	± 0.3
Portal vein blood flow, ml/kg/min						
CTR	22.2	± 1.3	17.4	± 1.0	19.1	± 0.9
HFA	21.6	± 1.4	18.0	± 1.2	19.3	± 2.3
HFR	23.1	± 2.0	18.4	± 1.3	19.9	± 1.6
Total glucose infusion rate, mg/kg/min						
CTR	0.0	± 0.0	9.0	± 3.0 ^A	10.2	± 2.4 ^A
HFA	0.0	± 0.0	5.7	± 0.8 ^A	8.4	± 1.2 ^A
HFR	0.0	± 0.0	4.9	± 0.6 ^A	8.5	± 1.2 ^A

Values are means ± SE; n = 5 per group. Dogs were 18h-fasted prior to study. A, $P < 0.05$ vs. basal period. CTR, chow control diet; HFA, high-fat diet; HFR, high-fructose diet; - PoG, no portal glucose; + PoG, portal glucose infusion.

Table 6.2.

Mean values for lactate, glycerol, and NEFA concentrations, and their net hepatic balance during the basal (-20 to 0 min) and experimental (P1, 60 to 90 min; P2, 150-180 min) periods of the hyperinsulinemic hyperglycemic clamp in CTR, HFA, and HFR groups

Group	Basal Period, min	Period 1 - PoG, min			Period 2 + PoG, min		
	-20 to 0	60	75	90	150	165	180
Arterial blood lactate, $\mu\text{mol/l}$							
CTR	397 \pm 111	663 \pm 86 ^A	628 \pm 73 ^A	642 \pm 88 ^A	643 \pm 78 ^A	688 \pm 87 ^A	693 \pm 121 ^A
HFA	373 \pm 30	523 \pm 27 ^{AC}	548 \pm 54 ^{AC}	565 \pm 64 ^{AC}	681 \pm 53 ^{AC}	702 \pm 72 ^{AC}	653 \pm 83 ^{AC}
HFR	308 \pm 29	295 \pm 24 ^B	284 \pm 25 ^B	325 \pm 38 ^B	371 \pm 67 ^B	400 \pm 77 ^B	442 \pm 52 ^B
Net hepatic lactate balance, $\mu\text{mol/kg/min}$							
CTR	-5.3 \pm 0.3	8.3 \pm 1.9 ^A	7.0 \pm 1.7 ^A	6.3 \pm 1.3 ^A	5.1 \pm 0.6 ^A	4.4 \pm 0.8 ^A	5.0 \pm 0.8 ^A
HFA	-7.4 \pm 0.7	3.3 \pm 0.6 ^{ABC}	3.1 \pm 0.2 ^{ABC}	2.6 \pm 0.3 ^{ABC}	1.7 \pm 0.9 ^{ABC}	1.1 \pm 1.2 ^{ABC}	1.2 \pm 1.0 ^{ABC}
HFR	-5.9 \pm 0.7	-4.3 \pm 1.0 ^B	-3.8 \pm 1.0 ^B	-3.4 \pm 0.9 ^B	-2.9 \pm 0.9 ^B	-3.3 \pm 0.9 ^B	-3.9 \pm 0.9 ^B
Arterial blood glycerol, $\mu\text{mol/l}$							
CTR	72 \pm 6	32 \pm 4 ^A	27 \pm 3 ^A	23 \pm 1 ^A	29 \pm 3 ^A	29 \pm 5 ^A	29 \pm 3 ^A
HFA	112 \pm 11 ^B	48 \pm 16 ^A	41 \pm 10 ^A	51 \pm 10 ^A	49 \pm 10 ^A	49 \pm 6 ^A	51 \pm 15 ^A
HFR	110 \pm 9 ^B	59 \pm 15 ^A	52 \pm 10 ^A	49 \pm 8 ^A	52 \pm 16 ^A	52 \pm 10 ^A	58 \pm 14 ^A
Net hepatic glycerol balance, $\mu\text{mol/kg/min}$							
CTR	-1.7 \pm 0.1	-0.7 \pm 0.2 ^A	-0.5 \pm 0.1 ^A	-0.5 \pm 0.1 ^A	-0.7 \pm 0.1 ^A	-0.6 \pm 0.1 ^A	-0.8 \pm 0.1 ^A
HFA	-2.1 \pm 0.2	-1.0 \pm 0.6 ^A	-0.7 \pm 0.2 ^A	-1.0 \pm 0.2 ^A	-1.1 \pm 0.3 ^A	-1.0 \pm 0.2 ^A	-1.2 \pm 0.5 ^A
HFR	-2.9 \pm 0.4 ^B	-1.3 \pm 0.4 ^A	-1.0 \pm 0.1 ^A	-1.0 \pm 0.2 ^A	-1.5 \pm 0.5 ^A	-1.2 \pm 0.3 ^A	-1.5 \pm 0.4 ^A
Arterial plasma NEFA, $\mu\text{mol/l}$							
CTR	831 \pm 73	154 \pm 30 ^A	136 \pm 27 ^A	118 \pm 33 ^A	84 \pm 17 ^A	109 \pm 30 ^A	102 \pm 20 ^A
HFA	902 \pm 111	142 \pm 26 ^A	146 \pm 35 ^A	135 \pm 25 ^A	136 \pm 49 ^A	119 \pm 30 ^A	115 \pm 30 ^A
HFR	938 \pm 112	258 \pm 46 ^A	216 \pm 42 ^A	170 \pm 36 ^A	179 \pm 79 ^A	156 \pm 40 ^A	215 \pm 81 ^A
Net hepatic NEFA balance $\mu\text{mol/kg/min}$							
CTR	-2.5 \pm 0.2	-0.2 \pm 0.2 ^A	-0.1 \pm 0.1 ^A	-0.2 \pm 0.1 ^A	-0.2 \pm 0.1 ^A	-0.3 \pm 0.1 ^A	-0.3 \pm 0.1 ^A
HFA	-3.1 \pm 0.4	-0.5 \pm 0.2 ^A	-0.4 \pm 0.2 ^A	-0.3 \pm 0.1 ^A	-0.4 \pm 0.2 ^A	-0.3 \pm 0.1 ^A	-0.4 \pm 0.2 ^A
HFR	-2.4 \pm 0.4	-0.8 \pm 0.2 ^A	-0.7 \pm 0.1 ^A	0.0 \pm 0.1 ^A	-0.5 \pm 0.5 ^A	-0.6 \pm 0.3 ^A	-1.0 \pm 0.6 ^A

Values are mean \pm SE; $n = 5$ per group. Dogs were 18h-fasted prior to study. A, $P < 0.05$ vs. basal period; B, $P < 0.05$ vs. CTR; C, $P < 0.05$, HFA vs. HFR.

Negative values for balance data indicate net hepatic uptake, whereas positive values indicate net hepatic output.

CTR, chow control diet; HFA, high-fat diet; HFR, high-fructose diet; PoG, portal glucose infusion.

CHAPTER VII

SUMMARY AND CONCLUSIONS

The incidence of obesity and diabetes has been increasing at a staggering rate within the United States (U.S.) and around the globe, with type 2 diabetes accounting for the majority of new diagnoses. Insulin resistance, defined as a decrease in the sensitivity of insulin target tissues (liver, skeletal muscle, and adipose tissue) to a physiologic rise in the hormone, is a common pathogenic factor underlying both obesity and type 2 diabetes. The causes of insulin resistance comprise genetic and acquired components, and obesity is one of the most common acquired factors associated with the development of insulin resistance in Western cultures [383]. Indeed, there have been dramatic lifestyle changes in recent decades, including increased caloric availability, excess energy consumption, and decreased energy expenditure (or physical activity), all of which might be causally linked to the increased prevalence of obesity and type 2 diabetes [4]. Given that high-fat and high-sugar-containing, energy dense and nutrient deficient foods have become increasingly available and preferentially consumed in Westernized cultures [6-12], considerable emphasis has been placed on their respective contributions to the development of obesity and insulin resistance. Excessive consumption of dietary fat and fructose has been associated with adipose tissue accretion, ectopic lipid deposition, whole-body insulin resistance, and perturbations in the regulation of glucose metabolism in laboratory animals and in humans. Thus, studies aimed at investigating the pathogenic links between diet and metabolic diseases are warranted. The overall objective of this

body of work was to elucidate the metabolic and hepatocellular consequences associated with chronic consumption of a high-fat and/or high-fructose diet, focusing on perturbations in the regulation of hepatic glucose uptake (HGU) and disposition by hyperglycemia, hyperinsulinemia, and portal vein glucose delivery – the primary determinants of HGU in vivo [26].

The liver acts as a dynamic regulator of glucose homeostasis during fasting and refeeding by virtue of its dynamic ability to switch from net glucose output to net glucose uptake, respectively. Previous studies have indicated that the liver is particularly vulnerable to nutritional insults induced by excess consumption of dietary fat or fructose [13-23]. In fact, several have suggested that hepatic insulin resistance, manifested as a diminished ability of insulin to suppress hepatic glucose production (HGP), is the first metabolic consequence to emerge upon initiation of a high-fat or high-fructose diet in laboratory animals [16-18, 23]. While the effects of high dietary fat or fructose on insulin's ability to suppress HGP have been extensively studied, their effects on HGU and disposition have not been clearly defined. This is due to both the complexity of its regulatory signals, and because it cannot be measured directly in humans or small animals. On the other hand, HGU can be measured directly in the dog. In fact, the accessibility of both the hepatic and portal veins, allowing repeated direct measurements of HGU in the basal state and in the course of experimental perturbations, is a major strength of the dog model.

Although impaired splanchnic (comprising the gut and liver tissues) glucose uptake is one of the metabolic sequelae associated with overt type 2 diabetes [200, 201, 204, 384], its temporal manifestation along the continuum of worsening insulin action

during the development of type 2 diabetes is poorly understood. Likewise, the combined effects of dietary fat and fructose, in quantities that mimic a Western diet, on the temporal development of glucose intolerance and impaired HGU are not known. Thus, in Specific Aim I, we explored how consumption of a high-fat, high-fructose diet (HFFD), coupled with a compromised pancreatic mass (via partial [65%] pancreatectomy), influenced the temporal development of impaired glucose tolerance, whole-body insulin resistance, and the ability of the liver to take up and store glucose in the presence of conditions that mimic the postprandial state. Our findings demonstrated that consumption of a HFFD results in impaired glucose tolerance in a relatively short period of time (4 weeks), which was due to both a beta cell defect and whole-body insulin resistance [339]. In addition, 13 weeks of HFFD feeding rendered the liver incapable of switching from net glucose output to net glucose uptake despite the presence of hyperinsulinemia, hyperglycemia, and intraportal glucose delivery [339]. Thus, the functional consequences of a HFFD on hepatic glucose metabolism were similar to those observed in type 2 diabetic individuals [200, 201], and suggest that impaired HGU may be an early manifestation of the disease.

The metabolic consequences associated with HFFD feeding in Specific Aim I were detected in response to a glucose challenge [339], which lacked other meal-associated factors that can influence the gastric emptying rate, insulin and glucagon secretion, and net hepatic glucose uptake (NHGU) [295-304]. In addition, any active involvement of the gut or endocrine pancreas in the response of the liver to a glucose challenge was eliminated because we had infused somatostatin to perform a pancreatic clamp. Thus, in Specific Aim II we wanted to investigate whether HFFD feeding impairs

NHGU during a more physiological mixed meal test, as it does in individuals with diabetes [203, 204]. Our findings demonstrated that 8 weeks of HFFD feeding elicited excessive postprandial hyperglycemia due to accelerated gastric emptying and glucose absorption, and markedly diminished NHGU [385]. Thus, the defect in NHGU seen in Specific Aim I in response to a glucose challenge and under clamped experimental conditions also existed in a mixed meal setting after chronic consumption of a HFFD. In addition, the mixed meal studies exposed a second metabolic defect as indicated by an enhanced rate of meal macronutrient absorption [385]. Additional studies aimed at exploring the mechanism(s) responsible for accelerated gastric emptying and glucose absorption in HFFD-fed animals are needed, as this too influences the timing and magnitude of postprandial glucose excursions in healthy and diabetic individuals [307, 308].

It is well known that the hepatic sinusoidal insulin level, the hepatic glucose load, and the route of glucose delivery (peripheral vs. intraportal) are the primary determinants of glucose uptake by the liver [26, 215]. The augmentation of HGU elicited by the intraportal route of glucose delivery has been attributed to a unique, neurally-mediated signal generated in the presence of a negative arterial-portal venous glucose gradient, termed the “portal glucose signal” [180, 182, 184, 193-195, 365, 386-389]. In response to ingestion of a glucose-containing meal, the portal signal works in concert with increased plasma glucose and insulin to orchestrate a coordinated response favoring enhanced HGU and glycogen synthesis (GSYN). Although the metabolic effects of intraportal glucose delivery have been studied in normal dogs and in the human, the molecular events linking the pleiotropic actions of the portal glucose signal to increased HGU and GSYN in vivo

have not been clearly defined. In addition, our findings in Specific Aim I suggested that HFFD feeding was associated with the loss of an intact portal glucose signal, but the molecular correlates to this phenotypic observation were not known. Thus, the objective of Specific Aim III was to identify the molecular “signature” associated with hyperinsulinemia, hyperglycemia, and portal glucose delivery in the livers of normal dogs, and to elucidate the mechanism(s) associated with impaired HGU under identical experimental conditions in insulin resistant dogs that had been fed a HFFD. Our findings demonstrated that delivery of glucose into the portal vein in the presence of hyperinsulinemia and hyperglycemia triggered a coordinated molecular response involving an increase in the catalytic activity of hepatic GK, and stimulation of hepatic GS activity, which collectively augmented HGU and GSYN *in vivo*. In contrast, HFFD feeding was associated with biochemical insulin resistance, a marked decline in hepatic GK protein content and activity, and loss of the stimulatory effects of portal glucose delivery on GK and GS activity. These mechanistic defects correlated with diminished HGU and GSYN (Figure 7.1).

Previously, Pagliassotti et al. [198] demonstrated rapid activation of liver GS in response to portal glucose delivery; however, the magnitude of the increase in NHGU suggested that additional mechanisms might also be involved. Our findings in Specific Aim III extend those made by Pagliassotti et al. [198], and indicate that the portal glucose signal also stimulates robust induction of hepatic GK expression and activity, in addition to activation of GS. These data provide novel mechanistic insight into the molecular physiology of the portal signaling mechanism under normal conditions, and suggest that impaired regulation of hepatic GK under insulin resistant conditions may be one of the

early molecular defects that contribute to the deterioration of glucose tolerance and development of postprandial hyperglycemia secondary to diminished HGU.

Follow-up studies in Specific Aim IV indicated that both a high-fat (HFA) and a high-fructose (HFR) diet impair HGU, GSYN, and GK activity in the presence of hyperinsulinemia, hyperglycemia, and portal glucose delivery. Nevertheless, the sum of their individual defects on HGU, GSYN, and GK exceeded those observed in Specific Aim III in response to consumption of a combination HFFD, suggesting that the relative contributions of fat and fructose to aberrant hepatic glucose disposition are not additive. Thus, high dietary fat and fructose either utilize the same pathway to impair HGU, or they signal through separate pathways which converge at the same rate-limiting, saturable step. The implications of these data when extended to the human population suggest that increased consumption of either nutrient might have a detrimental impact on glucose tolerance and risk of diabetes.

Previous studies have implicated liver lipid accumulation in the pathogenesis of hepatic insulin resistance induced by high-fat or high-fructose feeding [23, 146, 171]. In the present study, however, total liver triglyceride levels, and levels of other lipid metabolites (data not shown), did not significantly differ among groups. Likewise, dogs did not develop dyslipidemia or hyperglycemia when fed diets high in fat and/or fructose, yet their GK activity levels and HGU were markedly impaired. Thus, the mechanism(s) linking dietary insults to impaired regulation of GK and hepatic glucose disposition in vivo may be independent of liver lipid accumulation and glucolipototoxicity. These data are intriguing when considering that the dog only eats one meal per day, and the absorption of glucose in that meal is very slow such that the dog does not experience

significant postprandial hyperglycemia [309]. In contrast, humans consume at least 3 meals per day, and spend most of their day in the postprandial state. Thus, the adverse effects of a Western diet on glucose tolerance and hepatic glucose disposition might be magnified in humans.

The clinical significance of the findings presented herein is underscored by the fact that individuals with diabetes display a marked impairment not only in the ability of hyperinsulinemia and hyperglycemia to suppress HGP, but also in the ability of those postprandial stimuli to activate splanchnic glucose uptake and hepatic glycogen synthesis [200, 201, 203, 204]. As a result, they experience frequent bouts of postprandial hyperglycemia, one of the sequelae of diabetes that contributes to the elevation of their hemoglobin A1c and many of the complications associated with the disease [24, 25]. By diminishing the ability of the liver to buffer perturbations in blood glucose levels, high dietary fat and fructose consumption might promote the development of postprandial hyperglycemia, increase the load of glucose that must be disposed of by peripheral tissues and perhaps, precipitate a defect in the beta cell or muscle in a chronic setting. Altogether, the findings presented in this dissertation suggest that impaired HGU might be one of the early metabolic consequences associated with glucose intolerance induced by consumption of a Western diet. In addition, nutritional modulation of hepatic GK might be causally linked to the impaired regulation of HGU by insulin, glucose, and portal glucose delivery (Figure 7.2).

These studies raise a number of additional questions which could be further investigated. For example, what is the mechanism mediating the post-transcriptional decline in GK protein in response to high dietary fat and/or fructose consumption?

Processes such as oxidative stress [390, 391], nitrosative stress [392-394] ER stress [395], and inflammation [396, 397] have all been implicated in the development of insulin resistance in association with diet-induced obesity. However, a superficial assessment of markers of oxidative/nitrosative stress (gene expression of NADPH oxidase [Nox 2 and 4] and iNOS) and ER stress (phosphorylation of PERK on Thr980, eIF2 α on Ser51, and Bip protein levels) in the livers of HFFD-fed and CTR-fed dogs failed to show a difference between groups. The potential contribution of these processes to impaired regulation of hepatic GK in response to dietary insults needs to be addressed in more detail. Given that 4 weeks was the earliest time point in which we assessed glucose tolerance or HGU, it is possible that the liver had already undergone substantial adaptation at that time point. Thus, it would be interesting to go back in time, perhaps after 3 days or 1 week of HFFD (similar to some of the rodent studies discussed in Chapter I), and measure HGU with liver biopsy acquisition at the end of the study. This might enable us to capture the early molecular changes associated with HFFD feeding, and identify the pathogenic process leading to decreased GK activity and HGU after 4 weeks of feeding.

Another interesting question is whether the defect in HGU after 4 or more weeks of HFFD feeding is reversible if dogs are then switched back to their normal chow diet. We already know based on the findings presented in this dissertation that it is not reversible within 24 hours, given that all dogs received the same can of meat the day prior to the study, yet the defect in HGU was still manifest in HFA-, HFR-, and HFFD-fed animals during the clamp experiment. Initial assessments of HGU and GK activity could begin 3 days after switching from the HFFD to the CTR diet. If HGU and GK

activity are still impaired 3 days after switching to a normal chow diet, then one could reassess HGU and GK activity after 5 or 7 days. Furthermore, several different permutations of this experiment could be conducted. For example, we could switch dogs from the HFFD to a eucaloric or hypercaloric chow diet to investigate the impact of excess calories and/or body weight loss on the rapidity of the reversal of impaired HGU. These types of studies would provide insight into the effectiveness of lifestyle modification on improvements in hepatic glucose flux after short- or long-term consumption of a Western diet.

Another question to follow-up on would be whether pharmacologic activation of hepatic GK (GK activator or GKA) in HFFD-fed dogs could rescue their defect in HGU. Hyperinsulinemic hyperglycemic clamp studies could be conducted, but this time a GKA could be infused intraportally with and without portal glucose infusion. Use of somatostatin to perform the pancreatic clamp would enable us to isolate the liver-specific effects of the GKA. If the impairment in HGU is restored with intraportal GKA infusion, these data would suggest that the reduction in GK activity is causally linked to diminished HGU in HFFD-fed animals. In addition, intraportal glucose plus GKA infusion might shed light on whether activation of hepatic GK restores the ability of the portal glucose signal to augment HGU and GSYN. Conversely, would intraportal infusion of glucosamine, an inhibitor of GK, block the ability of hyperglycemia, hyperinsulinemia, and/or portal glucose delivery to augment HGU in normal dogs? This approach would shed light on whether the activation of GK is causally-linked to induction of HGU in response to the portal glucose signal.

Questions addressing the neural mediation of the portal glucose signal could also

be investigated. For example, would hepatic denervation or a selective hepatic vagotomy ablate the effect of portal glucose delivery on the induction of hepatic GK expression? If non-adrenergic, non-cholinergic nerves are involved in the induction of GK expression by portal glucose delivery, then activators and/or inhibitors of nitric oxide synthase or serotonin receptors, for example, could be infused intraportally in the absence and presence of portal glucose delivery. These experiments might shed light on the role of the nervous system in mediating the effects of portal glucose delivery on hepatic GK mRNA and activity.

Alternatively, would portal glucose delivery in the presence of basal insulin levels augment GK expression and activity? Hyperglycemic pancreatic clamps could be performed in which the hepatic sinusoidal insulin and glucagon concentrations are kept at a basal level, while the hepatic glucose load is doubled in the absence and presence of portal glucose delivery. These experiments would enable us to ascertain whether the portal glucose signal potentiates the ability of insulin to induce GK expression, or if it is acting independently of insulin through a neurally-mediated pathway. Furthermore, the same experiment could be conducted in the absence of basal insulin replacement to mimic insulin-dependent diabetes. Although the metabolic response of the liver to portal glucose delivery is lost after acute (somatostatin) or chronic (pancreatectomy) removal of insulin, it is possible that its effect on GK expression does not require insulin.

Finally, what is the response of the liver to a selective and physiologic increase in insulin or glucose alone after chronic consumption of a HFFD? In all of the aforementioned studies, glucose and insulin were concomitantly increased, so the relative contributions of hepatic insulin resistance and/or impaired glucose effectiveness to

diminished HGU and GSYN could not be delineated. Hyperinsulinemic euglycemic (4x basal insulin) and hyperglycemic euinsulinemic (2x basal hepatic glucose load) clamp studies could be performed to delineate between hepatic insulin resistance and impaired hepatic glucose effectiveness. In addition, the deuterated water technique could be utilized in the hyperinsulinemic clamps to see if impaired suppression of hepatic glucose production is due to impaired suppression of gluconeogenesis or glycogenolysis.

In contrast to dietary fat, there are currently no nutritional recommendations regarding the consumption of dietary fructose in the U.S. The findings presented in this dissertation demonstrate the need for additional studies aimed at elucidating the mechanisms through which chronic consumption of a HFFD impairs HGU and hepatic insulin sensitivity, and increases the risk for type 2 diabetes.

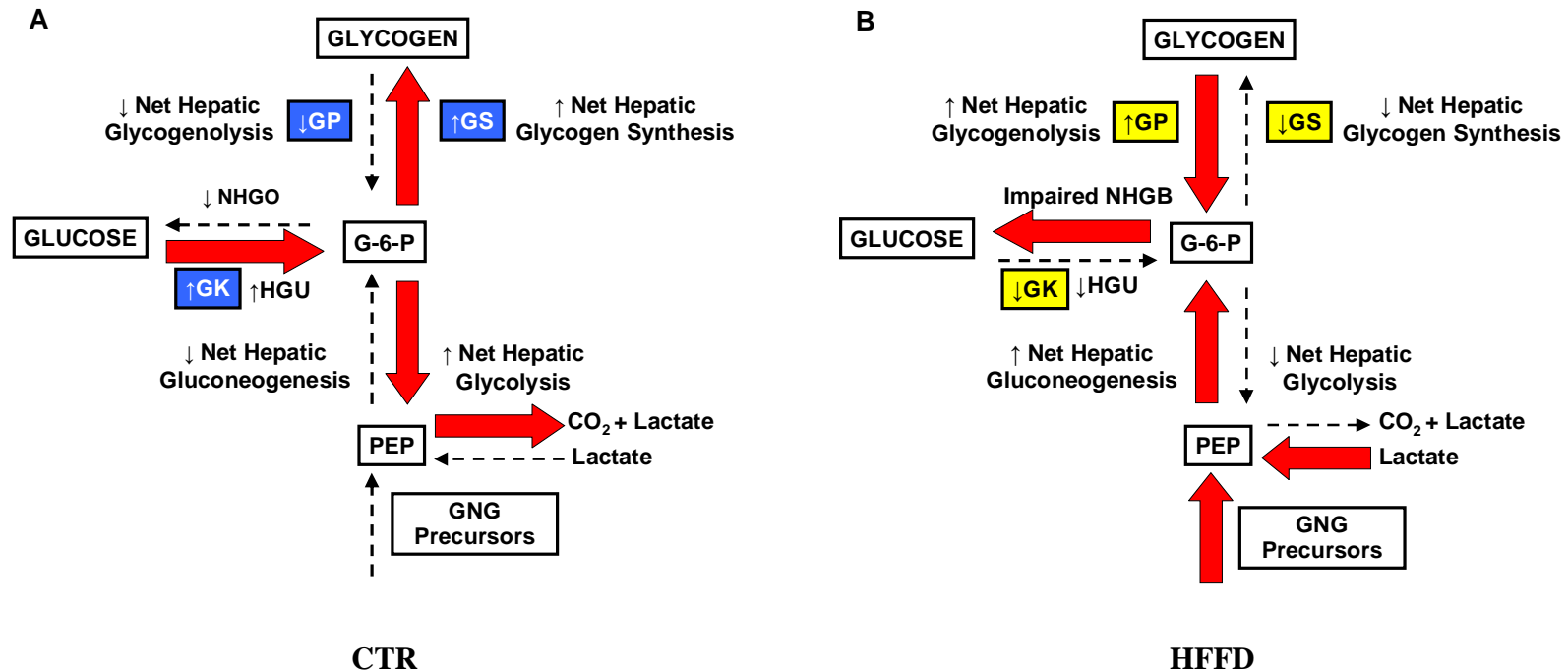
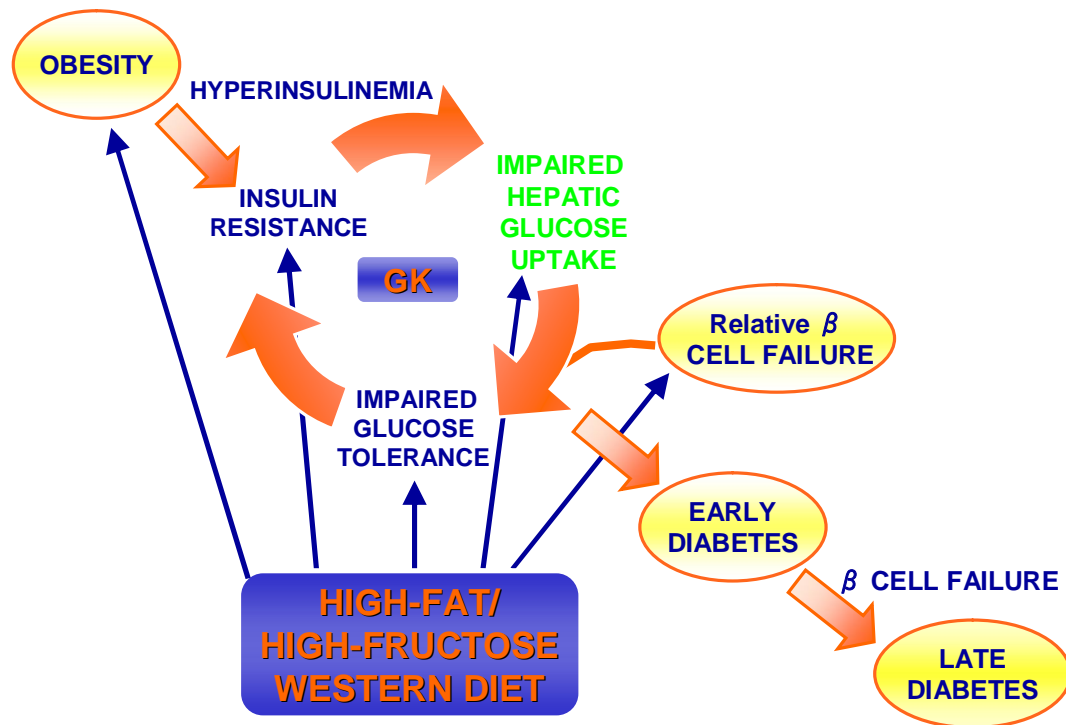


Figure 7.1: Altered hepatic glucose flux by high-fat, high-fructose diet (HFFD) feeding in the presence of hyperglycemia and hyperinsulinemia. A physiologic rise in glucose and insulin in normal, chow-fed control (CTR) dogs (A) suppresses net hepatic glucose output (NHGO) and stimulates an increase in hepatic glucose uptake (HGU) and net hepatic glycogen synthesis, glycolysis, and lactate output. These metabolic changes are associated with an increase in hepatic glucokinase (GK) and glycogen synthase (GS) activity, and a decrease in glycogen phosphorylase (GP) activity. On the other hand, HFFD feeding (B) significantly reduces hepatic GK protein content. As a result, a physiologic rise in glucose and insulin in HFFD-fed dogs is associated with impaired suppression of NHGO, and diminished HGU, net hepatic glycogen synthesis, and glycolysis in comparison to CTR. Furthermore, net hepatic lactate uptake persists in the presence of hyperinsulinemia and hyperglycemia, which contributes to inappropriately elevated net hepatic gluconeogenesis relative to CTR. These metabolic changes are associated with decreased GK and GS activity, and inappropriately increased GP activity relative to CTR.

METABOLIC STAGING OF TYPE 2 DIABETES



Adapted from Saltiel, A. R. J. Clin. Invest. 2000;106:163-164

Figure 7.2: Summary schematic of the metabolic staging of type 2 diabetes in the context of western diet-induced insulin resistance. The findings presented in this dissertation suggest that in the context of diet-induced insulin resistance, impaired hepatic glucose uptake (HGU) is manifest in the early stages of diabetes development, and contributes to the worsening of glucose tolerance and insulin action that occurs along the continuum of disease progression. Furthermore, our findings raise the possibility that impaired regulation of hepatic glucokinase (GK) is central to the defect in HGU and glucose tolerance in the early stages of the disease. Lastly, chronic consumption of a high-fat/high-fructose diet produces modest obesity and whole-body insulin resistance, and impairs glucose tolerance, HGU, and beta cell function. Each of these metabolic defects are associated with the development of type 2 diabetes. This raises the possibility that lifestyle intervention in the form of modifying the type of dietary constituents consumed in Westernized cultures might prove to be an effective approach in preventing or delaying the onset of type 2 diabetes in susceptible individuals. In addition, it is intriguing to speculate that a hepatoselective GK activator might have therapeutic potential in terms of preventing further impairment or even rescuing the defect in glucose tolerance and HGU in the early stages of type 2 diabetes.

REFERENCES

1. Flegal, K.M., et al., *Prevalence and trends in obesity among US adults, 1999-2008*. JAMA. 303(3): p. 235-41.
2. Ogden, C.L., et al., *Prevalence of overweight and obesity in the United States, 1999-2004*. JAMA, 2006. 295(13): p. 1549-55.
3. World Health Organization (2011) *Obesity and Overweight*. WHO website.
4. Ahima, R.S., *Digging deeper into obesity*. J Clin Invest, 2011. 121(6): p. 2076-9.
5. Centers for Disease Control and Prevention (2011) *National diabetes fact sheet: national estimates and general information on diabetes and prediabetes in the United States, 2011*. National diabetes fact sheet.
6. Glanz, K., et al., *How major restaurant chains plan their menus: the role of profit, demand, and health*. Am J Prev Med, 2007. 32(5): p. 383-8.
7. Glanz, K., et al., *Nutrition Environment Measures Survey in stores (NEMS-S): development and evaluation*. Am J Prev Med, 2007. 32(4): p. 282-9.
8. Wang, M.C., et al., *Socioeconomic and food-related physical characteristics of the neighbourhood environment are associated with body mass index*. J Epidemiol Community Health, 2007. 61(6): p. 491-8.
9. Bray, G.A., S.J. Nielsen, and B.M. Popkin, *Consumption of high-fructose corn syrup in beverages may play a role in the epidemic of obesity*. Am J Clin Nutr, 2004. 79(4): p. 537-43.
10. Bray, G.A. and B.M. Popkin, *Dietary fat intake does affect obesity!* Am J Clin Nutr, 1998. 68(6): p. 1157-73.
11. Bray, G.A. and B.M. Popkin, *Dietary fat affects obesity rate*. Am J Clin Nutr, 1999. 70(4): p. 572-3.
12. Tappy, L. and K.A. Le, *Metabolic effects of fructose and the worldwide increase in obesity*. Physiol Rev, 2010. 90(1): p. 23-46.
13. Bizeau, M.E. and M.J. Pagliassotti, *Hepatic adaptations to sucrose and fructose*. Metabolism, 2005. 54(9): p. 1189-201.
14. Bizeau, M.E., J.S. Thresher, and M.J. Pagliassotti, *Sucrose diets increase glucose-6-phosphatase and glucose release and decrease glucokinase in hepatocytes*. J Appl Physiol, 2001. 91(5): p. 2041-6.

15. Kim, J.K., J.K. Wi, and J.H. Youn, *Metabolic impairment precedes insulin resistance in skeletal muscle during high-fat feeding in rats*. *Diabetes*, 1996. 45(5): p. 651-8.
16. Kim, S.P., et al., *Primacy of hepatic insulin resistance in the development of the metabolic syndrome induced by an isocaloric moderate-fat diet in the dog*. *Diabetes*, 2003. 52(10): p. 2453-60.
17. Kraegen, E.W., et al., *Development of muscle insulin resistance after liver insulin resistance in high-fat-fed rats*. *Diabetes*, 1991. 40(11): p. 1397-403.
18. Pagliassotti, M.J. and P.A. Prach, *Quantity of sucrose alters the tissue pattern and time course of insulin resistance in young rats*. *Am J Physiol*, 1995. 269(3 Pt 2): p. R641-6.
19. Pagliassotti, M.J., K.A. Shahrokhi, and M. Moscarello, *Involvement of liver and skeletal muscle in sucrose-induced insulin resistance: dose-response studies*. *Am J Physiol*, 1994. 266(5 Pt 2): p. R1637-44.
20. Collier, G.R., et al., *More severe impairment of oral than intravenous glucose tolerance in rats after eating a high fat diet*. *J Nutr*, 1985. 115(11): p. 1471-6.
21. Jiang, M., et al., *Hypermethylation of hepatic glucokinase and L-type pyruvate kinase promoters in high-fat diet-induced obese rats*. *Endocrinology*, 2011. 152(4): p. 1284-9.
22. Oakes, N.D., et al., *Mechanisms of liver and muscle insulin resistance induced by chronic high-fat feeding*. *Diabetes*, 1997. 46(11): p. 1768-74.
23. Samuel, V.T., et al., *Mechanism of hepatic insulin resistance in non-alcoholic fatty liver disease*. *J Biol Chem*, 2004. 279(31): p. 32345-53.
24. Shimizu, H., et al., *Contribution of fasting and postprandial hyperglycemia to hemoglobin A1c in insulin-treated Japanese diabetic patients*. *Endocr J*, 2008. 55(4): p. 753-6.
25. Woerle, H.J., et al., *Impact of fasting and postprandial glycemia on overall glycemic control in type 2 diabetes Importance of postprandial glycemia to achieve target HbA1c levels*. *Diabetes Res Clin Pract*, 2007. 77(2): p. 280-5.
26. Cherrington, A.D., *Banting Lecture 1997. Control of glucose uptake and release by the liver in vivo*. *Diabetes*, 1999. 48(5): p. 1198-214.
27. Abumrad, N.N., et al., *Absorption and disposition of a glucose load in the conscious dog*. *Am J Physiol*, 1982. 242(6): p. E398-406.
28. van Dam, R.M., et al., *Dietary patterns and risk for type 2 diabetes mellitus in U.S. men*. *Ann Intern Med*, 2002. 136(3): p. 201-9.

29. van Dam, R.M., et al., *Dietary fat and meat intake in relation to risk of type 2 diabetes in men*. *Diabetes Care*, 2002. 25(3): p. 417-24.
30. Willett, W.C., *Dietary fat plays a major role in obesity: no*. *Obes Rev*, 2002. 3(2): p. 59-68.
31. Willett, W.C. and R.L. Leibel, *Dietary fat is not a major determinant of body fat*. *Am J Med*, 2002. 113 Suppl 9B: p. 47S-59S.
32. Astrup, A., *Dietary composition, substrate balances and body fat in subjects with a predisposition to obesity*. *Int J Obes Relat Metab Disord*, 1993. 17 Suppl 3: p. S32-6; discussion S41-2.
33. Bray, G.A., *Is dietary fat important?* *Am J Clin Nutr*. 93(3): p. 481-2.
34. Swinburn, B., G. Sacks, and E. Ravussin, *Increased food energy supply is more than sufficient to explain the US epidemic of obesity*. *Am J Clin Nutr*, 2009. 90(6): p. 1453-6.
35. Mendoza, J.A., A. Drewnowski, and D.A. Christakis, *Dietary energy density is associated with obesity and the metabolic syndrome in U.S. adults*. *Diabetes Care*, 2007. 30(4): p. 974-9.
36. Bray, G.A., et al., *Corrective responses in human food intake identified from an analysis of 7-d food-intake records*. *Am J Clin Nutr*, 2008. 88(6): p. 1504-10.
37. Blundell, J.E., et al., *Dietary fat and the control of energy intake: evaluating the effects of fat on meal size and postmeal satiety*. *Am J Clin Nutr*, 1993. 57(5 Suppl): p. 772S-777S; discussion 777S-778S.
38. Green, S.M. and J.E. Blundell, *Effect of fat- and sucrose-containing foods on the size of eating episodes and energy intake in lean dietary restrained and unrestrained females: potential for causing overconsumption*. *Eur J Clin Nutr*, 1996. 50(9): p. 625-35.
39. Sparti, A., et al., *Effect of an acute reduction in carbohydrate intake on subsequent food intake in healthy men*. *Am J Clin Nutr*, 1997. 66(5): p. 1144-50.
40. Tremblay, A., et al., *Nutritional determinants of the increase in energy intake associated with a high-fat diet*. *Am J Clin Nutr*, 1991. 53(5): p. 1134-7.
41. Gaitonde, M.K., *A spectrophotometric method for the direct determination of cysteine in the presence of other naturally occurring amino acids*. *Biochem J*, 1967. 104(2): p. 627-33.
42. Blundell, J.E. and J.I. Macdiarmid, *Passive overconsumption. Fat intake and short-term energy balance*. *Ann N Y Acad Sci*, 1997. 827: p. 392-407.

43. Arnett, D.K., et al., *Secular trends in dietary macronutrient intake in Minneapolis-St. Paul, Minnesota, 1980-1992*. Am J Epidemiol, 2000. 152(9): p. 868-73.
44. Prentice, A.M. and S.A. Jebb, *Obesity in Britain: gluttony or sloth?* BMJ, 1995. 311(7002): p. 437-9.
45. Kuczmarski, R.J., et al., *Increasing prevalence of overweight among US adults. The National Health and Nutrition Examination Surveys, 1960 to 1991*. JAMA, 1994. 272(3): p. 205-11.
46. Fung, T.T., et al., *Sweetened beverage consumption and risk of coronary heart disease in women*. Am J Clin Nutr, 2009. 89(4): p. 1037-42.
47. Brown, M.A., et al., *Dietary Fat and Carbohydrate Composition: Metabolic Disease*. 2011.
48. Drewnowski, A., *The real contribution of added sugars and fats to obesity*. Epidemiol Rev, 2007. 29: p. 160-71.
49. Bray, G.A., S. Paeratakul, and B.M. Popkin, *Dietary fat and obesity: a review of animal, clinical and epidemiological studies*. Physiol Behav, 2004. 83(4): p. 549-55.
50. Sonne-Holm, S. and T.I. Sorensen, *Post-war course of the prevalence of extreme overweight among Danish young men*. J Chronic Dis, 1977. 30(6): p. 351-8.
51. Monteiro, C.A., et al., *The nutrition transition in Brazil*. Eur J Clin Nutr, 1995. 49(2): p. 105-13.
52. Popkin, B.M., et al., *The nutrition transition in China: a cross-sectional analysis*. Eur J Clin Nutr, 1993. 47(5): p. 333-46.
53. Popkin, B.M., et al., *Body weight patterns among the Chinese: results from the 1989 and 1991 China Health and Nutrition Surveys*. Am J Public Health, 1995. 85(5): p. 690-4.
54. Popkin, B.M., et al., *Dietary and environmental correlates of obesity in a population study in China*. Obes Res, 1995. 3 Suppl 2: p. 135s-143s.
55. Sheppard, L., A.R. Kristal, and L.H. Kushi, *Weight loss in women participating in a randomized trial of low-fat diets*. Am J Clin Nutr, 1991. 54(5): p. 821-8.
56. *The National Diet-Heart Study Final Report*. Circulation, 1968. 37(3 Suppl): p. I1-428.

57. Boyd, N.F., et al., *Quantitative changes in dietary fat intake and serum cholesterol in women: results from a randomized, controlled trial*. Am J Clin Nutr, 1990. 52(3): p. 470-6.
58. Kasim, S.E., et al., *Dietary and anthropometric determinants of plasma lipoproteins during a long-term low-fat diet in healthy women*. Am J Clin Nutr, 1993. 57(2): p. 146-53.
59. Jeffery, R.W., et al., *A randomized trial of counseling for fat restriction versus calorie restriction in the treatment of obesity*. Int J Obes Relat Metab Disord, 1995. 19(2): p. 132-7.
60. Knopp, R.H., et al., *Long-term cholesterol-lowering effects of 4 fat-restricted diets in hypercholesterolemic and combined hyperlipidemic men. The Dietary Alternatives Study*. JAMA, 1997. 278(18): p. 1509-15.
61. Facchini, F.S., et al., *Insulin resistance as a predictor of age-related diseases*. J Clin Endocrinol Metab, 2001. 86(8): p. 3574-8.
62. Alberti, K.G. and P.Z. Zimmet, *Definition, diagnosis and classification of diabetes mellitus and its complications. Part 1: diagnosis and classification of diabetes mellitus provisional report of a WHO consultation*. Diabet Med, 1998. 15(7): p. 539-53.
63. Reaven, G.M., *Banting lecture 1988. Role of insulin resistance in human disease*. Diabetes, 1988. 37(12): p. 1595-607.
64. Mayer-Davis, E.J., et al., *Dietary fat and insulin sensitivity in a triethnic population: the role of obesity. The Insulin Resistance Atherosclerosis Study (IRAS)*. Am J Clin Nutr, 1997. 65(1): p. 79-87.
65. Gulliford, M.C. and O.C. Ukoumunne, *Determinants of glycated haemoglobin in the general population: associations with diet, alcohol and cigarette smoking*. Eur J Clin Nutr, 2001. 55(7): p. 615-23.
66. Marshall, J.A., R.F. Hamman, and J. Baxter, *High-fat, low-carbohydrate diet and the etiology of non-insulin-dependent diabetes mellitus: the San Luis Valley Diabetes Study*. Am J Epidemiol, 1991. 134(6): p. 590-603.
67. Marshall, J.A., et al., *Dietary fat predicts conversion from impaired glucose tolerance to NIDDM. The San Luis Valley Diabetes Study*. Diabetes Care, 1994. 17(1): p. 50-6.
68. Chen, M., R.N. Bergman, and D. Porte, Jr., *Insulin resistance and beta-cell dysfunction in aging: the importance of dietary carbohydrate*. J Clin Endocrinol Metab, 1988. 67(5): p. 951-7.

69. Fukagawa, N.K., et al., *High-carbohydrate, high-fiber diets increase peripheral insulin sensitivity in healthy young and old adults*. *Am J Clin Nutr*, 1990. 52(3): p. 524-8.
70. Swinburn, B.A., et al., *Deterioration in carbohydrate metabolism and lipoprotein changes induced by modern, high fat diet in Pima Indians and Caucasians*. *J Clin Endocrinol Metab*, 1991. 73(1): p. 156-65.
71. Lovejoy, J.C., et al., *Effect of a controlled high-fat versus low-fat diet on insulin sensitivity and leptin levels in African-American and Caucasian women*. *Metabolism*, 1998. 47(12): p. 1520-4.
72. Straznicky, N.E., et al., *Hypotensive effect of low-fat, high-carbohydrate diet can be independent of changes in plasma insulin concentrations*. *Hypertension*, 1999. 34(4 Pt 1): p. 580-5.
73. Lovejoy, J.C., *The influence of dietary fat on insulin resistance*. *Curr Diab Rep*, 2002. 2(5): p. 435-40.
74. Brons, C., et al., *Impact of short-term high-fat feeding on glucose and insulin metabolism in young healthy men*. *J Physiol*, 2009. 587(Pt 10): p. 2387-97.
75. Bisschop, P.H., et al., *Dietary fat content alters insulin-mediated glucose metabolism in healthy men*. *Am J Clin Nutr*, 2001. 73(3): p. 554-9.
76. Swinburn, B.A., P.A. Metcalf, and S.J. Ley, *Long-term (5-year) effects of a reduced-fat diet intervention in individuals with glucose intolerance*. *Diabetes Care*, 2001. 24(4): p. 619-24.
77. Knowler, W.C., et al., *Reduction in the incidence of type 2 diabetes with lifestyle intervention or metformin*. *N Engl J Med*, 2002. 346(6): p. 393-403.
78. Knowler, W.C., et al., *10-year follow-up of diabetes incidence and weight loss in the Diabetes Prevention Program Outcomes Study*. *Lancet*, 2009. 374(9702): p. 1677-86.
79. Tuomilehto, J., et al., *Prevention of type 2 diabetes mellitus by changes in lifestyle among subjects with impaired glucose tolerance*. *N Engl J Med*, 2001. 344(18): p. 1343-50.
80. Riccardi, G., R. Giacco, and A.A. Rivellese, *Dietary fat, insulin sensitivity and the metabolic syndrome*. *Clin Nutr*, 2004. 23(4): p. 447-56.
81. Maron, D.J., J.M. Fair, and W.L. Haskell, *Saturated fat intake and insulin resistance in men with coronary artery disease. The Stanford Coronary Risk Intervention Project Investigators and Staff*. *Circulation*, 1991. 84(5): p. 2020-7.

82. Parker, D.R., et al., *Relationship of dietary saturated fatty acids and body habitus to serum insulin concentrations: the Normative Aging Study*. Am J Clin Nutr, 1993. 58(2): p. 129-36.
83. Mayer, E.J., et al., *Usual dietary fat intake and insulin concentrations in healthy women twins*. Diabetes Care, 1993. 16(11): p. 1459-69.
84. Feskens, E.J., J.G. Loeber, and D. Kromhout, *Diet and physical activity as determinants of hyperinsulinemia: the Zutphen Elderly Study*. Am J Epidemiol, 1994. 140(4): p. 350-60.
85. Marshall, J.A., D.H. Bessesen, and R.F. Hamman, *High saturated fat and low starch and fibre are associated with hyperinsulinaemia in a non-diabetic population: the San Luis Valley Diabetes Study*. Diabetologia, 1997. 40(4): p. 430-8.
86. Stein, D.T., et al., *The insulinotropic potency of fatty acids is influenced profoundly by their chain length and degree of saturation*. J Clin Invest, 1997. 100(2): p. 398-403.
87. Dobbins, R.L., et al., *The composition of dietary fat directly influences glucose-stimulated insulin secretion in rats*. Diabetes, 2002. 51(6): p. 1825-33.
88. McGuinness, O.P., A. Friedman, and A.D. Cherrington, *Intraportal hyperinsulinemia decreases insulin-stimulated glucose uptake in the dog*. Metabolism, 1990. 39(2): p. 127-32.
89. McGuinness, O.P., et al., *Chronic hyperinsulinemia decreases insulin action but not insulin sensitivity*. Metabolism, 1990. 39(9): p. 931-7.
90. Paniagua, J.A., et al., *Monounsaturated fat-rich diet prevents central body fat distribution and decreases postprandial adiponectin expression induced by a carbohydrate-rich diet in insulin-resistant subjects*. Diabetes Care, 2007. 30(7): p. 1717-23.
91. Summers, L.K., et al., *Substituting dietary saturated fat with polyunsaturated fat changes abdominal fat distribution and improves insulin sensitivity*. Diabetologia, 2002. 45(3): p. 369-77.
92. Heine, R.J., et al., *Linoleic-acid-enriched diet: long-term effects on serum lipoprotein and apolipoprotein concentrations and insulin sensitivity in noninsulin-dependent diabetic patients*. Am J Clin Nutr, 1989. 49(3): p. 448-56.
93. Vessby, B., et al., *Substituting dietary saturated for monounsaturated fat impairs insulin sensitivity in healthy men and women: The KANWU Study*. Diabetologia, 2001. 44(3): p. 312-9.

94. Storlien, L.H., et al., *Fat feeding causes widespread in vivo insulin resistance, decreased energy expenditure, and obesity in rats.* Am J Physiol, 1986. 251(5 Pt 1): p. E576-83.
95. Kraegen, E.W., et al., *In vivo insulin resistance in individual peripheral tissues of the high fat fed rat: assessment by euglycaemic clamp plus deoxyglucose administration.* Diabetologia, 1986. 29(3): p. 192-8.
96. Woods, S.C., et al., *A controlled high-fat diet induces an obese syndrome in rats.* J Nutr, 2003. 133(4): p. 1081-7.
97. Shiraev, T., H. Chen, and M.J. Morris, *Differential effects of restricted versus unlimited high-fat feeding in rats on fat mass, plasma hormones and brain appetite regulators.* J Neuroendocrinol, 2009. 21(7): p. 602-9.
98. Rocchini, A.P., P. Marker, and T. Cervenka, *Time course of insulin resistance associated with feeding dogs a high-fat diet.* Am J Physiol, 1997. 272(1 Pt 1): p. E147-54.
99. Bergman, R.N., et al., *Abdominal obesity: role in the pathophysiology of metabolic disease and cardiovascular risk.* Am J Med, 2007. 120(2 Suppl 1): p. S3-8; discussion S29-32.
100. Kim, S.P., et al., *Nocturnal free fatty acids are uniquely elevated in the longitudinal development of diet-induced insulin resistance and hyperinsulinemia.* Am J Physiol Endocrinol Metab, 2007. 292(6): p. E1590-8.
101. Storlien, L.H., et al., *Influence of dietary fat composition on development of insulin resistance in rats. Relationship to muscle triglyceride and omega-3 fatty acids in muscle phospholipid.* Diabetes, 1991. 40(2): p. 280-9.
102. Park, Y.K. and E.A. Yetley, *Intakes and food sources of fructose in the United States.* Am J Clin Nutr, 1993. 58(5 Suppl): p. 737S-747S.
103. Marriott, B.P., N. Cole, and E. Lee, *National estimates of dietary fructose intake increased from 1977 to 2004 in the United States.* J Nutr, 2009. 139(6): p. 1228S-1235S.
104. Duffey, K.J. and B.M. Popkin, *High-fructose corn syrup: is this what's for dinner?* Am J Clin Nutr, 2008. 88(6): p. 1722S-1732S.
105. Gross, L.S., et al., *Increased consumption of refined carbohydrates and the epidemic of type 2 diabetes in the United States: an ecologic assessment.* Am J Clin Nutr, 2004. 79(5): p. 774-9.
106. Nielsen, S.J. and B.M. Popkin, *Changes in beverage intake between 1977 and 2001.* Am J Prev Med, 2004. 27(3): p. 205-10.

107. Putnam, J.J.a.A., J.E., *Food consumption, prices and expenditures, 1970-97.* , U.D.o.A.E.R.S.s. bulletin, Editor. 1999, US Government Printing Office: Washington, DC.
108. Yoshida, M., et al., *Surrogate markers of insulin resistance are associated with consumption of sugar-sweetened drinks and fruit juice in middle and older-aged adults.* J Nutr, 2007. 137(9): p. 2121-7.
109. Montonen, J., et al., *Consumption of sweetened beverages and intakes of fructose and glucose predict type 2 diabetes occurrence.* J Nutr, 2007. 137(6): p. 1447-54.
110. Palmer, J.R., et al., *Sugar-sweetened beverages and incidence of type 2 diabetes mellitus in African American women.* Arch Intern Med, 2008. 168(14): p. 1487-92.
111. Assy, N., et al., *Soft drink consumption linked with fatty liver in the absence of traditional risk factors.* Can J Gastroenterol, 2008. 22(10): p. 811-6.
112. Ouyang, X., et al., *Fructose consumption as a risk factor for non-alcoholic fatty liver disease.* J Hepatol, 2008. 48(6): p. 993-9.
113. Dhingra, R., et al., *Soft drink consumption and risk of developing cardiometabolic risk factors and the metabolic syndrome in middle-aged adults in the community.* Circulation, 2007. 116(5): p. 480-8.
114. McGuinness, O.P. and A.D. Cherrington, *Effects of fructose on hepatic glucose metabolism.* Curr Opin Clin Nutr Metab Care, 2003. 6(4): p. 441-8.
115. Shiota, M., et al., *Inclusion of low amounts of fructose with an intraportal glucose load increases net hepatic glucose uptake in the presence of relative insulin deficiency in dog.* Am J Physiol Endocrinol Metab, 2005. 288(6): p. E1160-7.
116. Shiota, M., et al., *Small amounts of fructose markedly augment net hepatic glucose uptake in the conscious dog.* Diabetes, 1998. 47(6): p. 867-73.
117. Cheeseman, C.I., *GLUT2 is the transporter for fructose across the rat intestinal basolateral membrane.* Gastroenterology, 1993. 105(4): p. 1050-6.
118. Colville, C.A., et al., *Kinetic analysis of the liver-type (GLUT2) and brain-type (GLUT3) glucose transporters in Xenopus oocytes: substrate specificities and effects of transport inhibitors.* Biochem J, 1993. 290 (Pt 3): p. 701-6.
119. Adelman, R.C., F.J. Ballard, and S. Weinhouse, *Purification and properties of rat liver fructokinase.* J Biol Chem, 1967. 242(14): p. 3360-5.
120. Hers, H.G. and T. Kusaka, *[The metabolism of fructose-1-phosphate in the liver].* Biochim Biophys Acta, 1953. 11(3): p. 427-37.

121. Heinz, F., W. Lamprecht, and J. Kirsch, *Enzymes of fructose metabolism in human liver*. J Clin Invest, 1968. 47(8): p. 1826-32.
122. Iynedjian, P.B., *Molecular physiology of mammalian glucokinase*. Cell Mol Life Sci, 2009. 66(1): p. 27-42.
123. Van Schaftingen, E., M. Detheux, and M. Veiga da Cunha, *Short-term control of glucokinase activity: role of a regulatory protein*. FASEB J, 1994. 8(6): p. 414-9.
124. Mayes, P.A., *Intermediary metabolism of fructose*. Am J Clin Nutr, 1993. 58(5 Suppl): p. 754S-765S.
125. Bode, C., H.K. Durr, and J.C. Bode, *Effect of fructose feeding on the activity of enzymes of glycolysis, gluconeogenesis, and the pentose phosphate shunt in the liver and jejunal mucosa of rats*. Horm Metab Res, 1981. 13(7): p. 379-83.
126. Koo, H.Y., et al., *Dietary fructose induces a wide range of genes with distinct shift in carbohydrate and lipid metabolism in fed and fasted rat liver*. Biochim Biophys Acta, 2008. 1782(5): p. 341-8.
127. Bjorkman, O. and P. Felig, *Role of the kidney in the metabolism of fructose in 60-hour fasted humans*. Diabetes, 1982. 31(6 Pt 1): p. 516-20.
128. Delarue, J., et al., *The contribution of naturally labelled ¹³C fructose to glucose appearance in humans*. Diabetologia, 1993. 36(4): p. 338-45.
129. Tounian, P., et al., *Effects of dexamethasone on hepatic glucose production and fructose metabolism in healthy humans*. Am J Physiol, 1997. 273(2 Pt 1): p. E315-20.
130. Tounian, P., et al., *Effects of infused fructose on endogenous glucose production, gluconeogenesis, and glycogen metabolism*. Am J Physiol, 1994. 267(5 Pt 1): p. E710-7.
131. Carmona, A. and R.A. Freedland, *Comparison among the lipogenic potential of various substrates in rat hepatocytes: the differential effects of fructose-containing diets on hepatic lipogenesis*. J Nutr, 1989. 119(9): p. 1304-10.
132. Da Silva, L.A., O.L. De Marcucci, and A. Carmona, *Adaptive changes in total pyruvate dehydrogenase activity in lipogenic tissues of rats fed high-sucrose or high-fat diets*. Comp Biochem Physiol Comp Physiol, 1992. 103(2): p. 407-11.
133. Park, O.J., et al., *Mechanisms of fructose-induced hypertriglyceridaemia in the rat. Activation of hepatic pyruvate dehydrogenase through inhibition of pyruvate dehydrogenase kinase*. Biochem J, 1992. 282 (Pt 3): p. 753-7.
134. Chong, M.F., B.A. Fielding, and K.N. Frayn, *Mechanisms for the acute effect of fructose on postprandial lipemia*. Am J Clin Nutr, 2007. 85(6): p. 1511-20.

135. McDevitt, R.M., et al., *Macronutrient disposal during controlled overfeeding with glucose, fructose, sucrose, or fat in lean and obese women*. *Am J Clin Nutr*, 2000. 72(2): p. 369-77.
136. Parks, E.J., et al., *Dietary sugars stimulate fatty acid synthesis in adults*. *J Nutr*, 2008. 138(6): p. 1039-46.
137. Ludwig, D.S., K.E. Peterson, and S.L. Gortmaker, *Relation between consumption of sugar-sweetened drinks and childhood obesity: a prospective, observational analysis*. *Lancet*, 2001. 357(9255): p. 505-8.
138. Tordoff, M.G. and A.M. Alleva, *Effect of drinking soda sweetened with aspartame or high-fructose corn syrup on food intake and body weight*. *Am J Clin Nutr*, 1990. 51(6): p. 963-9.
139. Anderson, J.W., et al., *Metabolic effects of fructose supplementation in diabetic individuals*. *Diabetes Care*, 1989. 12(5): p. 337-44.
140. Livesey, G. and R. Taylor, *Fructose consumption and consequences for glycation, plasma triacylglycerol, and body weight: meta-analyses and meta-regression models of intervention studies*. *Am J Clin Nutr*, 2008. 88(5): p. 1419-37.
141. White, J.S., *Straight talk about high-fructose corn syrup: what it is and what it ain't*. *Am J Clin Nutr*, 2008. 88(6): p. 1716S-1721S.
142. de Koning, L., et al., *Sugar-sweetened and artificially sweetened beverage consumption and risk of type 2 diabetes in men*. *Am J Clin Nutr*, 2011. 93(6): p. 1321-7.
143. Malik, V.S., et al., *Sugar-sweetened beverages and risk of metabolic syndrome and type 2 diabetes: a meta-analysis*. *Diabetes Care*, 2010. 33(11): p. 2477-83.
144. Hallfrisch, J., et al., *Effects of dietary fructose on plasma glucose and hormone responses in normal and hyperinsulinemic men*. *J Nutr*, 1983. 113(9): p. 1819-26.
145. Faeh, D., et al., *Effect of fructose overfeeding and fish oil administration on hepatic de novo lipogenesis and insulin sensitivity in healthy men*. *Diabetes*, 2005. 54(7): p. 1907-13.
146. Stanhope, K.L., et al., *Consuming fructose-sweetened, not glucose-sweetened, beverages increases visceral adiposity and lipids and decreases insulin sensitivity in overweight/obese humans*. *J Clin Invest*, 2009. 119(5): p. 1322-34.
147. Stanhope, K.L. and P.J. Havel, *Fructose consumption: recent results and their potential implications*. *Ann N Y Acad Sci*. 1190: p. 15-24.

148. Teff, K.L., et al., *Dietary fructose reduces circulating insulin and leptin, attenuates postprandial suppression of ghrelin, and increases triglycerides in women.* J Clin Endocrinol Metab, 2004. 89(6): p. 2963-72.
149. Stanhope, K.L. and P.J. Havel, *Fructose consumption: potential mechanisms for its effects to increase visceral adiposity and induce dyslipidemia and insulin resistance.* Curr Opin Lipidol, 2008. 19(1): p. 16-24.
150. Storlien, L.H., et al., *Effects of sucrose vs starch diets on in vivo insulin action, thermogenesis, and obesity in rats.* Am J Clin Nutr, 1988. 47(3): p. 420-7.
151. Thorburn, A.W., et al., *Fructose-induced in vivo insulin resistance and elevated plasma triglyceride levels in rats.* Am J Clin Nutr, 1989. 49(6): p. 1155-63.
152. Bizeau, M.E., J.S. Thresher, and M.J. Pagliassotti, *A high-sucrose diet increases gluconeogenic capacity in isolated periportal and perivenous rat hepatocytes.* Am J Physiol Endocrinol Metab, 2001. 280(5): p. E695-702.
153. Wachbroit, R. and D. Wasserman, *Research participation: are we subject to a duty?* Am J Bioeth, 2005. 5(1): p. 48-9; author reply W15-8.
154. Wei, Y., M.E. Bizeau, and M.J. Pagliassotti, *An acute increase in fructose concentration increases hepatic glucose-6-phosphatase mRNA via mechanisms that are independent of glycogen synthase kinase-3 in rats.* J Nutr, 2004. 134(3): p. 545-51.
155. Thresher, J.S., et al., *Comparison of the effects of sucrose and fructose on insulin action and glucose tolerance.* Am J Physiol Regul Integr Comp Physiol, 2000. 279(4): p. R1334-40.
156. Pagliassotti, M.J., et al., *Changes in insulin action, triglycerides, and lipid composition during sucrose feeding in rats.* Am J Physiol, 1996. 271(5 Pt 2): p. R1319-26.
157. Moore, M.C., et al., *Acute fructose administration decreases the glycemic response to an oral glucose tolerance test in normal adults.* J Clin Endocrinol Metab, 2000. 85(12): p. 4515-9.
158. Moore, M.C., et al., *Acute fructose administration improves oral glucose tolerance in adults with type 2 diabetes.* Diabetes Care, 2001. 24(11): p. 1882-7.
159. Shiota, M., et al., *Inclusion of low amounts of fructose with an intraduodenal glucose load markedly reduces postprandial hyperglycemia and hyperinsulinemia in the conscious dog.* Diabetes, 2002. 51(2): p. 469-78.
160. Agius, L. and M. Peak, *Intracellular binding of glucokinase in hepatocytes and translocation by glucose, fructose and insulin.* Biochem J, 1993. 296 (Pt 3): p. 785-96.

161. Shiota, M., K. Igawa, and D.W. Neal, *The effect of fructose on hepatic glucose uptake in conscious dogs is rapidly reversible*. *Diabetes*, 1999. 48(suppl 1): p. A457.
162. Van Schaftingen, E., *A protein from rat liver confers to glucokinase the property of being antagonistically regulated by fructose 6-phosphate and fructose 1-phosphate*. *Eur J Biochem*, 1989. 179(1): p. 179-84.
163. Hawkins, M., et al., *Fructose improves the ability of hyperglycemia per se to regulate glucose production in type 2 diabetes*. *Diabetes*, 2002. 51(3): p. 606-14.
164. Petersen, K.F., et al., *Stimulating effects of low-dose fructose on insulin-stimulated hepatic glycogen synthesis in humans*. *Diabetes*, 2001. 50(6): p. 1263-8.
165. Seoane, J., et al., *Glucose 6-phosphate produced by glucokinase, but not hexokinase I, promotes the activation of hepatic glycogen synthase*. *J Biol Chem*, 1996. 271(39): p. 23756-60.
166. Bezerra, R.M., et al., *A high fructose diet affects the early steps of insulin action in muscle and liver of rats*. *J Nutr*, 2000. 130(6): p. 1531-5.
167. Pagliassotti, M.J., Y. Wei, and M.E. Bizeau, *Glucose-6-phosphatase activity is not suppressed but the mRNA level is increased by a sucrose-enriched meal in rats*. *J Nutr*, 2003. 133(1): p. 32-7.
168. Wei, Y. and M.J. Pagliassotti, *Hepatospecific effects of fructose on c-jun NH2-terminal kinase: implications for hepatic insulin resistance*. *Am J Physiol Endocrinol Metab*, 2004. 287(5): p. E926-33.
169. Wei, Y., D. Wang, and M.J. Pagliassotti, *Fructose selectively modulates c-jun N-terminal kinase activity and insulin signaling in rat primary hepatocytes*. *J Nutr*, 2005. 135(7): p. 1642-6.
170. Wei, Y., et al., *Fructose-mediated stress signaling in the liver: implications for hepatic insulin resistance*. *J Nutr Biochem*, 2007. 18(1): p. 1-9.
171. Nagai, Y., et al., *The role of peroxisome proliferator-activated receptor gamma coactivator-1 beta in the pathogenesis of fructose-induced insulin resistance*. *Cell Metab*, 2009. 9(3): p. 252-64.
172. Kanuri, G., et al., *Role of tumor necrosis factor alpha (TNFalpha) in the onset of fructose-induced nonalcoholic fatty liver disease in mice*. *J Nutr Biochem*, 2011.
173. Spruss, A., et al., *Role of the Inducible Nitric Oxide Synthase in the Onset of Fructose-Induced Steatosis in Mice*. *Antioxid Redox Signal*, 2011.

174. Erion D.M., H.J.J., Yonemitsu S., Stark R., Dong J., Nagai Y., May T., Kahn M., Yu X.X., Murray S.F., Bhanot S., Monia B.P., Cline G.W., Samuel V.T., Shulman G.I., *Knockdown of Carbohydrate Response Element Binding Protein (ChREBP) in Liver Protects Against Fructose Induced Hyperlipidemia and Insulin Resistance*. *Diabetes*, 2009. 58: 1492-P.
175. Matsuzaka, T., et al., *Insulin-independent induction of sterol regulatory element-binding protein-1c expression in the livers of streptozotocin-treated mice*. *Diabetes*, 2004. 53(3): p. 560-9.
176. Aucouturier, J., et al., *Determination of the maximal fat oxidation point in obese children and adolescents: validity of methods to assess maximal aerobic power*. *Eur J Appl Physiol*, 2009. 105(2): p. 325-31.
177. Alves, T.C., et al., *Regulation of hepatic fat and glucose oxidation in rats with lipid-induced hepatic insulin resistance*. *Hepatology*, 2011. 53(4): p. 1175-81.
178. Ren, L., Chan, S.M.H., Zeng, X., Laybutt, D.R., Iseli, T.J., Kraegen, E.W., Cooney, G.J., Turner, N., Ye, J., *De novo lipogenesis induced hepatic steatosis and insulin resistance involve ER stress but not inflammation in contrast to lipid oversupply*, in *71st Scientific Sessions of the American Diabetes Association*. 2011, Diabetes: San Diego, CA.
179. Catena, C., et al., *Cellular mechanisms of insulin resistance in rats with fructose-induced hypertension*. *Am J Hypertens*, 2003. 16(11 Pt 1): p. 973-8.
180. Cardin, S., et al., *Portal glucose infusion increases hepatic glycogen deposition in conscious unrestrained rats*. *J Appl Physiol*, 1999. 87(4): p. 1470-5.
181. Shulman, G.I. and L. Rossetti, *Influence of the route of glucose administration on hepatic glycogen repletion*. *Am J Physiol*, 1989. 257(5 Pt 1): p. E681-5.
182. Adkins, B.A., et al., *Importance of the route of intravenous glucose delivery to hepatic glucose balance in the conscious dog*. *J Clin Invest*, 1987. 79(2): p. 557-65.
183. Adkins-Marshall, B.A., et al., *Interaction between insulin and glucose-delivery route in regulation of net hepatic glucose uptake in conscious dogs*. *Diabetes*, 1990. 39(1): p. 87-95.
184. Adkins-Marshall, B., et al., *Role of hepatic nerves in response of liver to intraportal glucose delivery in dogs*. *Am J Physiol*, 1992. 262(5 Pt 1): p. E679-86.
185. Barrett, E.J., et al., *Hepatic and extrahepatic splanchnic glucose metabolism in the postabsorptive and glucose fed dog*. *Metabolism*, 1985. 34(5): p. 410-20.

186. Ishida, T., et al., *Differential effects of oral, peripheral intravenous, and intraportal glucose on hepatic glucose uptake and insulin and glucagon extraction in conscious dogs*. J Clin Invest, 1983. 72(2): p. 590-601.
187. Bergman, R.N., J.R. Beir, and P.M. Hourigan, *Intraportal glucose infusion matched to oral glucose absorption. Lack of evidence for "gut factor" involvement in hepatic glucose storage*. Diabetes, 1982. 31(1): p. 27-35.
188. Moore, M.C., et al., *Neural and pancreatic influences on net hepatic glucose uptake and glycogen synthesis*. Am J Physiol, 1996. 271(2 Pt 1): p. E215-22.
189. Moore, M.C., et al., *Effect of hepatic denervation on peripheral insulin sensitivity in conscious dogs*. Am J Physiol Endocrinol Metab, 2002. 282(2): p. E286-96.
190. DeFronzo, R.A., et al., *Influence of hyperinsulinemia, hyperglycemia, and the route of glucose administration on splanchnic glucose exchange*. Proc Natl Acad Sci U S A, 1978. 75(10): p. 5173-7.
191. Vella, A., et al., *Effect of enteral vs. parenteral glucose delivery on initial splanchnic glucose uptake in nondiabetic humans*. Am J Physiol Endocrinol Metab, 2002. 283(2): p. E259-66.
192. Sacca, L., et al., *Differential effects of insulin on splanchnic and peripheral glucose disposal after an intravenous glucose load in man*. J Clin Invest, 1982. 70(1): p. 117-26.
193. Dicostanzo, C.A., et al., *Role of the hepatic sympathetic nerves in the regulation of net hepatic glucose uptake and the mediation of the portal glucose signal*. Am J Physiol Endocrinol Metab, 2006. 290(1): p. E9-E16.
194. Hsieh, P.S., et al., *Hepatic glucose uptake rapidly decreases after removal of the portal signal in conscious dogs*. Am J Physiol, 1998. 275(6 Pt 1): p. E987-92.
195. Moore, M.C. and A.D. Cherrington, *The nerves, the liver, and the route of feeding: an integrated response to nutrient delivery*. Nutrition, 1996. 12(4): p. 282-4.
196. Myers, S.R., et al., *Intraportal glucose delivery enhances the effects of hepatic glucose load on net hepatic glucose uptake in vivo*. J Clin Invest, 1991. 88(1): p. 158-67.
197. Myers, S.R., et al., *Intraportal glucose delivery alters the relationship between net hepatic glucose uptake and the insulin concentration*. J Clin Invest, 1991. 87(3): p. 930-9.
198. Pagliassotti, M.J., et al., *Comparison of the time courses of insulin and the portal signal on hepatic glucose and glycogen metabolism in the conscious dog*. J Clin Invest, 1996. 97(1): p. 81-91.

199. Pagliassotti, M.J., et al., *Magnitude of negative arterial-portal glucose gradient alters net hepatic glucose balance in conscious dogs*. *Diabetes*, 1991. 40(12): p. 1659-68.
200. Basu, A., et al., *Type 2 diabetes impairs splanchnic uptake of glucose but does not alter intestinal glucose absorption during enteral glucose feeding: additional evidence for a defect in hepatic glucokinase activity*. *Diabetes*, 2001. 50(6): p. 1351-62.
201. Basu, A., et al., *Effects of type 2 diabetes on the ability of insulin and glucose to regulate splanchnic and muscle glucose metabolism: evidence for a defect in hepatic glucokinase activity*. *Diabetes*, 2000. 49(2): p. 272-83.
202. Basu, R., et al., *Insulin dose-response curves for stimulation of splanchnic glucose uptake and suppression of endogenous glucose production differ in nondiabetic humans and are abnormal in people with type 2 diabetes*. *Diabetes*, 2004. 53(8): p. 2042-50.
203. Hwang, J.H., et al., *Impaired net hepatic glycogen synthesis in insulin-dependent diabetic subjects during mixed meal ingestion. A ¹³C nuclear magnetic resonance spectroscopy study*. *J Clin Invest*, 1995. 95(2): p. 783-7.
204. Krssak, M., et al., *Alterations in postprandial hepatic glycogen metabolism in type 2 diabetes*. *Diabetes*, 2004. 53(12): p. 3048-56.
205. Shulman, G.I., et al., *Glucose disposal during insulinopenia in somatostatin-treated dogs. The roles of glucose and glucagon*. *J Clin Invest*, 1978. 62(2): p. 487-91.
206. Cherrington, A.D., et al., *Insulin as a mediator of hepatic glucose uptake in the conscious dog*. *Am J Physiol*, 1982. 242(2): p. E97-101.
207. Sacca, L., R. Hendler, and R.S. Sherwin, *Hyperglycemia inhibits glucose production in man independent of changes in glucoregulatory hormones*. *J Clin Endocrinol Metab*, 1978. 47(5): p. 1160-3.
208. Cherrington, A.D., et al., *The role of insulin and glucagon in the regulation of basal glucose production in the postabsorptive dog*. *J Clin Invest*, 1976. 58(6): p. 1407-18.
209. Liljenquist, J.E., et al., *Evidence for an important role of glucagon in the regulation of hepatic glucose production in normal man*. *J Clin Invest*, 1977. 59(2): p. 369-74.
210. Rossetti, L., et al., *Mechanism by which hyperglycemia inhibits hepatic glucose production in conscious rats. Implications for the pathophysiology of fasting hyperglycemia in diabetes*. *J Clin Invest*, 1993. 92(3): p. 1126-34.

211. Barzilai, N., et al., *Glucosamine-induced inhibition of liver glucokinase impairs the ability of hyperglycemia to suppress endogenous glucose production.* Diabetes, 1996. 45(10): p. 1329-35.
212. Sindelar, D.K., et al., *Basal hepatic glucose production is regulated by the portal vein insulin concentration.* Diabetes, 1998. 47(4): p. 523-9.
213. Petersen, K.F., et al., *Mechanism by which glucose and insulin inhibit net hepatic glycogenolysis in humans.* J Clin Invest, 1998. 101(6): p. 1203-9.
214. Ramnanan, C.J., et al., *Molecular characterization of insulin-mediated suppression of hepatic glucose production in vivo.* Diabetes, 2010. 59(6): p. 1302-11.
215. Pagliassotti, M.J. and A.D. Cherrington, *Regulation of net hepatic glucose uptake in vivo.* Annu Rev Physiol, 1992. 54: p. 847-60.
216. Perley, M.J. and D.M. Kipnis, *Plasma insulin responses to oral and intravenous glucose: studies in normal and diabetic subjects.* J Clin Invest, 1967. 46(12): p. 1954-62.
217. Holste, L.C., et al., *Physiological changes in circulating glucagon alter hepatic glucose disposition during portal glucose delivery.* Am J Physiol, 1997. 273(3 Pt 1): p. E488-96.
218. Pagliassotti, M.J., et al., *Insulin is required for the liver to respond to intraportal glucose delivery in the conscious dog.* Diabetes, 1992. 41(10): p. 1247-56.
219. Shiota, M., et al., *Combined intraportal infusion of acetylcholine and adrenergic blockers augments net hepatic glucose uptake.* Am J Physiol Endocrinol Metab, 2000. 278(3): p. E544-52.
220. Cardin, S., et al., *Vagal cooling and concomitant portal norepinephrine infusion do not reduce net hepatic glucose uptake in the conscious dog.* Am J Physiol Regul Integr Comp Physiol, 2004. 287(4): p. R742-8.
221. DiCostanzo, C.A., et al., *The effect of vagal cooling on canine hepatic glucose metabolism in the presence of hyperglycemia of peripheral origin.* Metabolism, 2007. 56(6): p. 814-24.
222. An, Z., et al., *Effects of the nitric oxide donor SIN-1 on net hepatic glucose uptake in the conscious dog.* Am J Physiol Endocrinol Metab, 2008. 294(2): p. E300-6.
223. An, Z., et al., *A NO/sGC/cGMP dependent mechanism is involved in the regulation of net hepatic glucose uptake by hepatic nitric oxide in vivo.* Diabetologia, 2008. in press.

224. Moore, M.C., et al., *Hepatic portal venous delivery of a nitric oxide synthase inhibitor enhances net hepatic glucose uptake*. Am J Physiol Endocrinol Metab, 2008. 294(4): p. E768-77.
225. Moore, M.C., et al., *Interaction of a selective serotonin reuptake inhibitor with insulin in the control of hepatic glucose uptake in conscious dogs*. Am J Physiol Endocrinol Metab, 2004. 288: p. E556-63.
226. Moore, M.C., et al., *Portal infusion of a selective serotonin reuptake inhibitor alters hepatic and extrahepatic glucose disposal in conscious dogs*. Am J Physiol, 2004. 287: p. E1057-63.
227. Moore, M.C., et al., *Portal serotonin infusion and glucose disposal in conscious dogs*. Diabetes, 2004. 53(1): p. 14-20.
228. Bollen, M., S. Keppens, and W. Stalmans, *Specific features of glycogen metabolism in the liver*. Biochem J, 1998. 336 (Pt 1): p. 19-31.
229. Shimazu, T., *Glycogen synthetase activity in liver: regulation by the autonomic nerves*. Science, 1967. 156(779): p. 1256-7.
230. Shimazu, T. and A. Amakawa, *Regulation of glycogen metabolism in liver by the autonomic nervous system. 3. Differential effects of sympathetic-nerve stimulation and of catecholamines on liver phosphorylase*. Biochim Biophys Acta, 1968. 165(3): p. 349-56.
231. Ferre, T., et al., *Evidence from transgenic mice that glucokinase is rate limiting for glucose utilization in the liver*. FASEB J, 1996. 10(10): p. 1213-8.
232. Valera, A. and F. Bosch, *Glucokinase expression in rat hepatoma cells induces glucose uptake and is rate limiting in glucose utilization*. Eur J Biochem, 1994. 222(2): p. 533-9.
233. Chu, C.A., et al., *Rapid translocation of hepatic glucokinase in response to intraduodenal glucose infusion and changes in plasma glucose and insulin in conscious rats*. Am J Physiol Gastrointest Liver Physiol, 2004. 286(4): p. G627-34.
234. Kamata, K., et al., *Structural basis for allosteric regulation of the monomeric allosteric enzyme human glucokinase*. Structure, 2004. 12(3): p. 429-38.
235. Zhang, J., et al., *Conformational transition pathway in the allosteric process of human glucokinase*. Proc Natl Acad Sci U S A, 2006. 103(36): p. 13368-73.
236. Heredia, V.V., et al., *Glucose-induced conformational changes in glucokinase mediate allosteric regulation: transient kinetic analysis*. Biochemistry, 2006. 45(24): p. 7553-62.

237. Agius, L., *Control of glucokinase translocation in rat hepatocytes by sorbitol and the cytosolic redox state*. *Biochem J*, 1994. 298 (Pt 1): p. 237-43.
238. Iynedjian, P.B., *Mammalian glucokinase and its gene*. *Biochem J*, 1993. 293 (Pt 1): p. 1-13.
239. DeFronzo, R.A., et al., *Effects of insulin on peripheral and splanchnic glucose metabolism in noninsulin-dependent (type II) diabetes mellitus*. *J Clin Invest*, 1985. 76(1): p. 149-55.
240. Firth, R.G., et al., *Postprandial hyperglycemia in patients with noninsulin-dependent diabetes mellitus. Role of hepatic and extrahepatic tissues*. *J Clin Invest*, 1986. 77(5): p. 1525-32.
241. Ferrannini, E., et al., *The role of fractional glucose extraction in the regulation of splanchnic glucose metabolism in normal and diabetic man*. *Metabolism*, 1980. 29(1): p. 28-35.
242. Ludvik, B., et al., *Evidence for decreased splanchnic glucose uptake after oral glucose administration in non-insulin-dependent diabetes mellitus*. *J Clin Invest*, 1997. 100(9): p. 2354-61.
243. Magnusson, I., et al., *Increased rate of gluconeogenesis in type II diabetes mellitus. A ¹³C nuclear magnetic resonance study*. *J Clin Invest*, 1992. 90(4): p. 1323-7.
244. Chattopadhyay, M.B., et al., *Combined supplementation of vanadium and beta-carotene suppresses placental glutathione S-transferase-positive foci and enhances antioxidant functions during the inhibition of diethylnitrosamine-induced rat liver carcinogenesis*. *J Gastroenterol Hepatol*, 2004. 19(6): p. 683-93.
245. Caro, J.F., et al., *Liver glucokinase: decreased activity in patients with type II diabetes*. *Horm Metab Res*, 1995. 27(1): p. 19-22.
246. Torres, T.P., et al., *Restoration of hepatic glucokinase expression corrects hepatic glucose flux and normalizes plasma glucose in Zucker diabetic fatty rats*. *Diabetes*, 2009. 58(1): p. 78-86.
247. Froguel, P. and G. Velho, *Molecular Genetics of Maturity-onset Diabetes of the Young*. *Trends Endocrinol Metab*, 1999. 10(4): p. 142-146.
248. Froguel, P. and G. Velho, *Maturity-onset diabetes of the young*. *Curr Opin Pediatr*, 1994. 6(4): p. 482-5.
249. Froguel, P., et al., *Close linkage of glucokinase locus on chromosome 7p to early-onset non-insulin-dependent diabetes mellitus*. *Nature*, 1992. 356(6365): p. 162-4.

250. Velho, G., et al., *Impaired hepatic glycogen synthesis in glucokinase-deficient (MODY-2) subjects*. J Clin Invest, 1996. 98(8): p. 1755-61.
251. Postic, C., et al., *Dual roles for glucokinase in glucose homeostasis as determined by liver and pancreatic beta cell-specific gene knock-outs using Cre recombinase*. J Biol Chem, 1999. 274(1): p. 305-15.
252. O'Doherty, R.M., et al., *Metabolic impact of glucokinase overexpression in liver: lowering of blood glucose in fed rats is accompanied by hyperlipidemia*. Diabetes, 1999. 48(10): p. 2022-7.
253. Shiota, M., et al., *Glucokinase gene locus transgenic mice are resistant to the development of obesity-induced type 2 diabetes*. Diabetes, 2001. 50(3): p. 622-9.
254. Goresky, C.A., G.G. Bach, and B.E. Nadeau, *Red cell carriage of label: its limiting effect on the exchange of materials in the liver*. Circ Res, 1975. 36(2): p. 328-51.
255. Nelson, N., *A photometric adaptation of the Somogyi method for determination of glucose*. J Biol Chem, 1944. 153: p. 375-380.
256. Somogyi, M., *Determination of blood sugar*. J Biol Chem, 1945. 160: p. 69-73.
257. Somogyi, M., *Notes on sugar determination*. J Biol Chem, 1952. 195: p. 19-23.
258. Lloyd, B., et al., *Enzymic fluorometric continuous-flow assays for blood glucose, lactate, pyruvate, alanine, glycerol, and 3-hydroxybutyrate*. Clin Chem, 1978. 24(10): p. 1724-9.
259. Kadish, A.H., R.L. Litle, and J.C. Sternberg, *A new and rapid method for the determination of glucose by measurement of the rate of oxygen consumption*. Clin Chem, 1968. 14: p. 116-131.
260. Wide, L., Porath, J., *Radioimmunoassay of proteins with the use of Sephadex-doupled antibodies*. Biochim Biophys Acta, 1966. 130: p. 257-260.
261. Morgan, C.R. and A. Lazarow, *Immunoassay of insulin using a two-antibody system*. Proc Soc Exp Biol Med, 1962. 110: p. 29-32.
262. Ensick, J.W., *Immunoassays for glucagon*. Handbook of Experimental Pharmacology. 1983.
263. Faber, O.K., et al., *Characterization of seven C-peptide antisera*. Diabetes, 1978. 27 Suppl 1: p. 170-7.
264. O'Connell, S.E. and F.J. Zurzola, *A rapid quantitative determination of acetaminophen in plasma*. J Pharm Sci, 1982. 71(11): p. 1291-4.

265. Ameer, B., et al., *High-performance liquid chromatographic determination of acetaminophen in plasma: single-dose pharmacokinetic studies*. J Chromatogr, 1981. 226(1): p. 224-30.
266. Keppler, D. and K. Decker, *Glycogen: determination with amyloglycosidase*, in *Methods of enzymatic analysis*, H.U. Bergmeyer, Editor. 1974, Verlag Chemie Weinheim, Academic Press: New York. p. 1127-1131.
267. Folch, J., M. Lees, and G.H. Sloane Stanley, *A simple method for the isolation and purification of total lipides from animal tissues*. J Biol Chem, 1957. 226(1): p. 497-509.
268. Morrison, W.R. and L.M. Smith, *Preparation of Fatty Acid Methyl Esters and Dimethylacetals from Lipids with Boron Fluoride--Methanol*. J Lipid Res, 1964. 5: p. 600-8.
269. Livak, K.J. and T.D. Schmittgen, *Analysis of relative gene expression data using real-time quantitative PCR and the 2(-Delta Delta C(T)) Method*. Methods, 2001. 25(4): p. 402-8.
270. Barzilai, N. and L. Rossetti, *Role of glucokinase and glucose-6-phosphatase in the acute and chronic regulation of hepatic glucose fluxes by insulin*. J Biol Chem, 1993. 268(33): p. 25019-25.
271. Thomas, J.A., K.K. Schlender, and J. Larner, *A rapid filter paper assay for UDPglucose-glycogen glucosyltransferase, including an improved biosynthesis of UDP-14C-glucose*. Anal Biochem, 1968. 25(1): p. 486-99.
272. Gilboe, D.P., K.L. Larson, and F.Q. Nuttall, *Radioactive method for the assay of glycogen phosphorylases*. Anal Biochem, 1972. 47(1): p. 20-7.
273. Brun, C., *A rapid method for the determination of para-aminohippuric acid in kidney function tests*. J Lab Clin Med, 1951. 37(6): p. 955-8.
274. Altszuler, N., et al., *Carbohydrate metabolism of hypophysectomized dogs as studied with radioactive glucose*. Am J Physiol, 1956. 187(1): p. 25-31.
275. D'Alessio, D.A., et al., *Glucagon-like peptide 1 enhances glucose tolerance both by stimulation of insulin release and by increasing insulin-independent glucose disposal*. J Clin Invest, 1994. 93(5): p. 2263-6.
276. Royle, G.T., R.R. Wolfe, and J.F. Burke, *The measurement of glucose turnover and oxidation using radioactive and stable isotopes*. J Surg Res, 1983. 34(2): p. 187-93.
277. Ekberg, K., et al., *Contributions by kidney and liver to glucose production in the postabsorptive state and after 60 h of fasting*. Diabetes, 1999. 48(2): p. 292-8.

278. Moore, M.C., et al., *Hepatic glucose disposition during concomitant portal glucose and amino acid infusions in the dog*. Am J Physiol, 1998. 274(5 Pt 1): p. E893-902.
279. Moore, M.C., et al., *Nonesterified fatty acids and hepatic glucose metabolism in the conscious dog*. Diabetes, 2004. 53(1): p. 32-40.
280. Sindelar, D.K., et al., *A comparison of the effects of selective increases in peripheral or portal insulin on hepatic glucose production in the conscious dog*. Diabetes, 1996. 45(11): p. 1594-604.
281. Sindelar, D.K., et al., *The role of fatty acids in mediating the effects of peripheral insulin on hepatic glucose production in the conscious dog*. Diabetes, 1997. 46(2): p. 187-96.
282. Steele, R., et al., *Measurement of size and turnover rate of body glucose pool by the isotope dilution method*. Am J Physiol, 1956. 187(1): p. 15-24.
283. Cowan, J.S. and G. Hetenyi, Jr., *Glucoregulatory responses in normal and diabetic dogs recorded by a new tracer method*. Metabolism, 1971. 20(4): p. 360-72.
284. Commerford, S.R., et al., *Hyperglycemia compensates for diet-induced insulin resistance in liver and skeletal muscle of rats*. Am J Physiol Regul Integr Comp Physiol, 2001. 281(5): p. R1380-9.
285. Henriksen, J.E., et al., *Glucose-mediated glucose disposal in insulin-resistant normoglycemic relatives of type 2 diabetic patients*. Diabetes, 2000. 49(7): p. 1209-18.
286. Frey, C.F., C.G. Child, and W. Fry, *Pancreatectomy for chronic pancreatitis*. Ann Surg, 1976. 184(4): p. 403-13.
287. Slezak, L.A. and D.K. Andersen, *Pancreatic resection: effects on glucose metabolism*. World J Surg, 2001. 25(4): p. 452-60.
288. Bonner-Weir, S., D.F. Trent, and G.C. Weir, *Partial pancreatectomy in the rat and subsequent defect in glucose-induced insulin release*. J Clin Invest, 1983. 71(6): p. 1544-53.
289. Jonas, J.C., et al., *Chronic hyperglycemia triggers loss of pancreatic beta cell differentiation in an animal model of diabetes*. J Biol Chem, 1999. 274(20): p. 14112-21.
290. Ionut, V., et al., *Novel canine models of obese prediabetes and mild type 2 diabetes*. Am J Physiol Endocrinol Metab, 2010. 298(1): p. E38-48.

291. Rerup, C.C., *Drugs producing diabetes through damage of the insulin secreting cells*. Pharmacol Rev, 1970. 22(4): p. 485-518.
292. Wilson, G.L., et al., *Mechanisms of streptozotocin- and alloxan-induced damage in rat B cells*. Diabetologia, 1984. 27(6): p. 587-91.
293. Terauchi, Y., et al., *Glucokinase and IRS-2 are required for compensatory beta cell hyperplasia in response to high-fat diet-induced insulin resistance*. J Clin Invest, 2007. 117(1): p. 246-57.
294. Maiztegui, B., et al., *Islet adaptive changes to fructose-induced insulin resistance: beta-cell mass, glucokinase, glucose metabolism, and insulin secretion*. J Endocrinol, 2009. 200(2): p. 139-49.
295. Assan, R., et al., *Glucagon secretion induced by natural and artificial amino acids in the perfused rat pancreas*. Diabetes, 1977. 26(4): p. 300-7.
296. Balasse, E.O. and H.A. Ooms, *Role of plasma free fatty acids in the control of insulin secretion in man*. Diabetologia, 1973. 9(2): p. 145-51.
297. Crespin, S.R., W.B. Greenough, 3rd, and D. Steinberg, *Stimulation of insulin secretion by long-chain free fatty acids. A direct pancreatic effect*. J Clin Invest, 1973. 52(8): p. 1979-84.
298. Floyd, J.C., Jr., et al., *Stimulation of insulin secretion by amino acids*. J Clin Invest, 1966. 45(9): p. 1487-502.
299. Floyd, J.C., Jr., et al., *Insulin secretion in response to protein ingestion*. J Clin Invest, 1966. 45(9): p. 1479-86.
300. Gu, J.W., et al., *Sodium induces hypertrophy of cultured myocardial myoblasts and vascular smooth muscle cells*. Hypertension, 1998. 31(5): p. 1083-7.
301. Moore, M.C., et al., *Differential effect of amino acid infusion route on net hepatic glucose uptake in the dog*. Am J Physiol, 1999. 276(2 Pt 1): p. E295-302.
302. Seyffert, W.A., Jr. and L.L. Madison, *Physiologic effects of metabolic fuels on carbohydrate metabolism. I. Acute effect of elevation of plasma free fatty acids on hepatic glucose output, peripheral glucose utilization, serum insulin, and plasma glucagon levels*. Diabetes, 1967. 16(11): p. 765-76.
303. Hunt, J.N. and M.T. Knox, *A relation between the chain length of fatty acids and the slowing of gastric emptying*. J Physiol, 1968. 194(2): p. 327-36.
304. Hunt, J.N. and D.F. Stubbs, *The volume and energy content of meals as determinants of gastric emptying*. J Physiol, 1975. 245(1): p. 209-25.

305. Heading, R.C., et al., *The dependence of paracetamol absorption on the rate of gastric emptying*. Br J Pharmacol, 1973. 47(2): p. 415-21.
306. Bantle, J.P., *Dietary fructose and metabolic syndrome and diabetes*. J Nutr, 2009. 139(6): p. 1263S-1268S.
307. Horowitz, M., et al., *Relationship between oral glucose tolerance and gastric emptying in normal healthy subjects*. Diabetologia, 1993. 36(9): p. 857-62.
308. Jones, K.L., et al., *Gastric emptying in early noninsulin-dependent diabetes mellitus*. J Nucl Med, 1996. 37(10): p. 1643-8.
309. Davis, M.A., P.E. Williams, and A.D. Cherrington, *Effect of a mixed meal on hepatic lactate and gluconeogenic precursor metabolism in dogs*. Am J Physiol, 1984. 247(3 Pt 1): p. E362-9.
310. Drucker, D.J., *Biological actions and therapeutic potential of the glucagon-like peptides*. Gastroenterology, 2002. 122(2): p. 531-44.
311. Roberge, J.N. and P.L. Brubaker, *Secretion of proglucagon-derived peptides in response to intestinal luminal nutrients*. Endocrinology, 1991. 128(6): p. 3169-74.
312. Baggio, L.L. and D.J. Drucker, *Biology of incretins: GLP-1 and GIP*. Gastroenterology, 2007. 132(6): p. 2131-57.
313. Holst, J.J., et al., *Truncated glucagon-like peptide I, an insulin-releasing hormone from the distal gut*. FEBS Lett, 1987. 211(2): p. 169-74.
314. Kreymann, B., et al., *Glucagon-like peptide-1 7-36: a physiological incretin in man*. Lancet, 1987. 2(8571): p. 1300-4.
315. Mojsov, S., G.C. Weir, and J.F. Habener, *Insulinotropin: glucagon-like peptide I (7-37) co-encoded in the glucagon gene is a potent stimulator of insulin release in the perfused rat pancreas*. J Clin Invest, 1987. 79(2): p. 616-9.
316. Dupre, J., et al., *Glucagon-like peptide I reduces postprandial glycemic excursions in IDDM*. Diabetes, 1995. 44(6): p. 626-30.
317. Meier, J.J., et al., *Normalization of glucose concentrations and deceleration of gastric emptying after solid meals during intravenous glucagon-like peptide I in patients with type 2 diabetes*. J Clin Endocrinol Metab, 2003. 88(6): p. 2719-25.
318. Willms, B., et al., *Gastric emptying, glucose responses, and insulin secretion after a liquid test meal: effects of exogenous glucagon-like peptide-1 (GLP-1)-(7-36) amide in type 2 (noninsulin-dependent) diabetic patients*. J Clin Endocrinol Metab, 1996. 81(1): p. 327-32.

319. Wishart, J.M., et al., *Relation between gastric emptying of glucose and plasma concentrations of glucagon-like peptide-1*. *Peptides*, 1998. 19(6): p. 1049-53.
320. Miholic, J., et al., *Emptying of the gastric substitute, glucagon-like peptide-1 (GLP-1), and reactive hypoglycemia after total gastrectomy*. *Dig Dis Sci*, 1991. 36(10): p. 1361-70.
321. Qualmann, C., et al., *Glucagon-like peptide 1 (7-36 amide) secretion in response to luminal sucrose from the upper and lower gut. A study using alpha-glucosidase inhibition (acarbose)*. *Scand J Gastroenterol*, 1995. 30(9): p. 892-6.
322. Johnson, K.M., et al., *Intraportal GLP-1 infusion increases nonhepatic glucose utilization without changing pancreatic hormone levels*. *Am J Physiol Endocrinol Metab*, 2007. 293(4): p. E1085-91.
323. Johnson, K.M., et al., *Intraportally delivered GLP-1, in the presence of hyperglycemia induced via peripheral glucose infusion, does not change whole body glucose utilization*. *Am J Physiol Endocrinol Metab*, 2008. 294(2): p. E380-4.
324. Johnson, K.M., et al., *Endogenously released GLP-1 is not sufficient to alter postprandial glucose regulation in the dog*. *Endocrine*, 2011. 39(3): p. 229-34.
325. Phillips, W.T., J.G. Schwartz, and C.A. McMahan, *Rapid gastric emptying in patients with early non-insulin-dependent diabetes mellitus*. *N Engl J Med*, 1991. 324(2): p. 130-1.
326. Phillips, W.T., J.G. Schwartz, and C.A. McMahan, *Rapid gastric emptying of an oral glucose solution in type 2 diabetic patients*. *J Nucl Med*, 1992. 33(8): p. 1496-500.
327. Frank, J.W., et al., *Mechanism of accelerated gastric emptying of liquids and hyperglycemia in patients with type II diabetes mellitus*. *Gastroenterology*, 1995. 109(3): p. 755-65.
328. Loo, F.D., et al., *Gastric emptying in patients with diabetes mellitus*. *Gastroenterology*, 1984. 86(3): p. 485-94.
329. Nakanome, C., et al., *Disturbances of the alimentary tract motility and hypermotilinemia in the patients with diabetes mellitus*. *Tohoku J Exp Med*, 1983. 139(2): p. 205-15.
330. Bertin, E., et al., *Gastric emptying is accelerated in obese type 2 diabetic patients without autonomic neuropathy*. *Diabetes Metab*, 2001. 27(3): p. 357-64.
331. Schwartz, J.G., et al., *Rapid gastric emptying of a solid pancake meal in type II diabetic patients*. *Diabetes Care*, 1996. 19(5): p. 468-71.

332. Weytjens, C., et al., *Rapid gastric emptying of a liquid meal in long-term Type 2 diabetes mellitus*. Diabet Med, 1998. 15(12): p. 1022-7.
333. de La Serre, C.B., et al., *Propensity to high-fat diet-induced obesity in rats is associated with changes in the gut microbiota and gut inflammation*. Am J Physiol Gastrointest Liver Physiol, 2010. 299(2): p. G440-8.
334. Spruss, A. and I. Bergheim, *Dietary fructose and intestinal barrier: potential risk factor in the pathogenesis of nonalcoholic fatty liver disease*. J Nutr Biochem, 2009. 20(9): p. 657-62.
335. Bergheim, I., et al., *Antibiotics protect against fructose-induced hepatic lipid accumulation in mice: role of endotoxin*. J Hepatol, 2008. 48(6): p. 983-92.
336. Brun, P., et al., *Increased intestinal permeability in obese mice: new evidence in the pathogenesis of nonalcoholic steatohepatitis*. Am J Physiol Gastrointest Liver Physiol, 2007. 292(2): p. G518-25.
337. Cani, P.D., et al., *Metabolic endotoxemia initiates obesity and insulin resistance*. Diabetes, 2007. 56(7): p. 1761-72.
338. Erridge, C., et al., *A high-fat meal induces low-grade endotoxemia: evidence of a novel mechanism of postprandial inflammation*. Am J Clin Nutr, 2007. 86(5): p. 1286-92.
339. Coate, K.C., et al., *Chronic consumption of a high-fat/high-fructose diet renders the liver incapable of net hepatic glucose uptake*. Am J Physiol Endocrinol Metab, 2010. 299(6): p. E887-98.
340. Galassetti, P., et al., *A negative arterial-portal venous glucose gradient decreases skeletal muscle glucose uptake*. Am J Physiol, 1998. 275(1 Pt 1): p. E101-11.
341. Fueger, P.T., et al., *Regulation of insulin-stimulated muscle glucose uptake in the conscious mouse: role of glucose transport is dependent on glucose phosphorylation capacity*. Endocrinology, 2004. 145(11): p. 4912-6.
342. Wasserman, D.H., *Four grams of glucose*. Am J Physiol Endocrinol Metab, 2009. 296(1): p. E11-21.
343. Wasserman, D.H., et al., *The physiological regulation of glucose flux into muscle in vivo*. J Exp Biol. 214(Pt 2): p. 254-62.
344. DeFronzo, R.A., et al., *Regulation of splanchnic and peripheral glucose uptake by insulin and hyperglycemia in man*. Diabetes, 1983. 32(1): p. 35-45.
345. Iynedjian, P.B., A. Gjinovci, and A.E. Renold, *Stimulation by insulin of glucokinase gene transcription in liver of diabetic rats*. Journal of Biological Chemistry, 1988. 263(2): p. 740-744.

346. Iynedjian, P.B., et al., *Transcriptional induction of glucokinase gene by insulin in cultured liver cells and its repression by the glucagon-cAMP system*. J Biol Chem, 1989. 264(36): p. 21824-9.
347. Magnuson, M.A., et al., *Rat glucokinase gene: structure and regulation by insulin*. Proc Natl Acad Sci U S A, 1989. 86(13): p. 4838-42.
348. Agius, L., *Glucokinase and molecular aspects of liver glycogen metabolism*. Biochem J, 2008. 414(1): p. 1-18.
349. Cohen, P. and S. Frame, *The renaissance of GSK3*. Nat Rev Mol Cell Biol, 2001. 2(10): p. 769-76.
350. Parker, P.J., F.B. Caudwell, and P. Cohen, *Glycogen synthase from rabbit skeletal muscle; effect of insulin on the state of phosphorylation of the seven phosphoserine residues in vivo*. Eur J Biochem, 1983. 130(1): p. 227-34.
351. Patel, S., et al., *Tissue-specific role of glycogen synthase kinase 3beta in glucose homeostasis and insulin action*. Mol Cell Biol, 2008. 28(20): p. 6314-28.
352. Dong, X., et al., *Irs1 and Irs2 signaling is essential for hepatic glucose homeostasis and systemic growth*. J Clin Invest, 2006. 116(1): p. 101-14.
353. Moore, M.C., et al., *Effect of hepatic nerves on disposition of an intraduodenal glucose load*. Am J Physiol, 1993. 265(3 Pt 1): p. E487-96.
354. Shimazu, T., *Neuronal regulation of hepatic glucose metabolism in mammals*. Diabetes Metab Rev, 1987. 3(1): p. 185-206.
355. Niiijima, A., *Glucose-sensitive afferent nerve fibers in the liver and their role in food intake and blood glucose regulation*. J Auton Nerv Syst, 1983. 9(1): p. 207-20.
356. Schmitt, M., *Influences of hepatic portal receptors on hypothalamic feeding and satiety centers*. Am J Physiol, 1973. 225(5): p. 1089-95.
357. Ramnanan, C.J., Viswanathan S, Smith, M.S., Donahue, E.P., Farmer, B., Farmer, T.D., Neal, D.W., Williams, P.E., Lautz, M., Mari, A., Cherrington, A.D., Edgerton, D.S., *Brain insulin action augments hepatic glycogen synthesis without suppressing glucose production or gluconeogenesis in the dog*. J Clin Invest, 2011. in press.
358. Payne, V.A., et al., *Dual role of phosphofructokinase-2/fructose biphosphatase-2 in regulating the compartmentation and expression of glucokinase in hepatocytes*. Diabetes, 2005. 54(7): p. 1949-57.

359. Smith, W.E., et al., *Molecular coordination of hepatic glucose metabolism by the 6-phosphofructo-2-kinase/fructose-2,6- biphosphatase:glucokinase complex*. Mol Endocrinol, 2007. 21(6): p. 1478-87.
360. Wu, C., et al., *A potential role for fructose-2,6-bisphosphate in the stimulation of hepatic glucokinase gene expression*. Endocrinology, 2004. 145(2): p. 650-8.
361. Wu, C., et al., *Roles for fructose-2,6-bisphosphate in the control of fuel metabolism: beyond its allosteric effects on glycolytic and gluconeogenic enzymes*. Adv Enzyme Regul, 2006. 46: p. 72-88.
362. Roach, P.J., *Glycogen and its metabolism*. Curr Mol Med, 2002. 2(2): p. 101-20.
363. Ferrer, J.C., et al., *Control of glycogen deposition*. FEBS Lett, 2003. 546(1): p. 127-32.
364. Gomis, R.R., J.C. Ferrer, and J.J. Guinovart, *Shared control of hepatic glycogen synthesis by glycogen synthase and glucokinase*. Biochem J, 2000. 351 Pt 3: p. 811-6.
365. Cherrington, A.D., et al., *Factors which regulate net hepatic glucose uptake in vivo*. JPEN J Parenter Enteral Nutr, 1991. 15(3): p. 71S-73S.
366. Coate, K.C. and K.W. Huggins, *Consumption of a high glycemic index diet increases abdominal adiposity but does not influence adipose tissue pro-oxidant and antioxidant gene expression in C57BL/6 mice*. Nutr Res, 2010. 30(2): p. 141-50.
367. Newgard, C.B., D.W. Foster, and J.D. McGarry, *Evidence for suppression of hepatic glucose-6-phosphatase with carbohydrate feeding*. Diabetes, 1984. 33(2): p. 192-5.
368. Minassian, C., et al., *Liver glucose-6 phosphatase activity is inhibited by refeeding in rats*. J Nutr, 1995. 125(11): p. 2727-32.
369. Chu, C.A., et al., *Effects of free fatty acids on hepatic glycogenolysis and gluconeogenesis in conscious dogs*. Am J Physiol Endocrinol Metab, 2002. 282(2): p. E402-11.
370. Farrelly, D., et al., *Mice mutant for glucokinase regulatory protein exhibit decreased liver glucokinase: a sequestration mechanism in metabolic regulation*. Proc Natl Acad Sci U S A, 1999. 96(25): p. 14511-6.
371. Grimsby, J., et al., *Characterization of glucokinase regulatory protein-deficient mice*. J Biol Chem, 2000. 275(11): p. 7826-31.
372. Thomas, S.E., et al., *Diabetes as a disease of endoplasmic reticulum stress*. Diabetes Metab Res Rev. 26(8): p. 611-21.

373. Minassian, C., S. Tarpin, and G. Mithieux, *Role of glucose-6 phosphatase, glucokinase, and glucose-6 phosphate in liver insulin resistance and its correction by metformin*. *Biochem Pharmacol*, 1998. 55(8): p. 1213-9.
374. Francini, F., et al., *Changes induced by a fructose-rich diet on hepatic metabolism and the antioxidant system*. *Life Sci*, 2010. 86(25-26): p. 965-71.
375. Francini, F., et al., *Regulation of liver glucokinase activity in rats with fructose-induced insulin resistance and impaired glucose and lipid metabolism*. *Can J Physiol Pharmacol*, 2009. 87(9): p. 702-10.
376. Dipietro, D.L. and S. Weinhouse, *Hepatic glucokinase in the fed, fasted, and alloxan-diabetic rat*. *J Biol Chem*, 1960. 235: p. 2542-5.
377. Minderop, R.H., W. Hoepfner, and H.J. Seitz, *Regulation of hepatic glucokinase gene expression. Role of carbohydrates, and glucocorticoid and thyroid hormones*. *Eur J Biochem*, 1987. 164(1): p. 181-7.
378. Sharma, C., R. Manjeshwar, and S. Weinhouse, *Effects of Diet and Insulin on Glucose-Adenosine Triphosphate Phosphotransferases of Rat Liver*. *J Biol Chem*, 1963. 238: p. 3840-5.
379. Iynedjian, P.B., et al., *Differential expression and regulation of the glucokinase gene in liver and islets of Langerhans*. *Proc Natl Acad Sci U S A*, 1989. 86(20): p. 7838-42.
380. Iynedjian, P.B., C. Ucla, and B. Mach, *Molecular cloning of glucokinase cDNA. Developmental and dietary regulation of glucokinase mRNA in rat liver*. *J Biol Chem*, 1987. 262(13): p. 6032-8.
381. Penicaud, L., et al., *Development of obesity in Zucker rats. Early insulin resistance in muscles but normal sensitivity in white adipose tissue*. *Diabetes*, 1987. 36(5): p. 626-31.
382. Asterholm, I.W. and P.E. Scherer, *Enhanced metabolic flexibility associated with elevated adiponectin levels*. *Am J Pathol*. 176(3): p. 1364-76.
383. Schenk, S., M. Saberi, and J.M. Olefsky, *Insulin sensitivity: modulation by nutrients and inflammation*. *J Clin Invest*, 2008. 118(9): p. 2992-3002.
384. DeFronzo, R.A., *Pathogenesis of type 2 diabetes mellitus*. *Med Clin North Am*, 2004. 88(4): p. 787-835, ix.
385. Coate, K.C., et al., *A High-Fat, High-Fructose Diet Accelerates Nutrient Absorption and Impairs Net Hepatic Glucose Uptake in Response to a Mixed Meal in Partially Pancreatectomized Dogs*. *J Nutr*, 2011.

386. Cherrington, A.D., et al., *Hypoglycemia, gluconeogenesis and the brain*. Adv Exp Med Biol, 1991. 291: p. 197-211.
387. Hsieh, P.S., et al., *Importance of the hepatic arterial glucose level in generation of the portal signal in conscious dogs*. Am J Physiol Endocrinol Metab, 2000. 279(2): p. E284-92.
388. Hsieh, P.S., et al., *The head arterial glucose level is not the reference site for generation of the portal signal in conscious dogs*. Am J Physiol, 1999. 277(4 Pt 1): p. E678-84.
389. Moore, M.C., et al., *Chronic hepatic artery ligation does not prevent liver from differentiating portal vs. peripheral glucose delivery*. Am J Physiol Endocrinol Metab, 2003. 285(4): p. E845-53.
390. Evans, J.L., B.A. Maddux, and I.D. Goldfine, *The molecular basis for oxidative stress-induced insulin resistance*. Antioxid Redox Signal, 2005. 7(7-8): p. 1040-52.
391. Evans, J.L., et al., *Are oxidative stress-activated signaling pathways mediators of insulin resistance and beta-cell dysfunction?* Diabetes, 2003. 52(1): p. 1-8.
392. Charbonneau, A. and A. Marette, *Inducible nitric oxide synthase induction underlies lipid-induced hepatic insulin resistance in mice: potential role of tyrosine nitration of insulin signaling proteins*. Diabetes, 2010. 59(4): p. 861-71.
393. Perreault, M. and A. Marette, *Targeted disruption of inducible nitric oxide synthase protects against obesity-linked insulin resistance in muscle*. Nat Med, 2001. 7(10): p. 1138-43.
394. Tsuchiya, K., et al., *Chronic blockade of nitric oxide synthesis reduces adiposity and improves insulin resistance in high fat-induced obese mice*. Endocrinology, 2007. 148(10): p. 4548-56.
395. Ozcan, U., et al., *Endoplasmic reticulum stress links obesity, insulin action, and type 2 diabetes*. Science, 2004. 306(5695): p. 457-61.
396. Shoelson, S.E., L. Herrero, and A. Naaz, *Obesity, inflammation, and insulin resistance*. Gastroenterology, 2007. 132(6): p. 2169-80.
397. Shoelson, S.E., J. Lee, and A.B. Goldfine, *Inflammation and insulin resistance*. J Clin Invest, 2006. 116(7): p. 1793-801.